

**Fluorescent Dyes with Large Stokes Shifts of 80–200 nm for
Optical Microscopy and Nanoscopy**

Dissertation

for the award of the degree

“Doctor rerum naturalium” (Dr. rer. nat.)

of the Georg-August-Universität Göttingen

within the doctoral program in Chemistry

of the Georg-August University School of Science (GAUSS)

submitted by

Maksim Sednev

from Nizhny Tagil

Göttingen

2015

Thesis committee

Prof. Dr. Armin de Meijere, Institute of Organic and Biomolecular Chemistry, Georg-August-Universität Göttingen

Prof. Dr. Stefan W. Hell, Department of NanoBiophotonics, Max Planck Institute for Biophysical Chemistry

Members of the examination board

Reviewer: Prof. Dr. Armin de Meijere, Institute of Organic and Biomolecular Chemistry, Georg-August-Universität Göttingen

Second reviewer: Prof. Dr. Stefan W. Hell, Department of NanoBiophotonics, Max Planck Institute for Biophysical Chemistry

Further members of the Examination board

Prof. Dr. Ulf Diederichsen, Institute of Organic and Biomolecular Chemistry, Georg-August-Universität Göttingen

Prof. Dr. Claudia Höbartner, Research Group Nucleic Acid Chemistry, Max Planck Institute for Biophysical Chemistry and Institute of Organic and Biomolecular Chemistry, Georg-August-Universität Göttingen

Prof. Dr. Konrad Koszinowski, Institute of Organic and Biomolecular Chemistry, Georg-August-Universität Göttingen

Prof. Dr. Heinz Neumann, Department of Applied Synthetic Biology, GZMB, Georg-August-Universität Göttingen

Date of oral examination: 08.06.2015

Abstract

Bright and photostable fluorescent dyes with large Stokes shift are rare, though they are indispensable in optical microscopy, biology and chemistry. The rapid progress in super-resolution microscopy based on stimulated emission depletion (STED) phenomenon encouraged us to design and prepare new coumarins and a hybrid carborhodol dye. Variation of electron-withdrawing groups at C-3 and/or C-4 enabled us to create promising coumarin dyes possessing a 3-(2-pyridyl) group ($\lambda_{\text{abs}}/\lambda_{\text{em}} = 432/512$ nm in aqueous phosphate buffer), a 3-(pyrido[1,2-*a*]pyrrolo[2,1-*c*]pyrazinium) group (489/587 nm in MeOH) and a fused quinoline ring (453/617 nm in aqueous phosphate buffer). The new dyes were decorated with a polar phosphate group which provided sufficient solubility in aqueous solutions and a carboxylic group which was required for bioconjugation.

The hybrid carborhodol dye was obtained by a combination of (carbo)fluorescein and carbopyronine fluorophores. Due to the broad absorption and emission spectra of the carborhodol in the conjugated form (586/613 nm in aqueous phosphate buffer), the effective Stokes shift is larger in comparison with small Stokes shifts of the parent dyes. This allowed the use of carborhodol in two-color imaging schemes as well as in STED microscopy with a 775 nm depletion laser.

Table of contents

Table of contents.....	II
List of abbreviations	IV
Introduction.....	7
1 Physical background.....	9
1.1 Main principles of superresolution fluorescence microscopy.....	9
1.2 Large Stokes shift fluorophores	16
1.2.1 Fluorophores with a Stokes shift provided by photophysical processes	16
1.2.2 Fluorophores with a Stokes shift provided by photochemical processes	63
1.2.3 Multifluorophore constructs with pseudo-large Stokes shifts.....	67
1.3 Applications of large Stokes shift dyes in fluorescence nanoscopy.....	71
2 Main part	81
2.1 3-Heteroaryl-substituted coumarin dyes	81
2.1.1 Motivation and key structural elements	81
2.1.2 Synthesis of model compounds.....	84
2.1.3 Spectral properties of model coumarin dyes	87
2.1.4 Synthesis of water-soluble coumarins with a phosphate group ...	89
2.1.5 Spectral properties and imaging performance of coumarin 308 ..	90
2.1.6 Conclusion and outlook	93
2.2 3-Pyridiniumcoumarins	94
2.2.1 Motivation and key structural elements	94
2.2.2 Synthesis	95
2.2.3 Spectral properties.....	99
2.2.4 Conclusion and outlook	101
2.3 Synthesis of pyrido- and isoquinolino-fused coumarin dyes	102
2.3.1 Motivation and key structural elements	102
2.3.2 Synthesis of model hydrophilic compounds	103
2.3.3 Spectral properties of pyrido- and (iso)quinolinocoumarins	110
2.3.4 Synthesis of water-soluble quinolinocoumarin 378 and its spectral properties.....	112
2.3.5 Conclusion and outlook	113
2.4 Synthesis of a carborhodol dye	114
2.4.1 Motivation and key structural elements	114
2.4.2 Synthesis and chemical properties of carborhodol dyes	116
2.4.3 Properties and imaging performance of carborhodol dyes	123

2.4.4	Conclusion and outlook	130
3	Experimental part	132
3.1	General remarks	132
3.2	Experimental procedures.....	133
	Acknowledgments.....	193
	References.....	194
	Curriculum vitae	205

List of abbreviations

2C STED	two-color STED
4-MU	4-methylumbelliferone
AM1	Austin Model 1
APTS	8-aminopyrene-1,3,6-trisulfonic acid
BC	benzylcytosine
BG	benzylguanidine
BODIPY	boron-dipyrromethene
BOPIM	boron 2-(2-pyridyl)imidazole
Cbz	carboxybenzyl
CT	charge transfer
DCC	<i>N,N</i> -dicyclohexylcarbodiimide
DFT	density functional theory
DIEA	diisopropylethylamine
DMABN	4- <i>N,N</i> -dimethylaminobenzonitrile
DMAP	4- <i>N,N</i> -dimethylaminopyridine
DMF	<i>N,N</i> -dimethylformamide
DMSO	dimethyl sulfoxide
DOL	degree of labeling
dppf	1,1'-bis(diphenylphosphino)ferrocene
DRET	dark resonance energy transfer
dSTORM	direct STORM
EDC	1-ethyl-3-(3-dimethylaminopropyl)carbodiimide
ESIPT	excited-state intramolecular proton transfer
(F)PALM	(fluorescence) photoactivation localization microscopy
Fmoc	fluorenylmethoxycarbonyl

FRET	fluorescence resonance energy transfer
GSD	ground state depletion
GSDIM	GSD followed by individual molecule return
HATU	<i>O</i> -(7-azabenzotriazol-1-yl)- <i>N,N,N',N'</i> -tetramethyluronium hexafluorophosphate
HOMO	highest occupied molecular orbital
HPLC	high performance liquid chromatography
IC	internal conversion
ICT	intramolecular CT
IR	infrared
ISC	intersystem crossing
LDA	lithium diisopropylamide
MAO	monoamine oxidase
<i>m</i> CPBA	<i>m</i> -chloroperbenzoic acid
NHS	<i>N</i> -hydroxysuccinimidyl
NIR	near-IR
ODF	oligodeoxyfluoroside
PA-FP	photoactivatable fluorescent protein
PBS	phosphate buffered saline
pcFRET	photochromic FRET
PET	photoinduced electron transfer
PPA	polyphosphoric acid
PTCA	perylene-3,4,9,10-tetracarboxylic acid
PVA	polyvinyl acetate
QY	quantum yield
RESOLFT	reversible saturable optical fluorescent transitions
RFI	relative fluorescence intensity
SMLM	single-molecule localization methods

SNAFL	seminaphthofluorescein
SNAFR	seminaphthorhodafluor
SNARF	seminaphthofluorone
SNP	single nucleotide polymorphism
SRS	stimulated Raman-scattering source
STED	stimulated emission depletion
STORM	stochastic optical reconstruction microscopy
TBAF	<i>tert</i> -butylammonium fluoride
TBDMS	<i>tert</i> -butyldimethylsilyl
TBET	through-bond energy transfer
TFA	trifluoroacetic acid
THF	tetrahydrofuran
THP	2-tetrahydropyranyl
TICT	twisted ICT
UV	ultraviolet

Introduction

Fluorescence microscopy has become an essential tool in modern life sciences. A vast majority (~80%) of all microscopy investigations is still performed with conventional lenses and visible light, despite the significant achievements made by electron and X-ray microscopies.^[1] Biological tissues are transparent to visible light to a great extent. This inherent property gives a unique advantage to fluorescent microscopy over other methods and provides the possibility of non-invasive imaging of the interior parts of cells in three dimensions. Furthermore, various cellular constituents, such as proteins, nucleic acids or lipids, can be detected specifically when fluorescence tagging is employed.

However, a fundamental physical barrier known as the Abbe diffraction limit restricts the resolution of conventional fluorescence microscopy (in the visible range of 400–800 nm) to about 200 nm in the focal plane. Hence, submicron scale cell structures (for example, cristae of a mitochondrion) cannot be resolved. Luckily, as a result of recent innovations, several new super-resolution techniques that fundamentally overcome the diffraction barrier have been developed. For their pioneering work in improving the resolution of fluorescent microscopes, Stefan W. Hell, William E. Moerner and Eric Betzig were awarded with Nobel Prize in Chemistry 2014.

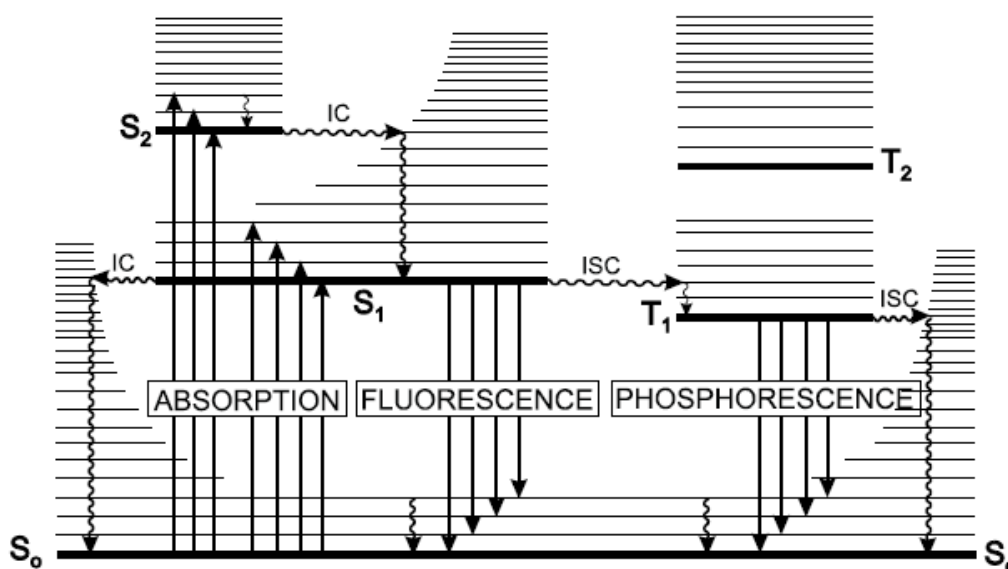
To obtain better results, these new microscopic methods often require more photostable fluorophores with higher binding specificity, greater brightness and an ability to switch between bright and dark states. Moreover, for multicolor imaging experiments, the spectral separation of different labels into two or more excitation or detection channels is required. In this regard, fluorophores with large Stokes shifts are particularly valuable, because they allow reducing the number of detection channels, avoiding cross-talk and simplifying the imaging scheme of a multicolor experiment. Unfortunately, photostable and bright fluorescent dyes with large Stokes shift are still rare and only a few of them are commercially available. Many suppliers offer fluorescent dyes and their conjugates with large Stokes shifts, but do not disclose their chemical structures and important photophysical properties. The lack of these data complicates the proper choice of the fluorescent dye for a particular imaging application. Furthermore, this also hampers the progress in basic research aimed at the creation of new fluorophores.

This work deals with the design and synthesis of new fluorophores with large Stokes shifts. The dissertation consists of two parts. The first part reviews the basic principles of super-resolution microscopy, the published data on large Stokes shift dyes and their use in super-resolution microscopy. The second part describes our own results and is further divided into four sections. In the first three sections, the synthesis of new coumarin-based dyes, their photophysical properties and application in super-resolution microscopy are described. The last section introduces new dyes – carborhodols, which represent asymmetric hybrids of fluorescein (or carbofluorescein) and carbopyronines. Owing to broader absorption and emission bands exhibited by carborhodols in comparison with parent carbopyronines or (carbo)fluoresceins, it was successfully used in two-color imaging as a large Stokes shift dye.

1 Physical background

1.1 Main principles of superresolution fluorescence microscopy

The processes associated with light absorption by a molecule can be conveniently illustrated by a Perrin-Jablonski diagram (see Scheme 1). It displays the relative positions of molecular energy levels and possible photophysical processes which follow the act of photon absorption. Thus, upon excitation, a molecule in the singlet ground state S_0 gains energy and enters one of the vibrationally excited levels of the singlet excited state S_1 . Since the energy gap between various vibrational levels is relatively small (in comparison to the gap between electronic states), the molecule undergoes a very fast (10^{-12} – 10^{-10} s) process of vibrational relaxation to the lowest vibrational level of S_1 . Afterwards, a few deactivation processes can take place. One of them is fluorescence, a radiative transition from the S_1 to one of the vibrationally excited levels of the ground state S_0 . After the very fast vibrational relaxation, the molecule occupies the ground state S_0 . The energy of the absorbed photon is higher than that of the emitted photon, and this explains the origin of the Stokes shift which is determined as a separation between the maxima of absorption and emission bands (usually measured in nm or cm^{-1}).



Scheme 1 Jablonski diagram: transitions between the ground and excited states and illustrating the origin and positions of absorption, emission, and phosphorescence bands.^[2]

Other deactivation processes are represented by internal conversion (IC) and intersystem crossing (ISC). Internal conversion is a nonradiative transition between two electronic states of the same spin multiplicity. This process can compete with other deactivation processes in solution where the excess energy can be transferred to the solvent through collisions of the excited molecule with the surrounding solvent molecules. Intersystem crossing is a nonradiative transition between two isoenergetic vibrational levels belonging to electronic states of different multiplicities. Formally, this process is forbidden and occurs slowly, unless there is a significant spin-orbit coupling. The presence of heavy atoms, such as Br, Se, I, Pb etc. increases spin-orbit coupling and therefore favors intersystem crossing. All deactivation processes reduce the probability of radiative $S_1 \rightarrow S_0$ transition and thus diminish the fluorescence QY. To obtain a large signal-to-noise ratio in fluorescence microscopy, fluorophores with large brightness (a product of extinction coefficient ϵ and fluorescence quantum yield Φ_{fl}) must be employed.

To obtain an image, the conventional confocal microscope – a standard tool in modern life sciences – rapidly scans a sample with a focused beam of light and collects emitted photons from all fluorescent species excited by this beam. According to the Abbe principle, light with wavelength λ , travelling in a medium with refractive index and converging with angle θ will make a spot of size d , described by Eq. 1.

$$d = \frac{\lambda}{2n\sin\theta} \quad \text{Eq. 1}$$

Objective lenses of modern microscopes have a semiaperture angle θ close to 67° , whereas the refractive index of common working media ranges from $n = 1.00$ (for air) to 1.52 (for immersion oil). If we illuminate the sample with green light having a wavelength of 500 nm, it will be impossible to focus light onto a spot smaller than 164 nm and resolve structures smaller than this spot. However, in many cases, a better optical resolution is desirable. For example, an adequate imaging and resolving of all parts of a nuclear pore complex of protein clusters is an extremely challenging task for fluorescence microscopy because of its small size (145 nm in diameter and 80 nm length^[3]) which is below the diffraction limit. Although electron microscopy provides better resolution, it is incompatible with live specimens and requires tedious preparation and fixation techniques, which can be destructive towards the features of interest.

Optical resolution of the light microscope considered to be limited by the diffraction limit for more than a century. However, after several super-resolution techniques have been established, the diffraction barrier was broken. The first of these techniques is stimulated emission depletion microscopy (STED).^[4] In the method of STED, a focused laser pulse excites fluorescence in a spot of a diffraction limited size (see Figure 1), and immediately after the excitation a red-shifted (to prevent re-excitation) doughnut-shaped STED beam is applied. It features zero intensity only at the very center and depletes the fluorescence of excited fluorophores on the periphery of the spot by stimulated emission ($S_1 \rightarrow S_0$).

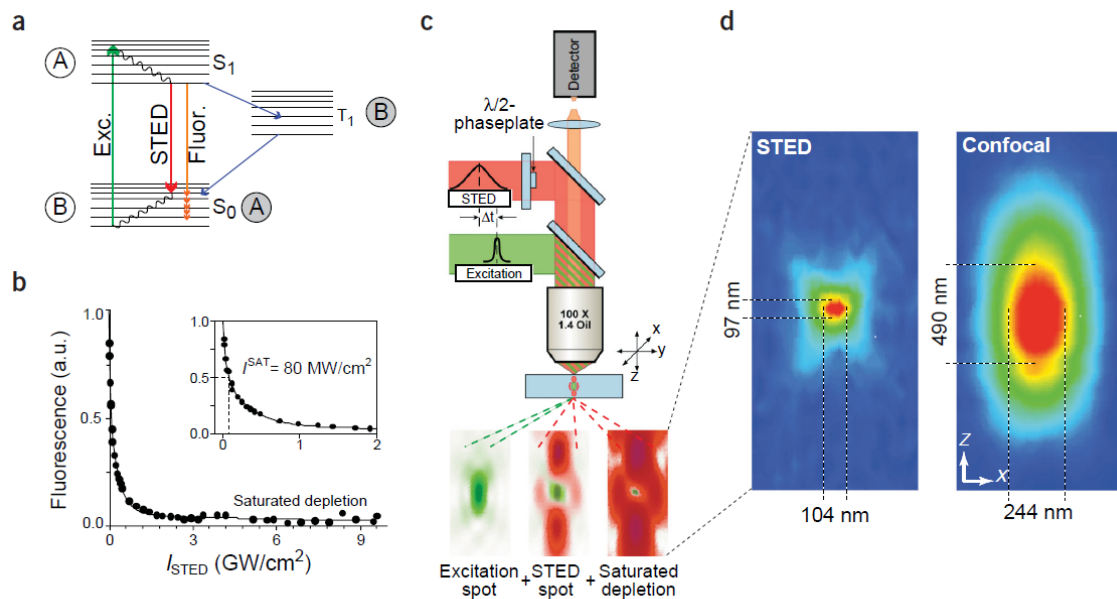


Figure 1 Physical conditions, setup and typical focal spot for STED:^[5] a) Energy diagram of an organic fluorophore. b) Saturated depletion of the excited state S_1 with increasing STED pulse intensity I_{STED} . c) Sketch of a point-scanning STED microscope. d) Fluorescent spot in the STED and in the confocal microscope.

In order to “squeeze” the central spot, the depletion rate should exceed the rate of spontaneous transition to the ground state S_0 . Typical values of fluorescence lifetimes for organic fluorophores ($\tau_{fl} \approx 10^{-9}$ s) and optical cross-sections for their $S_0 \rightarrow S_1$ transitions ($\sigma \approx 10^{-16} \text{ cm}^2$) imply that intensity of STED pulse $I_{STED} \gg I_S = (\sigma\tau_{fl})^{-1} \approx 10 \text{ MW}/\text{cm}^2$, where I_S is the effective saturation intensity which can be defined as the intensity at which probability of fluorescence is reduced by half. The optical resolution in STED is defined by Eq. 2.

$$d \approx \frac{\lambda}{2n \sin \theta \sqrt{1 + I_{STED}/I_S}} = \frac{d_C}{\sqrt{1 + I_{STED}/I_S}} \quad \text{Eq. 2}$$

The value d_C represents the resolution of a diffraction-limited system. According to Eq. 2, to obtain a significant improvement in resolution, very high pulse intensities I_{STED} should be applied. Such enormous light intensities ($>100 \text{ MW/cm}^2$) inevitably cause photobleaching of fluorophores, and therefore only highly photostable dyes are suitable for STED microscopy. In addition, to increase sensitivity and accordingly reduce imaging time, fluorophores with high fluorescence quantum yields are required.

Let us briefly consider the principles of another superresolution method – ground state depletion microscopy (GSD).^[6] In this method the triplet state T_1 of a fluorophore is used as a dark “off”-state B (see Figure 1a), instead of the ground state S_0 used in STED. Since lifetime of the triplet state T_1 is much longer than that of the singlet state S_1 , light intensities required for a saturable conversion of fluorophores to the triplet state T_1 are considerably smaller ($<10 \text{ KW/cm}^2$). However, not all molecules can be necessarily transferred to “dark” (triplet) states, and the fluorophores in the triplet (biradical) state, due to their long lifetimes and reactive nature of biradicals, can easily undergo various photochemical reactions which eventually lead to their bleaching. This problem is especially important in the presence of oxygen. Since the GSD parameters depend strongly on the nature of the fluorescent dyes and the environment, carefully chosen dyes and mounting media (oxygen scavengers) are required.^[7] Furthermore, wavelengths leading to excitation from T_1 to higher triplet states should be avoided.

The principles of STED and GSD microscopies were unified into the concept of reversible saturable optical fluorescent transitions (RESOLFT). This paradigm is applicable to all methods based on switching between two distinguishable and reversibly switchable, and thermally stable “bright” and “dark” states. Presumably, at least one transition between these states can be optically induced. The RESOLFT concept can be applied not only to transitions between electronic states, but also to various reversible photochemical transformations (isomerizations, cyclizations etc.). For example, in RESOLFT microscopy with photoswitchable fluorescent proteins,^[8] illumination with light of appropriate wavelength induces the E-Z isomerization of fluorescent proteins, which change their conformation, thus gaining or losing their ability to emit light. Low light intensities (a few W/cm^2) can be already sufficient to provide a full conversion and

overcome the diffraction barrier. The main disadvantage of reversibly switchable fluorescent proteins is their low fluorescence quantum yield. Therefore, for an acceptable image contrast, it is often necessary to use high protein concentrations. Moreover, formation of dimers and oligomers as well as moderate photostability can sometimes compromise biological imaging.^[9]

Along with photoswitchable proteins, photochromic organic compounds can also reversibly change their structure upon illumination. However, not many of them are fluorescent. This problem was circumvented in the method of photochromic energy transfer (pcFRET).^[10] In this method a combination of a photochromic and a fluorescent compound is used. One of the isomers of a photochromic compound absorbs visible light and is used as an energy acceptor for an excited fluorophore acting as a donor. As a result, the RESOLFT microscopy based on reversible switching of small fluorescent photochromic labels was implemented.^[11] Similarly to fluorescent proteins, only small light intensities are needed for efficient switching of photochromic compounds.

In comparison to RESOLFT techniques, where the position of the subdiffraction-sized emitting spot is known and well controlled, single-molecule localization microscopy (SMLM) methods rely on stochastic switching of single fluorophores. Stochastically distributed positions are sparse, contain only a small fraction of fluorophores in the bright state and do not overlap with each other, thus giving an opportunity to precisely localize these fluorophores using appropriate algorithms. It is important that at certain moment the distances between the “activated” (bright) markers are greater than the diffraction-limited distances (~ 200 nm), so that these markers can be localized and detected independently (separately). The localization precision (Δloc) depends on the number of collected photons N as defined by Eq. 3 (where Δ is the full width at half maximum of the point spread function).

$$\Delta loc \approx \frac{\Delta}{\sqrt{N}} \quad \text{Eq. 3}$$

Photoactivatable fluorescent protein (PA-FP) molecules that are initially found in a dark (non-fluorescent) state can be either reversibly or irreversibly activated by irradiation at one wavelength, and then can be visualized by excitation at a second wavelength. In a technique called (fluorescence) photoactivation localization microscopy ((F)PALM),^[12] a

sample with target proteins fused with PA-FPs is continuously excited by pulses of light from a laser at a wavelength close to the excitation maximum of the PA-FPs. The excitation is maintained until a large population of inactivated PA-FPs is obtained by reversible “bleaching”, thus creating sparse fields of individually resolvable single molecules. After recording several image frames (individual images), the “bleaching” process leads to a mean molecular separation larger than that needed for isolation of individual molecules which are still in the active state. At this point, a pulse from another laser at a shorter wavelength capable of reactivating the PA-FPs molecules from the inactive state is applied. The pulse duration and intensity is chosen so that the population of active PA-FPs is increased to higher, but still resolvable level. The process of “bleaching”, activation and recording is repeated many times ($>10^4$), until the whole set of inactivated molecules is used up. The signals from every molecule are summed across all recorded frames and then fitted using a mathematical algorithm giving position coordinates of the molecule and a standard deviation of this position. A final super-resolved image is rendered usually by representing each molecule as a two-dimensional Gaussian with the amplitude proportional to the number of collected photons and the standard deviation which depends on the localization precision. Genetically encoded labeling used in (F)PALM easily circumvents problems caused by unspecific binding. It is also compatible with live-cell imaging. However, fluorescent proteins often exhibit lower photon counts than organic dyes, and therefore, it can be difficult sometimes to obtain the full super-resolved image.

Another SMLM technique, stochastic optical reconstruction microscopy (STORM),^[13] is based on a similar fundamental principle as (F)PALM. However, instead of endogenously expressed PA-FPs, STORM relies on immunolabeling of the sample with antibodies tagged with optically switchable organic fluorophores. Originally, a pair of cyanine dyes, Cy3 and Cy5, known as “cyanine switch” was used. Cy3 served here as an “activator” that facilitates the transition of Cy5 to the “on”-state. The imaging procedure is pretty similar to that of (F)PALM: first, a red laser switches nearly all fluorophores to a stable dark state, and then a pulse of a green laser switches a small and random number of fluorophores to the “on”-state, and a frame is taken. This procedure is repeated many times, and at the end of the whole sequence, individual frames are processed and merged into a final image.

The necessity of double labeling of antibodies with activator-reporter pairs poses certain problems. To circumvent these problems, the so-called direct STORM (dSTORM)

method was proposed.^[14] In this technique, a green laser with a power 200 times higher than that in STORM was used. It efficiently turns a small subset of inactivated fluorophores (single dyes) to the bright state. A laser with a higher power made possible to use conventional and commercially available dyes (Cy5 and similar ones) making the experiment and sample preparation much easier than in the original STORM method.

In comparison to (F)PALM, organic fluorophores in (d)STORM allow obtaining a brighter stain and thus, a better image quality. However, as all techniques which rely on labeling with tagged antibodies, (d)STORM is also vulnerable to background noise caused by non-specific binding.

In addition to (F)PALM and STORM another super-resolution method was proposed. In ground state depletion microscopy followed by individual molecule return (GSDIM),^[15] stochastic single-molecule “on”-switching is performed without any photochemical transformation and relies only on basic transitions of standard markers. This technique operates using the same mechanism employed in GSD microscopy, i.e. transferring a synthetic dye to its triplet state T_1 (or another metastable dark state). But unlike GSD, GSDIM implies that a fluorophore recovers to its ground state S_0 only once. Images of the emitters are recorded, only when they spontaneously return to the ground state.

For the highest precision in localization, the number of emitted photons per switching cycle should be maximized (see Eq. 3). The relative brightness is proportional to the product of the molar extinction coefficient ϵ and the fluorescence quantum yield Φ_f of the fluorophore. For (F)PALM and STORM, fluorescent probes should also exhibit high switching reliability, high efficiency of transition to the “dark” state and a low fatigue rate. Furthermore, the reversible photobleaching and photoactivation rates should be balanced in a way that only a small fraction of fluorophores is activated at any particular time.

The image acquisition time in SMLM methods is defined by the number of the determined molecular positions needed for the reconstruction of the final image. Due to the intrinsic stochastic nature of all these methods it will be always not clear whether all positions of molecules have been recorded or not. This issue (when the image acquisition has to be stopped) is particularly important in live-cell imaging where the recording speed is crucial. In contrast to SMLM, in RESOLFT-type microscopy (including STED) the speed of the scanning process defines the acquisition time. The use of fast beam scanners

allowed recording of a $4.5 \mu\text{m}^2$ field of view with a focal spot size of 62 nm at video rates (STED with 28 frames per second).^[16] Moreover, there is a great potential in parallelization of the scanning procedure. In a recent report,^[17] it has been shown that RESOLFT microscopy can be effectively parallelized using two incoherently superimposed orthogonal standing light waves. The intensity minima of the resulting pattern act as more than 100 000 “doughnuts”. As a result, superresolution images of living cells in $12000 \mu\text{m}^2$ fields of view can be recorded in less than 1s using fluorescent proteins with a relatively slow switching kinetics.

One of the main advantages of fluorescent microscopy is the ability to use several fluorescent labels to target different specimens and produce multicolor images that help to identify many structural features of biological objects and interactions between them. Two-color STED (2C STED) using two separate sets of excitation and STED wavelengths for spectrally separated dyes has been reported.^[18] However, this approach is technically demanding. Another approach^[19] uses a standard fluorophore with a small Stokes shift (10-30 nm) in combination with a large Stokes shift (usually more than 80 nm) dye which have (partially) overlapping emission spectra. Two excitation wavelengths for two dyes are used to distinguish them. At the same time, due to similar emission spectra, only one STED beam can be used.

The common feature of many fluorescent dyes with large Stokes shifts is their relatively low brightness and poor photostability. These drawbacks limit their wide use in modern methods of optical microscopy, especially in STED nanoscopy. The present work deals with the design and synthesis of new bright and photostable fluorophores with large Stokes shift. In the following sections, common photophysical mechanisms providing large Stokes shifts as well as common classes of large Stokes shift dyes and their use in the imaging applications will be discussed.

1.2 Large Stokes shift fluorophores

1.2.1 Fluorophores with a Stokes shift provided by photophysical processes

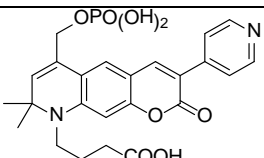
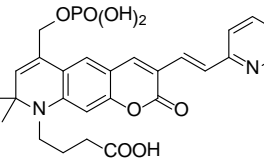
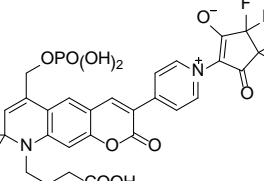
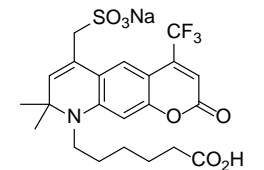
Upon excitation of a molecule, movements of electrons occur so fast (in ca. 10^{-15} s), that the atom nuclei in the molecule remain nearly stationary. In other words, the molecular geometry does not change in the course of absorption of a photon (Franck-Condon principle). However, the newly formed vibronic state is unstable, and the molecule quickly relaxes (in ca. 10^{-13}) to its equilibrium vibronic state. During this process, a part of the absorbed energy turns into heat. Similar transitions occur during emission. After a “fluorescence” photon is emitted, the molecule is found in the electronic state S_0 which retains the geometry of the excited state S_1 . After vibrational relaxation, a part of the energy of the absorbed photon is again converted into heat. Thus, the initially absorbed energy of a photon is partially converted to heat in the course of absorption and emission processes. In most cases, the dipole moment of a fluorophore in the excited state differs from that in the ground state. Therefore, after excitation, the solvent molecules that surround a molecule of the fluorophore undergo relaxation, leading to a relaxed excited state of lower energy. With increasing solvent polarity, the energy of the relaxed state becomes lower. As a result, the emission spectrum exhibits a red-shift. Geometrical relaxation and relaxation of the solvent media are two photophysical processes responsible for the generation of the Stokes shift. Therefore, in order to increase a Stokes shift, one should design molecules with large differences between equilibrated geometries and dipole moments in the ground and excited states.

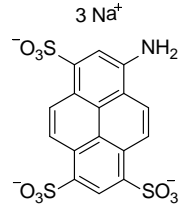
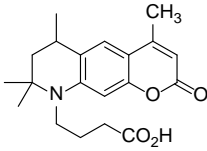
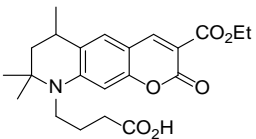
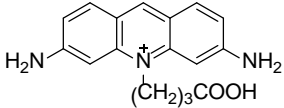
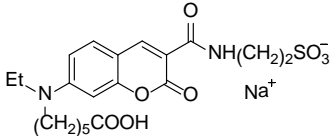
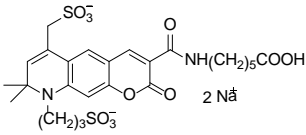
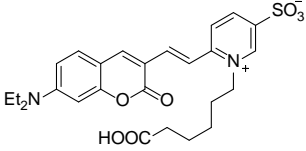
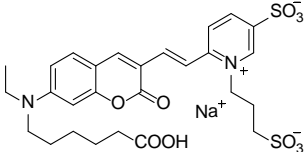
Unfortunately, these differences are difficult to predict, and the design of new fluorophores still remains mostly a matter of trial and error. Despite the significant advances in quantum-mechanical methods, it is still impossible to predict accurately all important properties of fluorescent dyes, such as band shapes and maxima of absorption and emission spectra in different solvents, Stokes shifts, molar extinction coefficients and fluorescence quantum yields. Therefore, when designing a new fluorophore, synthetic chemists often rely on the known data for similar dyes and general empirical guidelines. For example, in the case of fluorophores exhibiting intramolecular charge transfer (ICT) upon excitation, stronger or weaker acceptors and/or donors, or new π -systems can be introduced to the core fluorophore in order to “tune” the “push-pull” effect or expand the conjugation system of the fluorophore, thus providing bathochromic and bathofluoric shifts and increasing the molar extinction coefficient. However, regularities concerning the positions of these substituents at the dye scaffold are still unclear. A useful report

generalizing the structure-property relationships and providing detailed guidelines for the design of certain classes of fluorophores has been published recently.^[20]

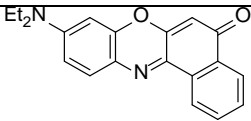
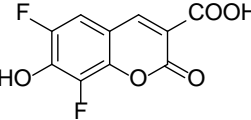
There is no general theory that could explain structure-property relationships, and it is difficult to design and prepare a new fluorophore with required properties. Only a few fluorophore classes, such as cyanine dyes, coumarins, rhodamines (xanthene dyes), carbo-pyronines, BODIPYs, Si-rhodamines and their hybrids have been widely used in life sciences. Among fluorescent dyes with large Stokes shift, coumarins (and hybrid dyes based on coumarins) are very important. Almost all commercially available fluorophores with large Stokes shifts with $\lambda_{\text{exc}} \geq 400$ nm contain a coumarin fragment (see Table 1). A few notable exceptions are represented by Lucifer Yellow and Atto dyes, 430LS and 490LS. Other dyes with large Stokes shifts include benzoxazole or triphenylpyrazoline derivatives. Although these dyes have good fluorescence quantum yields, they require UV light for excitation, which is often incompatible with imaging of biological samples.

Table 1 Selected commercially available dyes with large Stokes shift and with $\lambda_{\text{abs,max}} > 390$ nm.

Name	Structure	$\lambda_{\text{abs,max}}$, nm	$\lambda_{\text{em,max}}$, nm	ϵ , $\text{M}^{-1}\text{cm}^{-1}$	Φ_{fl}	τ_{fl} , ns	solvent
Abberior STAR 440SXP		436	515	22700	0.68	3.3	PBS
Abberior STAR 470SXP		472	624	29000	0.12	0.8	PBS
Abberior STAR 520SXP		522	632	42500	0.15	–	PBS
Alexa Fluor 430		431	541	16000	0.55	–	H ₂ O

Name	Structure	$\lambda_{\text{abs,max}}$, nm	$\lambda_{\text{em,max}}$, nm	ϵ , $\text{M}^{-1}\text{cm}^{-1}$	Φ_{fl}	τ_{fl} , ns	solvent
APTS		424	505	20000	–	–	H ₂ O
ATTO 390		390	479	24000	0.90	5.0	H ₂ O
ATTO 425		436	484	45000	0.90	3.6	H ₂ O
ATTO 465		453	508	75000	0.75	5.0	H ₂ O
ATTO 430LS	–	433	547	32000	0.65	4.0	PBS
ATTO 490LS	–	496	661	40000	0.30	2.6	PBS
Chro-meo 494	–	494	628	55000	–	–	PBS
DY-418		418	467	34000	–	–	EtOH
DY-431		442	496	35000	–	–	PBS
DY-480XL		500	630	50000	–	–	EtOH
DY-481XL		515	650	50000	–	–	EtOH

Name	Structure	$\lambda_{\text{abs,max}}$, nm	$\lambda_{\text{em,max}}$, nm	ϵ , $\text{M}^{-1}\text{cm}^{-1}$	Φ_{fl}	τ_{fl} , ns	solvent
DY-485XL		482	560	48000	–	–	H ₂ O
DY-510XL		493	585	40000	–	–	H ₂ O
DY-511XL		510	595	47000	–	–	EtOH
DY-520XL		520	664	50000	–	2.1	EtOH
DY-521XL		523	668	50000	–	–	EtOH
DY-601XL		606	663	85000	–	–	EtOH
DyLight 485-LS	Coumarin	485	559	50000	–	–	EtOH
DyLight 510-LS	Coumarin	509	590	50000	–	–	EtOH
DyLight 515-LS	Coumarin	519	648	50000	–	–	EtOH
DyLight 521-LS	Coumarin	526	666	50000	–	–	EtOH
Krome Orange	-	398	528	17665	–	–	H ₂ O
Lucifer Yellow CH		428	540	11500	0.21	–	H ₂ O

Name	Structure	$\lambda_{\text{abs,max}}$, nm	$\lambda_{\text{em,max}}$, nm	ϵ , $\text{M}^{-1}\text{cm}^{-1}$	Φ_{fl}	τ_{fl} , ns	solvent
Nile Red		552	636	43000	–	–	MeOH
Pacific Blue		400	447	29500	0.75	–	PBS
Pacific Green	–	410	500	–	–	–	H ₂ O
Pacific Orange	–	400	551	–	–	–	H ₂ O
V500	–	415	500	–	–	–	–

Coumarin itself (Figure 2) shows no fluorescence at room temperature and has only a weak absorption in the near UV region, but if C-6 or/and C-7 is substituted with an electron-donor group (such as hydroxyl or amino group), an intense blue-green emission appears. It originates due to a “push-pull” effect between the electron-donor group(s) at C-6(7) and the electron-withdrawing lactone moiety. 7-Hydroxy- and 7-aminocoumarins have a long history as laser dyes.^[21]

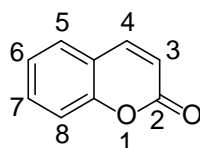


Figure 2 Coumarin (2*H*-chromen-2-one) and its atom numbering.

4-Methyl-7-hydroxycoumarin or 4-methylumbelliferone (4-MU) has the most red-shifted absorption band with a maximum at 360 nm ($\epsilon = 17000 \text{ M}^{-1}\text{cm}^{-1}$ in aqueous phosphate buffer at pH 10) and emits blue light with a maximum centered at 450 nm ($\Phi_{\text{fl}} = 0.63$, Stokes shift of 90 nm).^[22] Due to presence of the ionizable hydroxyl group with ($\text{pK}_{\text{a}} = 7.8$), the spectra of 4-MU are sensitive to pH changes. Fluorination of the 4-methylumbelliferone scaffold has minor effects on the absorption and fluorescence spectra, but fluorinated derivatives have higher fluorescence QYs and better photostability. In contrast, 7-hydroxy-4-trifluoromethylcoumarins have significantly lower QYs

than the parent compound. The hydroxyl group is slightly acidic, and it is ionized in basic solution. Therefore such compounds are soluble in water. However, if 7-hydroxycoumarins contain electron acceptor groups at C-3 or C-4, the fluorescence of their solutions rapidly fades out (due to decomposition).^[21b] 7-Hydroxycoumarins are emissive only in their anionic forms, and this makes them unattractive for applications at physiological pH values: these compounds will be neutral and, therefore, nonfluorescent. A great improvement is 6,8-difluoro-7-hydroxycoumarin (Pacific Blue^[22]) with a reduced pK_a of 3.7. The greater acidity makes this dye predominantly anionic at physiological pH. However, the anionic nature of this fluorophore is undesirable in some cases.^[23]

Introduction of acceptor aryl groups at C-3 of 7-hydroxy- or 7-aminocoumarins provides bathochromic and bathofluoric shifts, but, at the same time, significantly increases the rate of ISC. As a result, their fluorescent QYs decrease. These compounds can be used as efficient triplet sensitizers.^[24]

A “red” spectral shift and a higher acidity of 7-hydroxycoumarins were achieved by introducing electron-withdrawing groups at C-3 of the coumarin ring.^[25] Table 2 contains the spectral data for 7-hydroxycoumarins **1–9** and 4-cyano-7-hydroxycoumarins **10–14** with various substituents at C-3 (Figure 3). In aqueous borate buffer (pH 9), the spectra of compounds **1–7**, which have a heterocyclic residue at C-3 and an unsubstituted position 4, have an intense absorption band in the 405–439 nm range and an emission maximum between 470 and 500 nm. Compounds **8** and **9** with carboxylic and phenyl substituents at C-3 absorb and emit at shorter wavelengths ($\lambda_{\text{abs,max}}/\lambda_{\text{em,max}} = 386/448$ nm and 383/462 nm, respectively). Particularly remarkable is 7-hydroxy-2-thienylcoumarin **7** which has the most red-shifted fluorescence maximum (500 nm) and the largest Stokes shift (93 nm) in this group. The introduction of a 4-cyano group at C-4 results in considerable bathochromic and bathofluoric shifts (compared with the corresponding 4-unsubstituted analogs). All 3-substituted 4-cyano-7-hydroxycoumarins (compounds **10–14**) have absorption maxima in the range between 487 and 505 nm and exhibit bright yellow-orange fluorescence in basic aqueous solutions (except compound **14** with a 2-benzimidazolyl substituent which showed weak fluorescence). Interestingly, the benzazole-substituted 4-cyano-7-hydroxycoumarins retain large Stokes shifts typical for coumarin dyes. Closely related compounds were used as polarity-sensitive indicators of biochemical processes.^[26]

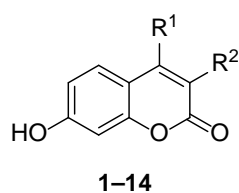


Figure 3 Substituted 7-hydroxycoumarins **1–14**.

Table 2 Spectral data of 7-hydroxycoumarins **1–9** and 4-cyano-7-hydroxycoumarins **10–14** with various substituents at C-3 in aqueous borate buffer at pH 9.

Compound	R ¹	R ²	$\lambda_{\text{abs,max}}$, nm	ϵ , M ⁻¹ cm ⁻¹	$\lambda_{\text{em,max}}$, nm	$\Delta\lambda^{\text{a}}$, nm
1	H	2-benzoxazolyl	427	44300	471	44
2	H	2-benzothiazolyl	439	47000	490	51
3	H	5-methyl-7-sulfonato-2-benzoxazolyl	431	44000	470	39
4	H	5-chloro-2-benzoxazolyl	425	30600 ^b	472	47
5	H	2-benzimidazolyl	427	33000 ^b	479	52
6	H	2-furyl	405	26300 ^b	489	84
7	H	2-thienyl	407	25000 ^b	500	93
8	H	COOH	386	15300 ^b	448	62
9	H	Phenyl	383	26100	462	79
10	CN	2-benzoxazolyl	494	33200	577	83
11	CN	2-benzothiazolyl	505	33100	595	90
12	CN	5-methyl-7-sulfonato-2-benzoxazolyl	494	23000 ^b	577	83
13	CN	5-chloro-2-benzoxazolyl	497	32400	577	80

Compound	R ¹	R ²	$\lambda_{\text{abs,max}}$, nm	ϵ , M ⁻¹ cm ⁻¹	$\lambda_{\text{em,max}}$, nm	$\Delta\lambda^{\text{a}}$, nm
14	CN	2-benzimidazolyl	487	25400 ^b	593 ^c	106

^aStokes Shift, ^bin MeOH, ^cweak fluorescence

Deligeorgiev et al.^[27] prepared the 3-(2-benzothiazolyl)-7-hydroxycoumarin **15** with a sulfonic acid residue ($\sigma_p = 0.09$ ^[28] in the Hammett equation) at C-6 (Figure 4). In aqueous solution, this coumarin ($\lambda_{\text{abs,max}} = 398$ nm) shows an absorption spectrum with a maximum shifted hypsochromically by 41 nm as compared with the analogous non-sulfonated compound **2** in aqueous borate buffer at pH 9. In contrast, the position of the fluorescence maximum ($\lambda_{\text{em,max}} = 487$ nm) stays virtually unchanged, and, as a result, this compound possesses a much larger Stokes shift of 89 nm. In coumarins **16** and **17**, extension of the coumarin skeleton by a benzene ring fused to C-5 and C-6 resulted in bathochromic (~20 nm) and bathofluoric (13 and 27 nm, respectively) shifts. The fluorescence QYs for sulphocoumarins **15–17**, in water, range from 0.28 for compound **15** to rather low values of ~0.12 for benzo[*f*]coumarins **16** and **17**.

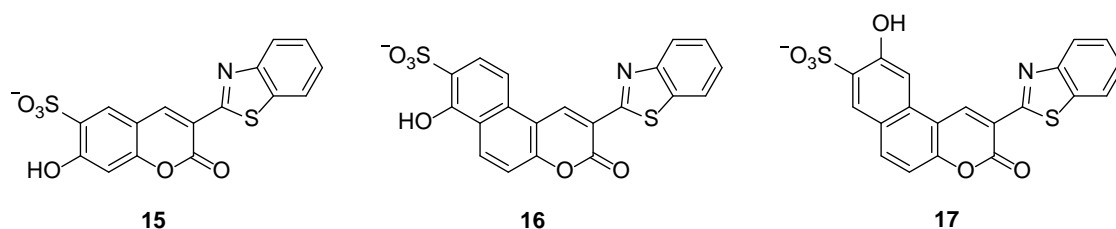


Figure 4 3-Benzothiazolylhydroxycoumarins **15–17** with sulphonic acid residues

The absorption spectra of 7-hydroxy-3-pyridylcoumarins **18–20** (Figure 5a) have an intense band with maxima located between 388 and 398 nm in aqueous NaHCO₃ (see Table 3). Upon excitation, these compounds emit intense blue light with a maximum at 469–471 nm. Remarkably, the spectra are weakly influenced by the attaching point in the pyridyl substituent and resemble those exhibited by 7-hydroxy-3-phenylcoumarin **9**. This result indicates the lack of strong direct conjugation between the coumarin and pyridine rings.^[29] Quaternization of the pyridine nitrogen causes pronounced bathochromic and bathofluoric shifts in the spectra of the 4-pyridyl isomer **23** (51 and 50 nm, respectively). In the case of 2- and 3-pyridyl isomers quaternized derivatives **21** and **22** displayed only small bathochromic shifts (~20 nm). According to the report,^[29] in the case of the 2-iso-

mer **21** steric constraints may prevent the formation of a planar π -electron system, whereas for the 3-isomer **22** no mesomeric stabilization is possible. Fluorescence efficiency of quaternized derivatives in aqueous solutions is very low. In contrast to them, quaternized 7-methoxy-3-pyridylcoumarins exhibit much stronger fluorescence. The authors assumed,^[29] that the ICT excited states of quaternized 7-hydroxy-3-pyridylcoumarins are better described by a corresponding quinoid structure (Figure 5b) which is expected to show intense phosphorescence at the expense of fluorescence.

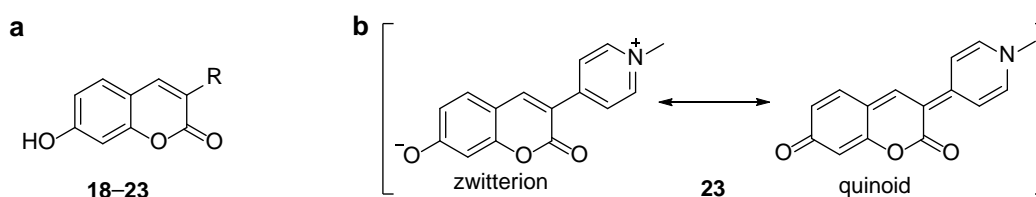


Figure 5 a) 3-Pyridyl-7-hydroxycoumarins **18–23**; b) Zwitterion- and quinoid-type resonance structures of compound **23**.

Table 3 Absorption and fluorescence maxima of 7-hydroxy-3-pyridylcoumarins and their quaternized derivatives in aq. solution of NaHCO_3 .^[29]

Compound	R	$\lambda_{\text{abs,max}}$, nm	ϵ , $\text{M}^{-1}\text{cm}^{-1}$	$\lambda_{\text{em,max}}$, nm	$\Delta\lambda^a$, nm
18	2-pyridyl	394	29000	469	75
19	3-pyridyl	388	26800	470	82
20	4-pyridyl	398	31700	471	73
21	1-methyl-2-pyridinio	414	32700	477	63
22	1-methyl-3-pyridinio	409	29400	472	63
23	1-methyl-4-pyridinio	449	38000	521	72

Similar tendencies were observed in the case of 7-aminocoumarins.^[30] Quaternized 4-pyridylcoumarins **25** and **26** (Figure 6) exhibited the most red-shifted absorption and emission spectra at 482–493 nm and 560–585 nm, respectively, and large Stokes shifts of 78 and 92 nm, whereas coumarin **24** with the 2-pyridinium fragment ($\lambda_{\text{abs,max}}/\lambda_{\text{em,max}} =$

440/494 nm) showed unchanged spectral properties in comparison to those of the non-quaternized analog.

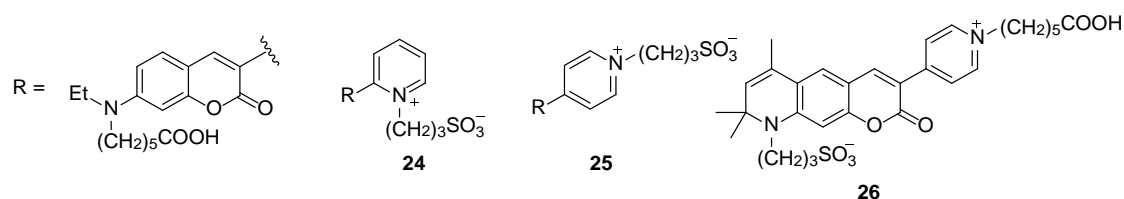


Figure 6 7-*N,N*-Dialkylamino-3-pyridiniumcoumarins **24–26**.

In an attempt to develop NIR fluorophores insensitive to thiols and suitable for the imaging of living systems, Richard et al.^[31] designed a series of water-soluble 7-hydroxycoumarin-hemicyanine hybrids **27–31** (see Figure 7). The extension of the conjugation in the aromatic system of the parent 7-hydroxycoumarin resulted in dramatic bathochromic and bathofluoric shifts. Thus, in aqueous phosphate buffer (pH 7.4), compounds **27**, **28** and **31** with one double bond ($n = 1$) between 7-hydroxycoumarin and indolium moieties have the absorption and emission maxima at 555–578 nm and 620–643 nm, respectively (Stokes shifts of 63–65 nm). Extension of the conjugation chain by an additional double bond ($n = 2$) had a little effect on the absorption spectra. Absorption maxima of compounds **29** and **30** are found at 564 and 592 nm, respectively. On the other hand, fluorescence spectra turned out to be more sensitive to the number of the double bonds between the coumarin and indolium fragments: emission maxima of **29** and **30** are shifted to 720 and 722 nm, respectively, and located already in the IR region of the visible spectrum (this corresponds to large Stokes shifts of 156 and 130 nm). However, despite their attractive spectral properties, fluorescence QYs in aqueous media are very low (<7.8%).^[31] The introduction of additional negatively charged sulfonate groups preventing dye-dye interactions did not solve the problem of low fluorescence QYs.

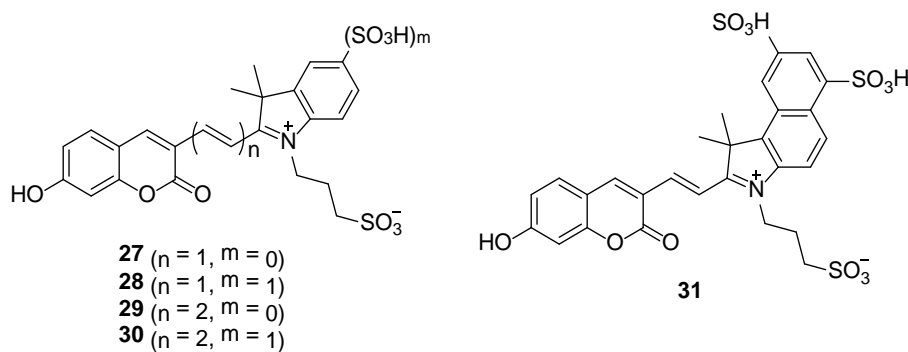
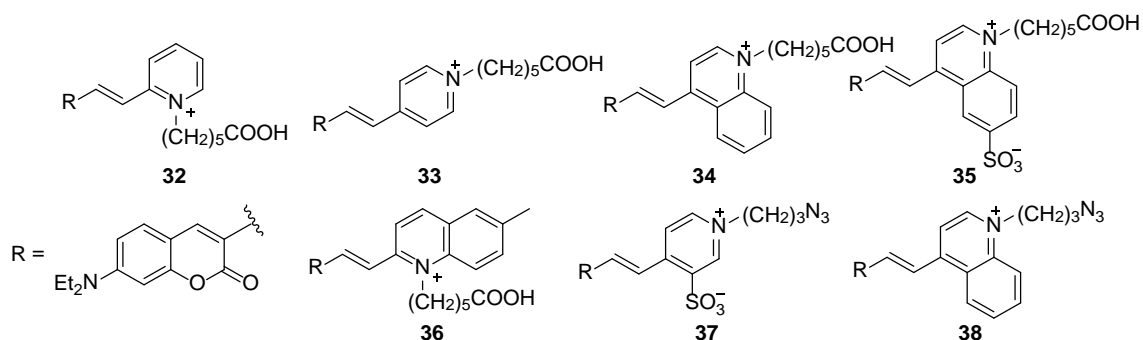


Figure 7 7-Hydroxycoumarin-hemicyanine hybrids **27–31**.

Dyomics GmbH used the same approach and designed similar 7-aminocoumarins as “Megastokes”-series of fluorescent dyes.^[30] 7-Diethylaminocoumarin-hemicyanine hybrid DY-601XL (Table 1) have the most red-shifted absorption maximum (606 nm in EtOH) in this series and emitted in the near-IR region with a Stokes shift of 57 nm ($\lambda_{\text{max,em}} = 663$ nm). The introduction of a *trans*-double bond between C-3 of the coumarin skeleton and the pyridinium moiety shifted the absorption to 480 nm (in EtOH) in the case of the 2-pyridinium substituent (compound **32**, Figure 8) and to 500 nm (in EtOH) in the case of the 4-pyridinium substituent (compound **33**) in comparison to corresponding analogs without the inserted double bond (coumarins **24** and **25**). In commercial dyes DY-480XL and DY-520XL, the introduction of a sulfonic acid residue on the pyridine rings resulted in an additional ~20 nm bathochromic shift. The presence of the sulfonate groups have an even more pronounced bathofluoric effect on the fluorescence spectra: thus, compounds **32** and **33**, which have no sulfonate groups, emit at 600 and 630 nm (Stokes shifts of 120 and 130 nm), respectively, whereas DY-480XL and DY-520XL – at 630 and 664 nm (Stokes shifts of 130 and 144 nm) in EtOH. The replacement of the pyridinium fragment with a quinolinium moiety in compounds **34–36** further shifted the absorption and fluorescence spectra towards the IR region and increased Stokes shifts to huge values of up to 160 nm (see Table 4 for further details). Closely related “clickable” fluorophores **37** and **38** were proposed for applications in (bio)orthogonal labeling schemes.^[32]

Figure 8 7-*N,N*-Diethylamino-3-vinylcoumarins **32–38**.Table 4 Spectral properties of 7-dimethylamino-3-vinylcoumarins **32–38**.

Compound	$\lambda_{\text{abs,max}}$, nm	ε , $\text{M}^{-1}\text{cm}^{-1}$	$\lambda_{\text{em,max}}$, nm	$\Delta\lambda^{\text{a}}$, nm	Solvent
32	480	–	600	120	EtOH
33	500	–	630	130	EtOH
34	540	–	695	155	MeOH
35	555	–	715	160	MeOH
36	520	–	655	135	MeOH
37 ^[32c]	544	53000	675	131	PBS
38 ^[32d]	549	27000	712	158	MeOH

In contrast to 7-hydroxycoumarins, 7-aminocoumarins do not exhibit significant pH sensitivity and are highly fluorescent over a wide range of pH values in their neutral forms. Methods of their synthesis and their photophysical properties were reviewed.^[33] The parent compound 7-aminocoumarin has the main band at 380 nm ($\varepsilon = 18000 \text{ M}^{-1}\text{cm}^{-1}$) in water and the emission maximum at 444 nm ($\Phi_{\text{fl}} = 0.55$ ^[34], Stokes shift of 64 nm). Amino groups, in particular if they are not or only partially alkylated are capable of forming hydrogen bonds with molecules of water. Therefore, simple 7-aminocoumarins are slightly soluble in water.^[21b] Absorption and emission maxima of 7-aminocoumarins slightly shift to longer wavelengths upon increasing the degree of alkylation of

the amino group.^[21a] A larger shift toward the red can be obtained through substitution with heteroaryl and trifluoromethyl groups in positions 3 and 4, respectively. Thus, the 4-trifluoromethyl group in laser dyes **39** (Coumarin 151) and **40** (Coumarin 307) provides bathochromic (28 and 29 nm, respectively, in EtOH) and bathofluoric (50 and 55 nm) shifts relative to analogous compounds **41** (Coumarin 120) and **42** (Coumarin 2) in the same solvent (see Figure 9). In addition, the introduction of a trifluoromethyl group at C-4 was found to reduce photobleaching by 20% in coumarin dyes.^[21c] The benzothiazole group in dye **47** (Coumarin 6) causes even larger shifts of 85 nm (in the absorption maximum) and 60 nm (in the emission maximum) and increases the extinction coefficient as compared with compound **44** (Coumarin 1).

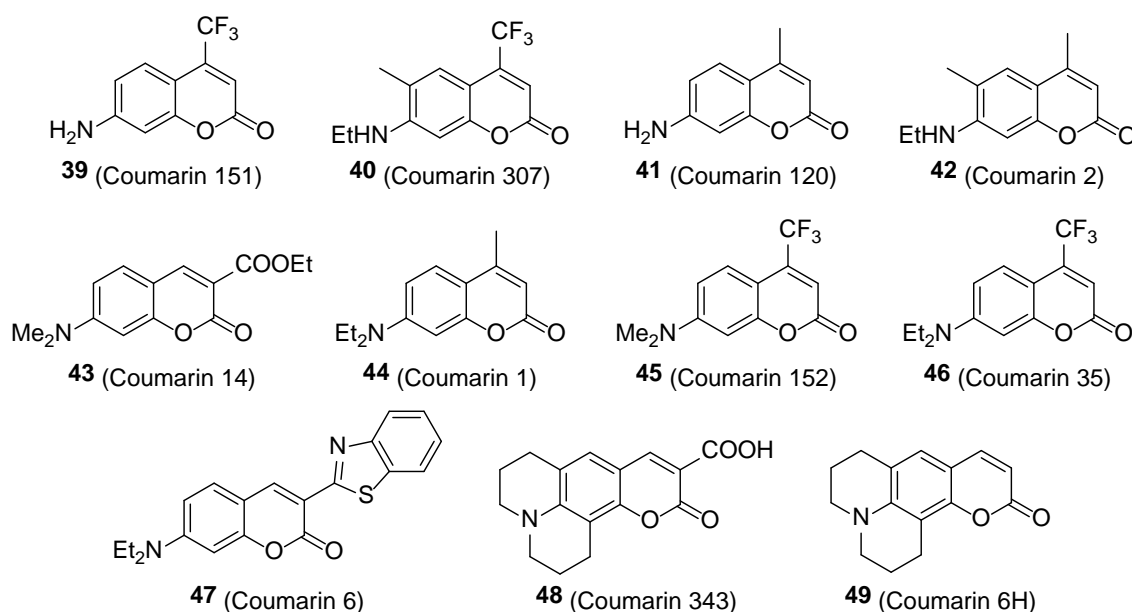


Figure 9 Coumarin laser dyes **39–49**.

As a rule, aminocoumarins have lower fluorescence efficiencies in highly polar solvents. This reduction is particularly sharp if the amino group at the position 7 is dialkylated (such amino groups cannot form hydrogen bonds with solvent molecules). It turns out that upon exciting the dyes with less rigid geometries, the rotation of the amino function facilitates an internal conversion of the initial ICT state to a non-emissive twisted charge-transfer (TICT) state with full charge separation (see Figure 10).^[21d, 21e, 21g, 35] This state is stabilized by electron-withdrawing groups at C-3 or C-4 and by electrostatic interaction with molecules of a polar solvent. As a result, coumarins **43**, **45** and **46** have poor fluorescence QYs in aqueous and alcoholic media. As expected, rigidization of the amino group

by incorporation into one or two six-membered rings as in compounds **48** and **49** led to a considerable improvement of the fluorescence efficiency, since in this case excitation yields a normal planar ICT state. It was also found that there is no need for rigidization if the amino group carries only one alkyl group. The rigidized amino groups are more strongly electron-donating than dimethyl- or diethylamino groups, therefore they shift absorption and emission bands further to longer wavelengths. The absorption and emission maxima of laser dye **48** (Coumarin 343) with a carboxylic group at C-3 shift 40 nm towards the blue upon addition of a base, which is consistent with a less withdrawing ability of carboxylate compared with non-ionized carboxylic group.^[21a]

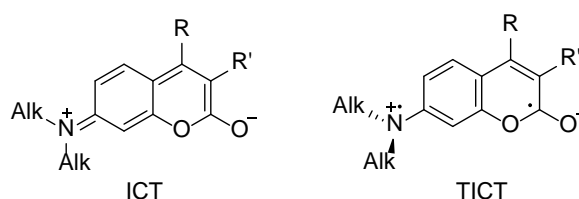


Figure 10 “Normal” intramolecular charge transfer (ICT) and twisted intramolecular charge transfer (TICT) excited states of 7-*N,N*-dialkylaminocoumarins.

To investigate the influence of the substitution at C-3 in laser dye **49** (Coumarin 6H) on lasing characteristics, coumarins **50–58** were prepared.^[21f] Variation of the functional group at C-3 from H to phenyl and other residues caused a red shift in wavelengths of the absorption and fluorescence maxima. Benzazole substituents (compounds **50–52** in Table 5) provided the largest bathochromic shift, but at the same time reduced the Stokes shift almost by a factor of two relative to the unsubstituted compound **49**. Phenyl and pyridyl substituents (compounds **54, 56–58**) moderately shifted absorption and emission bands toward the red spectral region retaining relatively large values of Stokes shifts (60–78 nm). Sulfonyl groups in coumarins **53** and **55** had an effect on spectral properties which is between the effects of the benzoxazolyl and pyridyl substituents.

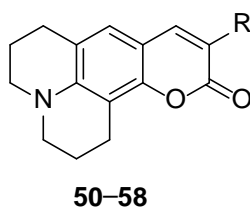
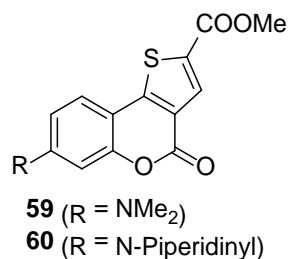


Figure 11 3-Substituted analogs of laser dye Coumarin 6H **50–58**.

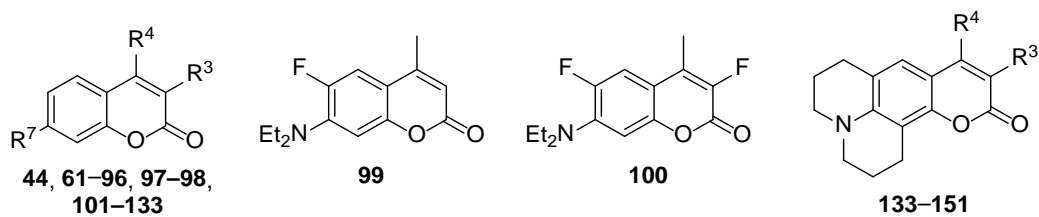
Table 5 Spectral properties of coumarins **49–58** in aq. EtOH (1:1).

Compound	R	$\lambda_{\text{abs,max}}$, nm	$\lambda_{\text{em,max}}$, nm	$\Delta\lambda$, nm	Φ_{fl}
49	H	404	488	84	0.96
50	2-benzimidazolyl	473	512	39	1.00
51	2-benzothiazolyl	490	526	36	0.96
52	2-benzoxazolyl	474	512	38	0.89
53	methylsulfonyl	442	488	46	0.87
54	phenyl	424	502	78	0.95
55	phenylsulfonyl	450	492	42	1.00
56	2-pyridyl	442	502	60	0.88
57	3-pyridyl	433	506	73	0.98
58	4-pyridyl	445	508	63	0.88

7-Aminothiено[3,2-*c*]coumarins (see Figure 12) contain a thiophene ring fused along positions 2 and 3 with the coumarin scaffold. The fused compounds **59** and **60** absorb violet light with maxima at 404 and 395 nm and emit blue light at 480 and 486 nm with large quantum efficiencies (0.82 and 1.00, respectively) in MeCN.^[36] The Stokes shifts (76 nm and 91 nm) were found to be somewhat larger than the Stokes shift for 7-diethylamino-4-methylcoumarin (63 nm^[21g]) in the same solvent.

Figure 12 7-Aminothiено[3,2-*c*]coumarins.

Replacement of the methyl group at C-4 in compounds **44** and **151** with an amino group led to coumarins **61–69**, **134** and **135** (see Figure 13 and Table 6), and this was accompanied by a hypsochromic shift in the absorption bands by 10–15 nm and by a hypsofluoric shift of the emission bands by approximately 20–30 nm.^[37] The authors explained this phenomenon with an increased charge transfer along the conjugation chain $4-R \rightarrow C(4)=C(3)$ which opposes the main conjugative interaction in the system $7-NR_2 \rightarrow C(2)=O$. Interestingly, substitution of the 4-monoalkylamino group by a more electron-donating 4-dialkylamino group in a transition series from compounds **62–65**, **70** and **71** to coumarins **66–69** and **72–74** induces a bathochromic shift of the absorption band by 7–19 nm, although the transition from 4-aminocoumarin **61** to 4-*N*-monoalkylaminocoumarins **62–65** does not produce any significant influence. According to the report, the reason for this discrepancy is the steric interaction between the 4-dialkylamino group and the 5-H atom which weakens p- π conjugation in the N-C(4)=C(3)-C(2)=O system. This effect is even more pronounced when the alkyl groups form a ring as in compounds **68** and **69**. Their absorption maxima are further bathochromically shifted by approximately 10 nm in comparison to coumarins **66** and **67**. Introduction of a 3-alkyl substituent further increases the steric hindrance and has a similar effect on the absorption maximum. Thus, compounds **70–74** have the main absorption bands shifted bathochromically by 6–13 nm compared to **63**, **64** and **69**. The positions of emission bands are influenced by similar effects as are the absorption spectra. One important exception is compound **62** which has a fluorescence maximum shifted by 30 nm towards longer wavelengths compared to compounds **63–65**. This behavior was attributed to steric hindrance between the *t*-butyl group and the 3-H atom in the excited state S₁ of coumarin **62**. Therefore, the degree of conjugation between the 4-substituent and the rest of the molecule is reduced. Dialkylamino groups possess greater vibrational degrees of freedom in comparison with morpholine, piperidine and monoalkylamino groups. This increases the probability of energy dissipation from the S₁ along nonradiative pathways. As a consequence, 4-*N,N*-dialkylaminocoumarins **66**, **67** and **76** exhibit lower emission efficiencies in EtOH than their analogs **61–65**, **68–75** and **77**.

Figure 13 Substituted 7-aminocoumarins **44**, **61**–**151**.Table 6 Spectral properties of coumarins **44**, **61**–**151** in EtOH.

	R ³	R ⁴	R ⁷	$\lambda_{\text{abs,max}}$, nm	$\lambda_{\text{em,max}}$, nm	$\Delta\lambda$, nm	Φ_{fl}
44	H	Me	NEt ₂	377	455	78	0.68
61	H	NH ₂	NEt ₂	350	410	60	0.58
62	H	NH <i>t</i> Bu	NEt ₂	349	445	96	0.62
63	H	NHCy	NEt ₂	349	414	65	0.67
64	H	NHBn	NEt ₂	350	410	60	0.68
65	H	NHCH ₂ CH ₂ OH	NEt ₂	349	412	63	0.63
66	H	NEt ₂	NEt ₂	356	440	84	<0.10
67	H	NBu ₂	NEt ₂	358	440	82	0.15
68	H	<i>N</i> -piperidyl	NEt ₂	365	447	82	0.36
69	H	<i>N</i> -morpholyl	NEt ₂	365	445	80	0.70
70	Cy	NHCy	NEt ₂	363	440	77	0.33
71	Bn	NHBn	NEt ₂	356	435	79	0.31
72	Et	<i>N</i> -morpholyl	NEt ₂	375	465	90	0.39
73	Cy	<i>N</i> -morpholyl	NEt ₂	376	464	88	0.76
74	Bn	<i>N</i> -morpholyl	NEt ₂	378	466	88	0.65

	R^3	R^4	R^7	$\lambda_{\text{abs,max}}$, nm	$\lambda_{\text{em,max}}$, nm	$\Delta\lambda$, nm	Φ_{fl}
75	H	<i>N</i> -morpholyl	<i>N</i> -pi-peridyl	360	455	95	0.49
76	H	NEt ₂	<i>N</i> -morpholyl	344	440	96	<0.10
77	H	<i>N</i> -morpholyl	<i>N</i> -morpholyl	350	450	100	0.31
78	Cl	Me	NEt ₂	388	476	88	0.81
79	Br	Me	NEt ₂	390	478	88	0.51
80	Cl	H	NEt ₂	398	485	87	0.69
81	Br	H	NEt ₂	400	482	82	0.50
82	I	H	NEt ₂	400	–	–	–
83	Cl	NHBn	NEt ₂	365	450	85	0.32
84	Br	NHBn	NEt ₂	365	450	85	0.23
85	Cl	<i>N</i> -morpholyl	NEt ₂	384	476	92	0.22
86	Br	<i>N</i> -morpholyl	NEt ₂	386	480	94	0.10
87	I	<i>N</i> -morpholyl	NEt ₂	391	–	–	–
88	Cl	Cl	NEt ₂	402	490	88	0.10
89	Br	Cl	NEt ₂	405	490	85	<0.10
90	I	Cl	NEt ₂	406	–	–	–
91	Cl	CH(COCH ₃) ₂	NEt ₂	405	490	85	0.41
92	Br	CH(COCH ₃) ₂	NEt ₂	408	490	82	0.24
93	I	CH(COCH ₃) ₂	NEt ₂	408	–	–	–

	R ³	R ⁴	R ⁷	$\lambda_{\text{abs,max}}$, nm	$\lambda_{\text{em,max}}$, nm	$\Delta\lambda$, nm	Φ_{fl}
94	Cl	Me	NH ₂	368	457	89	0.61
95	Br	Me	NH ₂	370	460	90	0.56
96	I	Me	NH ₂	380	–	–	–
97	F	H	NEt ₂	382	485	103	0.59
98	F	Me	NEt ₂	376	476	100	0.75
99	H	Me	NEt ₂	368	450	82	<0.10
100	F	Me	NEt ₂	362	480	118	<0.10
101	CHO	H	NEt ₂	446	494	48	<0.10
102	CHO	Me	NEt ₂	436	490	54	<0.10
103	CHO	Cl	NEt ₂	449	502	53	<0.10
104	CHO	<i>N</i> -morpholyl	NEt ₂	409	475	66	<0.10
105	CHO	NHBn	NEt ₂	379	460	81	<0.10
106	CHO	Cl	<i>N</i> -morpholyl	435	500	65	<0.10
107	CHO	<i>N</i> -morpholyl	<i>N</i> -morpholyl	392	480	88	<0.10
108	H	<i>N</i> -imidazolyl	NEt ₂	394	480	86	<0.10
109	H	<i>N</i> -benzimidazolyl	NEt ₂	399	480	81	<0.10
110	H	diethylamino-methyl	NEt ₂	379	468	89	<0.10
111	H	piperidin-1-ylmethyl	NEt ₂	382	465	83	<0.10

	R ³	R ⁴	R ⁷	$\lambda_{\text{abs,max}}$, nm	$\lambda_{\text{em,max}}$, nm	$\Delta\lambda$, nm	Φ_{fl}
112	H	morpholin-4-yl- methyl	NEt ₂	384	470	86	0.35
113	H	imidazol-1-yl- methyl	NEt ₂	378	480	102	0.28
114	H	benzimidazol-1- yl-methyl	NEt ₂	385	480	95	0.22
115	<i>N</i> -piperidyl	Me	NEt ₂	378	490	112	<0.10
116	<i>N</i> -morpholyl	Me	NEt ₂	377	480	103	<0.10
117	NH ₂	Me	NEt ₂	398	490	92	0.95
118	Ph	H	NEt ₂	401	484	83	0.92
	Ph	H	NEt ₂	397	480	83	0.73 ^a
119	Ph	Me	NEt ₂	383	475	92	0.86
120	<i>p</i> -tolyl	Me	NEt ₂	384	468	84	0.75
121	<i>o</i> -tolyl	Me	NEt ₂	383	454	71	1.00
122	<i>p</i> -phenoxy- phenyl	Me	NEt ₂	385	464	79	0.95
123	<i>p</i> -chlorophenyl	Me	NEt ₂	388	472	84	0.53
124	<i>o</i> -chlorophenyl	Me	NEt ₂	385	462	77	0.92
125	<i>p</i> -fluorophenyl	Me	NEt ₂	386	465	79	0.97
126	<i>o</i> -fluorophenyl	Me	NEt ₂	384	475	91	0.78
127	<i>p</i> -cyanophenyl	Me	NEt ₂	394	485	91	0.70
128	<i>o</i> -cyanophenyl	Me	NEt ₂	393	475	82	0.66

	R ³	R ⁴	R ⁷	$\lambda_{\text{abs,max}}$, nm	$\lambda_{\text{em,max}}$, nm	$\Delta\lambda$, nm	Φ_{fl}
129	Ph	<i>N</i> -morpholyl	NEt ₂	382	470	88	<0.10
130	Ph	Cl	NEt ₂	397	490	93	<0.10
131	Ph	CF ₃	NEt ₂	415	545	130	<0.10
132	β -styryl	H	NEt ₂	421	477	56	0.85 ^a
133	H	H	NEt ₂	380	462	82	0.29
134	H	NEt ₂	–	372	467	95	0.89
135	H	<i>N</i> -morpholyl	–	382	466	84	1.00
136	Cl	Me	–	404	495	91	0.95
137	Br	Me	–	404	485	81	0.65
138	I	Me	–	406	–	–	–
139	Cl	Cl	–	424	500	76	<0.10
140	Br	Cl	–	420	500	80	<0.10
141	I	Cl	–	423	–	–	–
142	F	H	–	392	505	113	0.72
143	F	Me	–	403	495	92	0.83
144	CHO	H	–	469	510	41	0.48
145	CHO	Me	–	454	508	54	0.81
146	CHO	Cl	–	468	520	52	<0.10
147	H	<i>N</i> -imidazolyl	–	415	495	80	0.63
148	H	morpholin-4-yl- methyl	–	400	490	90	1.00

	R ³	R ⁴	R ⁷	$\lambda_{\text{abs,max}}$, nm	$\lambda_{\text{em,max}}$, nm	$\Delta\lambda$, nm	Φ_{fl}
149	H	imidazol-1-yl- methyl	–	400	500	100	0.83
150	H	<i>N</i> -morpholyl	–	398	490	92	0.95
151	H	Me	–	394	474	80	0.86

^ain MeCN

The introduction of a halogen atom into the position 3 of the 7-aminocoumarin scaffold causes small bathochromic shifts of 10–25 nm relative to the corresponding unsubstituted coumarins.^[38] The absorption spectra of coumarins **78–93** and **136–141** (Table 6) are not very sensitive to the nature of the halogen atom at C-3. In the row from chlorine to iodine, the absorption maximum varies within a small interval ($\Delta\lambda = 0–5$ nm). However, emission bands of 3-chloro- and 3-bromocoumarins **78–81**, **83–86**, **88**, **89**, **91**, **92**, **94**, **95**, **136**, **137**, **139** and **140** are shifted bathofluorically by 10–45 nm compared with their analogs without the substituent at C-3. As expected, due to the quenching effect of the heavy atom, fluorescence efficiency drops in the series Cl → Br → I. Interestingly, the chlorine at C-3 in compounds **78**, **80**, **91**, **94**, and **136**, which have a hydrogen or alkyl substituent at C-4, enhances the fluorescence intensity compared to the analogous 3-unsubstituted coumarins. In contrast, in the case of coumarins **83**, **85**, **88** and **139**, substituents exhibiting positive mesomeric effects (amino groups or chlorine) at C-4 quench the emission. A decrease in the electron-donating ability of the substituent at C-4 in the series NHBn → N(CH₂CH₂)₂O → Me → H → Cl → CH(COCH₃)₂ is accompanied by bathochromic and bathofluoric shifts.

In comparison to other 3-halo-7-aminocoumarins, 3-fluoro derivatives (**97**, **98**, **142**, **143**) have the long-wavelength absorption maximum hypsochromically shifted by approximately 15 nm, thus resembling the spectral characteristics of 3-unsubstituted analogs.^[39] In the series of halogens, the fluorine atom participates most effectively in p- π conjugation, hindering the charge transfer from the 7-amino group to the pyrone ring in the ground state. The emission maxima of 3-fluorocoumarins nearly coincide with the fluorescence maxima of the corresponding 3-chlorocoumarins; and this means that 3-fluorocoumarins have larger Stokes shifts (92–113 nm). Fluorescence QYs of 7-amino-3-

fluorocoumarins in EtOH are high. However, the introduction of a fluorine atom into the position 6 in compounds **99** and **100** results in a significant decrease of emission efficiency.

The main absorption maximum of 7-amino-3-formylcoumarins (**101–107** and **144–146**) is shifted by 30–70 nm towards the red region of the visible spectrum compared with the analogous 3-unsubstituted 7-aminocoumarins.^[40] All coumarins in this series, except **144** and **145** with the julolidine fragment, exhibit weak fluorescence in EtOH and MeCN ($\Phi_{fl} < 0.10$). Decrease in the emission efficiency in case of coumarins with a rotating 7-amino group (**101–107**) can be attributed to the formation of TICT state which is stabilized by the strongly electron-withdrawing formyl group. The observed Stokes shifts were relatively small (41–54 nm) for compounds **101–103**, **106** and **144–146** with “small” substituents at C-4 (H, Me and Cl). On the other hand, bulky substituents, such as NHBn and *N*-morpholyl in coumarins **104**, **105** and **107** provided larger Stokes shifts (66–88 nm) which are more common for coumarin dyes.

Introduction of *N*-imidazolyl and *N*-benzimidazolyl fragments into the position 4 of the coumarin skeleton (compounds **108**, **109** and **147**) is accompanied by bathochromic (14–21 nm) and bathofluoric shifts (14–20 nm) in absorption and emission spectra in EtOH, respectively (as compared with 4-unsubstituted analogs).^[41] Additionally, the presence of *N*-heteroaryl residues leads to a significant decrease in the fluorescence QYs, which is most pronounced in the case of 7-*N,N*-diethylaminocoumarins **108** and **109**. The separation of the heteroaromatic fragments by a methylene group in compounds **110–114**, **148** and **149** is accompanied by a hypsochromic shift of 10–15 nm compared with compounds without the methylene group (**66**, **68**, **69**, **108**, **109**, **147** and **150**) and has virtually no effect on the location of the fluorescence maximum. The transition from coumarins **108**, **109** and **147** to coumarins **113**, **114** and **149** is also accompanied by an increase in emission intensities.

In the absorption spectra of compounds **118–128**, the position of the long-wavelength absorption band depends relatively weakly on the nature of the substituent on the phenyl ring.^[42] There is only a small (<10 nm) bathochromic shift of this spectral band in the transition from the electron-donating (Me, OPh) to electron-withdrawing groups (F, Cl, CN) in the *ortho*- or *para*-position. This indicates the presence of only a weak π - π conjugation between the aromatic substituent and the coumarin core. Another evidence for the

weak electronic interactions between 3-aryl groups and the rest of the fluorophore is illustrated by the similarity of the spectral properties of 3-phenyl derivatives **118** and **119** with those of the related 7-*N,N*-diethylaminocoumarin **133** and 7-*N,N*-dimethylamino-4-methylaminocoumarin **44** which have no aryl group at C-3. The position of the absorption maximum is affected more substantially by the nature of the 4-substituent. The increase in electron-withdrawing properties of the substituent series *N*-morpholyl – Me – Cl – H – CF₃ at C-4 is accompanied by a red-shift of the main absorption maximum of more than 30 nm. The fluorescence spectra are significantly more sensitive to the effects of the substituents. Thus, in EtOH, compounds **118–131** emit in the region of 460–545 nm. Compounds **118–128** exhibit particularly strong fluorescence. For coumarins **123–128**, the bathofluoric shift of the fluorescence maximum in the transition from the *ortho*- to the *para*-substituted derivatives amounts to 10–15 nm. In 7-*N,N*-diethylamino-3-(β -styryl)coumarin **132**, the presence of the *trans*-configured double bond leads to a bathochromic shift of 24 nm and has virtually no influence on the position of the fluorescence maxima and the value of the fluorescence QY^[43] as compared to 7-diethylamino-3-phenylcoumarin **118**.

Takechi et al.^[44] prepared 3-azolyl-7-*N,N*-diethylaminocoumarins **152–179** (Table 7) and studied the influence of the heterocycle nature and its substitution pattern on spectral properties. Thus, in EtOH, all the compounds exhibited red-shifts of the absorption (10–60 nm) and emission (3–35 nm) maxima combined with an increase in molar absorptivities (up to 1.7 times) compared to reference compound 7-*N,N*-diethylamino-3-phenylcoumarin **118** ($\lambda_{\text{abs,max}} = 398$ nm, $\lambda_{\text{flu,max}} = 477$ nm). The relative fluorescence intensity (RFI) turned out to be similar or even higher (up to 1.93 times) than that of the reference coumarin **118** (RFI = 1.00), except for 3-(1,3-thiazol-4-yl)- and 3-(1,3,4-oxadiazol-2-yl)-substituted compounds **172–175**. According to the magnitude of bathochromic and hyperchromic* shifts, heteroaromatic substituents can be arranged in the following order: 1,3,4-thiadiazol-2-yl (48 nm) > 1,3-thiazol-2-yl (39 nm) > 1,3,4-oxadiazol-2-yl (31 nm) > 1,3-oxazol-2-yl (26 nm). Values of the fluorescence maximum and the RFI exhibit a tendency to decrease in the order 1,3-thiazol-2-yl (495 nm, 1.42) \geq 1,3,4-thiadiazol-2-yl (494 nm, 1.01) > 1,3-oxazol-2-yl (481 nm, 1.02) \geq 1,3,4-oxadiazol-2-yl (480 nm, 0.35). The values of $\lambda_{\text{flu,max}}$ of coumarins with diazole substituents are similar to those of coumarins with

* Hyperchromic shift is an increase in the absorbance.

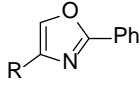
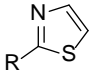
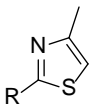
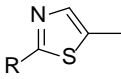
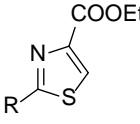
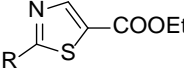
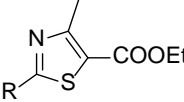
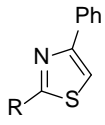
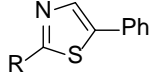
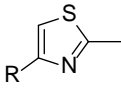
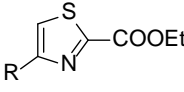
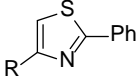
azole residues, but the presence of an additional nitrogen substantially decreases the emission intensity. The influence of 1,3-thiazolyl and 1,3,4-thiadiazolyl groups on the spectral properties is larger than the influence of the corresponding 1,3-oxazolyl and 1,3,4-oxadiazolyl groups. Authors^[44] suggested the sulfur lone pair in thiazoles is more delocalized than that of the oxygen in oxazole giving rise to a more effective π - π conjugation between the thiazole substituent and the coumarin ring. Furthermore, the low-lying *d* orbitals of the sulfur may also play an additional role in the conjugation. As a result, thiazole-containing compounds absorb and emit at longer wavelengths than the corresponding oxazole analogs.

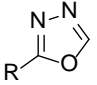
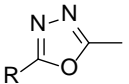
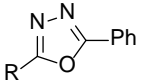
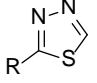
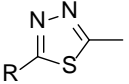
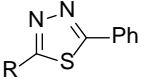
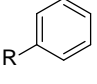
For regioisomeric 3-(phenyl-1,3-oxazolyl)coumarins **157**, **158**, **161** and **162** (see Table 7) the values of the $\lambda_{\text{abs,max}}$, $\lambda_{\text{flu,max}}$ and ϵ decrease in order: 5-phenyl-1,3-oxazol-2-yl (437 nm, 498 nm, 47300 M⁻¹cm⁻¹, respectively) > 2-phenyl-1,3-oxazol-5-yl (433 nm, 492 nm, 46900 M⁻¹cm⁻¹) > 4-phenyl-1,3-oxazol-2-yl (428 nm, 488 nm, 47300 M⁻¹cm⁻¹) > 2-phenyl-1,3-oxazol-4-yl (411 nm, 476 nm, 38800 M⁻¹cm⁻¹). The RFI decreased in the order: 2-phenyl-1,3-oxazol-5-yl (1.43) > 5-phenyl-1,3-oxazol-2-yl (1.32) > 4-phenyl-1,3-oxazol-2-yl (1.21) > 2-phenyl-1,3-oxazol-4-yl (1.15). The similar trends were observed for the corresponding sulfur analogs.

Variation of substituents in position 4 and 5 of the thiazole ring in 3-(1,3-thiazol-2-yl)coumarins **163–167**, **169** and **170** revealed that the values of $\lambda_{\text{abs,max}}$, $\lambda_{\text{flu,max}}$ and ϵ decreased in the order COOEt > Ph > Me > H in both 4- and 5-thiazole-substituted derivatives. Thus, an ethoxycarbonyl group at C-4 and C-5 of the thiazole has the largest influence on the absorption and fluorescence properties, whereas a methyl group has almost no or only a little effect. Moreover, the influence of an ethoxycarbonyl or a phenyl substituent at C-5 was greater than the effect of the same substituent at C-4 (due to the better push-pull effect between the 7-amino group of the coumarin and the electron-withdrawing group of the azole).

Table 7 Spectral properties of 7-*N,N*-diethylaminocoumarins with azole substituents at C-3 in EtOH.

Compound	$\lambda_{\text{abs,max}}$, nm	ϵ , $\text{M}^{-1}\text{cm}^{-1}$	$\lambda_{\text{em,max}}$, nm	$\Delta\lambda$, nm	RFI	
152		424	41100	481	57	1.02
153		425	42800	484	59	1.15
154		430	45200	483	53	0.96
155		443	48700	494	51	1.23
156		442	49700	493	51	1.49
157		428	43100	488	60	1.21
158		437	47300	498	61	1.32
159		422	40500	480	58	1.25
160		447	47900	504	57	1.45
161		433	46900	492	59	1.43

Compound	$\lambda_{\text{abs,max}}$, nm	ε , $\text{M}^{-1}\text{cm}^{-1}$	$\lambda_{\text{em,max}}$, nm	$\Delta\lambda$, nm	RFI
162 	411	38800	476	65	1.15
163 	437	45100	495	58	1.42
164 	437	45500	496	59	1.40
165 	439	45500	493	54	1.40
166 	449	50200	494	45	1.52
167 	463	60100	512	49	1.93
168 	463	59000	508	45	1.93
169 	441	46400	498	57	1.47
170 	453	54100	511	58	1.47
171 	408	38900	475	67	1.16
172 	418	39900	473	65	0.05
173 	412	40100	477	65	0.72

Compound	$\lambda_{\text{abs,max}}$, nm	ϵ , $\text{M}^{-1}\text{cm}^{-1}$	$\lambda_{\text{em,max}}$, nm	$\Delta\lambda$, nm	RFI
174 	429	44300	480	51	0.35
175 	428	44300	481	53	0.47
176 	437	50800	488	51	1.02
177 	446	48600	494	48	1.01
178 	446	48600	493	47	1.23
179 	458	58500	502	44	1.86
118 	398	34200	477	79	1.00

Regarding the synthetic routes leading to various 3-substituted coumarins, we conclude that many of them rely on the modern Pd-catalyzed C-C cross-couplings such as Suzuki, Heck and Sonogashira reactions applied to 3-halocoumarins.^[45] These transformations allow the introduction of arene, ethynylene and ethenylene moieties to the coumarin skeleton in one synthetic step. Taking advantage of these reactions and utilizing a combinatorial synthetic approach, Schiedel et al.^[46] prepared a compound library consisting of 34 coumarins with various substitution patterns. The “hits” (best dyes) were selected on the basis of fluorescence QYs and the possibility of further modifications (for applications as fluorescent labels). Thus, compound **180** (Figure 14) combines a very large Stokes shift of 162 nm ($\lambda_{\text{abs,max}}/\lambda_{\text{flu,max}} = 373/535$ nm, in EtOH) with a moderate quantum yield ($\Phi_{\text{fl}} = 0.18$), compounds **181** (395/478 nm), **182** (393/480 nm) and **183** (397/455 nm) have the highest emission efficiencies of 0.90, 0.62 and 0.98 in EtOH, respectively. Remarkably, compound **183** exhibited a higher fluorescence QY than the similar and

commercially available Coumarin 120 (**41**) (354/435 nm, $\Phi_{\text{fl}} = 0.88$, in EtOH). The 7- NH_2 -substituted compounds **180**, **182** and **183** can be linked to the biomolecule of interest through their modified amino groups.

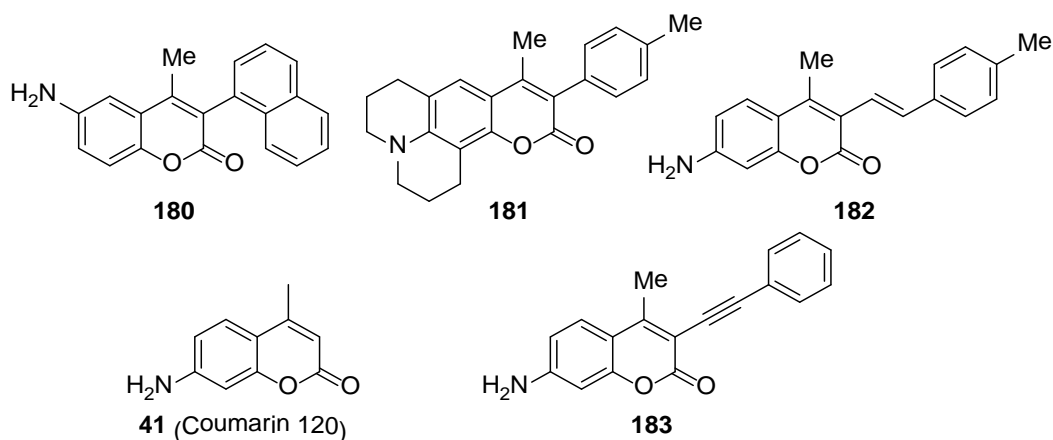


Figure 14 Coumarins prepared by a combinatorial method from 3-halocoumarins.

Another dye library was obtained by a “click” reaction of 3-azidocoumarins with various substituted alkynes.^[47] 7-Aminosubstituted coumarins exhibited strong fluorescence in EtOH (QYs 0.6–0.7) and a rather small dependence on the nature of the substituent attached to C-4 of the triazolyl ring. Thus, all 24 investigated 7-diethylaminocoumarins **184-R** (see Figure 15) have absorption and emission maxima in the narrow intervals 413–418 nm and 484–489 nm in aq. DMSO, respectively. Analogously, the absorption and emission bands of 7-aminocoumarins **185-R** with the julolidine fragment are grouped around 431–436 nm and 503–509 nm in aq. EtOH, respectively.

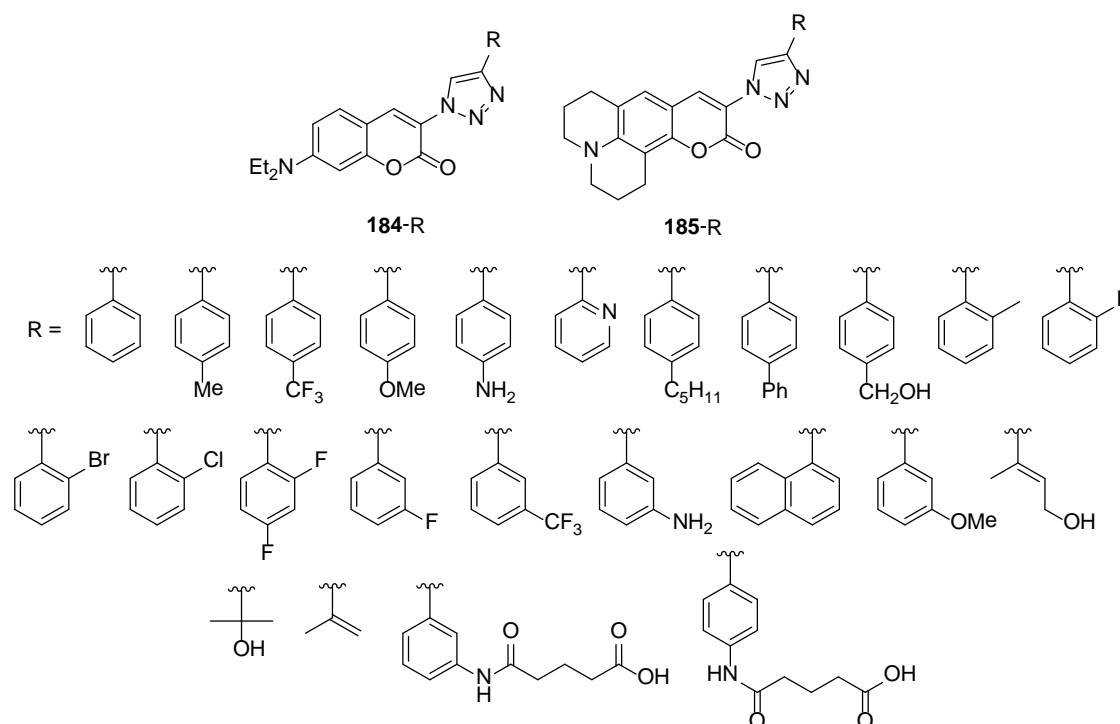


Figure 15 7-Amino-3-(1,2,3-triazol-1-yl)coumarins prepared by a combinatorial method.

Another series of coumarin dyes (Figure 16) was studied in order to evaluate the influence of various nitrogen-containing groups in position 7 on the optical spectra.^[48] The nitrogen atom incorporated into a piperidine fragment in compound **189-H** has a somewhat greater electron-releasing ability in comparison to the pyrrolidine-fused coumarin **188-H**. In ethanolic solutions, this results in a small bathochromic (8 nm) and a bathofluoric (4 nm) shift in the transition from compound **188-H** ($\lambda_{\text{abs,max}}/\lambda_{\text{flu,max}} = 370/440$ nm) to **189-H** (378/444 nm). The highest occupied molecular orbital (HOMO) of pyrrole has a node at the nitrogen atom. Therefore, the connection of an *N*-pyrrolyl moiety at C-7 of the coumarin diminishes π - π conjugation between the pyrrole and coumarin systems and decreases the extent of the ICT in the excited state of compounds **186-R** and **187-H** in comparison to 7-aminocoumarins. As a result, for compounds **186-H** ($\lambda_{\text{abs,max}} = 329$ nm), **186-F** ($\lambda_{\text{abs,max}} = 342$ nm) and **187-H** ($\lambda_{\text{abs,max}} = 316$ nm) relatively large hypsochromic shifts (24–40 nm) were observed, relative to the corresponding 7-amino-3-methyl- or 7-amino-3-trifluoromethylcoumarin (compounds **41** and **39**, respectively). Carbazole-coumarin hybrids **190-R** and **191-R** absorb in the near-UV region with a maximum at 353–376 nm and emit in the blue and green regions of the visible spectra. Notably, compounds **191-F** and **192-F** with the 4-trifluoromethyl group provide the

largest Stokes shifts of 163 and 124 nm. However, their emission intensities in EtOH are very low (less than 0.02).

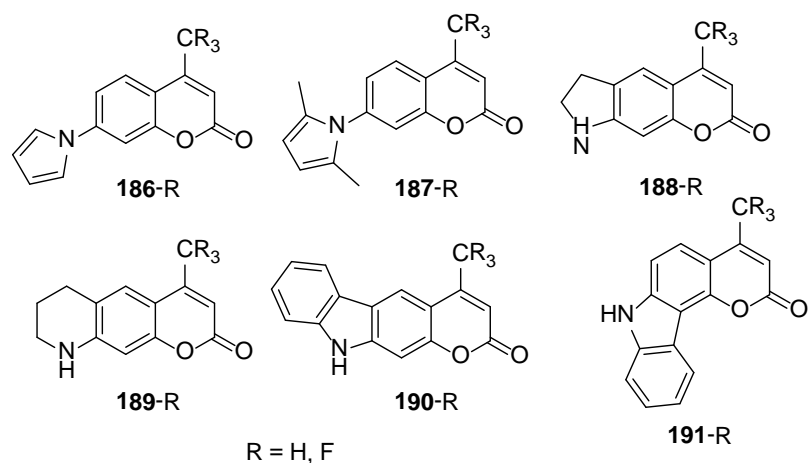


Figure 16 Coumarins **186-R–191-R** with various substitution patterns at nitrogen atom.

In the search for a novel fluorogenic indicator for monoamine oxidases (MAOs), Chen et al.^[49] prepared a number of fused pyrrolocoumarins (Figure 17) with various fusion patterns. In EtOH, compounds **192** and **193** with the nitrogen atom attached to C-7 turned out to be almost non-fluorescent. Compounds **194** ($\lambda_{\text{abs,max}}/\lambda_{\text{flu,max}} = 335/524$ nm) and **196** (330/517 nm) had very large Stokes shifts of 189 and 187 nm, respectively, in the series. However, their QYs in polar solvents were very low (0.08 and 0.06 in EtOH). Coumarin **195** (349/492 nm) provided the best combination of a large Stokes shift (143 nm) and a moderate fluorescence QY (0.36 in EtOH) in this series of pyrrolocoumarins.

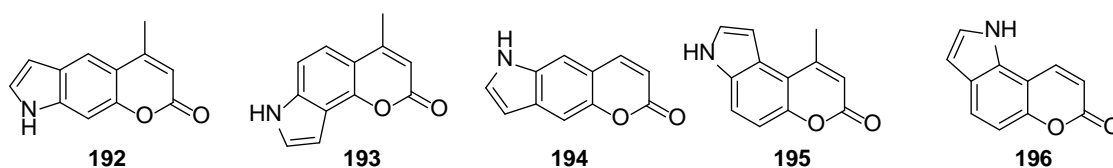


Figure 17 Pyranoidolones **192–196** as fused fluorophores with the coumarin core.

Fusion of 2-phenyl- and 2-*trans*-styrylimidazole systems with C-6 and C-7 positions of the coumarin scaffold (Figure 18) results in hypsochromic shifts of 30 and 7 nm as well as hypsofluoric shifts of 24 and 23 nm, respectively, and in a two-fold decrease in fluorescence QY in EtOH^[50] when compared with 7-*N,N*-diethylamino-4-methylcoumarin **44** ($\lambda_{\text{abs,max}}/\lambda_{\text{flu,max}} = 373/445$ nm, $\Phi_{\text{fl}} = 50\%$ ^[21a]).

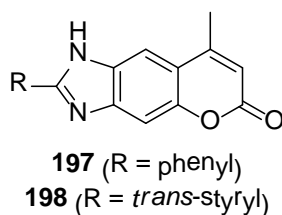
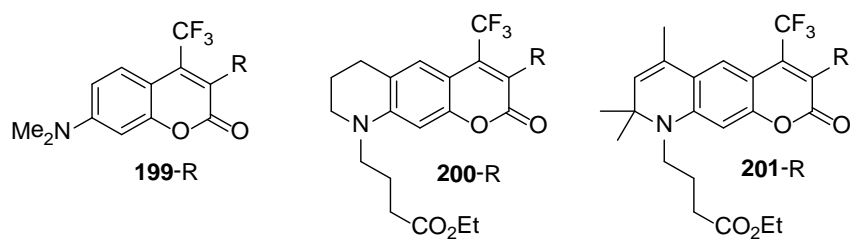


Figure 18 8-Methylchromeno[7,6-*d*]imidazol-6(1*H*)-ones **197–198** as fused fluorophores based on the coumarin core.

Coumarins **199-R–201-R** have various substituents at C-3 and different secondary amino groups at C-7. Comparison of compounds with the same 3-substituent revealed that a transition from compounds **199-R** to **201-R** provides red-shifts of 17 and 9 nm in the absorption bands and small red-shifts of 5 and 13 nm in the emission bands, respectively.^[45b] The substituents at C-3 have a stronger influence on the positions of the absorption and emission bands. Thus, compared to 3-unsubstituted coumarin **201-H** ($\lambda_{\text{abs,max}}/\lambda_{\text{flu,max}} = 424/527$ nm, in EtOH) the bathochromic shifts increased in the following order of substituents at C-3: 2-pyridyl (14 nm) \leq 4-pyridyl (16 nm) $<$ 2-thienyl (21 nm) $<$ *trans*-2-phenylethenyl (43 nm) $<$ *N*-(3-sulfopropyl)-4-pyridinio (50 nm) \leq *trans*-2-pyridylethenyl (51 nm) $<$ *N*-(3-sulfopropyl)-4-pyridinio (55 nm) \leq *trans*-4-pyridylethenyl (56 nm). Similar trends were observed in compounds **199-R** and **200-R**. For compounds **201-R** two new substituents were included, namely, *N*-(5-carboxypentyl)-2-pyridinioethenyl and *N*-(5-carboxypentyl)-4-pyridinioethenyl. These groups produce further red-shifts of 31 nm and 51 nm, respectively, in comparison to their non-quaternized analogs. For the emission bands, the bathofluoric shifts increase in a similar order. Exceptions are the 2-thienyl and 4-[*N*-(3-sulfopropyl)pyridinium] groups, which shift the emission bands very strongly to the red spectral region and show very large Stokes shifts of around 200 and 230 nm, respectively. In the former case, this effect, according to the authors,^[45b] is probably due to the strong electron-donating property of the 2-thienyl group. The fact that 4-[*N*-(3-sulfopropyl)pyridinium] group provides a much larger Stokes shift (230 nm) than the structurally similar 2-[*N*-(3-sulfopropyl)pyridinium] group (145–150 nm) was explained by a larger dipole moment. Similarly, 4-pyridyl substituents shift the emission bands more to the red compared with 2-pyridyl groups. Unfortunately, dyes with huge Stokes shifts exhibited low fluorescence QYs in EtOH.

Table 8 Spectral properties of 4-trifluoromethylcoumarins **199-R**–**201-R** in ethanolic solutions.

Compound	R	$\lambda_{\text{abs,max}}$, nm	ϵ , $\text{M}^{-1}\text{cm}^{-1}$	$\lambda_{\text{em,max}}$, nm	$\Delta\lambda$, nm	Φ_{fl}
199-R	2-thienyl	416	24400	611	195	0.13
	CH=CH-2-py	444	36600	578	134	0.64
	CH=CH-2-py-A ^a	475	9900	646	171	0.37
	CH=CH-4-py	449	28500	580	131	0.71
	CH=CH-4-py-A	500	13300	668	168	0.47
	4-py	413	18800	588	175	0.47
	4-py-A	439	11800	644	205	0.27
	CH=CH-ph	438	27600	576	138	0.49
200-R	4-py	430	13700	593	163	0.19
	4-py-B ^b	459	14800	655	196	0.34
	2-py	429	16400	578	149	0.20
	2-py-B	462	19200	607	142	0.11
201-R	4-py	440	18100	611	171	–
	2-py	438	17900	591	153	0.19
	2-py-B	479	22400	632	153	0.09
	4-py-B	474	12200	687	213	0.12
	2-thienyl	445	17400	636	191	0.16

Compound	R	$\lambda_{\text{abs,max}}$, nm	ϵ , $\text{M}^{-1}\text{cm}^{-1}$	$\lambda_{\text{em,max}}$, nm	$\Delta\lambda$, nm	Φ_{fl}
	CH=CH-ph	467	20000	598	131	0.58
	CH=CH-2-py	475	30400	602	127	0.80
	CH=CH-4-py	480	32100	609	129	0.68
	H	424	19600	527	103	0.45

^aA: The pyridine nitrogen is alkylated with an ω -carboxypentyl residue. ^bB: The pyridine ring is alkylated with an ω -sulfopropyl group.

In benzocoumarins (*2H*-benzochromen-2-ones) the annelation mode affects both the absorption and fluorescence properties. The values of absorption maxima for benzocoumarin derivatives in MeCN decrease in the order **203b** ($\lambda_{\text{abs,max}}/\lambda_{\text{flu,max}} = 390/491$ nm, $8600 \text{ M}^{-1}\text{cm}^{-1}$) > **202b** (382/465 nm, $15100 \text{ M}^{-1}\text{cm}^{-1}$) > **204b** (337/549 nm, $22500 \text{ M}^{-1}\text{cm}^{-1}$) with increasing absorbance (for structures, see Figure 19).^[51] The same tendency was observed for 3-ethoxycarbonylcompounds (**203a** > **202a** > **204a**). This was explained by the increase in extent of the CT between the benzocoumarin skeleton and the substituent at C-3. Among these benzocoumarins, compounds **202a** (ester type) and **203b** (acetyl type) showed the highest fluorescence efficiency. In contrast to the absorption maxima, the emission maxima shifted to longer wavelengths in the order **204** > **203** > **202**. The “linear” compounds **204a** (331/535 nm) and **6b** (337/549 nm) showed remarkably large Stokes shifts of 204 and 212 nm, respectively. These values are two-fold greater than those for “angular” compounds. However, the emission intensity of “linear” fused compounds is very poor and significantly inferior to that of the “angular” compounds.

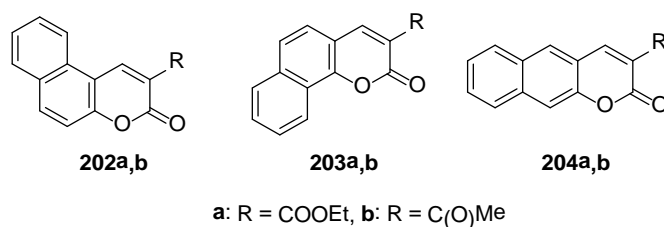


Figure 19 Benzocoumarins (*2H*-benzochromen-2-ones) **202–204** with various annelation modes.

In “iminocoumarins” the carbonyl oxygen in the position 2 is replaced with an imino group (see Figure 20). Sometimes these compounds exhibit photophysical properties

which are superior to those of the “parent” coumarins. Furthermore, in contrast to simple coumarins, the imino group can be easily modified allowing the synthesis of various derivatives. For example, iminocoumarin **205** shows a red-shifted absorption maximum ($\lambda_{\text{abs,max}} = 503 \text{ nm}$) in comparison with the “normal” coumarin **51** ($\lambda_{\text{abs,max}} = 467 \text{ nm}$), a well-known laser dye Coumarin 545.^[52] Compound **205** also has higher emission efficiency in pH-buffered aq. solutions (63% vs 10% for compound **51**). However, the observed Stokes shift (34 nm) is usually small for coumarin compounds. The modification potential of compound **205** was efficiently used in the design of various indicators and sensors for Zn^{2+} ,^[52] Cu^{2+} ,^[53] and F^{-} ^[54] and for the detection of alkaline phosphatase activity in living cells.^[55] Another iminocoumarin **206** contains a tetrahydroquinoxaline moiety and, when dissolved in neutral aq. buffer, with 143 nm exhibits a significantly larger Stokes shift ($\lambda_{\text{abs,max}}/\lambda_{\text{flu,max}} = 473 \text{ nm}/616 \text{ nm}$) than the dye **205**. Such a large Stokes shift was beneficial for signal detection in sensing fluoride ions.^[56]

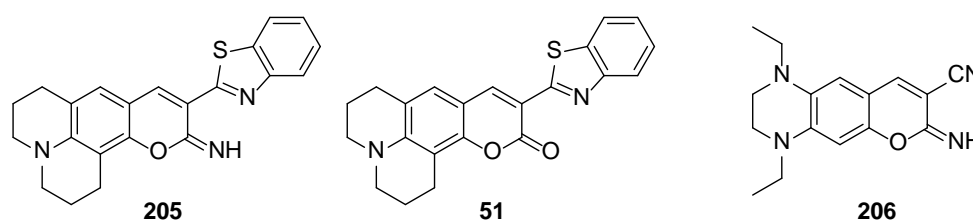


Figure 20 Iminocoumarins **205–206** and Coumarin 545 (**51**).

1,4-2*H*-Benzoxazin-2-ones, also known as “azacoumarins”, are coumarin analogs in which the carbon atom C-4 is replaced with a nitrogen (Figure 21). Similarly to the corresponding 7-aminocoumarins, 7-aminoazacoumarins **207-R** display strong fluorescence, but it is shifted towards the red spectral region due to a bathochromic effect of the heterocyclic nitrogen. This effect resembles the case of oxazine dyes (nitrogen and oxygen atoms at C-9 and C-10, respectively) which absorb and emit at longer wavelengths than the corresponding rhodamines (carbon and oxygen at C-9 and C-10, respectively). The spectral properties of compounds **207-R** in various solvents were thoroughly investigated.^[57] It was shown that the observed Stokes shift can reach an unusually high value of 183 nm, while the parent coumarin dyes showed Stokes shifts of 100 nm or less (in the same range of solvent polarity). A high fluorescence quantum yield of 93% in CHCl_3 was reported for compound **207-Me**. Large Stokes shifts of azacoumarins allowed using 7-*N,N*-dimethylamino-3-(*p*-formylstyryl)-1,4-benzoxazin-2-one **208** and benzoxazinone

vinylcinnamic acid **209** as fluorescent dyes in two-color cytometry together with fluorescein derivatives (which possess small Stokes shifts) using only one excitation wavelength.^[58] Although the emission efficiencies in polar protic media were reported only for a limited number of compounds, azacoumarins are interesting as scaffolds for the design of better large Stokes shift dyes which can be used in fluorescence microscopy.

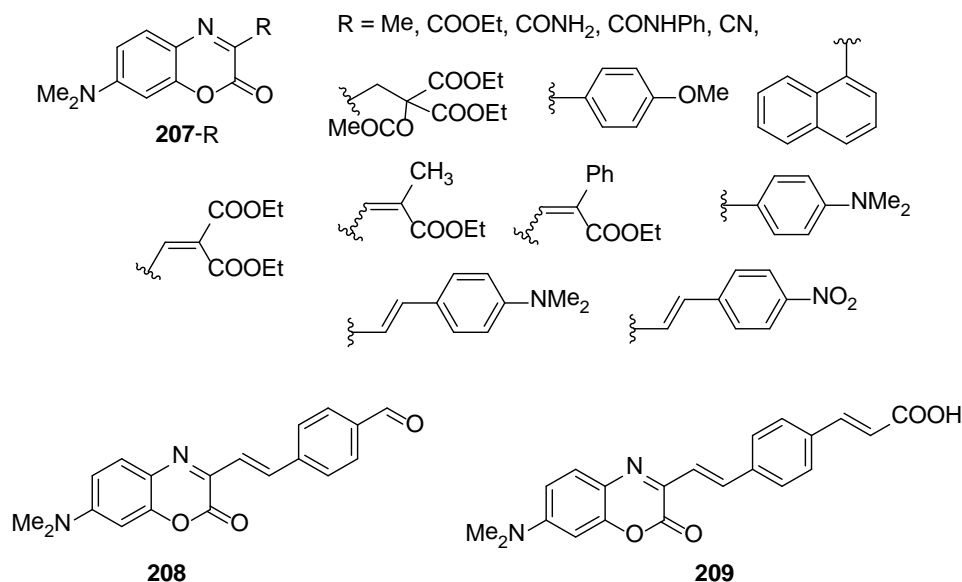


Figure 21 7-Aminoazacoumarins **207-R**, **208** and **209**.

Another way to provide bathochromic and bathofluoric shift is the extension of the π -conjugated system. In this respect, 8-*N,N*-dimethylamino-2-oxo-2*H*-benzo[*h*]chromenes **210** and **211** represent coumarins in which the π -conjugated system is extended by an additional benzene ring fused with positions 7 and 8 leading to a phenanthrene-like structure (Figure 22).

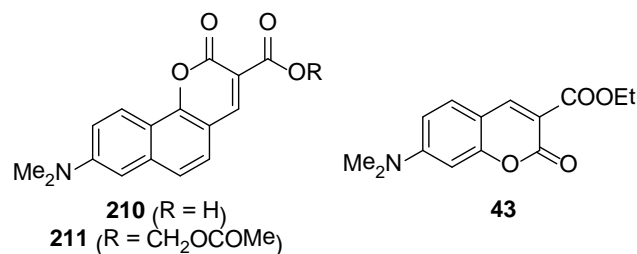


Figure 22 8-*N,N*-Dimethylamino-2*H*-benzo[*h*]chromen-2-ones **210** and **211**, and the parent coumarin **43**.

When dissolved in EtOH, compound **211** displays absorption and emission spectra maxima at 455 and 552 nm^[59] which corresponds to red-shifts of 43 and 92 nm, respectively, compared with the parent dye **43**, and a larger Stokes shift of 97 nm.^[21a] A relatively high fluorescence quantum yield of 29% in aq. media (in the presence of sodium dodecyl sulfate), high photostability and a bathochromic shift upon binding with magnesium ions rendered compound **210** useful as a probe for selective detection of intracellular magnesium ions in living cells without interference by calcium ions, and even as a candidate for the two-photon excitation mode.

2*H*-Benzo[*g*]chromenes **212** and **214** represent analogues of 7-*N,N*-dimethylamino-coumarin **213** with an additional benzene ring fused to positions 6 and 7 of the coumarin core (Figure 23).^[60] Due to their extended π -system, benzocoumarin **212** and benzoiminocoumarin **214** absorb and emit at much longer wavelengths relative to the corresponding parent coumarin **213** ($\Delta\lambda_{\text{abs}}$: 41 and 55 nm; $\Delta\lambda_{\text{em}}$: 110 and 137 nm) with larger quantum yields (61% and 67% in aqueous media, respectively). Emission bands are more shifted to the red than absorption, and this results in larger Stokes shifts of 152 and 139 nm compared with only 70 nm for compound **213**. Recently,^[61] benzocoumarin **215** was proposed as a red-emissive and photostable two-photon fluorescence probe for mitochondria. This compound showed high selectivity and robust staining ability together with low cytotoxicity and insensitivity to pH changes in the biologically relevant pH range.

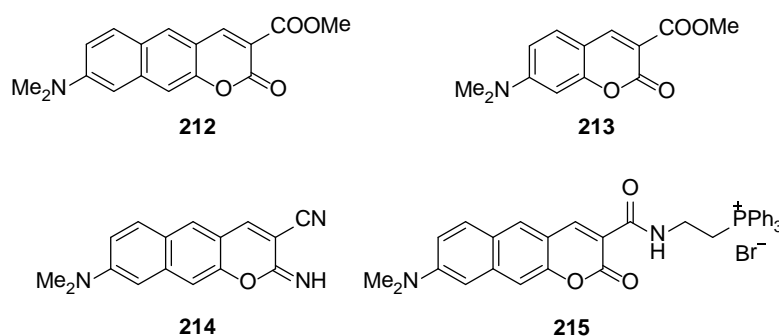


Figure 23 2*H*-Benzo[*g*]chromenes **212** and **214**, two-photon fluorescent probe **215** and the parent coumarin fluorophore **213**.

Here we abandon coumarin dyes and discuss the extension of the conjugated π -system in xanthene dyes. This approach could be applied to fluorescein, rhodol and rhodamine fluorophores. Fluorescent dyes with a red-shifted absorption band (compared with fluo-

rescein) – naphthofluoresceins **216-R** and **217-R** (Figure 24) – were used in flow cytometry.^[62] Although the annelation mode used in compounds **216-R** shifted absorption maximum by ~30–40 nm relative to fluorescein, it did not result in a significant increase of Stokes shift which remained small (max 32 nm). On the other hand, benzo[*c*]xanthene dyes **217-R** displayed a red-shifted absorption with maxima at 595–609 nm (in aqueous media) and much larger Stokes shifts of 56–77 nm. However, their fluorescence QYs did not exceed 15%.

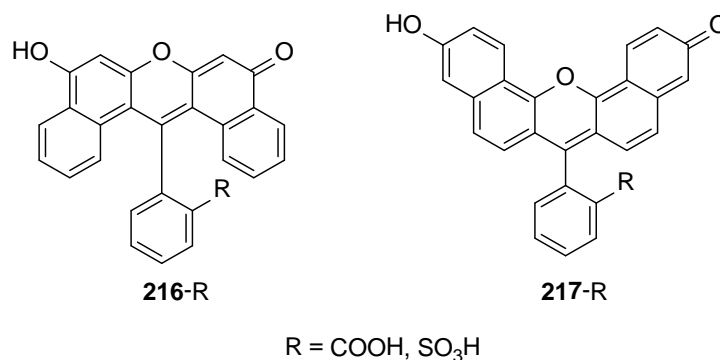


Figure 24 Naphthofluoresceins **216-R** and **217-R**.

Other benzo[*c*]xanthene dyes – seminaphthofluoresceins (SNAFLs) **218–222** and seminaphthorhodafluors (SNARFs) **223–231**^[63] – have only one fused benzene ring (Figure 25). They can be excited in the 550–650 nm range. Their pK_a values lie within the physiologically relevant pH range (between 7 and 8). They also have larger Stokes shifts (up to 85 nm) and good fluorescence QYs in aqueous media (up to 50%). Unlike the fluoresceins, they show not only two distinct absorption bands for the protonated and deprotonated forms, but also two emission bands (because the molecules do not dissociate in the excited state). Furthermore, the spectra have clearly defined isosbestic and iso-emissive wavelengths (where absorption or emission is pH independent). As a result, these compounds found numerous applications in ratiometric and fluorometric pH measurements^[64] and became commercially available. Apart from pH measurement, a number of SNAFL- and SNARF-based derivatives were used for detecting various metal ions,^[65] nitric oxide,^[66] thiols,^[67] peroxide^[68] and as a FRET partner for cyanine dye Cy5.^[69]

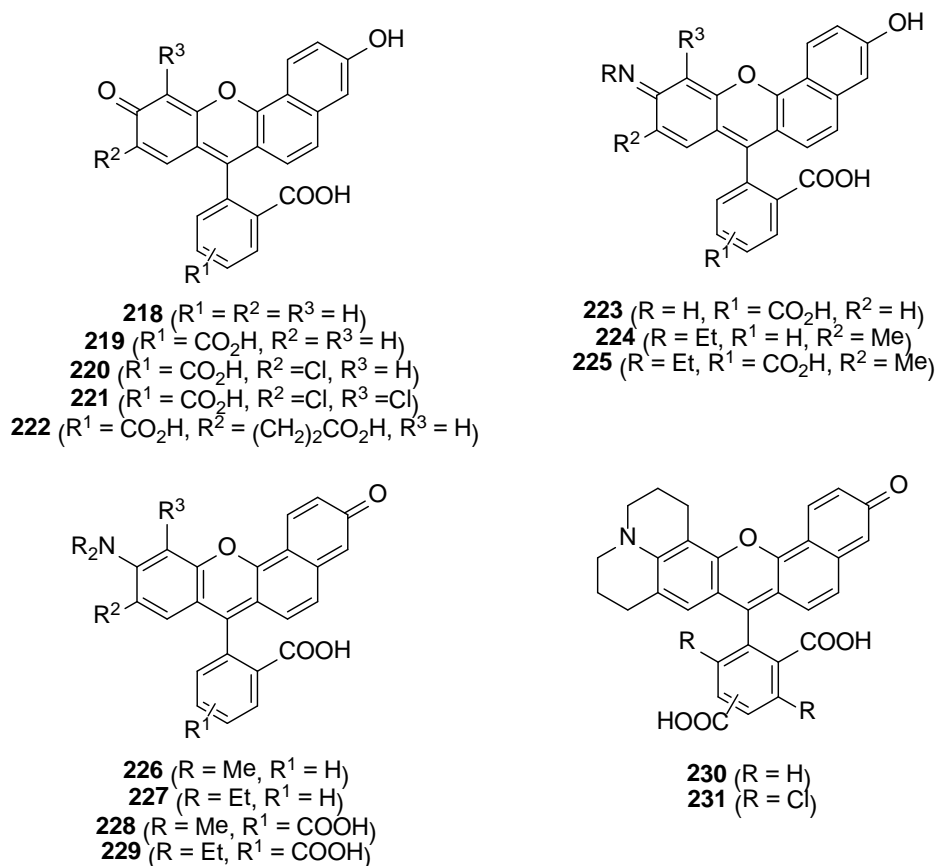


Figure 25 Seminaphthofluoresceins (SNAFLs) **218–222** and seminaphthorhodafluors (SNARFs) **223–231**.

Semiempirical calculations showed that [*a*]- and [*b*]-annelated benzoxanthenes should absorb and emit at significantly longer wavelengths than their [*c*]-annelated analogs.^[70] Based on these findings, Yang et al.^[71] developed and prepared seminaphthofluorones (SNAFRs) **232–237** (Figure 26). The annelation patterns and the position of the hydroxyl group were varied, and the spectral properties of the derivatives were evaluated. It was found that both these variables have a relatively small effect on the spectral properties of the *neutral forms* of SNAFRs in DMSO: all compounds have absorption maxima near 475 nm, and emission maxima near 600 nm. In contrast to neutral forms, the spectral properties of deprotonated SNAFRs depend on the annelation type and the position of hydroxyl group. Thus, compound **236** in its anionic form shows a NIR emission with a maximum at 789 nm, followed by **232** at 768 nm, **237** at 725 nm and **235** at 694 nm (in DMSO). Benzo[*c*]xanthene dye **233**, which is similar to SNAFL compounds, shows emission at the shortest wavelength (673 nm). The linearly annelated compound **237** is particularly interesting: in contrast to other SNAFRs, its anionic form exhibits an excep-

tionally large Stokes shift of 197 nm ($\lambda_{\text{abs}} = 536 \text{ nm}$, $\lambda_{\text{em}} = 733 \text{ nm}$) in aqueous phosphate buffer.

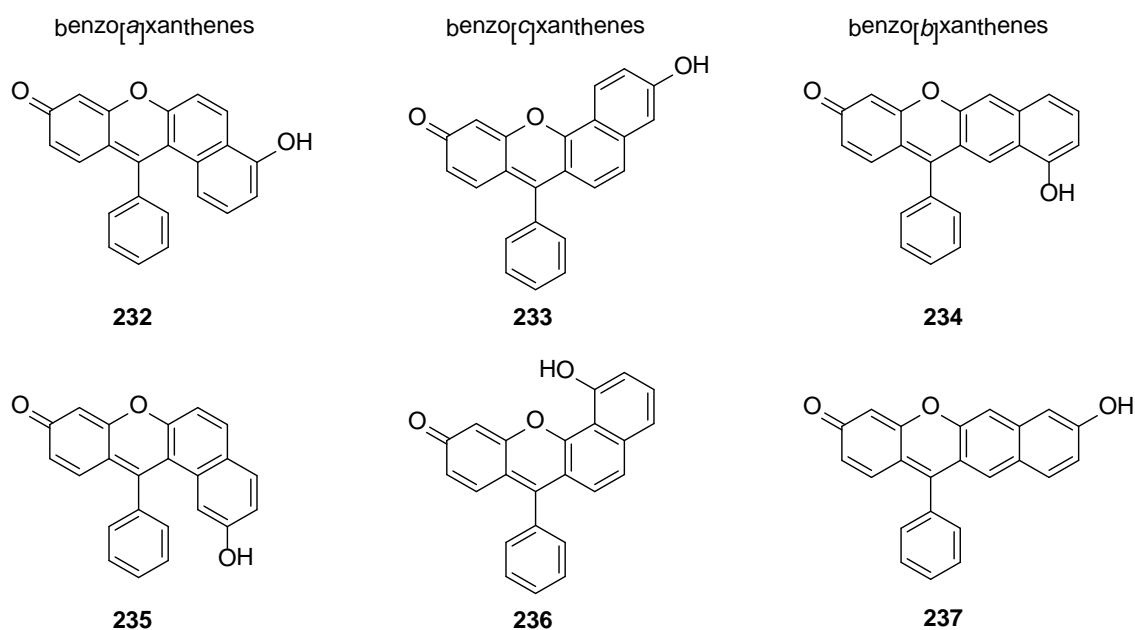


Figure 26 Seminaphthofluorones (SNAFRs) **232–237**.

A common feature of SNAFLs, SNARFs and SNAFRs is the sensitivity of their spectral properties to pH changes, but very often compounds with spectra insensitive to pH are needed. Rhodamine analogs with a xanthene core extended by one or two benzene rings provide this feature. Moreover, they have absorption and emission spectra shifted to the red in comparison with the “parent” rhodamines.^[72]

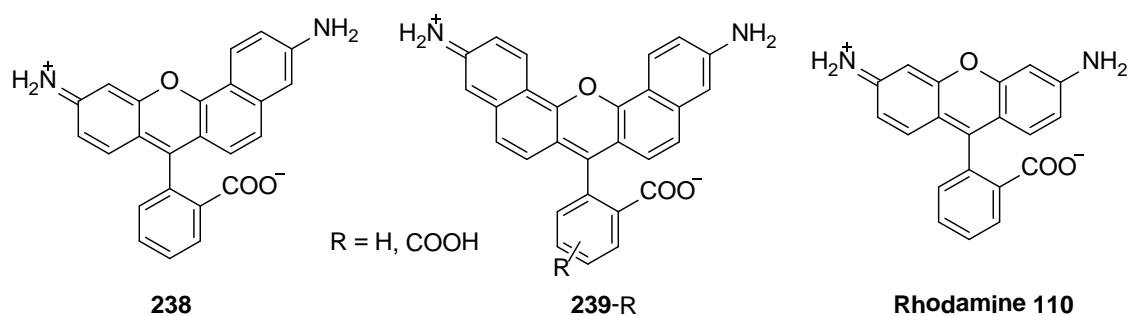


Figure 27 Seminaphthorhodamine **238**, naphthorhodamines **239-R** and parent dye Rhodamine 110.

Seminaphthorhodamine **238** (Figure 27) displays an absorption with a maximum at 535 nm (in a mixture of DMSO with aq. phosphate buffer, 1:9) which corresponds to a

bathochromic shift of 40 nm relative to parent Rhodamine 110. Its emission with a maximum at 628 nm (100 nm to the red from Rhodamine 110, Stokes shift 93 nm) exhibits a moderate QY of 19%. In the case of naphthorhodamine **239-H**, the introduction of an additional benzene ring results in further shifts of absorption and emission maxima to 578 and 668 nm, respectively (Stokes shift 98 nm, QY 10%), which are comparable to commercially available naphthofluorescein **217-COOH** (Figure 24) which absorbs and emits at 595 and 660 nm, respectively.

In order to take advantage of large Stokes shifts displayed by coumarins and strong fluorescence emission in the orange or red regions exhibited by rhodamines, hybrid compounds combining structural features of both fluorophores were designed.^[73]

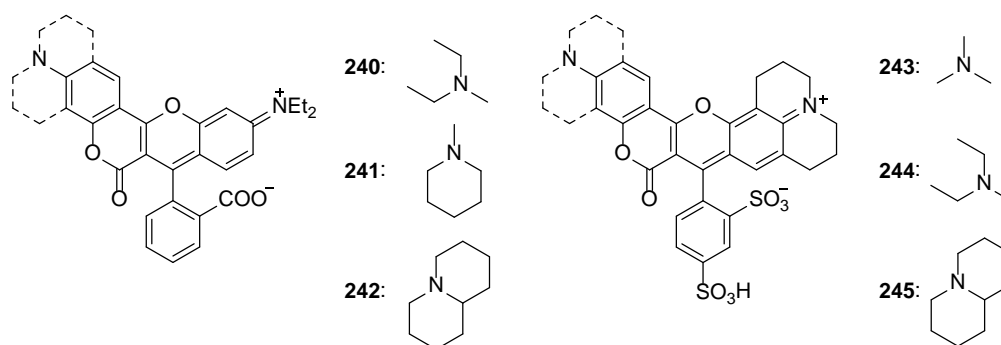


Figure 28 Rhodamine-coumarin hybrids **240–245**.

The emission and absorption spectra of compounds **240–242** (Figure 28) are sensitive to the acidity of the environment (due to the formation of the colorless and non-fluorescent spirocyclic forms under neutral and basic conditions). Moreover, at pH > 8 the coumarin ring opens. In solutions acidified with TFA (to prevent the formation of spirolactones) these compounds showed larger Stokes shifts (52–72 nm in water) than those for “normal” rhodamines. However, emission efficiencies in aqueous media were very low (<1%), possibly, due to the formation of aggregates. Spectral properties of hybrid dyes **243–245** are comparable to those of compounds **240–242**. However, due to the presence of two highly polar sulfonic acid groups in the *meso*-phenyl ring, which prevent the formation of aggregates, fluorescence QYs are considerably higher (9–10%).

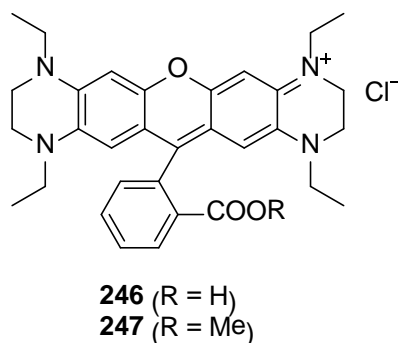


Figure 29 Rhodamine dyes **246** and **247** with 1,2,3,4-tetrahydropyrazine moieties.

Surprisingly, an introduction of two 1,2,3,4-tetrahydropyrazine moieties to the xanthene scaffold shifts absorption and emission bands towards longer wavelengths and also greatly increases the Stokes shift (Figure 29).^[74] The authors attributed this effect to an excited-state ICT which is greatly enhanced by the strong electron donor. Thus, compounds **246** ($\lambda_{\text{abs,max}}/\lambda_{\text{flu,max}} = 588/656$ nm) and **247** ($\lambda_{\text{abs,max}}/\lambda_{\text{flu,max}} = 597/662$ nm) have the largest Stokes shifts ever reported for rhodamine dyes (68 and 65 nm in 10% aqueous EtOH, respectively). For comparison, Rhodamine 6G exhibits a two-times smaller Stokes shift of 30 nm ($\lambda_{\text{abs,max}}/\lambda_{\text{flu,max}} = 525/555$ nm) under the same conditions. Similarly to dyes **240–242**, compound **246** exists in an equilibrium with its spirolactone form which is colorless. The position of this equilibrium is very sensitive to solvent polarity. In contrast to **246**, compound **247** in which the carboxylic acid function is blocked, cannot form the corresponding spirolactone. Unfortunately, fluorescence QYs in polar solvents were not reported for these compounds.

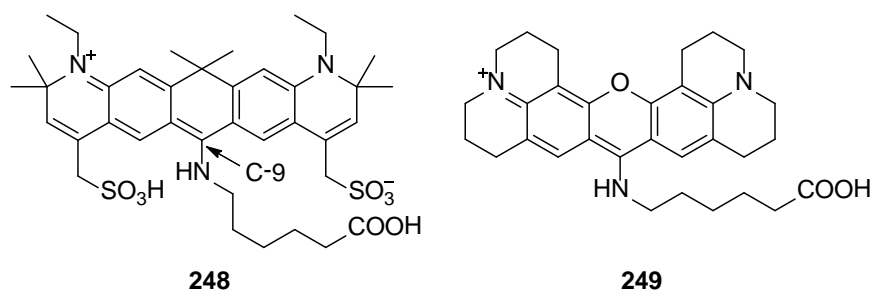


Figure 30 *Meso*-aminosubstituted carbopyronine **248** and pyronine **249**.

Substitution of the *meso*-position in carbopyronine or pyronine fluorophores with a primary amine results in a fundamental change of their photophysical properties.^[75] For

example, compounds **248** and **249** (Figure 30) in aqueous phosphate buffer absorb at 490 and 454 nm, respectively.^[76] This corresponds to an approximately 100 nm hypsochromic shift compared to the parent carbopyronine and pyronine unsubstituted at C-9. Furthermore, the introduction of amine substituents provides very large Stokes shifts (180 nm and 114 nm for compounds **248** and **249**) retaining high fluorescence QYs in aq. media (26% for **248** and 60% for **249**). Such combination of large Stokes shifts with high emission efficiencies in polar protic media is especially rare which makes these dyes truly unique. Interestingly, the introduction of secondary amino or primary arylamino substituents leads to substantially lower QYs of fluorescence.

Boron-dipyrromethene (BODIPY) fluorophores have a strong absorption of visible light, high fluorescence QYs and good photostability. Despite these attractive properties, very small Stokes shifts commonly displayed by many BODIPY dyes (ca. 10 nm) are disadvantageous to many applications including fluorescence microscopy. The reason is a so-called inner-filter effect, that is to say, the reduction of the emission intensity by self-absorption. On the other hand, BODIPYs have a great potential for synthetic modification.^[77] Therefore, many properties, such as the positions of absorption and emission maxima, the Stokes shift or hydrophilicity, can be readily tuned to a certain extent. However, increasing the Stokes shift for BODIPY dyes is not trivial. A typical synthetic modification of the BODIPY core, such as extending the π -conjugation chain, leads to bathochromic and bathofluoric shifts, but does not increase the Stokes shift. Chen et al.^[78] overcame this issue using a new approach. They hypothesized that by introducing thienyl substituents into positions 2 and 6 of the BODIPY core (see Figure 31 for the numbering scheme of the BODIPY fluorophore), a greater extent of the geometry relaxation upon photoexcitation could be achieved. A substantial amount of the excitation energy would dissipate through rotating thienyl groups during this process, and this would effectively lower the energy of the excited state. As a result, the emission energy would become much smaller than the excitation energy, thus increasing the Stokes shift.

Compound **250** with one thienyl moiety at C-2 (Figure 31) displays the absorption and emission maxima at 507 and 603 nm (in 75% aq. MeOH), respectively. This corresponds to an enormous (for BODIPY dyes) Stokes shift of 96 nm. The absorption and emission maxima of the symmetrical BODIPY derivative **251** were observed at 523 and 612 nm, respectively (the Stokes shift is 89 nm). Asymmetrical compound **250** exhibited a much stronger absorption ($\epsilon = 65\,000\text{ M}^{-1}\text{cm}^{-1}$ vs only $17\,000\text{ M}^{-1}\text{cm}^{-1}$ for **251**). However, the

emission efficiencies displayed by both compounds in protic solvents were rather low (< 10%). Interestingly, the introduction of phenyl substituents instead of thienyls into the same positions does not increase the Stokes shift. Similarly, the substitution with thienyl moieties at C-3, C-3,5 or C-1 also conserves small Stokes shifts observed for BODIPY dyes.

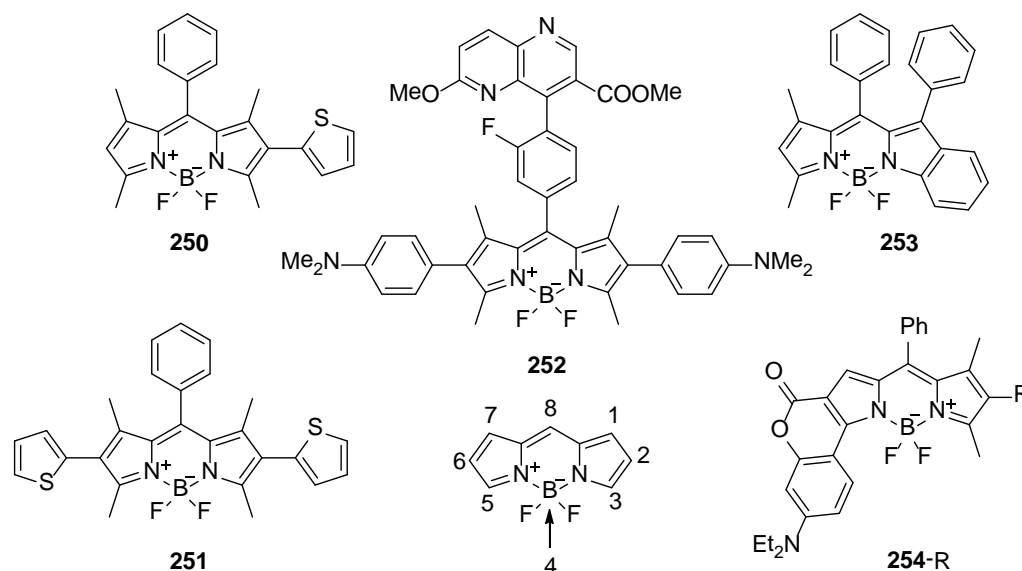


Figure 31 Large Stokes shift BODIPY dyes **250–254** and the atom numbering of the BODIPY fluorophore.

A Stokes shift of 186 nm ($\lambda_{\text{abs}} = 554$ nm, $\lambda_{\text{em}} = 740$ nm in CH_2Cl_2) was observed for compound **252**, and it represents the largest Stokes shift ever reported for BODIPY dyes.^[79] DFT calculations combined with resonance Raman spectroscopy showed that an ICT from the *p*-*N,N*-dimethylaminophenyl ring to the naphthyridyl unit is responsible for the lowest energy optical transition. Unfortunately, the fluorescence intensity in CH_2Cl_2 is very low ($\Phi_{\text{fl}} = 6\%$) and almost negligible in polar solvents (MeOH, MeCN, H_2O). Asymmetric benzo[*b*]fused BODIPY **253** was reported to show a broad absorption band centered at 512 nm and an emission band with a maximum at 655 nm (in CH_2Cl_2) resulting in a large Stokes shift of 143 nm.^[80]

Annulation of the coumarin unit with the BODIPY core was expected to shift absorption and emission maxima to the red spectral region and enlarge the Stokes shift compared with typical non-annulated BODIPY dyes.^[81] Indeed, *N,N*-diethylamino-substituted dyes **254-H** and **254-Et**, in MeOH, exhibit the absorption maxima at around 590 nm and emit in the NIR region (720 and 724 nm, respectively, Stokes shift of 130 nm). In polar sol-

vents, such as DMF or MeOH, fluorescence is significantly quenched ($\Phi_{fl} = 3\text{--}6\%$). The authors attributed this behavior to the formation of a twisted ICT excited state which they considered to be non-emissive in the case of 7-*N,N*-dialkylaminocoumarins.

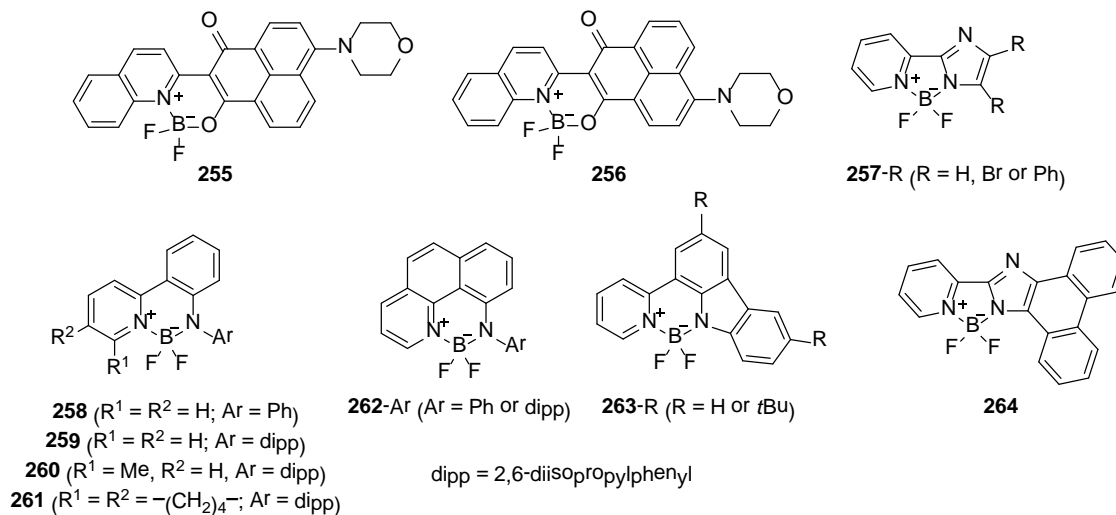


Figure 32 Fluorescent boron-fluorine complexes **255–264** with large Stokes shifts.

Isomeric compounds **255** and **256** (Figure 32) represent donor-acceptor complexes in which quinoline and phenalene-1,3-dione coordinate a BF₂ fragment and form a strong electron-acceptor moiety, while the morpholine part acts as a donor.^[82] Similar to all fluorophores displaying ICT upon excitation, spectral properties of these compounds significantly vary with solvent polarity. Interestingly, such a minor structural change as the change in the position of the donor morpholine fragment leads to quite different photophysical properties. Thus, in MeOH, absorption and emission maxima for compound **255** were observed at 419 and 564 nm, respectively, and the separation between them corresponds to a large Stokes shift of 145 nm. For the complex **256**, in the same solvent, the absorption maximum was observed at 461 nm, while the emission band had a maximum at 558 nm, i.e. the Stokes shift was significantly smaller (97 nm) compared with isomer **255**. The red-shifted emission band, the larger Stokes shift and broader emission band are consistent with a more efficient ICT process in the case of isomer **255**. Both compounds **255** and **256** exhibited high fluorescence QYs in polar protic MeOH, which is quite unusual for substances with such large Stokes shifts.

Asymmetrical anilido-pyridine boron difluoride dyes **258–261**, **262-Ar** and **263-R** (Figure 32) were specially designed to improve very small Stokes shifts of BODIPY dyes.^[83]

Compounds **258–261** absorb in the violet region of the visible spectrum ($\lambda_{\text{abs,max}} = 416\text{--}419$ nm in CH_2Cl_2). They have large Stokes shifts in the range of 95–114 nm and moderate QYs (27–33%). More rigid structures of **262-Ar** and **263-R** provided an efficient emission (QYs 60–83%) retaining large Stokes shifts. These dyes also showed exceptional photostability. Thus, under conditions, when Rhodamine 101 bleached in less than 2 h, the absorption profile of **258** remained essentially unchanged after 10 h of irradiation, dyes **262-Ph** and **262-dipp** were photostable for 16 h, and dyes with the carbazole fragment (**263-H** and **263-*t*Bu**) retained ca. 80% of their absorbance intensity after this time period.

Boron 2-(2-pyridyl)imidazole (BOPIM) complexes also exhibited larger Stokes shifts in contrast to BODIPYs. Compound **257-H** absorbs UV-light with a maximum absorbance at 293 nm and possesses a large Stokes shift of 66 nm ($\lambda_{\text{em,max}} = 362$ nm) and a small fluorescence QY of 3% in MeOH.^[84] Interestingly, the introduction of two bromine atoms (compound **257-Br**) leads to a bathochromic shift of 64 nm ($\lambda_{\text{abs,max}} = 357$ nm), a larger Stokes shift of 130 nm ($\lambda_{\text{em,max}} = 487$ nm) and a 10-fold increase in the fluorescence QY ($\Phi_{\text{fl}} = 31\%$). Absorption maxima of compounds **257-Ph** and **264** are further red-shifted (391 and 404 nm, respectively).^[85] Their emission maxima are at 525 and 531 nm, which correspond to Stokes shifts of 134 and 127 nm, respectively. Both compounds show moderate emission efficiencies in MeOH (12% and 14%). All BOPIM complexes displayed negative solvatochromism. More polar solvents shift the lowest-energy absorption bands towards the blue region of the UV-vis spectrum. This indicates that the $S_0 \rightarrow S_1$ absorption band has an ICT character, and the energy of the ground state decreases more than that of the excited state with increasing solvent polarity, and this effect makes the energy gap larger.

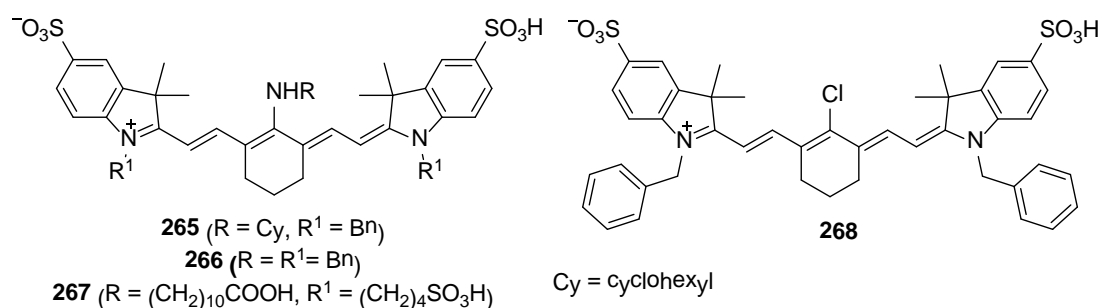


Figure 33 Heptamethine dyes **265–267** with large Stokes shift and their precursor **268**.

Heptamethine dyes **265–267** have an amino substituent attached to the methine chain (Figure 33). In this respect they are similar to compounds **248** and **249** with a C-N bond in the *meso*-position of carbopyronine and pyronine fluorophores. Heptamethine dyes **265–267** show very interesting spectral properties. Compared with precursor cyanine dyes, these compounds have larger Stokes shifts and high fluorescence QYs in water. For example, compounds **265–267** have broader spectra and much stronger fluorescence than dye **268**. Their solutions in water are blue-colored ($\lambda_{\text{abs,max}} = 600\text{--}617$ nm), whereas solutions of compound **268** are green, which corresponds to a hypsochromic shift of 180–190 nm.^[86] Fluorescent dyes **265–267** emit in the NIR region with large Stokes shifts of 140–155 nm (in water). However, emission efficiencies of **265** and **266** are rather low (~7%). Luckily, the introduction of two additional sulfonate residues results in a good fluorescence QY (37% for compound **267**) in aqueous solutions. In addition, compound **267** (also known as 4-Sulfonir) has a large molar absorptivity of $1.8 \times 10^5 \text{ M}^{-1} \text{ cm}^{-1}$, which together with the large QY provides high brightness in microscopy applications.

1.2.2 Fluorophores with a Stokes shift provided by photochemical processes

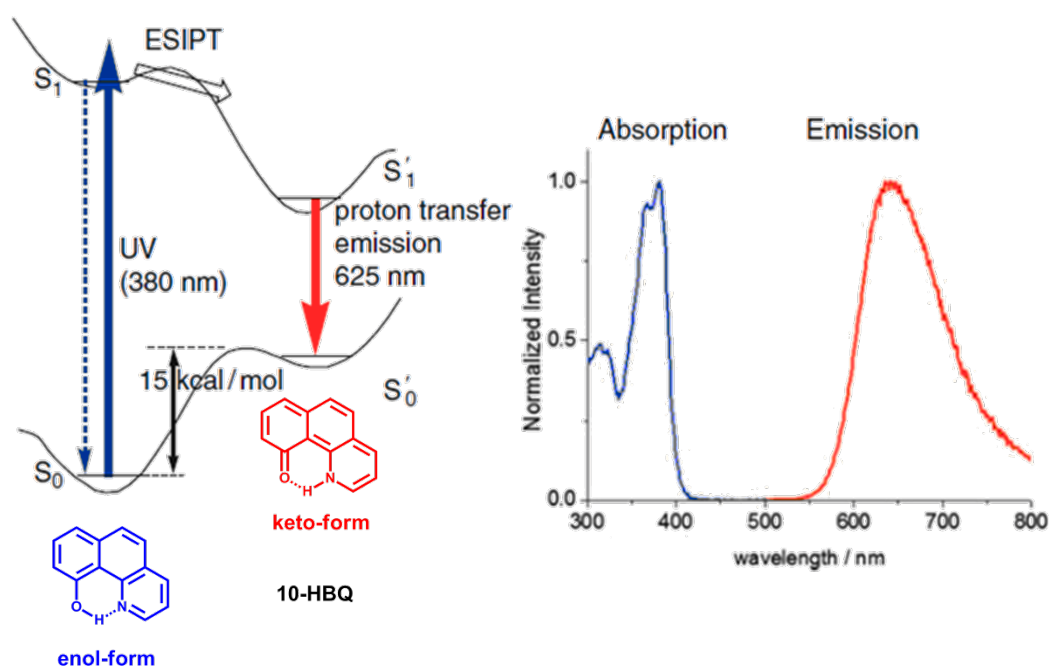
All compounds described in the previous section exhibited large Stokes shifts as a result of photophysical processes such as intramolecular charge transfer (ICT), solvent relaxation around a large excited dipole and steric relaxation of compounds with bulky groups. In contrast to these processes, there are other mechanisms providing large Stokes shifts. They involve adiabatic photochemical reactions leading to an emissive product with a chemical structure different from that of the starting molecule. A short overview of various photochemical mechanisms, such as excimer/exciple formation, excited state intramolecular proton transfer (ESIPT) and twisted ICT (TICT),^[87] providing large Stokes shifts is given below.

A molecule in the excited state can form a complex with an identical molecule (in the case of excimer formation) or a different molecule (in the case of exciple formation) in the ground state. The formation of these complexes may quench the emission,^[88] but sometimes an excimer/exciple can be emissive. For example, many aromatic hydrocarbons such as naphthalene or pyrene form excimers. The fluorescence band which corresponds to an excimer is red-shifted relative to the monomer and does not show vibronic

structure. The so called intramolecular excimers have two identical fluorophores which are linked by a short flexible chain. The formation of excimers or exciplexes involves diffusion processes or large intramolecular rearrangements. Therefore, it is diffusion-controlled and can be used to probe the local fluidity of the medium.^[89] For example, a concentration-dependent ability of the BODIPY label to form excimers with red-shifted emission was used to study the lipid transport and metabolism.^[90] The dual probes consisting of pyrene fluorophores attached to oligonucleotides were used for the detection of a single-base point mutation.^[91] In the course of adjacent binding of the modified nucleotides to a complementary target sequence, a pronounced spectral change from the blue monomer emission to the green excimer emission with a larger Stokes shift occurred (~140 nm) allowing a simple detection with a spectrofluorimeter. A similar approach used an exciplex formation between 1-pyrenemethylamine and *N*-methyl-*N*-naphthalene-1-ylethanediamine fragments attached to the 5'- or 3'-terminal phosphate groups of oligonucleotides upon binding to target sequence of a nucleic acid.^[92] The huge Stokes shift (100–150 nm) exhibited by this probe allowed detection of a single nucleotide polymorphism (SNP) DNA by a naked eye. Unlike other fluorescence probe approaches (e.g., FRET), the formation of excimers and exciplexes is more sensitive to the correct assembling of counterparts.

Incorporation of multiple fluorophores into the DNA scaffold can result in a multifluorophoric system with interesting photophysical properties (see review^[93]). For example, various fluorophores were introduced at C-1' of the D-ribose to replace nucleobases and produce artificial fluorescent deoxynucleosides (deoxyfluorosides).^[94] Afterwards, combinatorial libraries were prepared to reveal oligodeoxyfluorosides (ODFs) with best photophysical properties in the single-stranded state. In some ODFs, fluorophores formed excimers or exciplexes which emitted fluorescence with large Stokes shifts (up to 140 nm) and possessed large QYs in aq. buffers. In another case, a pyrene dye was attached to the C-2' position of D-ribose in the nucleotide of interest.^[95] In a molecule of the duplex RNA containing the modified nucleotide, the pyrene moiety resides outside the double-helical structure in the minor groove. When multiple pyrenes were introduced consecutively into the duplex RNA, strong excimer emission at around 480 nm (cf. 396 nm for the monomer) with a high QY was observed. Interestingly, with an increase in the number of incorporated pyrenes, the excimer fluorescence increased faster than linearly.

In the case of the excited state intramolecular proton transfer (ESIPT), a molecule in the excited state undergoes tautomerization, i.e. proton transfer from one basic site to another in the same molecule. The ESIPT reaction requires the formation of a hydrogen bond between a proton donor (hydroxyl, imino or amino group) and an acceptor group (for example, carbonyl or pyridine) which are located in close proximity. Upon excitation, a proton transfer takes place (acid-base properties of the excited state are different), forming a tautomer in the excited state S_1' , the geometry and electron distribution of which significantly differs from its corresponding normal species in the excited state S_1 (Scheme 2).^[96] The structural change during the ESIPT process may lead to unusually large Stokes shifts. Unfortunately, in protic solvents, the ESIPT emission is usually inhibited, and therefore, only fluorescence from the “normal” tautomer with a small Stokes shift is observed. Moreover, extending of the π -conjugation – a usual strategy for design of new fluorophores – may inhibit the ESIPT process.^[97]



Scheme 2 ESIPT process in 10-hydroxybenzo[*h*]quinoline.^[96]

Another process which could produce a large Stokes shift is the formation of twisted ICT states (TICT), which involves mutual twisting (in the excited state) of donor and acceptor parts of a molecule connected by a single bond and simultaneous charge transfer between them. In the TICT system, a donor D and an acceptor A are coplanar in the ground state, and the same coplanar arrangement is retained in the initially reached Franck-Condon

excited state. Due to the large π -overlap, mesomeric interaction between D and A is significant, and excitation can involve a (partial) charge transfer. In addition to an S_1 minimum for the planar geometry these systems can possess another low lying S_1 minimum for the perpendicularly twisted geometry with full charge separation, the TICT state. The latter can be populated in an adiabatic photoreaction which combines an excited-state intramolecular twist, electron transfer and solvent reorganization.^[98] For example, 4-*N,N*-dimethylaminobenzonitrile (DMABN) was found to exhibit a dual fluorescence in polar solvents. The emission spectrum of this compound consists of a “normal” band ($\lambda_{\text{abs,max}} = 361$ nm, in MeCN^[99]), which is analogous to emission bands exhibited by closely related benzene derivatives, and an “anomalous” band ($\lambda_{\text{abs,max}} = 492$ nm, in MeCN^[99]) with a large Stokes shift. These bands were ascribed to the excited state with the planar geometry (locally excited) and the TICT state with the twisted dimethylamino group, respectively.^[100] When the twisting of the dimethylamino group is hindered, as in the case of compound **270**, formation of the TICT state is impossible, and only the “normal” emission band is observed. At the same time, compound **271**, where the amino group is fixed in the twisted conformation, exhibits only fluorescence with a large Stokes shift (from the TICT state).^[101]

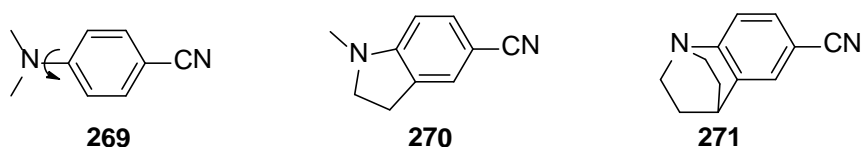
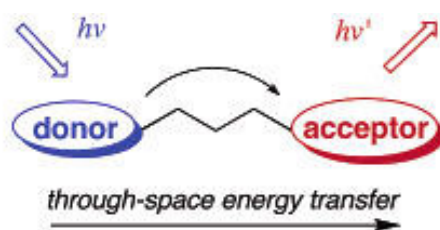


Figure 34 *p*-*N,N*-Dimethylaminobenzonitrile **269** which undergoes TICT in the excited state and model compounds **270** and **271**.

As a rule, emission efficiencies of compounds displaying the TICT are very low. In fact, many TICT states were found to be non-emissive and responsible for the rapid non-radiative decay of numerous important dyes (for example, in the case of 7-*N,N*-dialkylaminocoumarins^[21d, 21e, 21g, 35]) which leads to intramolecular fluorescence quenching. The latter effect may be due to the reduced value of the transition dipole moment (for transition $S_1 \rightarrow S_0$) which results from the lack of the orbital overlap between D^+ and A^- moieties.^[102] Therefore, a rational design to attain the TICT emission with a large Stokes shift and a high QY at the same time still remains a challenge.

1.2.3 Multifluorophore constructs with pseudo-large Stokes shifts

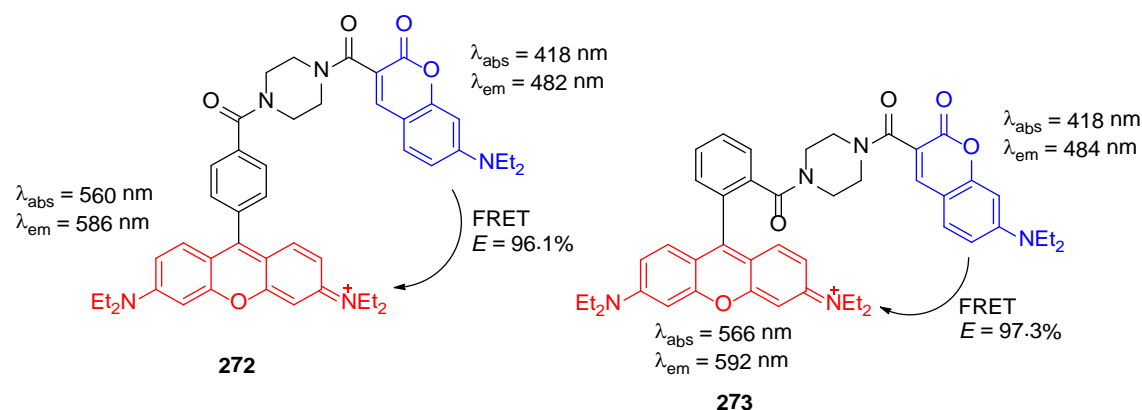
In order to address the problem of small Stokes shifts exhibited by most of the conventional fluorescent dyes, resonance energy transfer (RET) between two organic fluorophores, donor and acceptor, connected by a suitable linker, can be utilized to obtain dyads with pseudo-large Stokes shifts. Photophysical properties and applications of such molecular constructs, called energy transfer cassettes, have been reviewed recently.^[103] When both fluorophores are connected by a non-conjugating linker, the energy transfer occurs through space (Scheme 3). This process is usually called fluorescence resonance energy transfer (FRET) and occurs through non-radiative dipole-dipole coupling. According to the FRET theory,^[104] several requirements should be fulfilled for efficient FRET: (1) high fluorescence QY of the donor, (2) a substantial overlap between the donor emission band and the acceptor absorption band, (3) an appropriate alignment of the absorption and emission transition moments and their separation vector and (4) a sufficiently short distance (typically less than 10 nm) between the donor and acceptor.



Scheme 3 Energy transfer cassette based on FRET.^[105]

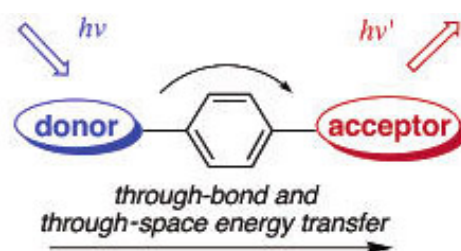
For example, FRET pairs **272** and **273** (Scheme 4) consist of the donor coumarin and the acceptor rhodamine dyes. Being excited in aqueous phosphate buffer at wavelengths where the coumarin donor moiety absorbs, they do not show any emission of the donor (coumarin) part. Instead, strong emission of the rhodamine acceptor around 590 nm was observed.^[106] This behavior is consistent with the very efficient intramolecular energy transfer between two dyes (with energy transfer efficiencies E 96.1% and 97.3%, respectively). The rigid piperazinyl linker connecting two fluorophores was found to be important for the efficient energy transfer. Thus, pseudo-large Stokes shifts of around 170 nm with good fluorescence QYs in aqueous media were obtained, a result which otherwise would be extremely difficult to realize using only one fluorophore. The drawback of

this approach is that an emission can be caused by exciting not only the donor, but also the acceptor part of the dyad.



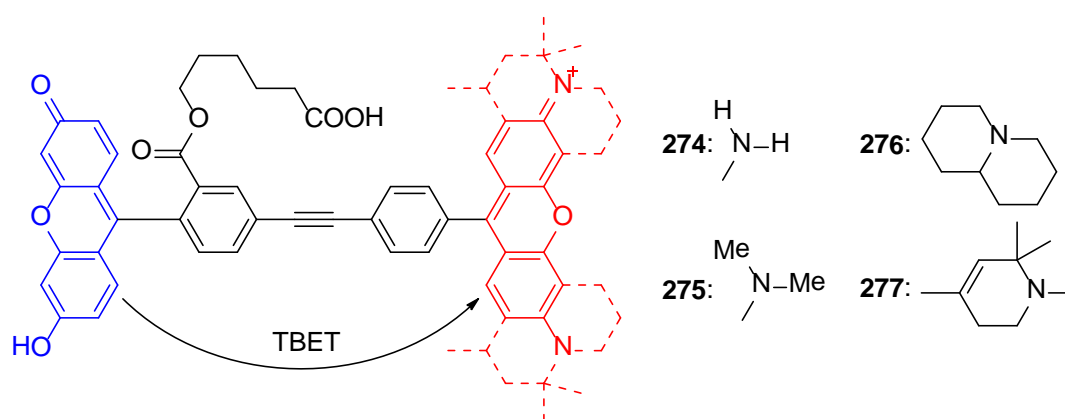
Scheme 4 FRET in 7-*N,N*-Diethylaminocoumarin-*N',N'',N''',N'''*-tetraethylrhodamine dye pairs **272–273**.

Although the FRET-based cassettes allow increasing apparent Stokes shift, this approach is still constrained by the requirement that the fluorescence of the donor must overlap with the absorption of the acceptor. If the donor and acceptor are linked by a π -electron system, the radiationless electronic energy transfer through bonds (Dexter and super-exchange mechanisms^[107]) and through space (Förster mechanism) may occur (Scheme 5). If the through-bond energy transfer (TBET) is fast relative to non-radiative decay pathways, then, unlike FRET-based cassettes, TBET is not constrained by this requirement. A good TBET-based cassette for labeling biological systems should meet the following requirements: (1) a strong absorbance of the donor component at the excitation wavelength, (2) a large fluorescence QY of the acceptor component, (3) the presence of a suitable linker which prevents the system from becoming planar and, therefore, from behaving as a single conjugated dye.^[105] TBET-based cassettes enable greater freedom for the selection of fluorophores than FRET-based ones. They can provide larger Stokes shifts and extend their emission further into the IR wavelength region.^[103]



Scheme 5 Energy transfer cassette based on TBET.^[105]

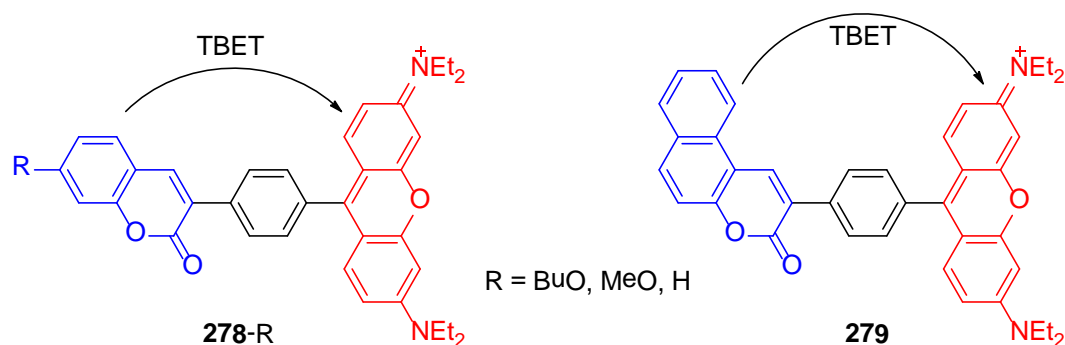
For example, compounds **274–277** (Scheme 6) display absorption maxima which are characteristic for their donor and acceptor components. They all have a fluorescein fragment and, therefore, absorb strongly around 512 nm (in EtOH). Upon excitation with an Ar laser at 488 or 514 nm, these cassettes emit fluorescence at 538, 582, 603 and 616 nm (pseudo-Stokes shifts: 28, 70, 91 and 104 nm), respectively, and almost no fluorescence from the donor, which corresponds to nearly 100% energy transfer efficiency.^[105] Furthermore, the fluorescein fragment in cassettes **274–277** was found to be considerably more stable to photobleaching than fluorescein itself which is known to be poorly photostable. In a typical experiment, cassette **276** retained 95% of its original fluorescence level, whereas the fluorescence of fluorescein in the same solution had decreased by 55%. This behavior was attributed to a fast energy transfer from the fluorescein donor fragment to the rhodamine acceptor in the cassette. As a result, intersystem crossing cannot compete with this process, and the triplet states, which are believed to be the main cause of photobleaching in case of fluorescein, are not significantly populated.



Scheme 6 TBET in fluorescein-rhodamine dye pairs **274–277**.

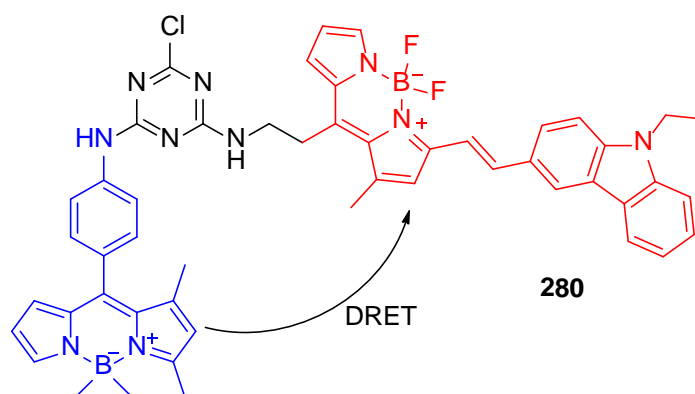
Remarkably, cassettes **278-R** and **279** (Scheme 7) have only negligible spectral overlap between the donor emission and the acceptor absorption bands.^[108] They displayed the absorption band of the rhodamine and coumarin parts at around 560 nm and 350 nm (in case of **278-R**) or 370 nm (for **279**), respectively. Upon excitation of the cassettes **278-R** and **279** in a solution of phosphate buffer with MeOH (3:2) at the coumarin absorption maximum, only the rhodamine emission at around 582 nm with moderate QYs (<27%) was observed. The absence of the coumarin emission indicates that the energy-transfer efficiencies were nearly perfect (>99%). The pseudo-Stokes shifts of up to 230 nm are

much larger than those of fluorescein-rhodamine TBET cassettes and those of the typical FRET-based rhodamine systems.



Scheme 7 TBET in coumarin-*N,N,N',N'*-tetraethylrhodamine dye pairs **278-R** and **279**.

If the donor dye in the FRET or TBET cassette has a very high value of the fluorescence QY, this may often lead to a fluorescence “leaking” from the donor due to inefficient energy transfer. In order to overcome this problem, the “dark” resonance energy transfer (DRET) concept was proposed.^[109] In this approach, a “dark” dye with very low fluorescence QY is used as the donor component. Upon excitation, a very efficient and fast energy transfer occurs due to large spectral overlap of the donor-acceptor pair and high extinction coefficient of the acceptor, despite the low quantum yield and short excited-state lifetime of the donor. For example, the absorption spectrum of compound **280** (Scheme 8) displayed a characteristic absorption band of the donor fragment (shown blue) at around 494 nm and an absorption band of the acceptor fragment at around 577 nm (shown red). Upon excitation of this compound with 470 nm light in EtOH, only the strong ($\Phi_{fl} = 0.38$) and characteristic emission of the acceptor part with a maximum at 617 nm was observed. Transient absorption spectra showed, that the decay profile of the donor alone only exhibited a single decay component of 33 ps, whereas the decay time constant of the donor component in the DRET-pair was much shorter (1.2 ps). These data led to the conclusion that the energy absorbed by the donor is efficiently transferred to the acceptor (96% efficiency) without quenching by any non-radiative intramolecular rotations.



Scheme 8 DRET in BODIPY-based dye pair **280**.

1.3 Applications of large Stokes shift dyes in fluorescence nanoscopy

There are not so many examples of studies in which a large Stokes shift dye (or its combination with a “normal” dye) is used as a fluorescent label in optical super-resolution microscopy. This is obviously due to the lower photostability and brightness of most dyes with large Stokes shift. However, there are some modern bright and photostable large Stokes shift dyes which have been successfully applied in optical “nanoscopy”. For example, the suitability of light from a multicolor stimulated-Raman-scattering (SRS) source for gaining STED resolution was successfully demonstrated with silica beads which were labeled with the commercially available coumarin dye ATTO425 and imaged in a simple custom-built STED microscope.^[110] Unlike the supercontinuum light source used in another STED microscope,^[16] the optical power of the SRS light source, which consists of a microchip laser coupled to a fiber where SRS occurred, is preserved within narrow peaks in a comb-like spectrum, the output light is linearly polarized, and light suitable for STED is produced below 630 nm. Thus, for ATTO425, STED was performed at 532 nm (the fundamental wavelength from the comb spectrum of the SRS light source). Excitation of the fluorophore was accomplished using a 440 nm diode laser. Due to simplicity, compactness, broad spectral output and low cost, SRS sources could become an attractive option for spectrally flexible STED imaging.

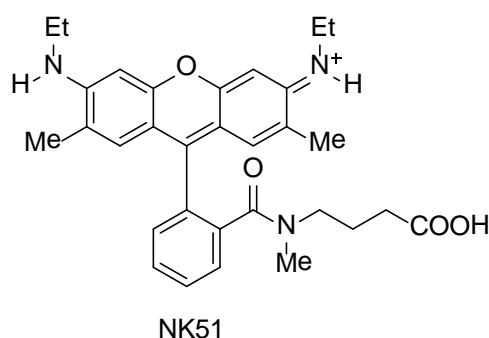


Figure 35 Rhodamine dye NK51.

In another report, the commercially available coumarin dye DY-485XL (see Table 1 for structure) was used together with the small Stokes shift rhodamine dye NK51 (Figure 35) to demonstrate the advantages and illustrate the principles of isoSTED (a combination of STED and 4Pi* microscopies to improve resolution along the Z-axis). Two-color isoSTED enables imaging of the spatial distribution of two or more (biological) objects at the nanoscale in three dimensions.^[19] The coumarin dye DY-485XL displays a similar emission spectrum as rhodamine dye NK51, whereas its excitation spectrum is blue-shifted by ~50 nm (Figure 36). This combination of fluorophores allowed using only one STED beam at 647 nm and two readily available excitation lasers with emission at 488 nm (for DY-485XL) and 532 nm (for NK51). In this study, mitochondrial outer membrane protein Tom20 was labeled by indirect immunostaining with dye DY-485XL, and the matrix protein mtHsp70 – with dye NK51. The images were recorded by subsequent excitation of the sample at 488 nm (channel 1) and 532 nm (channel 2) and depletion of the fluorescence by stimulating emission at 647 nm. The residual excitation cross-talk between two channels was efficiently removed by linear unmixing applied to the raw data. These dual-color images were the first example of the optical super-resolution microscopy providing separate images of two proteins of an organelle inside the whole cell with a nanoscale 3D resolution in the 50-nm range for both channels.

* 4Pi-microscope is a variation of confocal microscope, where the improvement in axial resolution achieved by using two opposing lenses focused to the same location.

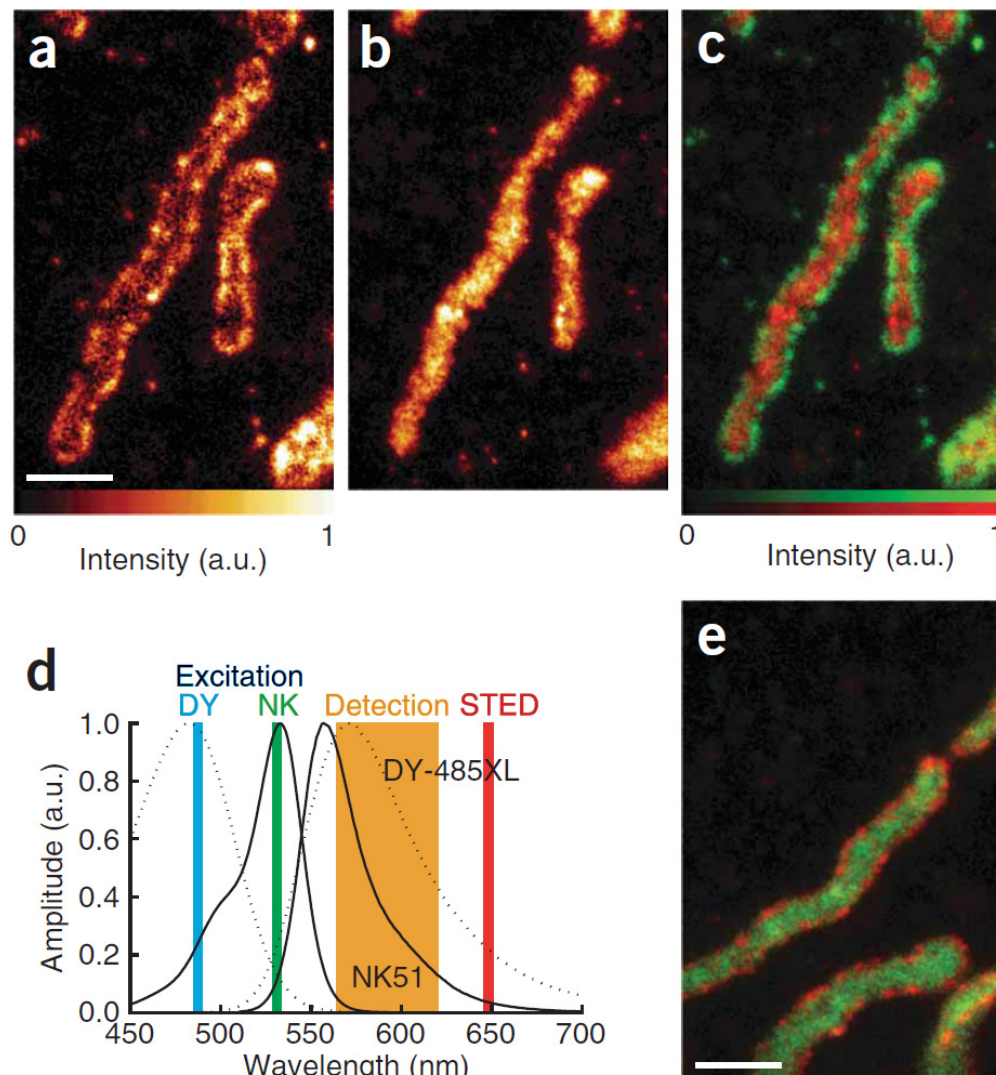


Figure 36 Two-color isoSTED imaging of mitochondria in Vero cells.^[19] (a,b) Distribution of the outer membrane protein Tom20 labeled with the organic fluorophore DY-485XL (a) and of the NK51-labeled matrix protein mtHsp70 (b). (c) Overlay of the two images showing Tom20 in green and mtHsp70 in red. (d) Excitation and absorption spectra for DY-485XL (dotted line) and NK51 (solid line). The two fluorophores are separated by subsequently exciting the sample at 488 nm (DY-485XL) and 532 nm (NK51). Both dyes are depleted by stimulated emission at 647 nm. (e) Reverse staining as a control (Tom20 with NK51 and Hsp70 with DY-485XL) yields similar results as the initial recording (c). Scale bars = 1 μ m.

Another commercially available coumarin dye DY-480XL with a large Stokes shift and the optical spectra similar to those of DY-485XL was used together with rhodamine dye KK114.^[111] This study dealt with an investigation of the spatial organization of the synaptotagmin 1 (Syt1) surface pool in hippocampal presynaptic boutons. For that, dual-color isoSTED microscopy^[112] was used. In order to reveal the localization of surface-stranded Syt1 at synapses, Syt1 was stained with KK114. The synapses were identified by labeling pre- and postsynaptic markers RIM1, RIM2 (RIM) and Homer1 with the dye

DY-480XL. The dyes were excited sequentially at fixed wavelengths of 530 nm (for DY-480XL) and 635 nm (for KK114). Since both dyes have similar emission spectra, STED pulses only at one wavelength of 775 nm were required. Emission of both fluorophores was detected in the range of 660–700 nm (in separate channels). After deconvolution, the final super-resolved images were obtained (see Figure 37).

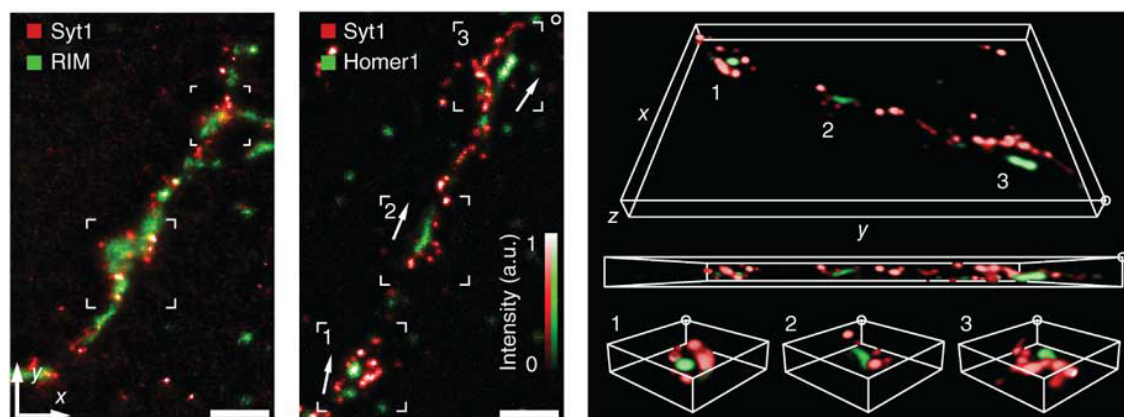


Figure 37 The localization of the surface-stranded protein Syt1 at synapses revealed by three-dimensional dual-color isoSTED nanoscopy.^[112] Syt1 was labeled with KK114 (red); postsynaptic markers RIM1, RIM2 (RIM) – with DY-480XL (green). Scale bars = 1 μm .

In material science, dual-color STED microscopy was successfully applied to localize and investigate the repartition of fluorescent polymer nanoparticles of ca. 100 nm size in nanofibers.^[113] Usually the BODIPY dyes are not used in STED microscopy due to their very small Stokes shifts (and therefore, a significant risk of re-excitation by the STED beam). However, the hydrophobic polymerizable BODIPY dye B504-MA (Figure 38) found to be applicable in STED nanoscopy. It was used to label the polymer nanoparticles, whereas the PVA matrix was stained with a water-soluble derivative of perylenetetracarboxylic acid (PTCA) which has a comparatively large Stokes shift. This combination of fluorophores allowed using the excitation by different lines of the same argon laser (458 nm for PTCA and 514 nm for B504-MA). The emission spectra of these fluorophores overlap considerably. Therefore, efficient depletion using a single STED beam at 592 nm could be achieved. The nanoparticle sizes and nanofiber thicknesses were shown to be in good agreement with the values obtained by electron microscopy.

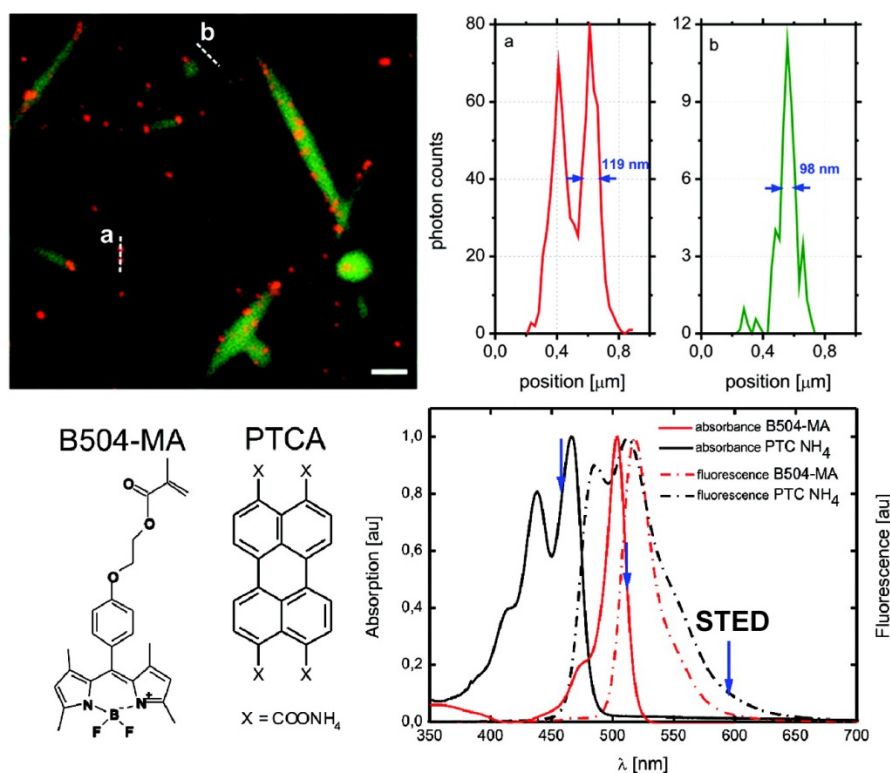


Figure 38 The STED image (raw data) of polystyrene nanoparticles (labeled with B504-MA, shown red) immobilized within PVA nanofibers (labeled with PTCA, shown green).^[113] Scale bar = 680 nm.

One of the brightest commercially available dyes with a large Stokes shift Chromeo494* was used together with a carbopyronine dye Atto 647N in a dual color STED microscopy in order to investigate the dynamics of and epidermal growth factor (EGF) epidermal growth factor receptor (EGFR) in living cells.^[114] For this purpose, a fused protein EGFR-SNAP_f expressed by HEK293 cells was labeled with BG-Chromeo494 (a conjugate of Chromeo494 with benzyl guanidine). The SNAP_f-sequence (polypeptide) also known as SNAP-tag specifically recognizes the BG conjugates and participates in an efficient S_N2-type reaction resulting in a permanent covalent bond between SNAP_f and the fluorophore. This methodology enables one to obtain the EGFR-SNAP_f-Chromeo494 conjugate. On the other hand, the recombinantly expressed fused protein EGF-CLIP_f was labeled with BC-ATTO647N (conjugate of ATTO647N with benzyl cytosine). Similarly to SNAP_f, CLIP_f sequence specifically recognizes BC derivatives. As a result of this reaction, the labeled exogenous protein EGF-CLIP_f-ATTO647N was formed. During incubation of EGFR-SNAP_f-Chromeo494 with EGF-CLIP_f-ATTO647N, EGF specifically

* Nowadays, a brighter dye with similar optical spectra – Abberior Star 520SXP – is available.

binds to EGFR. This resulted in the double staining of the EGFR-EGF complex with two dyes suitable for two-color STED imaging.

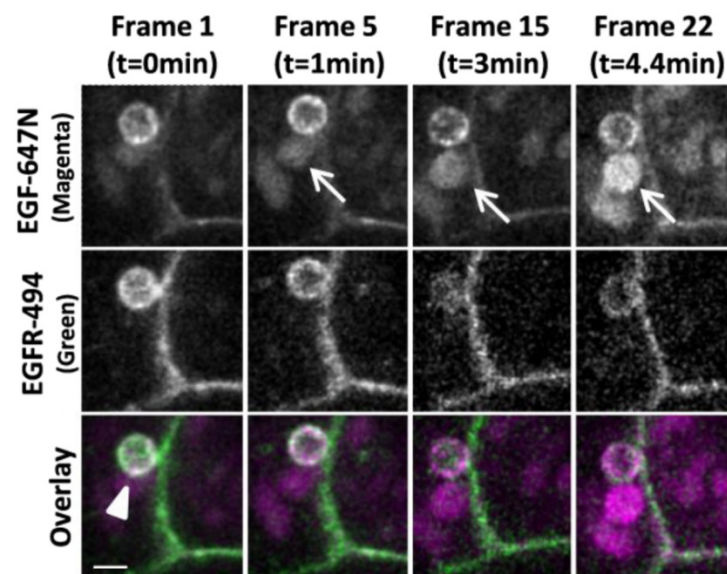


Figure 39 A time series of 2-color STED images (raw data) of living cells (HEK293) labeled with EGF-CLIP₇-ATTO647N (magenta) and EGFR-SNAP₇-Chromeo494 (green).^[114] Scale bar = 1 μ m.

Imaging was performed by sequential excitation of fluorophores with synchronized pulsed lasers at 532 nm (for Chromeo494) and 640 nm (for ATTO647N) and depletion with a tunable mode-locked Ti:Sapphire laser at 760 nm. A time series of STED images (see Figure 39) showed that shortly after EGF stimulation, an endosome-like structure containing the ATTO674N label began to form. This result was the first example of two-color live cell STED imaging and showed that STED microscopy has a great potential in revealing biologically relevant processes in living cells.

Owing to enhanced optical resolution, STED microscopy allows resolution of single vesicles in cells. Using dual color STED, Dean et al.^[115] found that after 15 min treatment of neurons with glycine (to induce neural activity), a vesicular transport protein synaptotagmin IV (syt-IV) was present on vesicles at synapses which are distinct from synaptic vesicles. At the same time, synaptotagmin I (syt-I) was shown to be localized to synaptic vesicles. For these experiments, syt-IV or syt-I were labeled with ATTO565, while synaptophysin (a protein ubiquitous in synaptic vesicles) was stained with the large Stokes shift dye DY-485XL. Excitation of ATTO565 was achieved with a diode laser at 532 nm. DY-485XL was excited with the 470 nm line from a laser diode source. STED

beam at 647 nm was used to deplete fluorescence of both dyes. Fluorescence detection for both dyes was realized in the window 560–600 nm.

In another report,^[116] two-color super-resolution STED microscopy was successfully used to assess the distribution of IQ motif containing GTPase activating protein (IQGAP1) and phosphorylated Rho GTPases Rac1 and Cdc42 as well as the change in their expression levels upon stimulation of *P. aeruginosa* cells with *N*-3-oxo-dodecanoyl-L-homoserine lactone (3O-C₁₂-HSL, a signaling molecule). IQGAP1 and Rac1/Cdc42 were immunochemically stained with ATTO647N and the large Stokes shift dye Abberior Star 470SXP, respectively. Images were acquired with a commercially available Leica TCS STED microscope.

Mace et al.^[117] revealed, using dual-color STED microscopy, that in natural killer cells NK92, lytic granules (specialized secretory lysosomes secreted by NK cells for the elimination of diseased and tumorigenic targets) are closely associated with F-actin and thus secreted through minimally sized clearances. For imaging, NK cells were fixed, permeabilized and stained for F-actin with phalloidin Alexa Fluor 488. The lytic granule component perforin was labeled with the large Stokes shift dye Pacific orange which was conjugated to the anti-perforin antibody.

In another example, topological mapping of presynaptic proteins with nanoscale resolution at the calyx of Held* was realized by dual-color STED microscopy.^[118] Two synaptic protein components, the vesicular glutamate transporter (VGluT1) and synapsin were indirectly labeled with Atto565 and the large Stokes shift dye DY-485XL, respectively, using standard immunohistochemistry protocols. Excitation was performed with pulsed laser irradiation at 470 nm (for DY-485XL) and 532 nm (for Atto565). A pulsed STED laser at 647 nm depleted the fluorescence of both fluorophores. The enhanced resolution provided by STED microscopy revealed synaptic vesicles lacking synapsin which was impossible to demonstrate using conventional confocal microscopy (Figure 40).

* Calyx of Held is a large synapse in the mammalian auditory central nervous system.

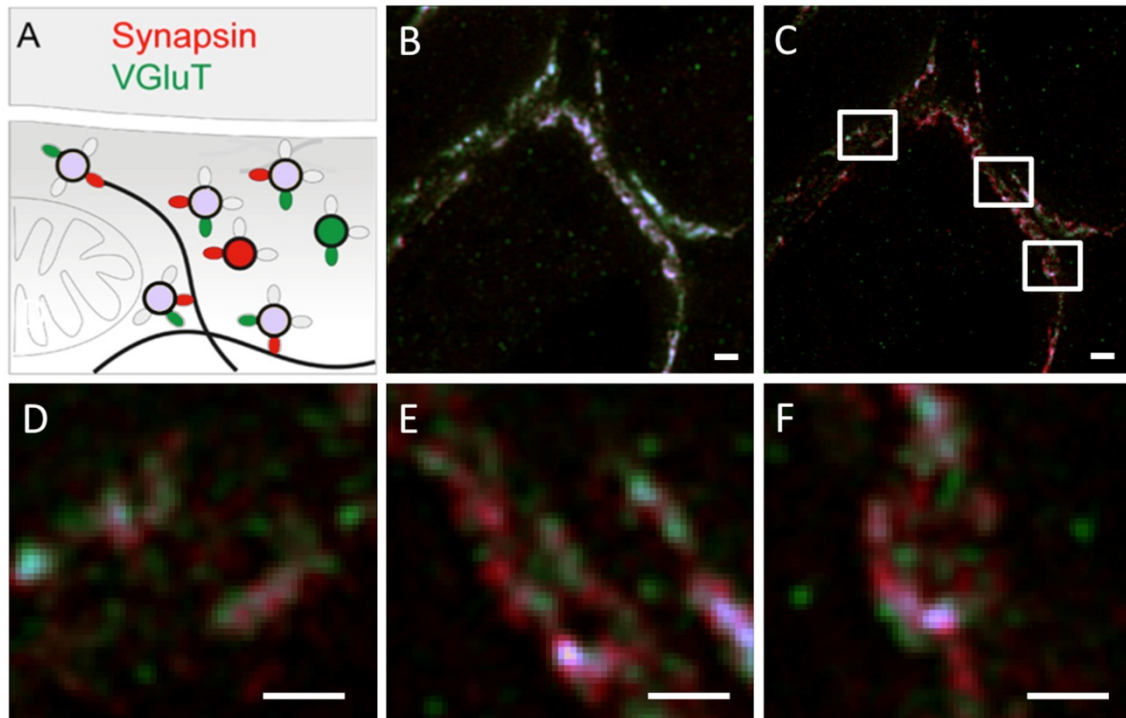


Figure 40 Dual color STED nanoscopy of synapsin (labeled with DY-485XL, shown red) and VGLuT1 (labeled with Atto565, shown green) distribution in the calyx of Held.^[118] (A) Schematic diagram depicting the hypothesized interplay of synapsin and synaptic vesicles (VGLuT1) in a glutamatergic terminal. (B) Dual-color confocal and (C) STED images of synapsin and VGLuT1 distribution in the calyx. Scale bars = 1 μm . (D,E,F) Magnified views of the subregions marked in C in clockwise order of their appearance. Scale bar = 500 nm.

The lateral resolution provided by STED (~ 70 nm) was sufficient to discriminate *cis*- and *trans*-Golgi cisternae in a HeLa cell, which are typically separated by at least 200 nm. In a test experiment on two-color STED imaging, transmembrane protein GPP130, which is localized to the *cis*-Golgi network, was labeled with the large Stokes shift dye Star 470SXP, whereas protein p230, which is found in the *trans*-Golgi network, was stained with Star 635.^[45b] Another large Stokes shift dye Star 520SXP together with Star 635 was used in a dual-color STED imaging experiment which allowed the assessment of the localization of collagen I (an abundant component of the extracellular matrix) within Golgi ministacks upon treatment with nocodazole and showed that collagen I is retained at the *cis* face.^[119] This result led the authors to a conclusion that the flow of collagen through the Golgi ministack was inhibited.

Dual-color STED microscopy provided morphological evidence for the organization of anoctamins (voltage sensitive calcium-activated chloride channels) and cyclic nucleotide-gated (CNG) channels in distinct domains, thus indicating the existence of signaling

microdomains in cilia of the olfactory sensory neuron (OSN).^[120] In addition, the staining patterns for anoctamins ANO2 and ANO6 observed in high-resolved STED images supported the idea that ANO2 and ANO6 form oligomeric complexes in olfactory cilia. Large Stokes shift dye V500 (BD Horizon) was used for staining tubulin, whereas anoctamins and CNG channels were immunochemically stained with Oregon Green 488 – a conventional dye with a small Stokes shift. Images were acquired using two excitation sources at 458 nm (for V500) and 514 nm (for Oregon Green 488) and one STED laser (592 nm). V500 and Oregon Green 488 emission was detected at 465–500 and 540–585 nm, respectively.

The large Stokes shift dyes Star 440SXP and Star 520SXP (Abberior) were utilized in colocalization studies on Norbin (neuron-specific cytosolic protein which interacts with the metabotropic glutamate receptor) and postsynaptic density protein 95 (PSD-95) in neurons.^[121] Neuron spines have a submicrometer size, and therefore all constituting proteins appear as more or less colocalized in a confocal microscope. Using super-resolution microscopy methods – 3D-SIM and STED, authors showed that Norbin associates with actin rather than with PSD-95 in dendritic spines.

In a study on the function of the Arf1/COPI protein machinery at cellular lipid droplets (LDs) in mammalian NRK cells, two-color STED microscopy revealed that β' COP (a component of COPI machinery) localize to the lipid droplet surface.^[122] For this study, β' COP and the LD marker perilipin3 were immunochemically labeled with the large Stokes shift dye Star 470SXP and the conventional dye ATTO647N, respectively. Images were acquired in a custom-built microscope with a STED laser tuned to either 760 or 770 nm for the depletion. Two pulsed diode laser lasing at 510 and 640 nm were used for the excitation of Star 470SXP and ATTO647N. Fluorescence detection was realized at 570–616 nm (for Star 470SXP) and 665–705 nm (for ATTO647N).

Using multiple super-resolution imaging techniques, including two-color gated STED (gSTED) microscopy, which provided spatial resolution down to ~50 nm, Johnson et al.^[123] found that endogenous TFG protein tightly colocalized with both inner and outer subunits of COPII (protein coating a vesicle which transports proteins from the rough endoplasmic reticulum to the Golgi apparatus). For immunochemical staining, large Stokes shift dyes Star 440SXP and DyLight 488 were used together with small Stokes

shift dyes Alexa Fluor 488, 568 and 647. Imaging was performed using the commercial Leica TCS STED system.

2 Main part

2.1 3-Heteroaryl-substituted coumarin dyes

2.1.1 Motivation and key structural elements

Coumarins are unique among other fluorophores with large Stokes shifts caused by photoinduced ICT. Many coumarins combine moderately high extinction coefficients (20 000–50 000 and large Stokes shifts with good fluorescence quantum yields in polar protic solvents. The synthesis of coumarins has been pioneered long ago beginning with the work of Perkin^[124] published in 1868. Modern catalytic methods involving C-H activation^[125] represent one of the recent highlights in this area. Most of these synthetic methods are simple, rather straightforward, and require available starting materials and a relatively small number of synthetic steps.

In all coumarin dyes presented in this work, 7-*N,N*-dialkylaminocoumarin ($\lambda_{\text{abs,max}}/\lambda_{\text{em,max}} = 380/460$ nm in MeOH for 7-*N,N*-diethylaminocoumarin) was chosen as a starting scaffold for the design of new fluorescent dyes with large Stokes shift. The introduction of a 2,2,4-trimethyl-1,2-dihydropyridine ring provides a small red-shift of 5-10 nm,^[45a] rigidizes the dye skeleton, improves the photostability and anchors the 7-amino group preventing the coumarin from transition to a non-emissive TICT state,^[21d, 21e, 21g, 35] and thus enhancing the fluorescence QY in polar solvents. The methyl group at the double bond can be easily modified to introduce various polar groups, such as hydroxyl, sulfonate, phosphonate or phosphate. These groups increase the solubility in aq. media and prevent the fluorophores from aggregation, thus improving the fluorescence QY. At the same time, they are known to have only a minor effect on the positions of absorption and emission maxima.

Unlike alkylsulfonic acids, monoalkyl phosphates and alkylphosphonic acids are dibasic acids. Therefore, upon dissociation they give doubly charged anions which are less prone to aggregation and non-specific binding than the monocharged sulfonates. Comparison of pK_a^1 and pK_a^2 values for monoalkyl phosphates vs. alkylphosphonic acids (1.54–1.80 and 6.31–6.84 vs. 2.33–2.74^[126] and 7.76–8.48,^[127] respectively) leads to a conclusion that at physiological pH of 7.3–7.4 the former compounds are better ionized (and their aggrega-

tion is suppressed more efficiently). Due to the double negative charge, monoalkyl phosphates are resistant to nucleophilic attacks and, in particular, to basic hydrolysis. Taking into account all these pieces of information we chose the monophosphate ester as a polar solubilizing unit for the fluorescent dyes presented in this work.

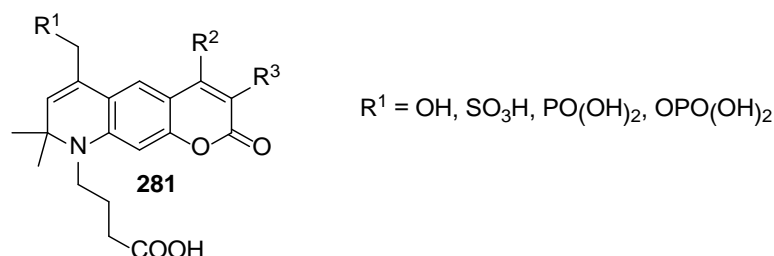


Figure 41 Coumarins with the 2,2,4-trimethyl-1,2-dihydropyridine fragment and various polar groups.

The carboxylic acid residue in coumarin **281** (see Figure 41) is required for bioconjugation. It can be activated by formation of an amino-reactive ester (e.g. an *N*-hydroxysuccinimidyl ester), and used in the reaction with biomolecules having free amino groups (e.g. proteins). The carboxylic group may be attached to the nitrogen via a linker with variable length. A linker having three CH_2 groups was found to provide better hydrolytic stability of *N*-hydroxysuccinimidyl esters than a shorter linker derived from propanoic acid.^[111b]

The substituents R^2 and R^3 determine the photophysical properties of the coumarin fluorophore. They can be varied to a great extent. It is known that electron-acceptor groups at C-3 and/or C-4 of the coumarin fragment facilitate the degree of ICT and increase “push-pull” effects in the fluorophore. Therefore, these groups determine the positions of absorption and emission bands, and can shift them towards the red end of the visible spectrum.

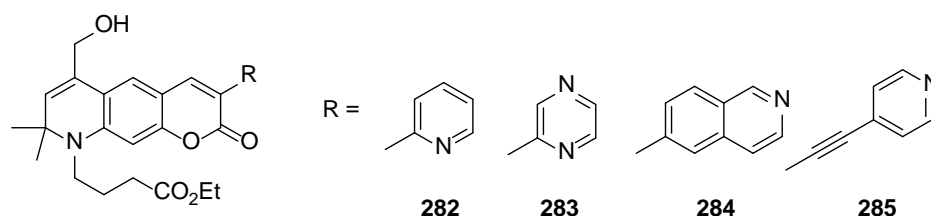
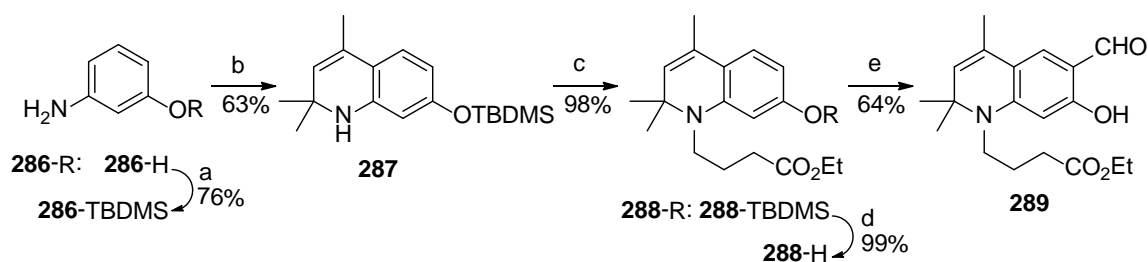


Figure 42 Model coumarins **282–285** with a variable electron-acceptor group at C-3.

7-Amino-3-phenylcoumarins have an attractive combination of large Stokes shifts and acceptable QYs in polar solvents.^[42] However, their absorption bands are found in the violet region of the visible spectrum. One can expect that the introduction of a strong electron-withdrawing substituent on the phenyl ring could provide red-shifts in absorption and emission bands. Many electron-withdrawing groups are available, and their acceptor properties were quantified as σ -constants in the Hammett equation. In this regard, the nitro group represents an interesting candidate as it is relatively easy to introduce, and it has one of the largest values of the σ -constant (0.78).^[128] Unfortunately, fluorophores containing the nitro group often display very poor emission efficiency in polar solvents (probably, due to formation of the non-emissive TICT state). On the other hand, it is known that many properties of nitrobenzene are similar to those of pyridine. Due to the larger electronegativity of the nitrogen atom (in comparison to the carbon) and the inability of the lone electron pair to participate in delocalization, pyridine represents a π -deficient heterocycle, and 2-pyridyl and 4-pyridyl groups exhibit strong $-I$ and $-M$ effects. Indeed, an introduction of 2- or 4-pyridyl groups at C-3 of the 7-*N,N*-dialkylamino-coumarin scaffold provided a bathochromic shift of ~ 20 nm (in EtOH) in comparison with analogous 3-phenyl-substituted coumarins.^[21f] The pyrazinyl group has an additional nitrogen atom in the cycle which further increases the π -deficiency. The quinolyl and isoquinolyl groups provide an extension of the conjugation chain and can cause further bathochromic and bathofluoric shifts. We expected that a 4-pyridylethynyl group would also provide an extension of the conjugation chain and a small $-M$ -effect enhanced by the neighboring π -deficient pyridine ring. Thus, at the beginning of this work, we decided to synthesize coumarins **282–285** without phosphate groups (see Figure 42). This would allow us to evaluate and compare the properties of the said groups, and probably obtain dyes with large Stokes shifts and good fluorescence QYs. In view of the apparent lack of photostable and bright fluorescent dyes applicable in two-color STED imaging (only a few fluorescent dyes were successfully applied in two-color STED: DY-480XL, DY-485XL, Chromeo 494, Abberior STAR 440SXP), the design of new dyes with large Stokes shift is particularly important. Moreover, live-cell imaging requires more cell-permeable dyes for all spectral regions.

2.1.2 Synthesis of model compounds

The universal coumarin precursor **289** was prepared in five steps starting from commercially available *m*-aminophenol **286-H** (see Scheme 9). First, the phenolic residue in compound **286-H** was protected with *t*-butyldimethylsilyl chloride (TBDMSCl) using the standard protocol. The protected TBDMS derivative **286-TBDMS** was then converted to 2,2,4-trimethyl-1,2-dihydroquinoline **287** using a modified Skraup reaction with acetone catalyzed by anhydrous Yb(OTf)₃.^[129] The anilinic nitrogen in compound **287** is hindered by adjacent methyl groups, and its alkylation required relatively harsh conditions. Nevertheless, reaction of ethyl 4-iodobutanoate with **287** in neat DIEA at 110 °C afforded the ester **288-TBDMS** after 48 h in an excellent yield. Next, the hydroxyl group in **288-TBDMS** was deprotected with tetrabutylammonium fluoride in THF, and the resulting phenol **288-H** was then formylated according to Vilsmeier-Haack to furnish the silicic aldehyde **289**.

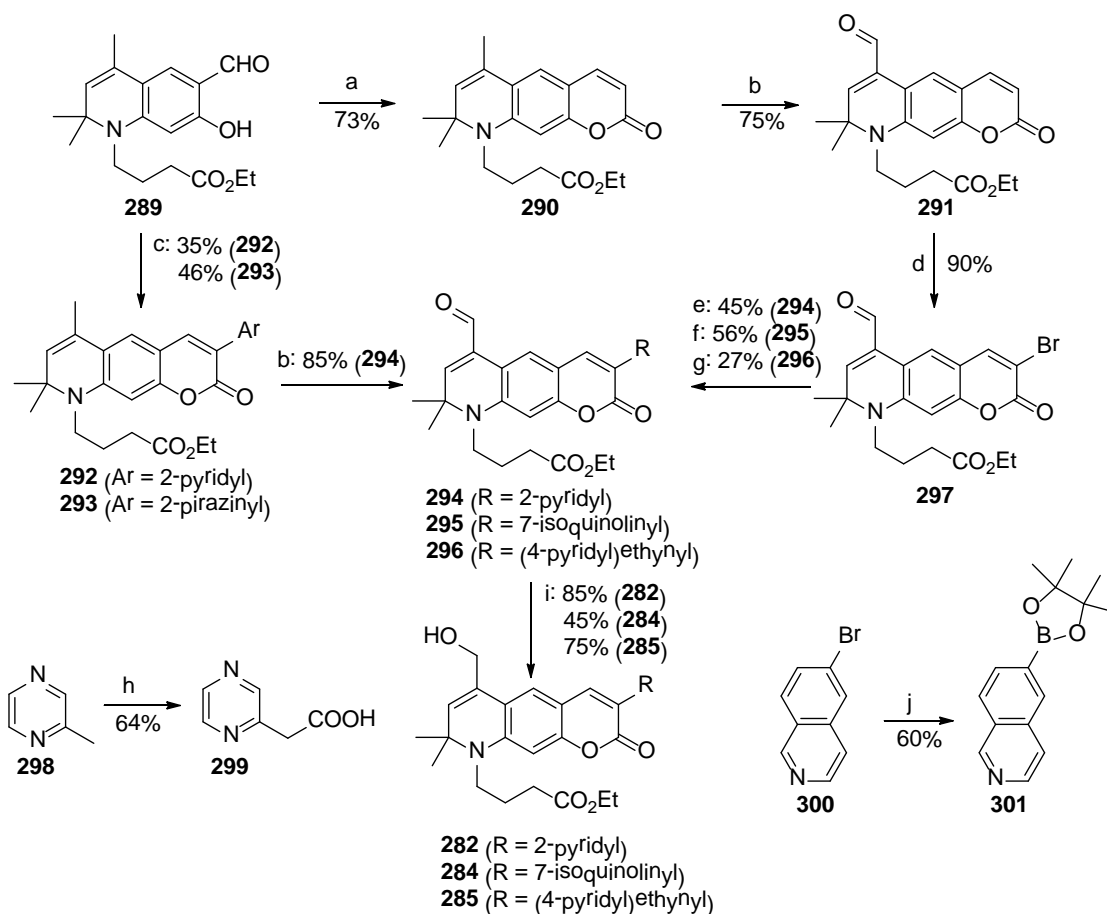


Scheme 9 Synthesis of the universal precursor **289**: a) TBDMSCl, imidazole, DMF, 0 to 55 °C, 2 h; b) acetone, Yb(OTf)₃, r.t., 16 h; c) ethyl 4-iodobutanoate, DIEA, 110 °C, 48 h; d) TBAF·3H₂O, THF, 0 °C, 5 min; e) POCl₃, DMF, 60 °C, 1.5 h.

In order to obtain the target dyes **282–285** using precursor **289**, two synthetic approaches were employed. According to the first approach, the coumarin ring was formed in the course of the esterification reaction which involved phenol **289** and a heteroaryl acetic acid followed by a Knoevenagel condensation (route *c* in Scheme 10). 2-Pyridylacetic acid is commercially available. 2-Piperazinylacetic acid **299** was conveniently prepared by lithiation of 2-methylpiperazine **298** with *t*BuLi followed by quenching the resulting lithiated derivative with dry ice. In initial experiments we found out that compound **299** being dissolved in ethyl acetate readily loses carbon dioxide, if the solution is evaporated at elevated temperatures (>40 °C). To our delight, when all operations were performed at room temperature or below, the compound **299** could be isolated with a moderate yield.

This tendency to lose carbon dioxide is even more pronounced in the case of (6-methylpyrimidin-4-yl)acetic acid: in an attempted synthesis according to the same method, the decarboxylation readily occurred already upon acidification of the reaction mixture (even at low temperatures).

The second approach employs 3-bromocoumarin **297** and its Pd-catalyzed cross-coupling reactions with 2-(tributylstannyl)pyridine (route *e*), boronic ester **301** (route *f*) or 4-pyridylacetylene (route *g*). Aryl bromide **297** was obtained from the universal precursor **289** in three steps. First, the coumarin ring was formed in the course of a Wittig reaction of **289** with (ethoxycarbonylmethylene)triphenylphosphorane followed by the cyclization reaction. In initial trials we tried to brominate compound **290**, but along with the desired aryl bromide, we also obtained substantial amounts of the corresponding allyl bromide. Therefore, before the bromination, we oxidized the methyl group attached to the C=C bond into a formyl group using SeO₂ in dioxane. Final bromination of aldehyde **291** proceeded smoothly and rapidly in acetic acid at room temperature and afforded the required bromocoumarin **297** in a high yield.



Scheme 10 Synthesis of the model 3-substituted coumarins **282**, **284** and **285**: a) (ethoxycarbonylmethylene)triphenylphosphorane, xylene, 140 °C, 3 h; b) SeO₂, dioxane, reflux, 2 h; c) heteroarylacetic acid, EDC·HCl, NEt₃, DMAP, CH₂Cl₂/DMF, 30 °C, 20 h; d) Br₂, AcOH, r.t., 15 min; e) 2-(tributylstannyl)pyridine, Pd(PPh₃)₄, dioxane, 110 °C, overnight; f) **301**, Pd(PPh₃)₄, 2 M aq. Na₂CO₃, toluene, 110 °C, overnight; g) 4-ethynylpyridine, Pd₂(dba)₃, P(*t*Bu)₃, CuI, NEt₃, THF, r.t., 8 h; h) MeI, MeCN, 70 °C, overnight; i) NaBH₄, CeCl₃, THF/MeOH, 0 °C, 15 min; k) LDA, THF, -78 °C, 1 h; then CO₂, -78 °C → r.t., overnight; l) *t*BuLi, THF, -78 °C, 20 min; then B(O*i*Pr)₃, -78 °C → r.t., overnight; then AcOH, pinacol, r.t., 2 h.

Having coumarin **297** at hand, we tried to perform Stille, Suzuki and Sonogashira reactions and obtain compounds **294–296** with 2-pyridyl, 7-isoquinolinyl and (4-pyridyl)ethynyl groups, respectively. The Stille and Suzuki coupling reactions employed Pd(PPh₃)₄ as a catalyst and proceeded in a clean fashion, although the preparative yields did not exceed 56%. In contrast, a Sonogashira reaction in the presence of Pd(PPh₃)₄ and CuI did not occur at all. When Pd₂(dba)₃ and P(*t*Bu)₃ were used to form a more active Pd-catalyst in the reaction mixture, a very low conversion of **297** was observed, even when the whole amount of alkyne was consumed. Only with a two-fold excess of 4-ethynylpyridine which was added to the reaction mixture in four portions over an eight-

hour interval, we obtained a modest yield (27%) of **296** and observed a 33% conversion of the starting material **297**. Pinacol boronate **301** was prepared from 6-bromoisoquinoline **300** in the course of a lithium-halogen exchange followed by a reaction of the resulting organolithium compound with $B(OiPr)_3$, and a transesterification of the intermediate diisopropyl boronate with pinacol in the presence of acetic acid. 4-Ethynylpyridine was kindly provided by Dr. S. Nizamov.

Reduction of conjugated aldehydes **294–296** to the corresponding allylic alcohols can be complicated by 1,4-reduction. In order to minimize the amount of undesired products resulting from 1,4-reduction, we utilized Luche's reduction procedure.^[130] According to it, $NaBH_4$ in the presence of $CeCl_3$ reduced compounds **294–296** in the 1,2-fashion and afforded model coumarins **282,284** and **285**.

2.1.3 Spectral properties of model coumarin dyes

Table 9 presents the most important photophysical properties of compounds **282**, **284**, **285** and **293**. Thus, coumarin **293** with a pyrazinyl group at C-3 has the absorption maximum at 451 nm, when dissolved in CH_2Cl_2 or MeOH. Upon excitation, it emits green light with the maximum at 506 (in CH_2Cl_2) or 535 nm (in MeOH). The observed bathochromic shift of 29 nm upon transition from CH_2Cl_2 to MeOH corresponds to the general trend exhibited by many other coumarin dyes.^[21e] This behavior is attributed to a better stabilization of the excited state S_1 by a more polar solvent. The red-shift of the fluorescence maximum is also accompanied by a significant decrease of fluorescence quantum yield from 0.78 in CH_2Cl_2 to 0.08 in MeOH. One possible explanation of this phenomenon could be a photoinduced electron transfer (PET) accelerated in polar MeOH. In the course of this process, in the excited state S_1 , an electron from one of the lone pairs of the pyrazine moiety fills the vacant place in the half-occupied HOMO of the fluorophore, and thus makes the emission impossible. This kind of electron transfer can take place only if the molecular orbital, which contains the lone pair electrons, has a higher energy than the HOMO of the fluorophore in the ground state. A comparison of the calculated energies for the highest-energy orbital, which is occupied by the electron lone-pair, in nitrogen heterocycles gave the following values for pyrazine and pyridine: -10.25 eV and -9.93 eV, respectively (by AM1 method).^[131] These values were also in accordance with experimental pK_a -values (0.4 and 5.2),^[132] and revealed that a PET from the nitrogen atom in

the pyridine moiety should proceed more readily. In contrast to this conclusion, coumarin **282** with a 2-pyridyl fragment shows no sign of emission quenching and displays a high fluorescence QY in MeOH. Another explanation of the fluorescence quenching might be formation of a hydrogen bond between the lone electron pairs of the 2-pyrazinyl moiety in **293** in the excited state S_1 and a molecule of MeOH. This phenomenon may create an additional non-radiative decay path for compound **293**. If this explanation were true, it is still unclear why the same interaction does not lead to the fluorescence quenching in the case of compound **282**.

The positions of absorption and emission maxima for compound **282** were found to be close to those of the analogous dye **56** possessing the julolidine fragment.^[21f] The transition from a 2-pyridyl to a 7-isoquinolinyl substituent (compound **284**) did not influence the shape and the position of the long-wavelength absorption maximum, but provided a small bathofluoric shift of 13 nm, thus increasing the observed Stokes shift from 67 to 80 nm. Coumarin **285** with a (4-pyridyl)ethynyl substituent at C-3 had the most red-shifted absorption maximum in this series, but its value of Stokes shift (54 nm) turned out to be rather low: the emission maximum was centered at 511 nm. All coumarins **282**, **284–285** displayed high fluorescence QYs in MeOH in the range of 0.62–0.72. Due to these attractive spectral properties model coumarins **282**, **284–285** were chosen for further development (phosphorylation).

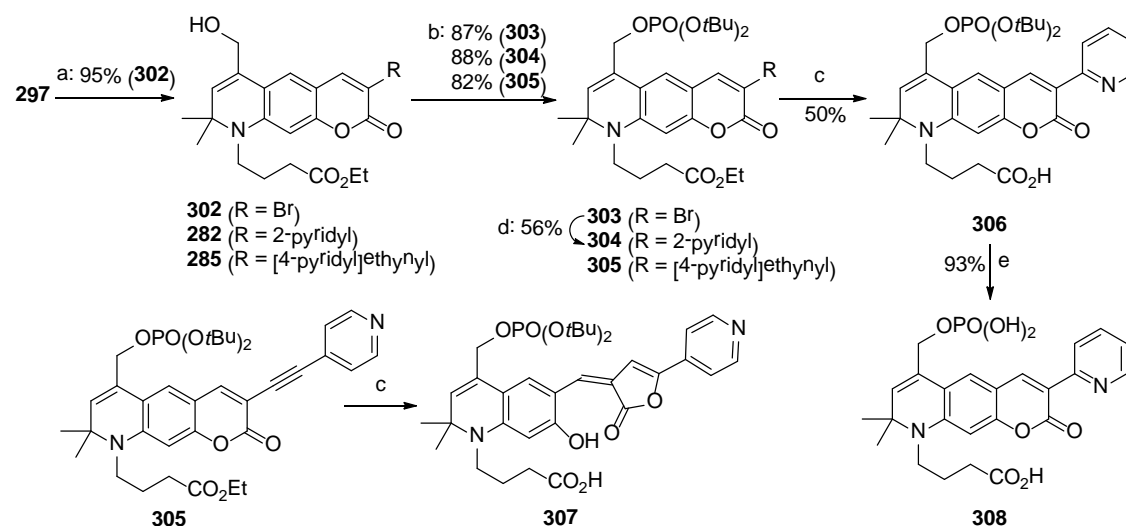
Table 9 Spectral properties of model coumarins **282**, **284**, **285**, **293** and phosphorylated coumarin **43** in various solvents.

Compound	$\lambda_{\text{abs,max}}$, nm	ϵ , $\text{M}^{-1}\cdot\text{cm}^{-1}$	$\lambda_{\text{em,max}}$, nm	$\Delta\lambda$, nm	Φ_{fl}	Solvent
282	431	32000	498	67	0.67	MeOH
284	431	41100	511	80	0.72	MeOH
285	457	44200	511	54	0.62	MeOH
293	451	39200	506	55	0.74	CH_2Cl_2
293	451	39600	535	84	0.08	MeOH
308	432	20400	512	80	0.81	PBS 7.4

2.1.4 Synthesis of water-soluble coumarins with a phosphate group

For the synthesis of 3-heteroaryl-substituted coumarins with a phosphorylated CH_2OH group we used the route presented in Scheme 11. Aldehyde **297** with the bromine substituent at C-3 was reduced using Luche's reduction method.^[130] According to the known procedure,^[133] alcohol **302** readily reacted with di-*tert*-butyl *N,N*-diisopropylphosphoramidite in the presence of 1*H*-tetrazole and gave the intermediate phosphite which was not isolated and directly oxidized in the reaction mixture with *m*CPBA providing the phosphate **303** in a high preparative yield (87% in two synthetic steps).

At this point, we tried to improve the synthetic yield of the cross-coupling reactions of bromide **303** in comparison with the analogous reactions of **297** (see section 2.1.2) and, at the same time, to reduce the possibility of any side reactions at high temperatures. For this purpose, we attempted a cross-coupling reaction of coumarin **303** with 2-(tributylstannyl)pyridine at room temperature in the presence of a highly active Pd catalyst prepared *in situ* from $\text{Pd}(\text{OAc})_2$ and $\text{P}(\text{tBu})_3$. Unfortunately, at room temperature, this reaction did not proceed at all. At 110 °C, the starting bromide **303** had disappeared completely in the reaction mixture after 2 h. However, the coupling product – coumarin **304** with the 3-(2-pyridyl) substituent – was isolated with an only moderate yield of 56%.



Scheme 11 Synthesis of water-soluble coumarins with a primary phosphate group: a) NaBH_4 , CeCl_3 , THF/MeOH , 0 °C, 15 min; b) $i\text{Pr}_2\text{NP}(\text{OtBu})_2$, 1*H*-tetrazole, CH_2Cl_2 , 40 °C, 1 h; then *m*CPBA, 0 °C, 15 min; c) aq. NaOH , THF/MeOH , r.t., overnight; d) 2-(tributylstannyl)pyridine, $\text{Pd}(\text{OAc})_2$, $\text{P}(\text{tBu})_3$, toluene, 110 °C, 2 h; e) TFA, CH_2Cl_2 , r.t., 1 h.

The same phosphorylation procedure^[133] was applied to coumarins **282** and **285** and provided phosphates **304** and **305** in good yields of 88 and 82%, respectively. Compounds **304** and **305** already have all the functionalities required for the new 3-heteroaryl-coumarin dyes. The carboxylic acid and phosphate groups are orthogonally protected as ethyl and *tert*-butyl esters, respectively. They should be removed in the next synthetic steps. Isolation and handling of free phosphates involves aqueous solutions and reverse-phase chromatography. Thus, we decided to cleave the ethyl ester function first. Saponification of ester **304** afforded carboxylic acid **306** with a rather moderate yield of 50%. A possible side reaction, which may decrease the yield of the desired product, could involve the opening of the coumarin ring followed by the formation of a salt of *cis*-coumarinic acid. This process is known to be reversible, and the cyclization to the starting coumarin takes place upon acidification. However, under prolonged action of a base, the *cis*-coumarinate isomerizes to the *trans*-isomer which cannot cyclize back to the starting coumarin upon acidification.^[33] Both *tert*-butyl groups in compound **306** were easily removed upon treatment with trifluoroacetic acid, and the target dye **308** was isolated in an excellent yield.

Unexpectedly, all attempts to saponify the ester function in coumarin **305** having a (4-pyridyl)ethynyl substituent did not result in the required product. After addition of 1 M NaOH to a solution of ester **305** in a THF/MeOH mixture, the reaction mixture immediately changed its color from yellow-green (characteristic for coumarins **282**, **284–285**, **304** and **305**) to dark-red. Thin-layer chromatography showed the presence of a red-colored and weakly fluorescent compound as a main product. Although this product was not isolated, we suspect that the basic hydrolysis led to the opening of the coumarin ring, and the resulting carboxylate anion attacked the triple bond which is activated towards a nucleophilic addition by the presence of the neighboring pyridine ring. If this is true, then compound **307** with a five-membered lactone ring and an extended π -conjugated system was formed, and this can explain the appearance of the intense red color.

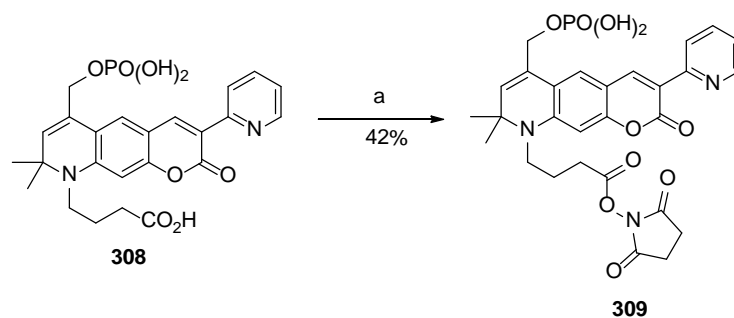
2.1.5 Spectral properties and imaging performance of coumarin **308**

As expected, the phosphate residue in compound **308** provided solubility in aqueous PBS buffer (pH 7.4) and a large fluorescence quantum yield. Upon dissociation of the phos-

phate group, dye molecules gain negative charges. Due to electrostatic repulsion, the resulting anions are much less prone to aggregation which is believed to be responsible for the reduced fluorescence quantum yields observed for the hydrophobic dyes in polar solvents.^[134] In coumarin **308**, the introduction of the phosphate group and the transition from MeOH to the aqueous buffer did not change the position of the absorption maximum (see Table 9). However, the value of molar absorptivity became somewhat smaller in comparison to the parent dye **282**. The position of the fluorescence maximum of phosphorylated coumarin **308** shifted towards longer wavelengths by 14 nm and resulted in a larger Stokes shift of 80 nm.

To prepare bioconjugates for immunochemical staining, the dye must be attached to an antibody or another target molecule by means of a strong covalent bond. This bond must be stable enough and withstand such operations as chromatography, washing, permeabilization, fixation and mounting (in the case of immunochemical staining). In this respect, a peptide bond between the carboxylic group of the dye and a primary amino group represents a viable option. If we consider the labeling of antibodies, modification of lysine residues, due to their relatively high abundance in mammalian proteins, may provide high degrees of labeling and improve the fluorescence signal. For the formation of a peptide bond in aqueous medium, the carboxylic group of any dye (and coumarin **308**) must be converted to an active ester, such as *N*-hydroxysuccinimidyl, 4-sulfotetrafluorophenyl, tetrafluorophenyl or sulfodichlorophenyl ester, or to a carbonyl azide.^[135] *N*-Hydroxysuccinimidyl esters provide a good balance between the reactivity towards amines and hydrolytic stability under basic conditions (pH > 7–8). Under these conditions the aliphatic amines cannot be protonated, and therefore, they readily undergo acylation.

The *N*-hydroxysuccinimidyl ester **309** was prepared from *N*-hydroxysuccinimide and coumarin **308** which was activated with HATU in the presence of NEt₃ (Scheme 12). In order to reach complete conversion of the starting dye, the long reaction time (16 h) and large excesses of *N*-hydroxysuccinimide, HATU and NEt₃ were used. However, the overall reaction was not clean, and the preparative yield of **309** was only modest (42%). This result may be explained with competitive esterification of the phosphate group.^[136]



Scheme 12 Synthesis of NHS-ester **309**: a) *N*-hydroxysuccinimide, HATU, Et₃N, DMF, r.t., 16 h.

The performance of the phosphorylated coumarin **308** in optical microscopy is illustrated in Figure 43. This figure shows the images of microtubules immunolabeled with dye **308** bound to secondary antibodies. Pictures in Figure 43 represent confocal and STED images obtained in a fluorescence microscope. The superresolution STED image was acquired using a 405 nm laser as the excitation source, the STED beam applied at 590 nm and the detection window between 510 and 560 nm. Under these conditions, the new dye provided an optical resolution of ca. 50 nm. Owing to its large Stokes shift (80 nm) and the emission band which overlaps with the emission of dyes Alexa Fluor 488 and Oregon Green (with small Stokes shifts), phosphorylated coumarin **308** can be successfully employed in multicolor STED experiments. Similar dyes were already used in single-color STED microscopy and showed sub-diffractive optical resolution of approximately 70 nm.^[137] For realizing a two-color STED imaging using one of these dyes and coumarin **308**, it is sufficient to add to the optical setup a second laser for the excitation (at 488 nm) of Alexa Fluor 488 or Oregon Green dyes.

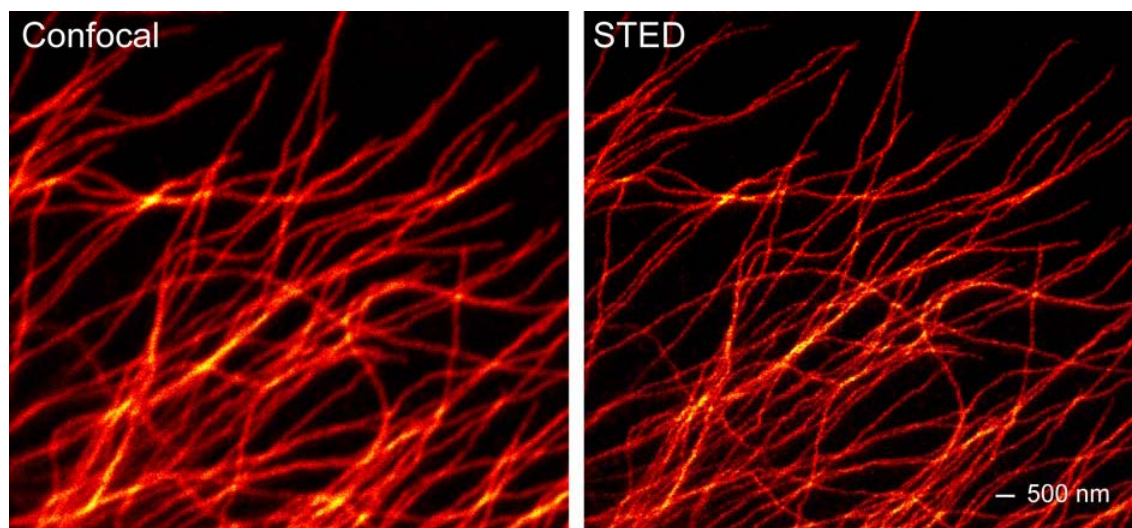


Figure 43 Confocal and STED microscopy images of microtubules stained with coumarin **308**. The mammalian cell was fixed and immunolabeled with a primary and secondary antibody (the latter was conjugated with compound **308**). Excitation at 405 nm; detection at 510–560 nm; STED at 590 nm (STED power ca. 84 mW at the back focal plane).

2.1.6 Conclusion and outlook

New coumarins with 3-heteroaryl and a 3-(4-pyridyl)ethynyl groups have been prepared from the universal precursor **289** using two different synthetic routes. These approaches enabled us to shift the absorption and emission maxima of new compounds towards the red spectral region. Thus, synthesized compounds **282**, **284–285**, **293** and **308** have absorption and emission maxima in the ranges of 431–457 nm and 498–535 nm, respectively. Coumarin **293** with 3-(2-piperidyl)-group had a low emission efficiency in MeOH, whereas compounds **282**, **284–285** and **308** provided good fluorescence QYs and large Stokes shifts. The presence of the primary phosphate group in coumarin **308** provided good solubility and a high fluorescence QY in aqueous media. The confocal and super-resolution images of microtubules stained with compound **308** demonstrated good signal-to-noise ratio and very good optical resolution (~ 50 nm under STED conditions). Detection and co-localization of various biological objects can be achieved with dye **308** and a conventional “green” dye with small Stokes shift (for example, Oregon Green 488), using one detection channel and two excitation sources (405 and 488 nm lasers, respectively). Compounds **284–285** also “deserve” further improvement by the introduction of polar groups, which is expected to increase their solubility in aqueous media, fluorescence QYs and brightness in optical microscopy.

2.2 3-Pyridiniumcoumarins

2.2.1 Motivation and key structural elements

As a rule, the neutral electron-withdrawing groups attached to C-3 and/or C-4 of the 7-aminocoumarin fluorophore do not shift the absorption maximum of the dye further than 450 nm.* Compounds **310** and **311** (Abberior Star 470SXP)^[45a] (Figure 44) possess the substituent at C-3 which has a betaine structure with the positively charged nitrogen atom; they absorb in the green region of the visible spectrum with a maximum at about 520 nm. The large bathochromic shift may be explained by strong $-I$ - and $-M$ -effects (for 4-*N*-methylpyridinium group $\sigma = 2.57$ ^[138] in the Hammett equation) of the quaternized pyridine ring which is in a direct polar conjugation with the amino group at C-7. As a result, this group facilitates the ICT from the 7-amino group shifting the absorption and emission bands towards the red region of the visible spectrum.

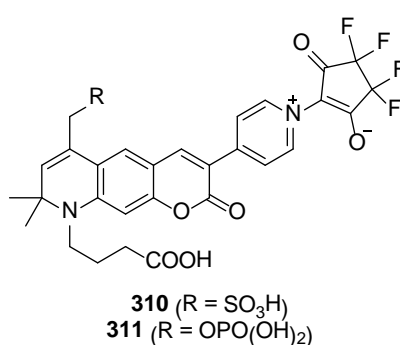


Figure 44 Coumarins **310** and **311**.

Despite the attractive spectral properties, coumarins **310** and **311** have very low fluorescence QYs in polar solvents. The presence of the tetrafluorocyclopentadienone fragment which can rotate around the C-N bond, thus creating an additional pathway for a non-radiative deactivation of the excited state S₁, might be responsible for poor emission efficiencies. Commercially available dyes DY-480XL, DY-481XL, DY-485XL, DY-510XL, DY-511XL, DY-520XL, DY-521XL possess a quaternized pyridine ring, attached to the 3-position of the coumarin via a *trans*-double bond. These dyes have spectral properties

* A notable exception is the combination of a CF₃-group at C-4 and an (hetero)arylvinyl group at C-3 which is known to produce large bathochromic and bathofluoric shifts.^[48]

similar to those of **310** and **311**, and their QYs have not been disclosed. The other dyes with large Stokes Shift, ATTO 490LS and Chromeo 494, also absorb in the yellow region, but their structures are unknown. Therefore, a direct comparison of their structures and properties with those of compounds **310**, **311** and Dyomics dyes is very difficult.

It is known that the boron-fluorine complexes with *N,N*- or *N,O*-bidentate ligands, such as boron-dipyromethenes (BODIPYs),^[77] boron 2-(2-pyridyl)imidazoles (BOPIMs),^[84] and complexes with (2-quinolin-2-yl)phenol,^[139] are often fluorescent. Despite the presence of nitrogen atoms with partial positive charges, some of these compounds display high fluorescence QYs even in polar solvents. Taking into account these regularities, we decided to prepare new coumarin dyes with a quaternized pyridine ring which constitutes a part of a BF₂ complex. For example, coumarin **312** contains a 2-(2-hydroxyphenyl)pyridine fragment as a chelating ligand. This compound is structurally similar to the strongly fluorescent BF₂ complexes with the (2-quinolin-2-yl)phenol ligand.^[139] The fragment attached to C-3 in compound **313** resembles the BOPIM complexes and has a 2-(2-pyrrolyl)pyridine moiety which chelates the BF₂ fragment. We also used the opportunity to link the nitrogen atoms of pyridine and pyrrole rings in the 2-(2-pyrrolyl)pyridine fragment via two methylene groups. This leads to a rigid heterocyclical system with the quaternized pyridine ring **314**.

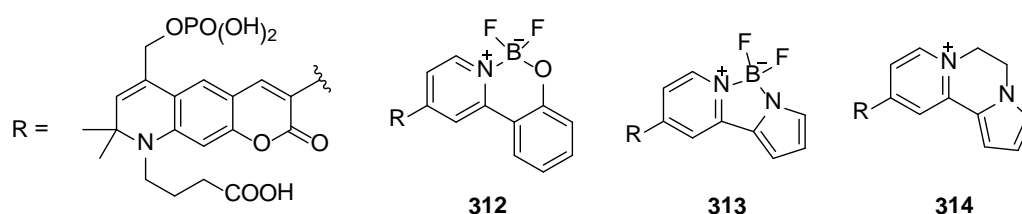
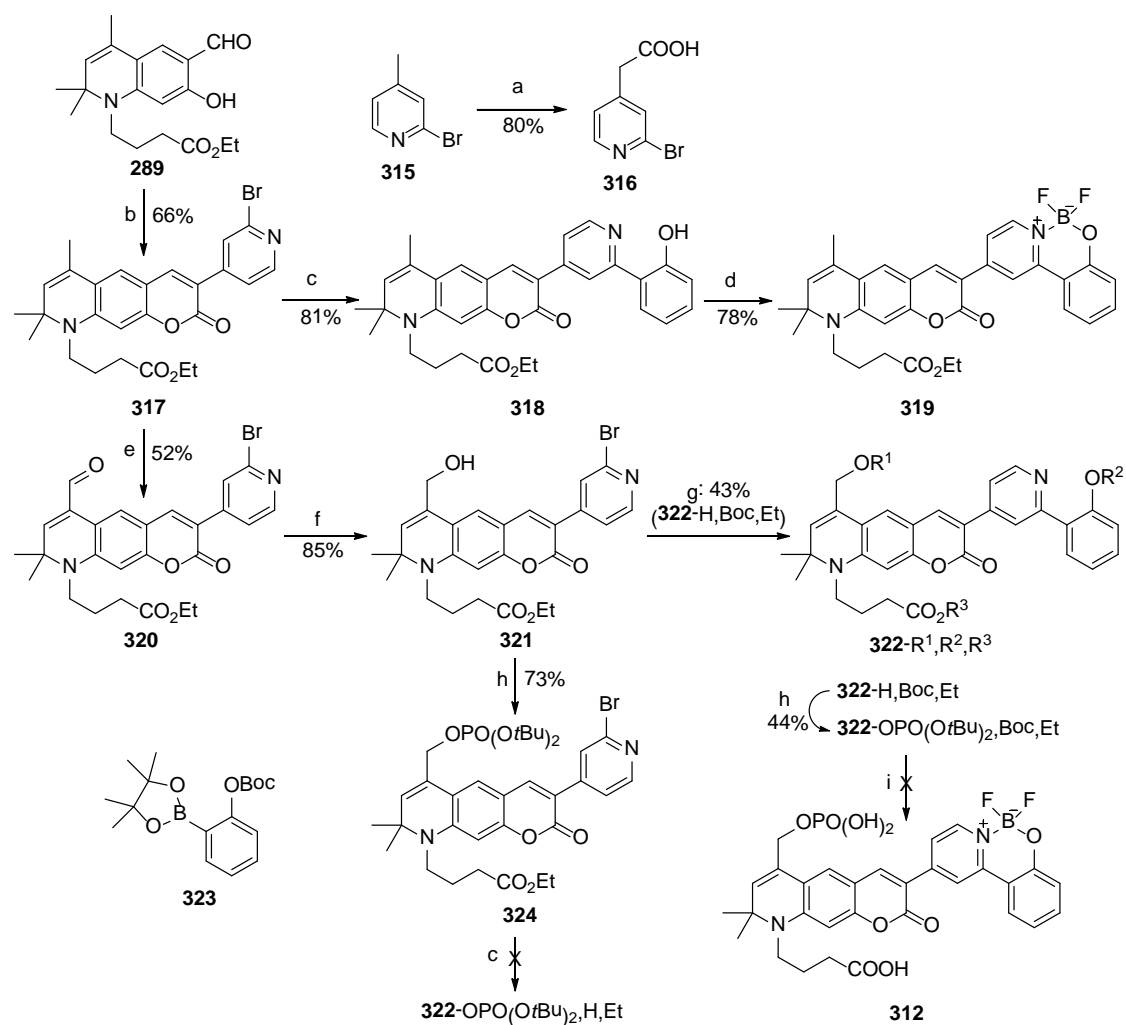


Figure 45 Phosphorylated coumarins with a pyridinium group at C-3.

2.2.2 Synthesis

The preparation of the lipophilic dye **319** and an attempt to synthesize its phosphorylated analog **312** are given in Scheme 13. Analogously to 3-heteroaryl coumarins, building block **317** was prepared by esterification of salicylic aldehyde **289** with 4-(2-bromopyridyl)acetic acid activated by DCC, and a subsequent Knoevenagel condensation. Similarly to compound **299**, heteroaryl acetic acid **316** was prepared from 2-bromo-

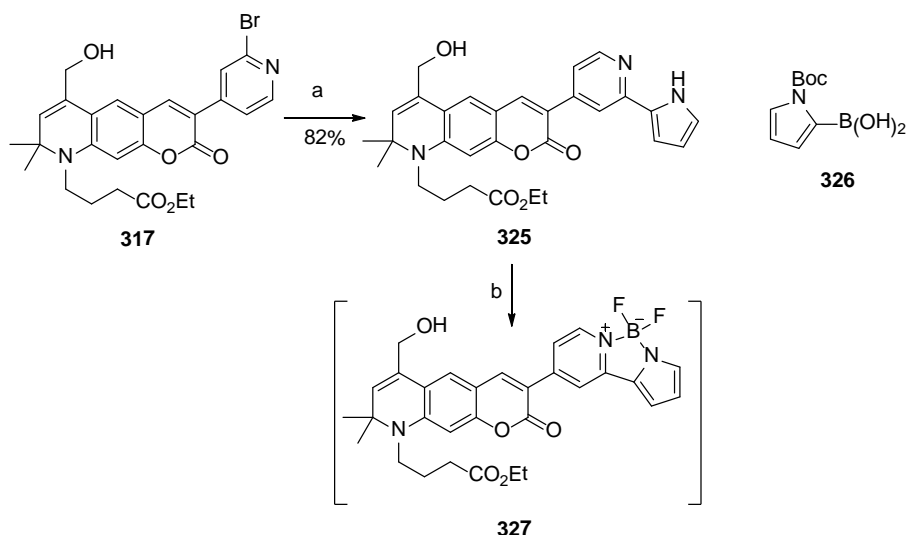
4-picoline **315**. At this step, in order to evaluate spectral properties and stability of the corresponding coumarin-BF₂ complex in polar protic solvents, we decided to prepare model compound **319** without the phosphate group. For this purpose, bromopyridyl-coumarin **317** was subjected to a Suzuki reaction with 2-hydroxyphenylboronic acid to give coumarin **318** which contains the *N,O*-bidentate ligand. A chelation of BF₃·Et₂O by compound **318** readily occurred in toluene in the presence of NEt₃ and afforded coumarin-BF₂ complex **319** in a good yield. When dissolved in MeOH, this compound did not decompose upon prolonged standing, and therefore we decided to prepare the water-soluble analog **312**. A detailed discussion and comparison of the spectral properties of coumarins **317**–**319** is given below in Section 2.2.3.



Scheme 13 Synthesis of phosphorylated coumarin **312**: a) LDA, THF, -78 °C, 1 h; then CO₂, -78 °C → r.t., overnight; b) **316**, DCC, NEt₃, DMAP, CH₂Cl₂/DMF, 30 °C, 20 h; c) 2-hydroxyphenylboronic acid, Pd(PPh₃)₄, toluene, aq. Na₂CO₃, 120 °C, overnight; d) BF₃·Et₂O, NEt₃, toluene, r.t., overnight; e) SeO₂, dioxane, reflux, 3 h; f) NaBH₄, CeCl₃, THF/MeOH, 0 °C, 5 min; g) **323**, Pd(PPh₃)₄, toluene, aq. Na₂CO₃,

120 °C, overnight; h) *i*Pr₂NP(*O**t*Bu)₂, 1*H*-tetrazole, CH₂Cl₂, 40 °C, 1 h; then *m*CPBA, 0 °C, 15 min; i) aq. NaOH, THF, water, r.t., overnight; then TFA, CH₂Cl₂, r.t., 1 h; then BF₃·Et₂O, NEt₃, THF, r.t., 40 min.

For the synthesis of coumarin **312** – a phosphorylated analog of compound **319** – the allylic methyl group of bromopyridyl coumarin **317** was subjected to the same series of oxidation and reduction reactions as in the case of 3-heteroaryl coumarins in order to obtain alcohol **321** (Scheme 13). The phosphorylation according to the phosphoramidite method provided bromopyridyl coumarin **324** with a phosphate group. Unfortunately, attempted Suzuki reactions of **324** with 2-hydroxyphenylboronic acid failed to afford the desired compound **322-OPO(*O**t*Bu),H,Et**, even though a number of various catalysts and ligands were tested. In contrast, a Suzuki reaction of coumarin **321** with *O*-*tert*-butoxycarbonyl-protected pinacol ester **323** proceeded well and gave compound **322-H,Boc,Et** in a moderate yield. The presence of a *tert*-butoxycarbonyl group, which masks the phenolic hydroxyl group, is important in the next step, in which a phosphate group is going to be attached to the allylic hydroxyl group using the protocol described above. The resulting compound **322-OPO(*O**t*Bu)₂,Boc,Et** was subjected to a series of deprotection and complexation reactions in a one-pot fashion. First, the ethyl ester group was cleaved by basic hydrolysis. Then the *tert*-butyl groups on the phosphate function and the *tert*-butoxycarbonyl group attached to the aromatic hydroxyl were removed with TFA. Finally, upon exposure to BF₃·Et₂O in the presence of NEt₃, compound **312** was formed. However, due to instability on SiO₂ or RP-SiO₂, all attempts to isolate compound **312** in a pure form failed.

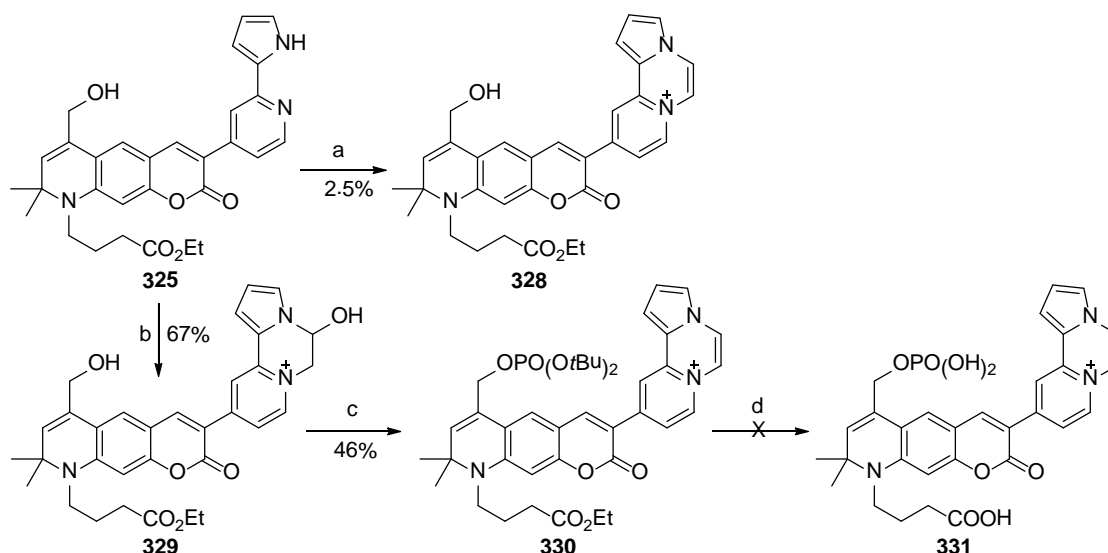


Scheme 14 Failed synthesis of coumarin- BF_2 complex **327**: a) **326**, $\text{Pd}(\text{PPh}_3)_4$, toluene, aq. Na_2CO_3 , 120 °C, overnight, then 150 °C, 30 min; b) $\text{BF}_3 \cdot \text{Et}_2\text{O}$, NEt_3 , THF, r.t., overnight.

An attempted synthesis of the model coumarin **327** with a BF_2 residue bound to the *N,N*-bidentate 2-(2-pyrrolyl)pyridine ligand is presented in Scheme 14. The pyrrolyl residue was introduced to bromopyridylcoumarin **317** by a Suzuki reaction with the commercially available *N-tert*-butoxycarbonyl protected 2-pyrrolylboronic acid **326**. The pyrolysis of the reaction mixture at 150 °C cleaved the *tert*-butoxycarbonyl-protecting group and provided coumarin **325** in good yield. The reaction of **325** with $\text{BF}_3 \cdot \text{Et}_2\text{O}$ in THF in the presence of NEt_3 yielded a red fluorescent solution. However, upon quenching the reaction mixture with MeOH or H_2O , the fluorescent product (complex **327**) decomposed and left the yellow-colored starting material **325**. Thus, coumarin **327** turned out to be even less stable than coumarin **312**.

Then we studied the feasibility of the preparation of the lipophilic analog of the dye **314**. The straightforward synthetic route involves a reaction of compound **325** with dibromoethane (Scheme 15). To our surprise, the only fluorescent product observed in this reaction mixture was the dehydrogenated compound **328**. However, the preparative yield was very low, even when prolonged reaction times, elevated temperatures and saturation of the reaction mixture with air were applied. Due to the interesting and promising spectral properties of compound **328** (see Section 2.2.3 for further details), we decided to develop a more efficient synthetic route. For that, we tried to condense compound **325** with chloroacetaldehyde diethyl acetal. Under the known conditions,^[140] the reaction did not proceed at all after heating for 2 h at 100 °C. However, when an excess of this acetal and

a stoichiometric amount of NaI were added, the starting material **325** was completely consumed after 2 days at 100 °C. Notably, the product of this transformation – compound **329** – did not readily undergo dehydration to **330** when exposed to acid. This behavior may be attributed to the inability of this rigid polycyclic system to adopt the antiperiplanar conformation in the transition state of the elimination reaction. The phosphorylation reaction transformed both hydroxyl groups present in compound **329** into the corresponding phosphates. As a result, the hydroxyl belonging to the hemiaminal fragment was converted to a good leaving group and readily eliminated during the isolation procedure. Thus, coumarin **330** with the pyrido[1,2-*a*]pyrrolo[2,1-*c*]pyrazinium moiety at C-3 was obtained. However, the final deprotection step failed to give compound **331**. Probably, the attack of the hydroxide ion on the double bond prone to undergo nucleophilic addition triggered the decomposition reaction.



Scheme 15 Synthesis of coumarins with a pyrido[1,2-*a*]pyrrolo[2,1-*c*]pyrazinium substituent: a) $\text{BrCH}_2\text{CH}_2\text{Br}$, 130 °C, 3 days; b) $\text{ClCH}_2\text{CH}(\text{OEt})_2$, NaI, DMF, 100 °C, 5 h; c) $i\text{Pr}_2\text{NP}(\text{OtBu})_2$, 1*H*-tetrazole, CH_2Cl_2 , 40 °C, 1 h; then *m*CPBA, 0 °C, 15 min; d) aq. NaOH, THF, water, r.t., overnight; then TFA, CH_2Cl_2 , r.t., 1 h.

2.2.3 Spectral properties

Spectral properties of synthesized compounds **317–319**, **325**, **328** were measured in MeOH and are presented in Table 10. Introduction of the bromine atom to the pyridine ring in coumarin **317** caused bathochromic and bathofluoric shifts of 14 and 4 nm, respectively, in comparison with the parent coumarin **282**. Interestingly, the presence of the

bromine atom, which usually quenches the emission by increasing the rate of intersystem crossing,^[141] did not have any effect on the fluorescence QY of **317**.

2-(2'-Hydroxyphenyl)pyridine is known to undergo an ESIPT process upon excitation.^[142] In the case of coumarin **318**, which has the 2-(2'-hydroxyphenyl)pyridyl moiety, ESIPT may also be responsible for the low fluorescence QY in MeOH. Upon excitation, the excited state S_1 of the "normal" (enol)-tautomer is formed initially. Afterwards, due to the increased basicity of the pyridinic nitrogen and acidity of the phenolic hydroxyl, a very fast proton transfer takes place within the molecule resulting in the formation of the non-emissive keto-tautomer **318K** (see Figure 46) in the excited state S_1' . A small fraction of molecules that did not undergo ESIPT gives rise to a very weak fluorescence with a "normal" (typical for coumarin dyes) Stokes shift of 66 nm.

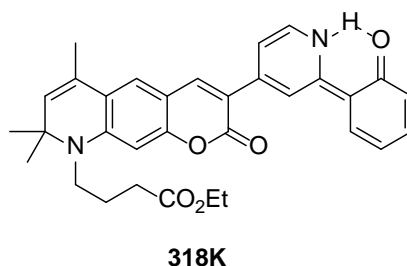


Figure 46 Keto-tautomer **318K** of coumarin **318** formed due to ESIPT from the phenolic hydroxyl to the pyridine nitrogen.

Coordination of the BF_2 moiety with 2-(2-hydroxyphenyl)pyridyl fragment in coumarin **318** completely suppresses the ESIPT. As a result, emission efficiency of the complex **319** significantly increases in comparison to the parent compound **318**. Moreover, the partial positive charge on the pyridinic nitrogen facilitates the ICT in coumarin **319** and leads to large bathochromic and bathofluoric shifts (26 and 53 nm relative to compound **318**).

The unfavorable geometry and the lower acidity of the pyrrole ring in the 2-(2'-pyrrolyl)pyridyl fragment of compound **325** apparently makes the ESIPT impossible. As a consequence, this compound shows only one emission band with a maximum at 505 nm with a "normal" Stokes shift of 73 nm and a good fluorescence QY in MeOH. The presence of the pyrrole ring does not influence the positions of absorption and fluorescence maxima, when compared to 3-(2-pyridyl)coumarin **282**.

Among all compounds presented in this section, coumarin **328** with the polycyclic and rigid pyrido[1,2-*a*]pyrrolo[2,1-*c*]pyrazinium substituent displays the most red-shifted absorption and emission maxima. In addition, this compound features a large Stokes shift of 98 nm and a high value of the fluorescence QY in MeOH. These attractive spectral properties make this fluorophore particularly interesting for further developments (e.g. decoration with polar groups and amino-reactive residues).

Table 10 Spectral properties of 3-pyridiniumcoumarins and their precursors in MeOH.

Compound	$\lambda_{\text{abs,max}}$, nm	ϵ , $\text{M}^{-1}\cdot\text{cm}^{-1}$	$\lambda_{\text{em,max}}$, nm	$\Delta\lambda$, nm	Φ_{fl}
317	445	38400	515	70	0.72
318	440	40000	506	66	0.005
319	466	32400	559	93	0.38
325	432	33650	505	73	0.50
328	489	n/d	587	98	0.56

2.2.4 Conclusion and outlook

The new coumarins **319** and **328** with a positively charged 4-pyridinium fragment attached to C-3 have been prepared from the universal precursor **289**. Both compounds exhibited absorption maxima beyond 450 nm and emitted light in the green-yellow spectral region with large Stokes shifts. Phosorylated analog of **319** apparently had a poor hydrolytic stability, and could not be isolated in pure form. Absorption and emission maxima of coumarin **328** are close to those of commercial dyes Chromeo 494, DY-480XL, DY-485XL, DyLight 485-LS and Abberior Star 470SXP. Therefore, it is particularly interesting to develop a synthetic approach to a water-soluble analog of **328** and evaluate its performance in optical microscopy in comparison with commercially available dyes.

2.3 Synthesis of pyrido- and isoquinolino-fused coumarin dyes

2.3.1 Motivation and key structural elements

Coumarin dyes are known to have moderate photostabilities in aqueous media. For example, the average numbers of the excitation cycles before bleaching (μ) for coumarins was found to be approximately 2 to 3 orders of magnitude smaller than the corresponding values for rhodamine dyes.^[143] This poorer photostability can be explained by a generally higher chemical reactivity of the coumarin fluorophore towards Michael addition of nucleophiles and a larger triplet quantum yield in comparison with rhodamines. Due to its comparatively long lifetime, the formation of the lowest triplet state is believed to be the main bleaching pathway. Moreover, the high irradiation intensities applied in confocal and super-resolution (STED) microscopies, can give rise to multiphoton absorption. As a result, various photochemical reactions from the higher excited states S_n may form additional photobleaching channels which cause further deterioration of the fluorophore in the sample of interest.

For coumarins without substituents at C-3 and C-4, a photodimerization reaction may represent a prevailing photodegradation mechanism.^[144] In the case of 7-*N,N*-diethylamino-4-methylcoumarin two main photobleaching paths were identified: (1) dealkylation of the 7-diethylamino group with formation of 7-monoethylamino- and 7-aminocoumarins and (2) oxidation of the methyl group at C-4 to carboxylic acid via intermediate formation of 4-hydroxymethylene- and 4-formyl derivatives.^[145] The formation of oxidation products during irradiation often involves “self-sensitized” oxidation processes. According to this mechanism, a transfer of the excitation energy between a dye molecule in the triplet state T_1 and triplet oxygen occurs initially. Afterwards, the resulting singlet oxygen oxidizes the dye in the ground state S_0 .^[146]

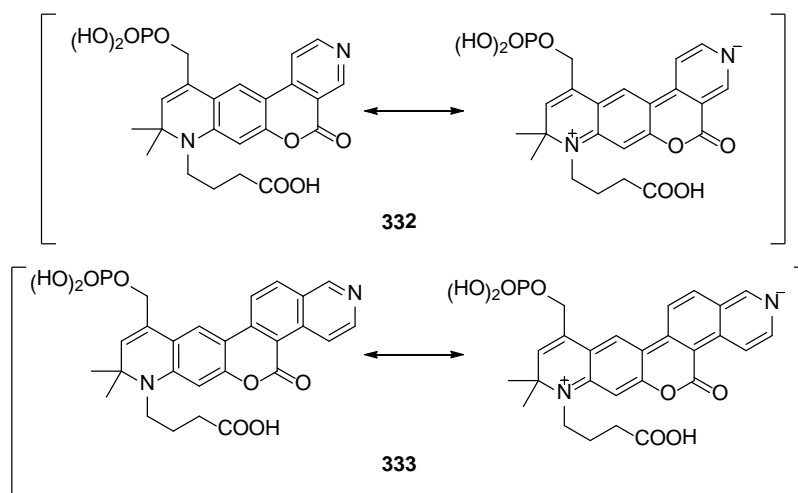


Figure 47 Phosphorylated pyrido- and isoquinolino-fused coumarins **332** and **333** and corresponding mesomeric structures showing the participation of the pyridin and isoquinoline moieties in delocalization of the lone electron pair on the nitrogen atom of the 7-amino group.

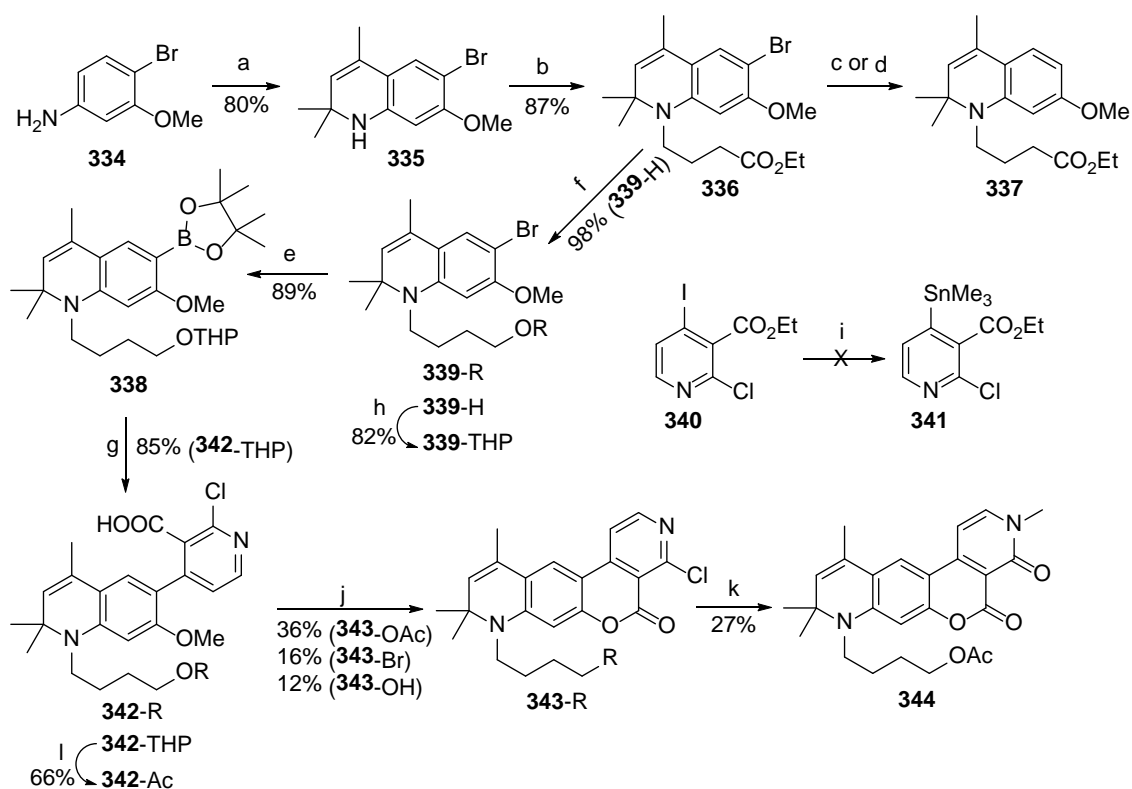
Benzo[*c*]coumarins do not have a reactive double bond conjugated with the carbonyl group of coumarin and, therefore, cannot undergo photodimerization. Fusion with an additional benzene ring results in bathochromic and bathofluoric shifts in comparison with the corresponding 3,4-unsubstituted analogs.^[147] Taking into account these attractive features of benzo[*c*]-fused coumarins, we decided to prepare pyrido[3,4-*c*]-fused coumarin **332** and isoquinolino[3,4-*f*]-fused coumarin **333** (Figure 47). Similarly to the fused benzene fragment in benzo[*c*]coumarins, pyridine and isoquinoline moieties in dyes **332** and **333** provide planar and rigid molecular frameworks and protect “critical” positions susceptible to (photo)oxidation and photodimerization. Furthermore, due to the negative mesomeric effect, they could participate in delocalization of the lone electron pair of the amino group at C-7 to the pyridine or isoquinoline nitrogen. This delocalization facilitates ICT in the excited state and provides large shifts of absorption and emission spectra towards the red region of the visible spectrum.

2.3.2 Synthesis of model hydrophilic compounds

A route to the model compound **343-OH** without the phosphate group is given in Scheme 16. Similarly to the syntheses of 3-substituted coumarins described in Sections 2.1 and 2.2, we started to assemble the pyrido- and isoquinolino-fused coumarins with the preparation of the universal precursor **336**. The latter was prepared in two steps with a high overall yield starting from the commercially available 4-bromo-3-methoxyaniline

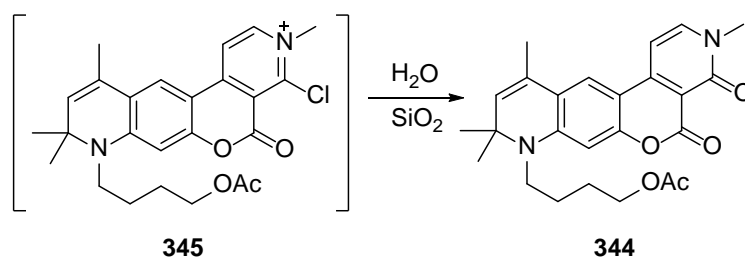
334. The chemical transformations described earlier (see Section 2.1.2) afforded compound **336**. It represents an aryl bromide which can be used in cross-coupling reactions with an organometallic derivative of the nicotinic acid with a leaving group at C-4 (as in compound **341**). After unmasking the phenolic group at C-7, the resulting intermediate is expected to form the desired pyridocoumarin. However, the required organometallic compounds, which can serve as coupling partners for the synthesis of pyridocoumarins, are predominantly unknown, probably due to their instability (we found only one example^[148]). All attempts to prepare the trimethylstannyl-substituted nicotinic acid ester **341** failed. Therefore, we decided to synthesize an organometallic derivative from the precursor **336** and couple it with halonicotinic acid derivatives, many of which are commercially available. To our regret, all Pd-catalyzed borylation and stannylation reactions yielded only the product of debromination **337**.

The traditional method for the preparation of boronic esters involves the trapping of an aryllithium reagent with a borate ester. In this respect, compound **336** is incompatible with this method due to the presence of the ester group. Therefore, we reduced ester **336** with LiAlH_4 and obtained alcohol **339-H** in an excellent yield. Later, in the final steps of the synthesis, the hydroxyl group could be easily converted to the amino-reactive *N*-hydroxysuccinimidyl carbonate and used for bioconjugation. For the reaction with *t*BuLi, the hydroxyl group in compound **339-H** was protected and used as a tetrahydropyranyl derivative. The intermediate bromide **339-THP** was subjected to lithium-bromine exchange, and the organolithium compound was then quenched with triisopropyl borate. Direct transesterification in the reaction mixture using pinacol in the presence of acetic acid afforded boronate ester **338**. The following Suzuki cross-coupling between **338** and commercially available 2-chloro-4-iodonicotinic acid proceeded smoothly and gave the biaryl **342-THP** in good yield. The methoxy and tetrahydropyranyl groups in compound **342-THP**, in principle, could be removed in one synthetic step using two equivalents of BBr_3 . However, initial experiments showed that even a large excess of BBr_3 cleaved only the tetrahydropyranyl group and left the methoxy group intact. To overcome this problem, we replaced the THP group with the acetate protective group using the known one-pot procedure.^[149] After that, acetate **342-Ac** was subjected to a reaction with BBr_3 . Unfortunately, the demethylation turned out to be sluggish, and a large excess of BBr_3 was required to provide full consumption of the starting material **342-Ac** in an acceptable time.



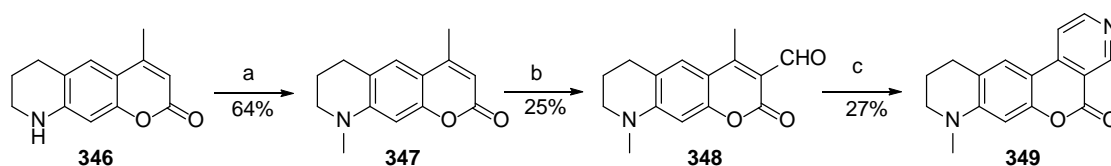
Scheme 16 Synthesis of the model coumarins **343-OH** and **344**: a) acetone, Yb(OTf)₃, r.t., 16 h; b) ethyl 4-iodobutanoate, DIEA, 105 °C, 64 h; c) hexabutyliditin, Pd(PPh₃)Cl₂, toluene, 110 °C, 3 days; d) bis(pinacolato)diboron, PdCl₂(dppf), AcOK, DMSO, 80 °C, overnight; e) *t*BuLi, THF, -78 °C, 45 min; then B(O*i*Pr)₃, -78 °C → r.t., overnight; then AcOH, pinacol, r.t., 1 h; f) LiAlH₄, THF, 0 °C → r.t.; 2.5 h; g) 2-chloro-4-iodonicotinic acid, Pd(PPh₃)₄, aq. Na₂CO₃, toluene/EtOH, reflux, 18 h; h) 3,4-dihydro-2*H*-pyrane, TsOH·H₂O, CH₂Cl₂; 0 °C → r.t., overnight; i) hexamethylditin, Pd(PPh₃)Cl₂, dioxane, 100 °C, overnight; j) BBr₃, CH₂Cl₂, 0 °C → r.t., overnight; k) MeI, MeCN, 75 °C, 2 days; l) AcOH, AcCl, r.t., 1 h.

As expected, in the course of this process a spontaneous ring closure occurred, and the pyridocoumarin core skeleton was formed. The harsh reaction conditions caused partial cleavage of the acetate protective group. As a result, three main products were obtained in this reaction: acetate **343-OAc**, alcohol **343-OH** and bromide **343-Br**. In the experiments aimed at the quaternization of the pyridine nitrogen in compound **343-OAc** we isolated methylpyridonocoumarin **344** which apparently resulted from hydrolysis of the *N*-methylated 2-chloropyridine **345** during chromatographic isolation on SiO₂ (Scheme 17).



Scheme 17 Decomposition of compound **345** on silica during the isolation procedure.

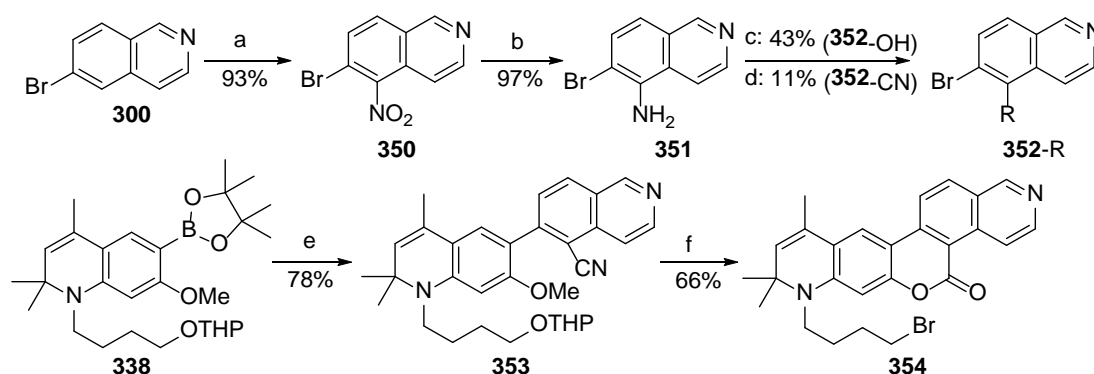
Searching for faster and more efficient synthetic routes to pyridocoumarins, we tried to condense formamide with 3-formyl-4-methylcoumarin **348** which, in turn, was prepared from commercially available compound **346** in two steps. We found that condensation of **348** with formamide occurs in the presence of conc. H_2SO_4 at elevated temperatures (Scheme 18). Under these conditions, the full conversion of **348** was not reached due to decomposition of formamide, and target compound **349** was isolated in a low yield of 27%.



Scheme 18 Synthesis of model coumarin **349**: a) trimethyl phosphate, 195 °C, overnight; b) POCl_3 , DMF, 50 °C, 10 min; c) formamide, H_2SO_4 , 90 °C, overnight.

For the synthesis of the model isoquinolinocoumarin **354** we used another synthetic approach which is, however, analogous to the one depicted in Scheme 16. The cross-coupling partner for the boronate ester **338** was prepared from the commercially available 6-bromoisoquinoline **300** in three synthetic steps (Scheme 19). First, the bromoisoquinoline **300** was nitrated with a mixture of conc. H_2SO_4 and HNO_3 . The regioselectivity of this reaction was good, and the expected isomer **350** was isolated in excellent yield. In the next step, the nitro compound **350** was reduced to the corresponding aromatic amine **351** using iron in the presence of NH_4Cl , which acted as a weak acid. The method of generation of the diazonium cation from compound **351** plays an important role in the following reaction with CuCN . Thus, when **351** was treated with aq. HNO_2 (prepared *in situ* from NaNO_2 and H_2SO_4), only phenol **352-OH** was isolated as the main product.

Under water-free conditions, when the corresponding diazonium cation was generated by action of *t*-butyl nitrite on compound **351** in DMSO,^[150] the target nitrile **352-CN** was obtained, although in a low yield.



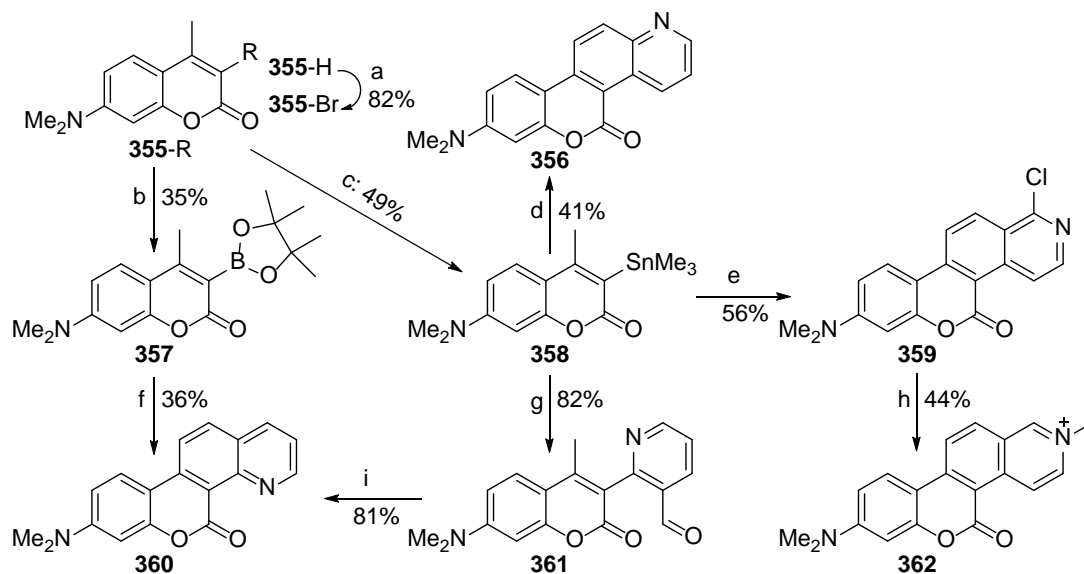
Scheme 19 Synthesis of the model coumarin **354**: a) HNO_3 , H_2SO_4 , r.t., 2 h; b) iron powder, NH_4Cl , $\text{EtOH}/\text{H}_2\text{O}$, r.t., 50 min; c) NaNO_2 , H_2SO_4 , CuCN , NaCN , H_2O , toluene, 0 °C, 30 min; then 70 °C, 2.5 h; d) *t*BuONO, CuCN , DMSO, 40 °C, 1.5 h; e) **352-CN**, $\text{Pd}(\text{PPh}_3)_4$, aq. Na_2CO_3 , toluene, 110 °C, overnight; f) conc. aq. HBr , 130 °C, 3 h.

A cross-coupling reaction of compound **352-CN** with boronate ester **338** gave the biaryl **353**. The final deprotection followed by the intramolecular cyclization in refluxing aqueous HBr afforded isoquinolinocoumarin **354** in a good yield. Upon standing, solutions of compound **354** spontaneously formed a red colored substance which may result from an alkylation of the pyridine nitrogen with the alkyl bromide part of another molecule of compound **354**.

In another synthetic approach leading to (iso)quinolinocoumarins, the key step is a cross-coupling reaction between organoboron compounds of the type **357** or organotin compounds of the type **358** and halopyridinecarboxaldehydes with the vicinal halogen and formyl groups (Scheme 20). The subsequent intramolecular condensation of the formyl group, which belongs to the pyridine fragment, with the methyl group at C-4 of the coumarin leads to an additional benzene ring, thus resulting in the (iso)quinolinocoumarin fluorophore.

The preparation of organometallic compounds **357** and **358** was started with the bromination of the commercially available 7-*N,N*-dimethylamino-4-methylcoumarin **355-H** with bromine in AcOH . Then bromide **355-Br** was subjected to Pd-catalyzed borylation and stannylation reactions to afford boronate ester **357** and 3-(trimethylstannyl)coumarin **358**,

respectively. Along with the desired product **357**, the borylation reaction produced substantial amounts of the debrominated compound **355-H** which, due to its similar R_f , significantly complicated the chromatographic isolation of **357**. The stannylation of **355-Br** with hexamethylditin was carried out according to the known protocol for the closely related *2H*-pyran-2-ones,^[151] and proceeded cleanly, though the preparative yield of compound **358** was moderate. When the less toxic hexabutylditin was used, the stannylation did not occur at all.



Scheme 20 Synthesis of model coumarins **356**, **360** and **362**: a) Br_2 , AcOH, r.t., 15 min; b) bis(pinacolato)diboron, $\text{PdCl}_2(\text{dppf})$, AcOK, dioxane, 80 °C; c) Sn_2Me_6 , $\text{Pd}(\text{PPh}_3)_4$, toluene, 110 °C, overnight; d) 3-bromopyridine-2-carbaldehyde, CuCl, LiCl, $\text{Pd}(\text{PPh}_3)_4$, DMSO, 60 °C, overnight; e) 2-chloro-4-iodopyridine-3-carbaldehyde, CuCl, LiCl, $\text{Pd}(\text{PPh}_3)_4$, DMSO, 60 °C, overnight; f) 2-bromopyridine-3-carbaldehyde, $\text{Pd}(\text{PPh}_3)_4$, aq. Na_2CO_3 , toluene, 110 °C, overnight; g) 2-bromopyridine-3-carbaldehyde, CuCl, LiCl, $\text{Pd}(\text{PPh}_3)_4$, DMSO, 60 °C, overnight; h) MeI, DMF, 100 °C, overnight; i) Cs_2CO_3 , EtOH, r.t., 3 h.

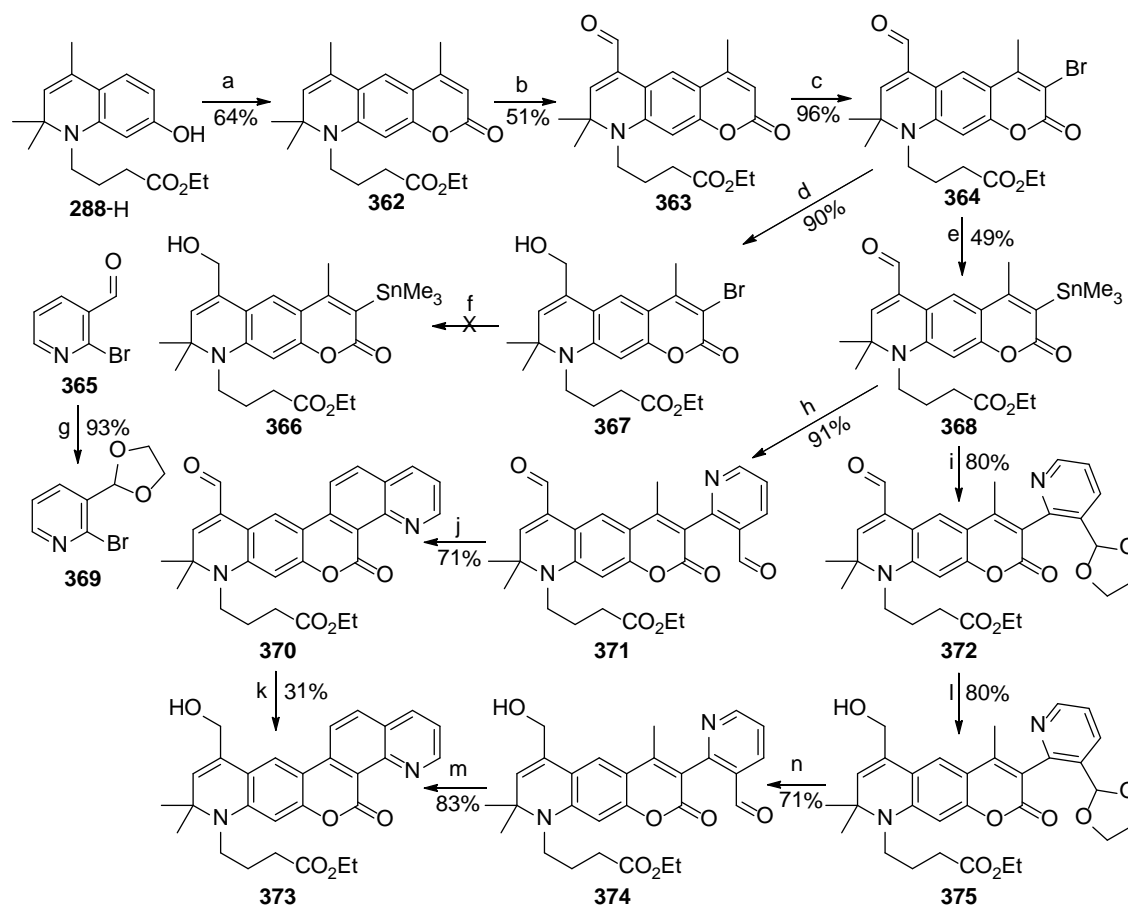
In the course of a Suzuki reaction of the boronate ester **357** with 2-bromopyridine-3-carbaldehyde, a spontaneous intramolecular cyclization with the formation of quinolinocoumarin **360** took place. In a related Stille coupling of the organotin compound **358** with 2-bromopyridine-3-carbaldehyde, in the absence of a strong base, it was possible to isolate the intermediate biaryl **361**. The Corey modification of the Stille coupling procedure^[152] provided an excellent yield of **361**. The intramolecular cyclization of coumarin **361** readily occurred in EtOH in the presence of catalytic amounts of Cs_2CO_3 and afforded quinolinocoumarin **360**. Surprisingly, in the Stille reactions of compound **358** with 3-bromopyridine-2-carbaldehyde and 2-chloro-4-iodopyridine-3-carbaldehyde only

the cyclized products **356** and **359**, respectively, were isolated. In an attempt to convert the chloropyridine moiety in compound **359** into an *N*-methylpyridone fragment (as in compound **344**), the quaternized isoquinolinocoumarin **362** was obtained as a main product.

The structure of quinolinocoumarin **373** (Scheme 21) is closer to the target coumarin **333**, than, for example, the structure of coumarin **360**. In the synthesis of model compound **373**, phenol **288-H** was subjected to a Pechmann condensation with ethyl acetoacetate and gave coumarin **362**. SeO₂ in dioxane selectively oxidized the methyl group at the C=C-bond in dihydroquinoline fragment of coumarin **362**, and aldehyde **363** was formed. The subsequent bromination of **363** with bromine in AcOH gave compound **364**. The organotin derivative **368** was obtained from **364** by a Pd-catalysed stannylation with hexamethylditin. In the later steps, the synthetic strategy was essentially the same as for compound **360**. Thus, a Stille coupling reaction of **368** with 2-bromopyridine-2-carbaldehyde **365** led to the formation of biaryl **371** as an intermediate, which cyclized to quinolinocoumarin **370** in the presence of Cs₂CO₃ in EtOH. The reduction of **370** with NaBH₄ was found to give many products. As a result, the preparative yield of coumarin **373** was very low. One of the main side-products of this reduction is an unidentified overreduced unpolar substance which was readily oxidized to compound **373** on a TLC plate or in solution while standing in air. The re-oxidation of the reaction mixture with Bu₄NIO₄ directly after full consumption of compound **370** helped to provide an acceptable preparative yield of quinolinocoumarin **373**. In contrast to quinolinocoumarin **370**, 3-heteroarylated coumarins could be reduced in excellent yields. Therefore, we decided to perform the ring closure reaction after the reduction step in order not to expose the sensitive heterocyclic system to strong reducing agents. However, bromide **367** with the reduced aldehyde group did not react with hexamethylditin. This result indicates that the reduction step should be undertaken only after stannylation.

In new synthetic approach, 2-bromopyridine-3-carbaldehyde **365** was protected as a dioxolane moiety by reaction with ethylene glycol. The product of this reaction – compound **369** – was introduced into a Stille reaction with organotin compound **368** and afforded the biaryl **372**. As expected, reduction of **372** proceeded cleanly and gave the coumarin **375** in a high yield. The subsequent deprotection with TsOH in aqueous acetone afforded compound **374** with a free aldehyde group. Treatment of **374** with Cs₂CO₃ in EtOH induced an intramolecular condensation and yielded the target quinolinocoumarin

373. Despite two additional steps, the overall yield in the synthetic sequence **368** → **372** → **375** → **374** → **373** (38%) is almost twice as high as the overall yield achieved in the shorter sequence **368** → **371** → **370** → **373** (20%).



Scheme 21 Synthesis of model coumarin **373**: a) ethyl acetoacetate, ZnCl₂, EtOH, 90 °C, 20 h; b) SeO₂, dioxane, 100 °C, 3 h; c) Br₂, AcOH, r.t., 10 min; d) NaBH₄, CeCl₃, THF, MeOH, 0 °C, 10 min; e) Sn₂Me₆, Pd(PPh₃)₄, toluene, 110 °C, 25 h; f) Sn₂Me₆, Pd(PPh₃)₄, toluene, 110 °C, overnight; g) ethylene glycol, TsOH·H₂O, toluene, reflux, 5 h; h) 2-bromopyridine-3-carbaldehyde, CuCl, LiCl, Pd(PPh₃)₄, DMSO, 60 °C, overnight; i) **369**, CuCl, LiCl, Pd(PPh₃)₄, DMSO, 60 °C, overnight; k) NaBH₄, EtOH, THF, r.t., 5 min; then aq. HClO₄, Bu₄NIO₄, r.t., 5 min; l) NaBH₄, MeOH, THF, 0 °C, 5 min; m) Cs₂CO₃, EtOH, r.t., 1.5 h; n) acetone, H₂O, TsOH·H₂O, reflux, overnight.

2.3.3 Spectral properties of pyrido- and (iso)quinolinocoumarins

Spectral properties of pyrido- and (iso)quinolinocoumarins are presented in Table 11. When dissolved in CH₂Cl₂ or MeOH, pyridocoumarin, **343**-OAc absorbs in the violet region of the visible spectrum with a maximum at 405 nm. The position of the emission maximum and the relative fluorescence intensity significantly depend on the solvent. Thus, in CH₂Cl₂, **343**-OAc emits green light with a maximum at 530 nm (large Stokes

shift of 125 nm) and a QY of 15%. In MeOH, the fluorescence maximum is shifted to 571 nm indicating an enormous Stokes shift of 166 nm. However, due to a very low fluorescence QY in MeOH (and presumably in other polar solvents), pyridocoumarin **343**-OAc is not particularly useful. Another interesting feature of **343**-OAc is emission of light in the solid-state upon irradiation of the powdered **343**-OAc with a 365 nm UV lamp. Similarly to pyridocoumarin **343**-OAc, compound **349** exhibited a very low QY in MeOH. Transition from pyridocoumarin **343**-OAc to pyridonocoumarin **344** resulted in bathochromic shifts of 17–22 nm and hypsofluoric shifts of 33–47 nm (depending on the solvent). As a result, Stokes shifts displayed by compound **344** turned out to be smaller than the Stokes shift observed for compound **343**-OAc and closer to values typical for coumarins (75–100 nm). The relative fluorescence intensity of **344** showed a pronounced dependence on the nature of solvent. In polar MeOH, the fluorescence QY of **344** was only a third of the value found in CH₂Cl₂.

Table 11 Spectral properties of pyrido- and (iso)quinolinocoumarins **343**-OAc, **344**, **349**, **355**-H, **356**, **360**, **362**, **373** and **378**.

Compound	$\lambda_{\text{abs,max}}$, nm	ϵ , M ⁻¹ ·cm ⁻¹	$\lambda_{\text{em,max}}$, nm	$\Delta\lambda$, nm	Φ_{fl}	Solvent
343 -OAc	405	16700	530	125	0.15	CH ₂ Cl ₂
343 -OAc	405	17100	571	166	0.01	MeOH
344	422	11500	497	75	0.56	CH ₂ Cl ₂
344	427	18800	524	97	0.20	MeOH
347 ^a	378	n/d	458	80	1.00	EtOH
349	377	14200	500	123	0.02	MeOH
355 -H ^b	366	21800	447	81	n/d	EtOH
356	411	16700	577	166	0.11	MeOH
360	420	13200	560	140	0.29	MeOH
362	467	13400	608	141	0.26	MeOH

373	438	19300	574	136	0.27	MeOH
378	453	n/d	617	164	0.01	PBS 7.4

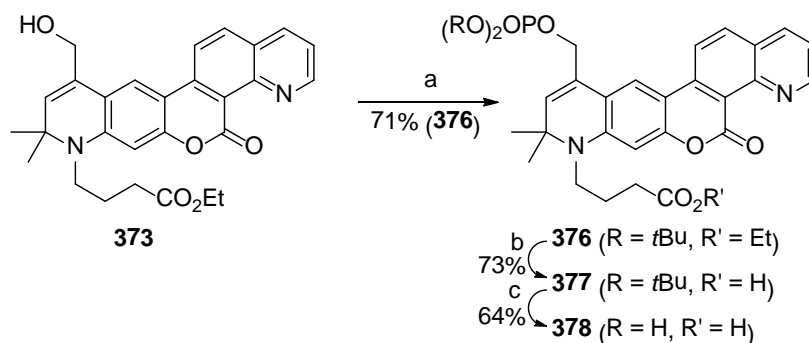
^adata from ref.^[153]; ^bdata from ref.^[154]

The quinoline moiety in compounds **356** and **360** shifts the absorption maxima (by 45 and 56 nm in MeOH, respectively) towards the red region of the visible spectrum relative to their precursor **355-H**. The bathochromic effect is more pronounced in the case of compound **360**, where the pyridine nitrogen can participate in delocalization of the lone pair of the 7-dimethylamino group. Upon excitation, compounds **356** and **360** emit yellow fluorescence with large Stokes shifts of 166 and 140 nm, respectively. Both compounds **356** and **360** displayed moderate QYs in MeOH, but the emission efficiency of **356** is lower. Isoquinolinocoumarin **362** with a quaternized pyridine nitrogen showed the most red-shifted values of absorption and fluorescence maxima and a large Stokes shift. Despite the presence of a positive charge, compound **362** possessed a satisfactory QY of 26%. Quinolinocoumarin **373** is a close structural analog of compound **360** and displayed essentially the same values of Stokes shift and QY as compound **360**. At the same time, due to the presence of a 2,2,4-trimethyl-1,2-dihydropyridine moiety, the maxima of the absorption and fluorescence spectra were red-shifted by 14–18 nm relative to **360**.

2.3.4 Synthesis of water-soluble quinolinocoumarin **378** and its spectral properties

The model coumarin dye **373** displays a good combination of a large Stokes shift and a satisfactory fluorescence QY in MeOH. In addition, due to the presence of the hydroxyl and masked carboxyl groups, it has two sites for further synthetic modifications. Thus, for the preparation of a water-soluble quinolinocoumarin with a primary phosphate residue, coumarin **373** was subjected to phosphorylation using the phosphoramidite method mentioned earlier. In initial experiments, the phosphorylation with $(t\text{BuO})_2\text{PNiPr}_2$ proceeded rapidly and cleanly. However, the following treatment with *m*CPBA at room temperature yielded many products, possibly due to the epoxidation of the C=C-bond in the quinoline residue and/or formation of the quinoline *N*-oxide. To our delight, when the oxidation procedure was carried out at $-78\text{ }^\circ\text{C}$, phosphorylated product **376** was formed in a good yield (Scheme 22). The subsequent saponification of **376** with aq. NaOH in MeOH led to

compound **377**, which was deprotected with TFA in CH_2Cl_2 , and afforded the water-soluble coumarin **378**.



Scheme 22 Synthesis of the water-soluble coumarin **378** decorated with a primary phosphate group: a) $(t\text{BuO})_2\text{PNiPr}_2$, 1*H*-tetrazole, CH_2Cl_2 , 40 °C, 40 min; then *m*CPBA, CH_2Cl_2 , -78 °C, 1 h; b) aq. NaOH, MeOH, r.t., 3 h; c) TFA, CH_2Cl_2 , 0 °C, 40 min.

Solutions of compound **378** in a PBS buffer at pH 7.4 exhibited an absorption with a maximum at 453 nm (Table 11) and an emission band in the orange-red spectral region with a maximum at 617 nm (Stokes shift 164 nm). Transition from MeOH to aqueous solutions resulted in a considerable decrease in fluorescence (<1%). The possible explanation is that the single phosphate group probably cannot prevent molecules of **378** with a large, planar, extended and hydrophobic framework from the formation of non-fluorescent aggregates. However, we expect that the fluorescence will improve upon conjugation with proteins. For example, it was the case with dye Abberior Star 520SXP which displayed QY of 0.6% in a free state in aqueous PBS buffer, but its conjugates with antibodies turned out to be much brighter and are successfully used in optical super-resolution microscopy.

2.3.5 Conclusion and outlook

Coumarins with a pyridine or an (iso)quinoline fragment fused with positions 3 and 4 of the coumarin scaffold have been synthesized using three different synthetic approaches. Pyridocoumarins **343**-OAc and **349** did not provide the desired bathochromic shift and an acceptable fluorescence QYs in polar media, despite the large Stokes shifts. Transition to pyridonocoumarin **344** allowed us to improve emission efficiency, but it is still lower than that of commercial dyes Alexa Fluor 430, Atto 425, Atto 430LS and Abberior Star

440SXP with comparable optical spectra. (Iso)quinolinocoumarins demonstrated large Stokes shifts and moderate fluorescence QYs in MeOH. However, the introduction of a primary phosphate residue did not help to improve emission efficiency of compound **378** in aqueous media. Nevertheless, in a conjugated form, this dye may demonstrate a better emitting performance, and therefore requires further testing.

2.4 Synthesis of a carborhodol dye

2.4.1 Motivation and key structural elements

Hybrid fluorophores are assembled from fragments which can be considered as parts of traditional fluorescent dyes. Very often, these compounds combine properties and features of the parent dyes. For example, rhodols belong to the xanthene dyes and may be regarded as hybrids of rhodamines and fluorescein (see Figure 48). Spectral properties of fluorescein, the simplest unsubstituted rhodamine (R = H) and the simplest rhodol (R = H) are very close ($\lambda_{\text{abs,max}}/\lambda_{\text{flu,max}} = 485/514, 496/520$ and $494/520$ nm, respectively, in basic aqueous solutions). For alkyl-substituted rhodols the absorption and fluorescence maxima are situated approximately between the maxima for fluorescein and the corresponding symmetric alkyl-substituted rhodamine. Unlike the parent fluorescein, rhodols are relatively photostable.^[155] Under neutral conditions, rhodols do not form zwitterionic species, and therefore are less susceptible to the formation of nonfluorescent spirolactones which are often not desirable.

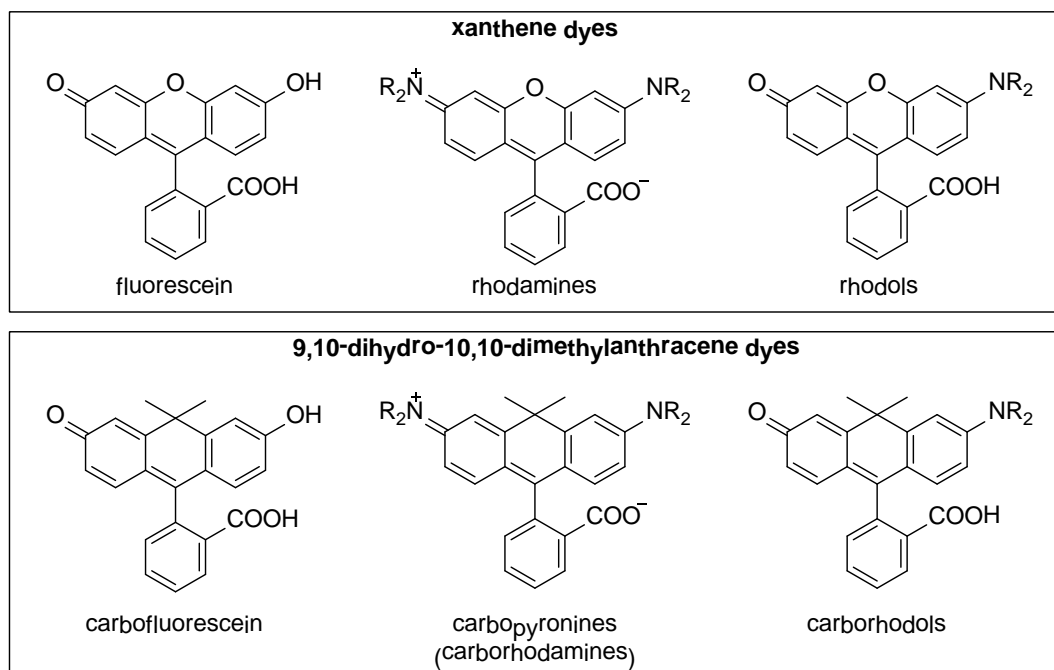


Figure 48 Rhodols and new carborhodol dyes as fluorescein-rhodamine and carbofluorescein-carbopyronine hybrids, respectively.

Other hybrid fluorophores are known. For example, those obtained by “crossbreeding” rhodamines with coumarins.^[73] These hybrid dyes inherited certain features from both parent fluorophores, e.g. the emission in the orange-red spectral region from rhodamines and large Stokes shifts which are typical for coumarins.

The replacement of the oxygen atom at C-10 of xanthene dyes with an isopropylidene bridge leads to 9,10-dihydro-10,10-dimethylantracene dyes. Owing to the positive inductive effect of two methyl groups in the 10-position and the completely new conjugation pattern in the fluorophore, the absorption and fluorescence maxima of carbofluorescein and carborhodamines (carbopyronines) are red-shifted by ca. 50–60 nm relative to the corresponding fluorescein and rhodamines. Following the same pattern as in the case of rhodol dyes, carbofluorescein and carborhodamine may be combined into a completely new fluorophore – carborhodol. This combination is particularly interesting because it enables design of a new, simple and uncharged fluorophore with asymmetric electron density distribution which can lead to a larger Stokes shift and other new properties. Due to the presence of two methyl groups at C-10, the new fluorophore will emit orange-red light. Such red-emitting fluorophores are of particular importance for micros-

copy applications because the cellular autofluorescence is negligible in this spectral region.

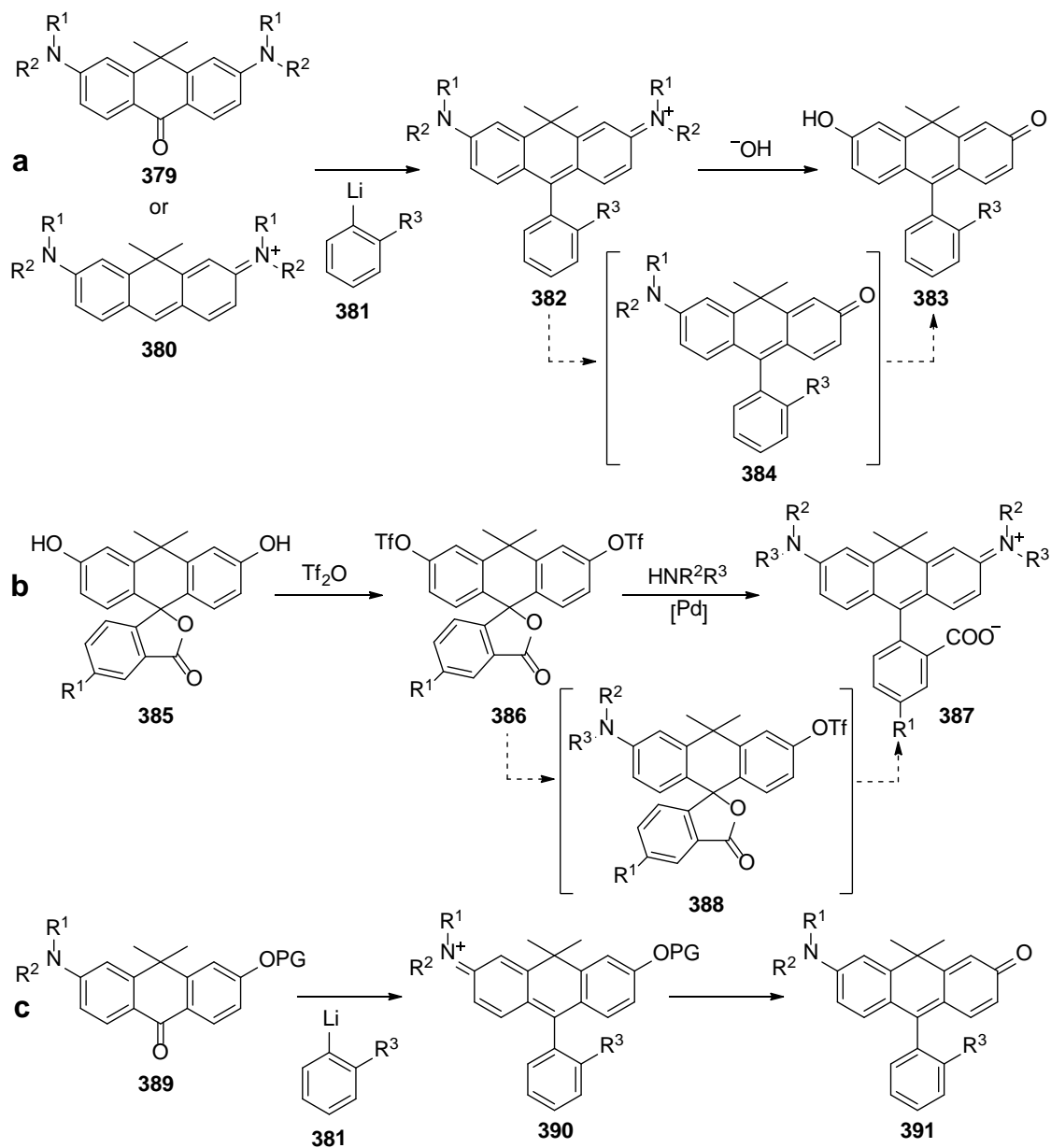
2.4.2 Synthesis and chemical properties of carborhodol dyes

The classic strategy for the preparation of carborhodamines (carbopyronines) utilizes addition of an aryllithium species **381** to *N,N,N',N'*-tetrasubstituted diaminoanthrone **379**^[156] or to carbopyronine **380**^[157] (route *a* in Scheme 23). In one report^[156a] a transformation of carbopyronine **382** into carbofluorescein **383** by alkaline hydrolysis was described. In principle, this reaction must proceed via an intermediate formation of carborhodol **384**. However, the hydrolysis rate of compound **384** may exceed that of the starting compound **382** making this method inefficient for the preparation of **384**.

After the present work had been finished, an alternative route to carbopyronines was reported^[158] (route *b* in Scheme 23). In this new approach carbofluorescein **385** was first converted to the corresponding triflate **386**. The subsequent coupling of **386** with secondary amines according to a Buchwald-Hartwig protocol provided carbopyronines **387** in good yields. As in the case of hydrolysis of **382**, the reaction of compound **386** with amines must proceed via intermediate **388** which is, in fact, a carborhodol precursor. Provided that the coupling rates for **386** and **388** are comparable (which seems reasonable because the presence of the remote amino group in compound **384** should not significantly change the electron density at the carbon atom attached to the triflate group in comparison to the starting ditriflate **386**), the reaction of **386** with one equivalent of the secondary amine could give compound **388** in an acceptable yield. Moreover, in the same report^[158] a novel strategy for the synthesis of carbofluorescein **385** was developed. In principle, this method, with some modifications, could allow the synthesis of a carbofluorescein with phenolic hydroxyls protected with two different protective groups. If such an intermediate were available, one of its protected hydroxyl groups could be selectively deprotected and converted to the corresponding triflate. A subsequent Buchwald-Hartwig coupling of the monotriflate could yield a carborhodol precursor which is similar to compound **388**, without the formation of carbopyronines as side products.

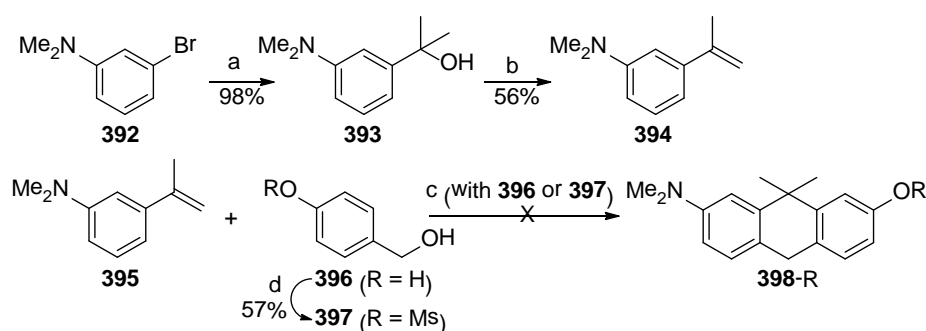
In our pioneering synthetic approach to carborhodols we decided to use the route *c* (Scheme 23) which is analogous to the classic synthetic approach to carbopyronines (route *a*). In the key step of our approach, aryllithium compound **381** reacts with the

protected anthrone **389** and yields the protected carborhodol **390**. Removal of the protecting group from the phenolic hydroxyl leads to the target carborhodol **391**. In contrast to the route *b*, our approach allows introducing tetrahydroisoquinoline and julolidine fragments to the final fluorophore. These structural features “rigidize” the framework of a fluorescent dye and provide better photostability and larger fluorescence QYs, even in polar solvents. Thus, carborhodols with a julolidine fragment are also expected to be photostable and efficient red emitting fluorescent dyes.



Scheme 23 a) Classic synthetic route to carbopyronines **382** and carbofluoresceins **383** via bis(dialkyl-amino)anthrones **379** or 9-unsubstituted carbopyronines **380**; b) Synthetic approach to carbopyronines based on a Buchwald-Hartwig amination of carbofluorescein triflates **386**; c) Synthetic approach to carborhodols used in this work.

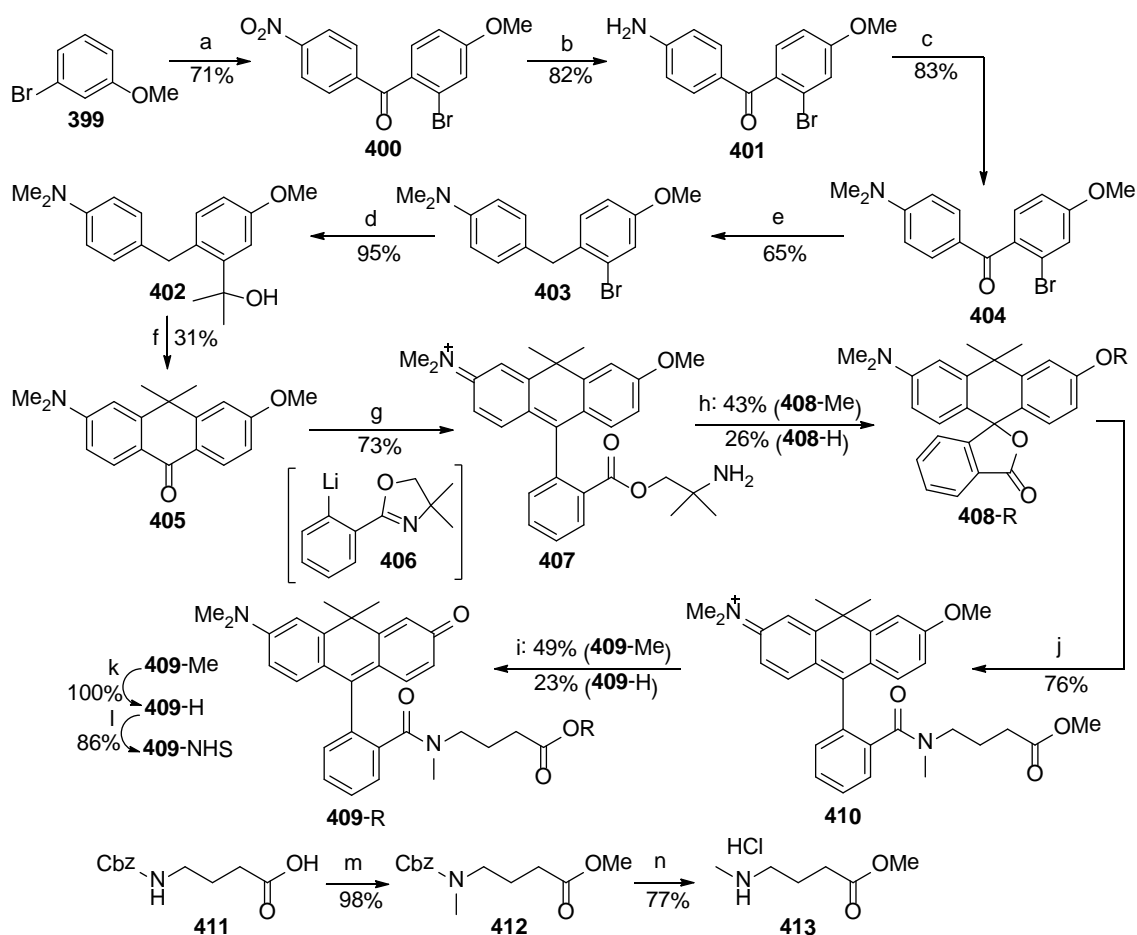
Initially, in order to develop the synthesis of anthrones **389**, we were going to use the procedure which worked well for the synthesis of diaminoanthrones **379**.^[156] To this end, 3-bromo-*N,N*-dimethylaniline **392** was subjected to lithium-bromine exchange, and the resulting aryllithium compound was “quenched” with acetone to yield alcohol **393** (Scheme 24). Subsequent water elimination in boiling chlorobenzene in the presence of KHSO_4 provided the building block **394** with an isopropylidene group. Unfortunately, an attempted condensation of **394** with either benzylic alcohol **396** or its protected derivative **397** promoted by BCl_3 and PPA did not lead to the desired product **398-R**.



Scheme 24 Attempts to prepare the carborhodol precursor **398-R** by a condensation of the building block **395** with **396** or **397**: a) BuLi , THF, $-78\text{ }^\circ\text{C}$, 20 min; then acetone, $-78\text{ }^\circ\text{C} \rightarrow \text{r.t.}$, 1 h; b) KHSO_4 , chlorobenzene, $140\text{ }^\circ\text{C}$, 15 min; c) BCl_3 , CH_2Cl_2 , $0\text{ }^\circ\text{C} \rightarrow \text{r.t.}$, overnight; then PPA, H_3PO_4 , $110\text{ }^\circ\text{C}$, 2 h; d) MsCl , KOH , H_2O , 10 min, r.t.

In a modified approach, 3-bromoanisole **399** was subjected to a Friedel-Crafts acylation with *p*-nitrobenzoyl chloride to afford the benzophenone **400** (Scheme 25). The nitro group in compound **400** was successfully reduced to the primary amino group with SnCl_2 . *N*-Methylation of aminobenzophenone **401** was carried out according to a known procedure^[159] and provided *N,N*-dimethylaminobenzophenone **404**. For the introduction of the isopropanol fragment, that will provide the geminal dimethyl group in the final carborhodol, the carbonyl group in compound **404** has to be protected, for example, as a dimethyl acetal. However, the attempted acetalization using $\text{HC}(\text{OMe})_3$ in the presence of montmorillonite K10 and TsOH ,^[160] or $\text{CF}_3\text{SO}_3\text{H}$ ^[161] failed to provide the required compound. The transformation of benzophenone **404** to the corresponding diaryldichloromethane^[162] was successful, but the subsequent reaction with MeONa ^[163] did not afford the required dimethyl acetal. Therefore, in order to be able to perform a lithium-bromine exchange, benzophenone **404** was reduced with NaBH_4 in the presence of AlCl_3 ,^[164] and thus the diarylmethane **403** was obtained. The lithium-bromine exchange in **403** followed

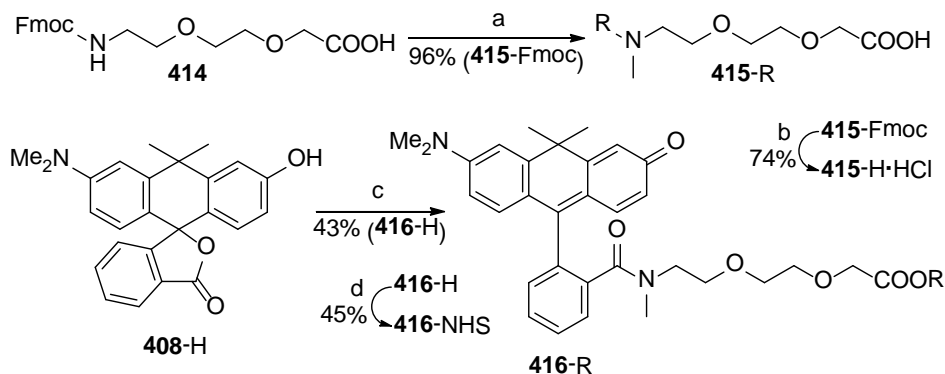
by a reaction with acetone provided carbinol **402**. The cyclization of compound **402** readily occurred in the presence of AlCl_3 in CH_2Cl_2 .^[165] The intermediate 9,10-dihydro-10,10-dimethyl derivative (not shown in Scheme 25) represents a leuco-form of the fluorescent dye. It was readily oxidized in air with the formation of colored products, and therefore it was oxidized without isolation directly with KMnO_4 . As a result, the keto group was restored, and anthrone **405** was formed. Having the important intermediate **405** at hand and using the known methodology,^[156d, 157] we easily performed the final transformations. The aryllithium compound **406**, which contains the masked carboxylic function, was generated from 2-(2-bromophenyl)-4,4-dimethyl-4,5-dihydrooxazole and *t*BuLi and introduced to the reaction with ketone **405**. During the work-up procedure, a spontaneous ring-opening of the oxazolidinone cycle took place, and ester **407** was formed. The deprotection of the carboxylic group was accomplished by heating in 20% aq. HCl. These harsh conditions also caused the partial cleavage of the aryl methyl ether, and a mixture of two products (**408-Me** and **408-H**) was obtained. The carboxyl group in compound **408-Me** was activated by POCl_3 . In the subsequent reaction of the intermediate acid chloride with an excess of the amino ester **413**, the required amide **410** was obtained (along with *N*-methyl-2-pyrrolidone which formed in the course of cyclization of **413** under basic conditions). It is noteworthy that compound **408-H** can also be amidated according to the method described above (the substitution of the phenolic hydroxyl with a chlorine atom does not occur). The reaction partner **413** was prepared in two steps from *N*-carboxybenzyl (Cbz) protected 4-aminobutyric acid **411**. In the first step, methylation with MeI in the presence of Ag_2O provided the Cbz-protected methyl ester **412**. Deprotection of the Cbz-protecting group was accomplished by hydrogenation on Pd/C. In order to prevent the resulting methyl *N*-methylaminobutyrate from a spontaneous cyclization, it was necessary to perform the deprotection step in the presence of HCl. As a result, the hydrochloride **413** was obtained. Demethylation of the methyl ether group in amide **410** with BBr_3 was accompanied by the concomitant cleavage of the methyl ester leading to a mixture of compounds **409-Me** and **409-H**. Methyl ester **409-Me** could be easily converted to the target dye **409-H** by saponification of the ester group. The amino-reactive NHS-ester **409-NHS** was prepared in MeCN using *N*-hydroxysuccinimide in the presence of HATU and NEt_3 . Notably, the stability of **409-NHS** was found to be fairly good: during storage of a sample at $-20\text{ }^\circ\text{C}$ under Ar for about a year, the content of the active ester was still about 70% according to HPLC.



Scheme 25 General approach to carborhodols: a) *p*-nitrobenzoyl chloride, AlCl₃, CH₂Cl₂, reflux, 3 h; b) SnCl₂·2H₂O, HCl, DME, EtOH, r.t., overnight; c) NaBH₃CN, paraform, AcOH, 0 °C → r.t., overnight; e) NaBH₄, AlCl₃, THF, 0 °C; then reflux, 2 h; d) BuLi, THF, -78 °C, 40 min; then acetone, -78 °C → r.t.; f) AlCl₃, CH₂Cl₂, 0 °C, 6 h; then r.t., 10 h; then KMnO₄, acetone, -18 °C, 2 h; g) 2-(2-bromophenyl)-4,4-dimethyl-4,5-dihydrooxazole, THF, *t*BuLi, -78 °C, 40 min to form compound **406**; then compound **405**, THF, -78 °C → r.t., 1 h; h) aq. HCl, 80 °C, 6.5 h; j) POCl₃, ClCH₂CH₂Cl, 80 °C, 2 h; then **413**, MeCN, NEt₃, r.t., 15 min; i) BBr₃, CH₂Cl₂, r.t., 1 h; k) aq. NaOH, THF, r.t., 1 h; l) *N*-hydroxysuccinimide, HATU, MeCN, DMF, NEt₃, r.t., overnight; m) MeI, Ag₂O, DMF, 0 °C → r.t., overnight; n) H₂, Pd/C, EtOH, *i*PrOH, HCl, r.t., 2 h.

We also prepared the similar hybrid dye **416-H** with a longer and more hydrophilic linker (Scheme 26). For the preparation of the new linker, the Fmoc-protected amino acid **414** (kindly provided by Dr. Matthias Bischoff) was subjected to a one-pot reductive *N*-methylation.^[166] Deprotection of resulting compound **415-Fmoc** in DMF in the presence of piperidine provided *N*-methylamino acid **415-H** in an excellent yield. Amidation of compound **408-H** with amino acid **415-H** afforded carborhodol **416-H**. We expected that the hydrophilic linker would improve the imaging performance of the carborhodol by reducing aggregation of the dye molecules in aqueous solutions. Unfortunately, the NHS-

ester **416**-NHS was less stable than **409**-NHS, and the quality of the images obtained with its bioconjugates was worse than in the case of **409**-NHS.

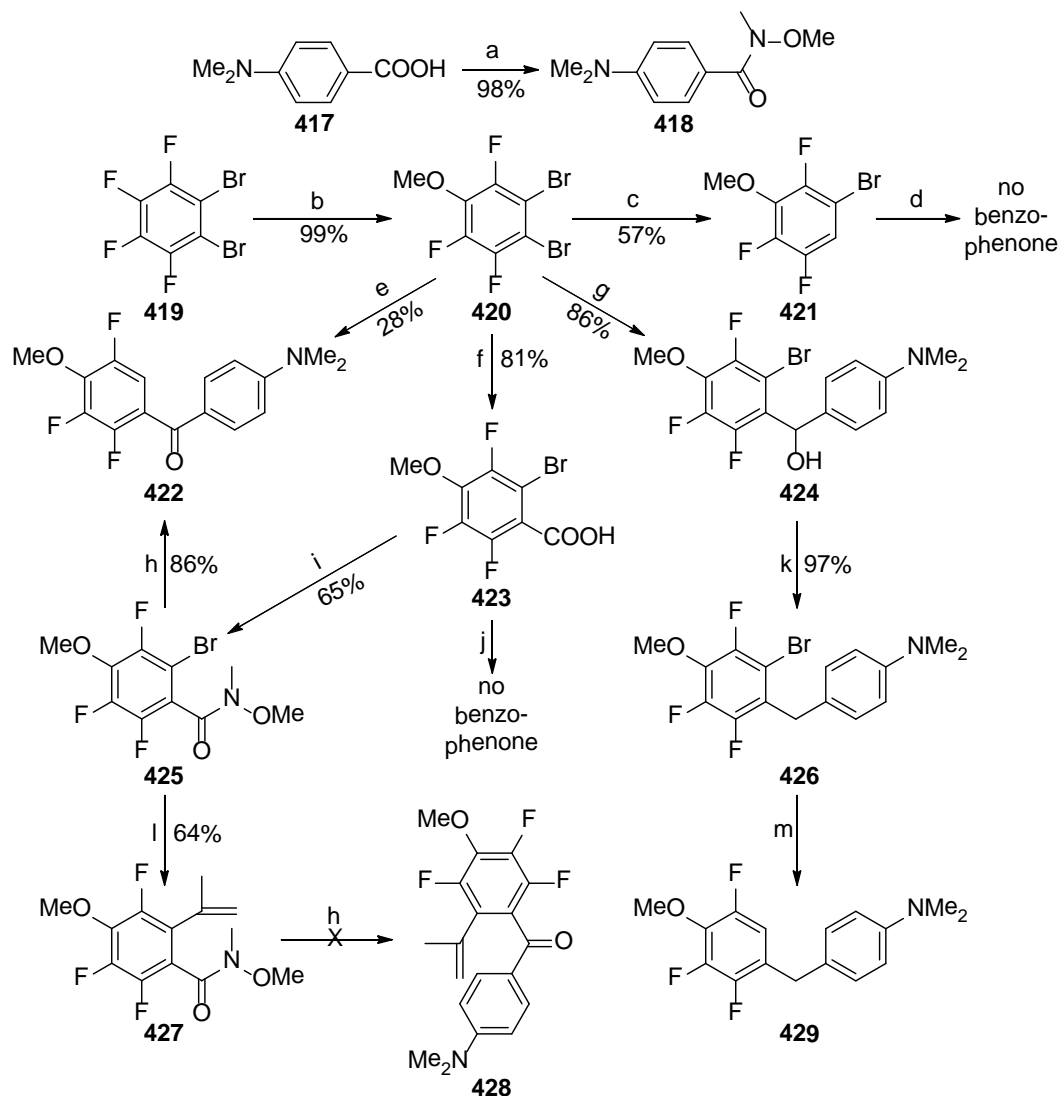


Scheme 26 Synthesis of carborhodol **416**-H with the hydrophilic linker: a) CH_2O , TFA, CHCl_3 , H_2O , $4\text{ }^\circ\text{C} \rightarrow \text{r.t.}$, 30 min; then Et_3SiH , r.t., 30 min; b) piperidine, DMF, r.t., 30 min; then aq. HCl; c) POCl_3 , $\text{ClCH}_2\text{CH}_2\text{Cl}$, $80\text{ }^\circ\text{C}$, 1.5 h; then **415**-H·HCl, THF, NEt_3 , overnight; d) *N*-hydroxysuccinimide, HATU, NEt_3 , MeCN, r.t., overnight.

Fluorinated analogs of fluorescein (for example, Oregon Green) are known to possess significantly better photostability in comparison with the parent fluorophore. At the same time, the influence of fluorine substituents on the positions of absorption and emission maxima, fluorescence QYs and fluorescence lifetimes is rather small. According to Sun et al.,^[167] the improved resistance to photobleaching may be explained by shorter triplet lifetimes of fluorinated derivatives, which reduce the probability of any photochemical processes, or by a general lower (photo)chemical reactivity of fluorinated compounds in comparison with their analogs without fluorine substituents.

Taking into account these favorable properties of fluorinated fluoresceins, we decided to incorporate fluorine atoms into the carborhodol scaffold. Commercially available 1,2-dibromo-3,4,5,6-tetrafluorobenzene **419** (Scheme 27) was considered as a precursor for the fluorescein “half” of the resulting hybrid fluorophore. Selective nucleophilic substitution of the fluorine atom with methoxide anion gave the anisole **420**.^[168] In compound **420**, the bromine atom in the *para*-position to the methoxy group was selectively replaced with Li, and the resulting organolithium compound was quenched with aqueous EtOH to afford bromide **421**.^[168a] Compound **421** represents a fluorinated analog of anisole **399** which was used as a precursor for the synthesis of carborhodol **409**-H. However, the same synthetic sequence used for compound **409**-H failed in the case of the synthesis of the fluorinated carborhodol. Attempted Friedel-Crafts acylation of anisole **421** with *p*-nitro-

benzoyl chloride to form the corresponding fluorinated benzophenone did not proceed at all, probably due to a lower chemical reactivity of compound **421** towards electrophiles as compared with compound **399**.



Scheme 27 Attempts to obtain compound **428**, a precursor of the fluorinated analogs of hybrid fluorescein – carbopyronine dyes: a) triphosgene, NEt_3 , $\text{HN}(\text{OMe})\text{Me}\cdot\text{HCl}$, CH_2Cl_2 , $0\text{ }^\circ\text{C} \rightarrow \text{r.t.}$, 3 h; b) MeONa , MeOH , reflux, 6 h; c) BuLi , Et_2O , $-78\text{ }^\circ\text{C}$, 4 h; then aq. EtOH , $-78\text{ }^\circ\text{C} \rightarrow \text{r.t.}$, overnight; d) *p*-nitrobenzoylchloride, AlCl_3 , $\text{ClCH}_2\text{CH}_2\text{Cl}$, reflux, 3.5 h; e) BuLi , THF , $-78\text{ }^\circ\text{C}$, 30 min; then compound **418**, $-78\text{ }^\circ\text{C}$, 30 min; then $0\text{ }^\circ\text{C}$, 10 min; f) BuLi , THF , $-78\text{ }^\circ\text{C}$, 30 min; then CO_2 , $-78\text{ }^\circ\text{C} \rightarrow \text{r.t.}$; g) BuLi , Et_2O , $-78\text{ }^\circ\text{C}$, 15 min; then *p*-*N,N*-dimethylaminobenzaldehyde, $-78\text{ }^\circ\text{C} \rightarrow \text{r.t.}$, 3 h; h) *p*-*N,N*-dimethylaminophenylmagnesium bromide, THF , $0\text{ }^\circ\text{C}$, 1 h; then r.t., 1 h; i) triphosgene, NEt_3 , $\text{HN}(\text{OMe})\text{Me}\cdot\text{HCl}$, CH_2Cl_2 , $0\text{ }^\circ\text{C} \rightarrow \text{r.t.}$, 1.5 h; j) SOCl_2 , DMF , r.t., 1 h; then *N,N*-dimethylaniline, AlCl_3 , CH_2Cl_2 , $0\text{ }^\circ\text{C} \rightarrow \text{r.t.}$; then reflux, 6 h; k) Et_3SiH , TFA , CH_2Cl_2 , $40\text{ }^\circ\text{C}$, 7 h; l) isopropenylboronic acid, toluene, $\text{Pd}(\text{PPh}_3)_4$, aq. Na_2CO_3 , EtOH , $110\text{ }^\circ\text{C}$, overnight; m) BuLi , THF , $-78\text{ }^\circ\text{C}$, 30 min; then acetone, $-78\text{ }^\circ\text{C} \rightarrow \text{r.t.}$, 2 h.

Another ketone synthesis is the reaction of organolithium or organomagnesium compounds with Weinreb amides.^[169] To apply this method for the synthesis of the fluorinated benzophenone **428**, dibromide **420** was converted with one equivalent of BuLi to the corresponding organolithium compound, which was then acylated with the Weinreb amide **418**. In the course of this reaction, the second bromine atom “disappeared”, and although the product – benzophenone **422** – was isolated, it could not be used in further synthetic steps. Interestingly, when the organolithium compound prepared from compound **420** and one equivalent of BuLi, was treated with a stronger electrophile, such as CO₂ or *p*-*N,N*-dimethylaminobenzaldehyde, the corresponding products, benzoic acid **423** and alcohol **424**, retained the second bromine. In principle, the acid chloride prepared from compound **423** can serve as an acylation reagent in the Friedel-Crafts reaction with *N,N*-dimethylaniline to give the important benzophenone intermediate. Unfortunately, all our trials to provide the desired product failed. We also prepared the Weinreb amide **425** and treated it with *p*-*N,N*-dimethylaminophenylmagnesium bromide, and again, the bromine atom was “lost” in the course of the reaction. Ionic hydrogenation^[170] of alcohol **424** with Et₃SiH and TFA provided the diarylmethane **426**, the important intermediate analogous to compound **403**. To our regret, in the next synthetic step, the lithium-bromine exchange followed by reaction with acetone yielded debrominated compound **429** as a main product.

In the search for new synthetic methods which do not involve organometallic reagents, we turned our attention towards Pd-catalyzed reactions. In this respect, isopropenylboronic acid can be used for the introduction of the isopropenyl group which will later form the isopropylidene bridge at C-10 of the final carborhodol scaffold. Thus, in a Suzuki reaction of compound **425** with isopropenylboronic acid, coupling product **427** was successfully obtained. However, the subsequent reaction of amide **427** with *p*-*N,N*-dimethylaminophenylmagnesium bromide yielded only traces of the benzophenone **428**.

2.4.3 Properties and imaging performance of carborhodol dyes

Table 12 presents the most important photophysical properties of carborhodol dyes **408-H** and **409-H**, their precursor **409-Me**, conjugates of **409-H** with antibodies and the related data for compound KK114,^[171] which was used together with **409-H** in two-color imaging experiments.

Table 12 Photophysical properties of carborhodol dyes **408-H** and **409-H**, their precursor **408-Me** and dye KK114 at room temperature

Compound	$\lambda_{\text{abs,max}}$, nm	ϵ , $\text{M}^{-1}\cdot\text{cm}^{-1}$	$\lambda_{\text{em,max}}$, nm	$\Delta\lambda$, nm	Φ_{fl}	τ^{a} , ns	Solvent
408-Me	513, 549	18250, 18430	585	72, 36	0.01	–	MeOH ^b
408-H	515, 553	30000, 37400	585 (broad)	70, 32	0.11	–	MeOH ^b
408-H	560	34300	598	38	0.94	–	MeOH ^c
409-H	573 (broad)	41000	613	40	0.64	4.0	MeOH
409-H	586	59000	613	27	0.32	2.5	PBS ^d
409-H ·AB ^e	586 (broad)	–	613	27	0.39	1.3	PBS ^d
409-H ·AB ^f	586 (broad)	–	613	27	0.09	1.6	PBS ^d
KK114	636	90000	660	24	0.53	3.6	PBS ^d
KK114·AB	636	–	660	24	0.40	3.6	PBS ^d

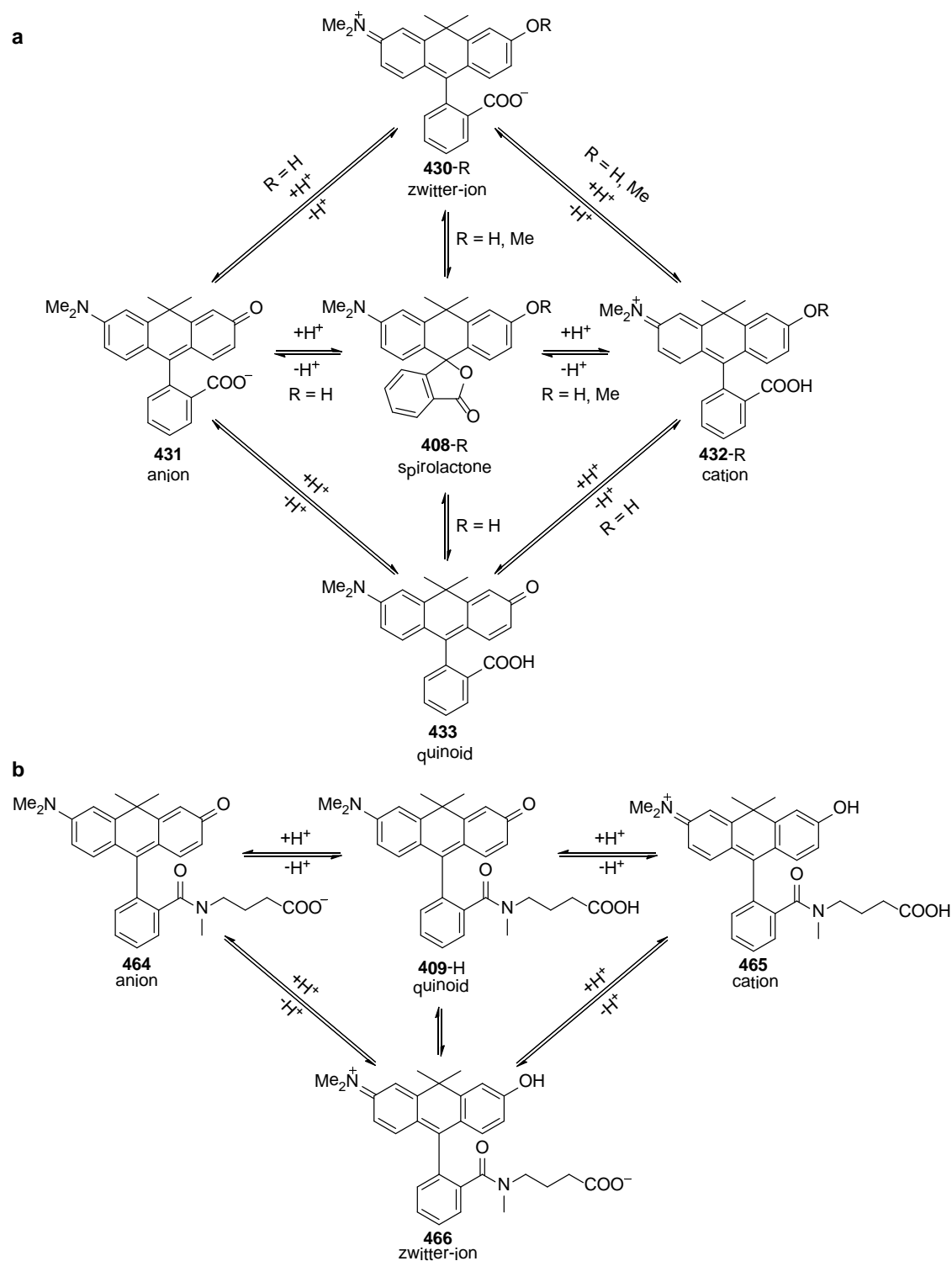
^aLifetime of the excited state S_1 . ^bWith 0.1% v/v TFA. ^cWith 0.1% v/v NEt_3 . ^dPhosphate-buffered saline, pH 7.4. ^eConjugate with sheep-antimouse antibody, degree of labeling (DOL): 5.2. ^fConjugate with goat-anti-rabbit antibody, DOL: 13.

Like fluorescein,^[172] methylcarborhodol **408-Me** and carborhodol **408-H** (along with their spirolactone form) may exist in a complex equilibrium between zwitter-ion **430-R**, anion **431** (only for **408-H**), cation **432-R**, and quinoid **433** (only for **408-H**, Scheme 28a). The position of this equilibrium is influenced by the polarity and acidity of the environment. In neutral MeOH, compounds **408-Me** and **408-H** predominantly exist in their “closed” spirolactone forms, and therefore, their solutions are almost colorless with a slight red tint which may be caused by small concentrations of open forms **430-R** and/or **433**. Upon acidification with TFA, the solutions readily become red-colored, which may correspond to the formation of the “open” protonated forms **432-R**. Absorption and emission spectra of **432-Me** and **432-H** in acidic MeOH were found to be almost identical. Thus, in the absorption spectra two maxima around 515 and 550 nm with comparable intensities were observed, whereas emission spectra of both compounds displayed a maximum at 585 nm. The fluorescence QY of **431-H** turned out to be significantly higher than that of compound **431-Me**. A similar trend was observed in rhodol dyes: conversion of the *O*-substi-

tuted rhodols to *O*-free dyes induced a drastic increase in the fluorescence intensity.^[173] Upon addition of 0.1% v/v NEt₃ to the methanolic solution of **408-Me**, no color change occurred. In contrast, under the same conditions, compound **408-H** formed the red-colored deprotonated “open” form **430-H** which displayed intense fluorescence in the orange-red region of the visible spectrum ($\lambda_{\text{em,max}} = 598 \text{ nm}$, $\Phi_{\text{fl}} = 0.94$). Carborhodol **409-H** cannot form a spirolactone or spirolactame ring and, therefore, under neutral and basic conditions exists in the open quinoid form (Scheme 28b). Maxima of its absorption and emission spectra in MeOH are red-shifted by 13–15 nm in comparison with carborhodol **408-H**. Upon transition to aqueous media, the absorption maximum of compound **409-H** undergoes a further bathochromic shift of 13 nm, whereas the maximum position of the emission spectrum stays nearly unchanged. Interestingly, in MeOH, the extinction coefficient is lower than in PBS buffer, but owing to the broader band, the oscillator strength is approximately the same. Remarkably, the absorption band of antibody conjugates **409-H**·AB is broadened as well.

The fluorescence QY of the free dye **409-H** in PBS buffer (0.32) was found to be a factor of two lower than in MeOH (0.64). QYs of the antibody conjugates depend on the degree of labeling (DOL) which shows the average amount of the dye residues attached to one antibody molecule with $M \approx 150\,000$. Thus, the antibody conjugate with a relatively high DOL (5.2) displayed a QY of 39% in aqueous PBS buffer. As the values of DOL reached 13 and 15, the QYs decreased to 9 and 4%, respectively. For the highest imaging brightness, it is necessary to maximize the values of $\varepsilon \times \text{DOL} \times \Phi_{\text{fl}}$. In this respect, the conjugates of **409-H** with DOL = 5.2 are advantageous (provided that the extinction coefficient ε for the dye **409-H** is the same in the free state and in conjugates).

Another important feature of the new carborhodol dye is the shortened fluorescence lifetimes τ in the conjugated state. Thus, the lifetimes were found to be 1.2–1.6 ns, whereas dye KK114 displays constant τ values in the range of 3.3–3.7 ns.^[111b] The difference in lifetimes can be used in multilifetime STED^[174] to discriminate between two proteins labeled with dyes **409-H** and KK114.



Scheme 28 a) The acid-base equilibrium between the colorless “closed” forms of compounds **408-R** and colored “open” forms **430-R**, **431**, **432-R** and **433**. b) The acid-base equilibrium between neutral and charged forms of compound **409-H**.

The Stokes shift of carborhodol **409-H** in aqueous PBS was found to be relatively small (27 nm). However, due to the broad absorption and emission bands, the “effective” value

is higher. In other words, the hybrid dye **409-H** can be efficiently excited with green light (for example, with the 514 nm line of an argon laser), while the emitted light is red (Figure 49). This remarkable and useful feature is not typical for the rhodamine and carbopyronine dyes and enables use of carborhodol **409-H** in two-color imaging. As a second dye, we used a bright and photostable near-emitting fluorescent marker KK114 (for its chemical structure, see ref.^[171]). The main spectral parameters of KK114 are given in Table 12 and Figure 49. Conjugates of KK114 with antibodies exhibited essentially the same absorption and emission spectra as KK114 in the free state, except for a very small red-shift of the absorption band. Owing to a substantial overlap of the emission spectra of carborhodol **409-H** and the benchmark dye KK114, the same detection channel and the same STED laser can be used for both fluorophores.

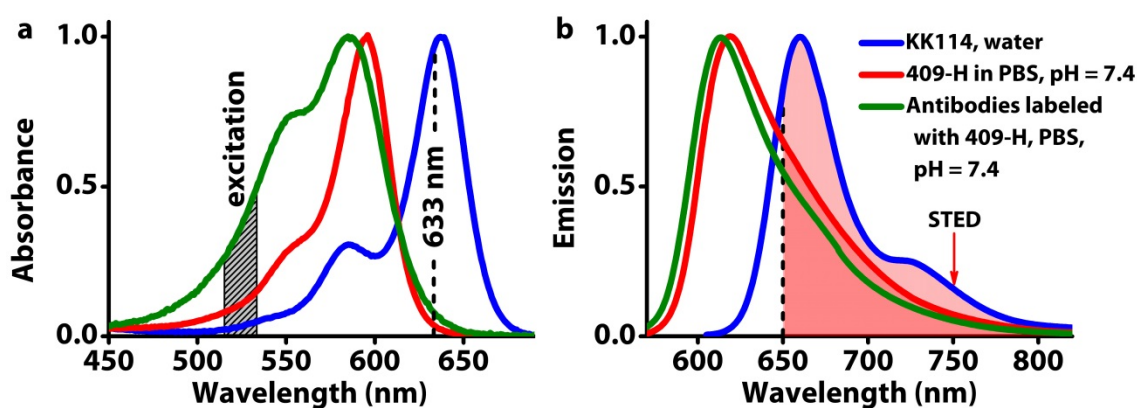


Figure 49 Normalized absorption (a) and emission (b) spectra of compound **409-H**, its conjugate with goat anti-rabbit antibody, and the reference dye KK114. Excitation regions (514–532 nm and 633–640 nm, respectively), detection area (650–800 nm) and a STED wavelength (750 nm) are shown.

In multicolor imaging the crosstalk observed in the course of the excitation with different light sources has to be low. To evaluate the crosstalk between two excitation channels, mammalian tubulin was labeled with compound **409-H** or ATTO594 and KK114 dyes (Figure 50). Imaging was performed in a confocal microscope with two excitation lasers (514 and 633 nm), and emission was collected beyond 650 nm. Mowiol was used as an embedding medium. KK114 displayed a relatively low level of crosstalk upon excitation at 514 nm (10–15%). Atto594 showed a high crosstalk (up to 60%) in the “KK114 channel”, while **409-H** proved to have negligible crosstalk as expected. This result shows that the dye pair **409-H**/KK114 provides much lower crosstalk than the ATTO594/KK114 pair, and therefore, may be advantageously used in two-color imaging and colocalization studies even without linear unmixing or other image processing techniques.

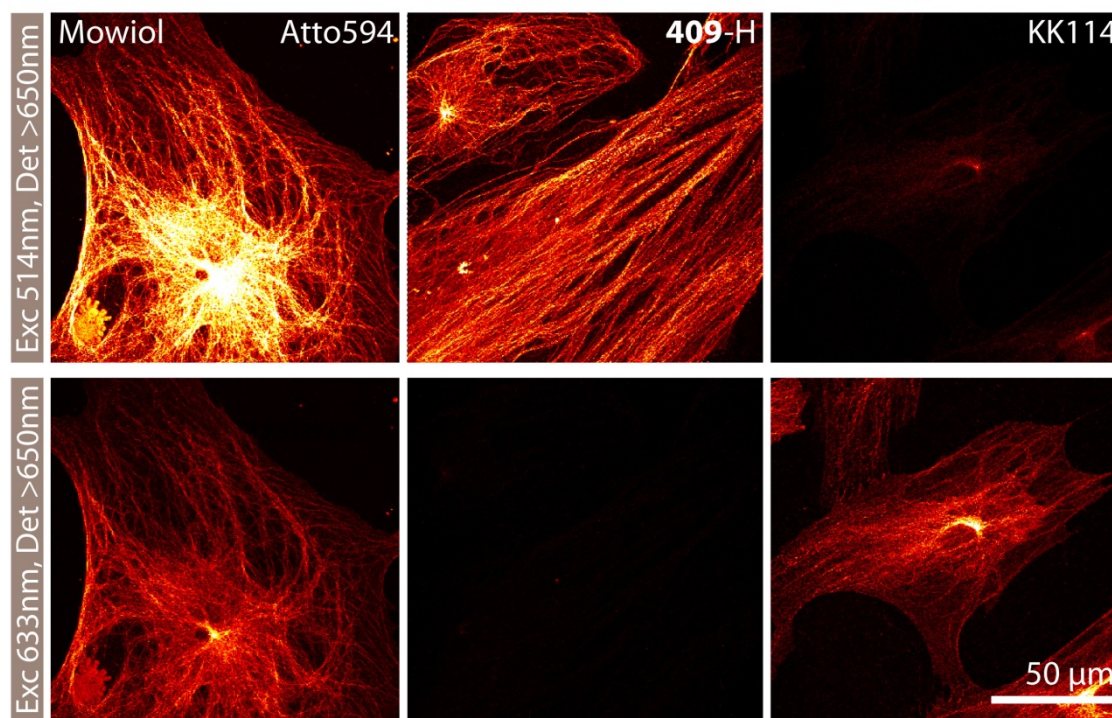


Figure 50 Immunofluorescence imaging and comparison of the crosstalk observed between compound **139**-H or ATTO594, and KK114 dyes in mowiol, two excitation sources (514 and 613 nm), and one detection channel (650–750 nm).

Figure 51 shows fluorescence images of cells labeled with **409**-H (mitochondria) and KK114 (peroxysomes) and embedded in Mowiol. Although some crosstalk is visible in “KK114”, both objects are well discernible.

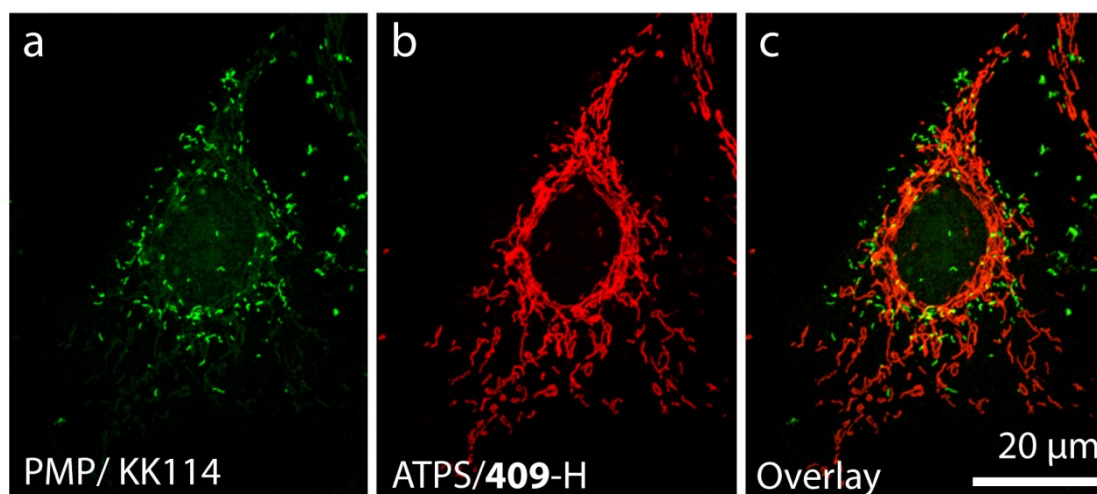


Figure 51 Dual color imaging with dyes **409-H** and KK114. A subunit of the mitochondrial ATP synthase and the peroxysomal protein PMP70 were labeled in Vero cells using dyes **409-H** and KK114, respectively. Imaging was performed in a custom-made microscope; excitation with laser light at 640 nm (a) and 532 nm (b), respectively; confocal detection between 650 and 690 nm. (c) Overlay of (a) and (b). To discriminate the structures, the pictures in the “KK114 channel” and “**409-H** channel” are pseudocolored in red and green, respectively.

To test the new carborhodol in super-resolution STED microscopy, the vimentin cytoskeleton in Vero cells was immunolabeled with compound **409-H**. Imaging was performed in a custom-built STED microscope with excitation at 532 nm ($\sim 40 \mu\text{W}$) and a STED irradiation at 760 nm ($\sim 200 \text{ mW}$). The confocal detection was carried out in the 650–690 nm range. As visible in Figure 52, the performance of carborhodol **409-H** is very good, even though the STED wavelength is shifted by more than 140 nm to the red from the emission maximum. The optical resolution achieved with dye **409-H** was about 80 nm. At the same time, the best resolution of this STED microscope obtained with different dyes was in the range of 40–50 nm. The reason for lower STED resolution with **409-H** might be photobleaching. Although we expected carborhodol **409-H** to be more photostable than fluorescein, its photostability apparently cannot reach the values typical for rhodamine dyes. Under STED conditions compound **409-H** bleaches significantly faster than rhodamine dye KK114, which is considered to be one of the best STED dyes.^[156d] Trying to improve the photostability of carborhodol dyes, we planned to replace three hydrogen atoms in the fluorescein “half” of the molecule with fluorine. Similar structural modifications applied to the fluorescein resulted in a series of Oregon Green dyes which showed significantly better resistance against photobleaching.^[167] Although we failed to prepare the fluorinated analog of **409-H**, the synthetic transformations pre-

sented in Scheme 27 may be useful for the design of other fluorinated 10,10-dimethylantracene-9(10*H*)-ones.

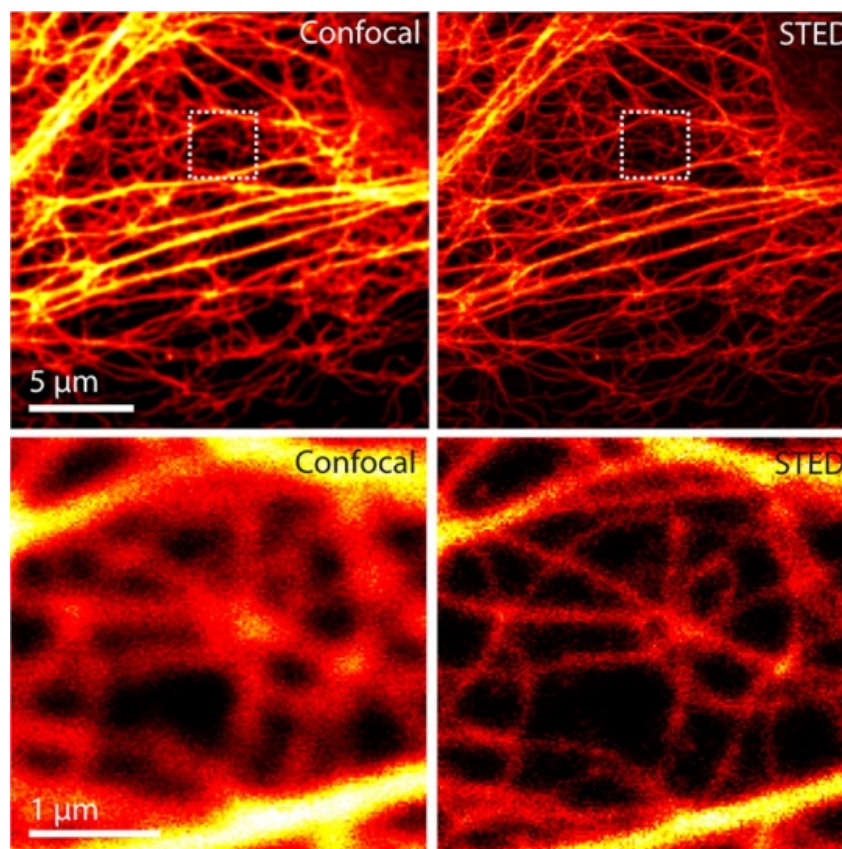


Figure 52 STED imaging with compound **409-H**. The vimentin cytoskeleton of mammalian cells was labeled with compound **409-H**. Top: confocal and STED images of the same region of the sample. Bottom: close-ups of the boxed regions in the upper panels.

2.4.4 Conclusion and outlook

A general synthetic approach to new hybrid dyes – carborhodols – has been developed. The new dyes provided bright protein conjugates and low crosstalk in two-color imaging when used together with the benchmark red-emitting dye KK114. Another remarkable feature is the relatively short lifetime in the conjugated form. This allows the use of carborhodols in multilifetime microscopy experiments with other dyes possessing longer lifetimes. The synthetic route to carborhodols given in Scheme 25 can be used for the preparation of structurally diverse dyes with extended conjugation (for example, compounds with 1,2-dihydro-1,2,2,4-tetramethylpyridine fragments). However, the necessity of lithium-halogen exchange at the two key steps restricts the synthetic freedom. Another

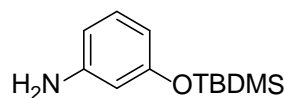
prospective piece of research is the future evaluation of the cell permeability of carborhodol **409-H** and its derivatives.

3 Experimental part

3.1 General remarks

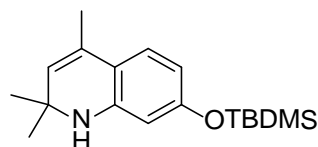
UV-visible absorption spectra were recorded on a Varian Cary 4000 UV-Vis spectrophotometer, and the fluorescence spectra on a Varian Cary Eclipse fluorescence spectrophotometer. The fluorescence quantum yields were determined by comparison with the reference dyes with the known quantum yields (for a detailed description, see: www.horiba.com/fileadmin/uploads/Scientific/Documents/Fluorescence/quantumyieldstrad.pdf). A MICROTOF spectrometer equipped with ESI ion source Apollo and direct injector with LC autosampler Agilent RR 1200 was used for obtaining high resolution mass spectra (ESI-HRMS). ESI-HRMS were obtained also on APEX IV spectrometer (Bruker). HPLC system (Knauer): Smartline pump 1000 (2×), UV detector 2500, column thermostat 4000 (25 °C), mixing chamber, injection valve with 20 and 100 µL loop for the analytical and preparative columns, respectively; 6-port-3-channel switching valve; analytical column: Eurospher-100 C18, 5 µm, 250×4 mm, 1.1 mL/min; solvent A: water + 0.1 v/v% TFA; solvent B: MeCN + 0.1 v/v% TFA; detection at 254 nm or as specified. Analytical TLC was performed on MERCK ready-to-use plates with regular silica gel 60 (F254) and UV-detector (unless specified otherwise). Preparative column chromatography was performed on silica gel 60 (40–63 µm) from Macherey-Nagel (Germany). NMR device: Varian (Agilent) 400-MR (400 MHz) unless specified otherwise. Coupling constants (*J*) are given in Hz. In the APT mode, the ¹³C signals of the methyl (CH₃) and methyne (CH) groups are “positive” (+), while the signals of methylene groups (CH₂) and carbons without attached hydrogen atoms are “negative” (–). Reactions were carried out upon magnetic stirring in Schlenk flasks equipped with septa or reflux condensers with bubble counters under argon using a standard manifold with vacuum and argon lines. Freeze-drying of the dye solutions in aqueous acetonitrile was performed with ALPHA 2–4 LD plus device with the cooler maintained at –80 °C (Martin Christ, Germany).

3.2 Experimental procedures



3-[(*tert*-Butyldimethylsilyl)oxy]aniline (**286-TBDMS**)

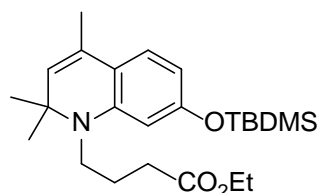
Compound **286** was prepared according to the published procedure.^[175] 3-Aminophenol (21.8 g, 0.200 mol) and imidazole (34 g, 0.50 mol) were dissolved in DMF (200 mL), the solution was cooled with an ice-water bath, and TBDMSCl (36.1 g, 0.24 mol) was added in one portion. The cooling bath was removed, the reaction mixture was allowed to warm-up to room temperature, and stirred for 1 h. DMF (ca. 150 mL) was evaporated *in vacuo* at 55 °C, the residue was diluted with EtOAc (250 mL), washed with sat. aq. NaHCO₃ (twice), water (several times), brine and dried over MgSO₄. After evaporation of solvents, the oily residue was dried *in vacuo* (0.5 Torr) to a constant weight. Purification by column chromatography (gradient elution with *n*-hexane to *n*-hexane/Et₂O = 5/1) afforded compound **286-TBDMS** (R_f = 0.24 in *n*-hexane/Et₂O = 8/1) as a clear oil (34.1 g, 76%). ¹H NMR (300 MHz, CDCl₃): δ = 0.21 (s, 6 H, 2×Me), 0.99 (s, 9 H, *t*Bu), 3.60 (br. s, 2 H, NH₂), 6.18 (m, 1 H, Ar), 6.25 (m, 2 H, Ar), 6.98 (m, 1 H, Ar) ppm.



7-[(*tert*-Butyldimethylsilyl)oxy]-1,2-dihydro-2,2,4-trimethylquinoline (**287**)

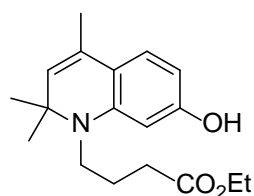
Anhydrous ytterbium(III) triflate (4.2 g, 6.8 mmol, 6.5 mol%, freshly dried *in vacuo* at 130 °C for 4 h) was added in one portion to a solution of compound **286-TBDMS** (23.3 g, 0.1045 mol) in dry acetone (300 mL). The reaction mixture was stirred at r.t. for 16 h. Acetone was evaporated *in vacuo*, the residue was dissolved in AcOEt, washed with sat. aq. NaHCO₃ (twice), water, brine and dried over MgSO₄. After evaporation of solvents, the oily residue was dried *in vacuo* (0.5 Torr) to a constant weight. Purification by column chromatography (gradient elution with *n*-hexane to *n*-hexane/Et₂O = 10/1) afforded compound **287** (R_f = 0.86, *n*-hexane/Et₂O = 8/1) as a clear oil (19.85 g, 63% yield). ¹H NMR (400 MHz, CDCl₃): δ = 0.20 (s, 6 H, 2×Me), 0.99 (s, 9 H, *t*Bu), 1.27 (s, 6 H, 2×Me), 1.97 (d, J = 1.2 Hz, 3 H, Me), 3.63 (br. s, 1 H, NH), 5.20 (q, J = 1.2 Hz, 1 H), 5.99 (d, J = 2.4, 1 H, Ar), 6.15 (dd, J = 8.2 and 2.4 Hz, 1 H, Ar), 6.92 (d, J = 8.2 Hz, 1 H, Ar) ppm. ¹³C NMR (125.7 MHz, CDCl₃): δ = -4.4, 18.2, 18.6, 25.7, 30.9, 51.9,

104.7, 108.9, 115.9, 124.5, 126.1, 128.3, 144.5, 156.1 ppm. HRMS (ESI, C₁₈H₂₉NOSi): 302.1940 (found [M-H]⁻), 302.1946 (calc.); HRMS (ESI, C₁₈H₂₉NOSi): 304.2096 (found [M+H]⁺), 304.2091 (calc.).



1-[3-(Ethoxycarbonyl)propyl]-7-[(*tert*-butyldimethylsilyl)oxy]-1,2-dihydro-2,2,4-trimethylquinoline (288-TBDMS)

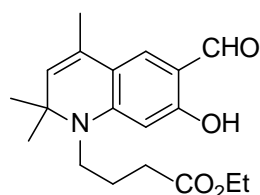
DIEA (11.8 g, 91.7 mmol) was added to a mixture of compound **288** (13.9 g, 45.87 mmol) and ethyl 3-iodobutyrate (13.3 g, 55.05 mmol) in a screw-cup bottle, and the reaction mixture was stirred with heating (110 °C) for 2 days. After cooling, the reaction mixture was diluted with Et₂O, passed through a plug of SiO₂ (eluting with Et₂O), and the filtrate evaporated *in vacuo*. The residue was dissolved in *n*-hexane/Et₂O (3/1) mixture, washed with water, brine and dried over MgSO₄. The product **288-TBDMS** was isolated by a short path column chromatography (*n*-hexane → *n*-hexane/Et₂O 10/1; *R*_f = 0.59 in *n*-hexane/Et₂O = 10/1); yield 18.75 g (98% yield) of a clear oil. ¹H NMR (400 MHz, CDCl₃): δ = 0.21 (s, 6 H, 2×Me), 0.99 (s, 9 H, *t*Bu), 1.27 (t, *J* = 7.2 Hz, 3 H, Et), 1.28 (s, 6 H, 2×Me), 1.91 (m, 2 H, CH₂), 1.94 (d, *J* = 1.2 Hz, 3 H, Me), 2.38 (m, 2 H, CH₂), 3.21 (m, 2 H, NCH₂), 4.16 (q, *J* = 7.2 Hz, 2 H, Et), 5.11 (q, *J* = 1.2 Hz, 1 H), 6.03 (d, *J* = 2.4, 1 H, Ar), 6.12 (dd, *J* = 8.2 and 2.4 Hz, 1H, Ar), 6.90 (d, *J* = 8.2 Hz, 1H, Ar) ppm. ¹³C NMR (125.7 MHz, CDCl₃): δ = -4.3, 14.3, 18.3, 18.7, 23.5, 25.8, 28.2, 31.8, 43.3, 56.8, 60.4, 103.1, 107.1, 117.2, 124.4, 127.1, 127.6, 145.0, 156.4, 173.1 ppm.



1-[3-(Ethoxycarbonyl)propyl]-1,2-dihydro-7-hydroxy-2,2,4-trimethylquinoline (288-H)

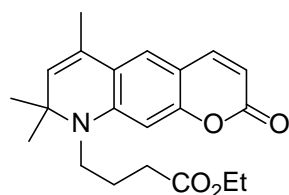
A solution of TBAF·3H₂O (7.66 g, 24.31 mmol) in THF (50 mL) was added to a solution of ester **288-TBDMS** (16.90 g, 40.53 mmol) in THF (60 mL) at 5 °C. After 5 min, the reaction mixture was diluted with Et₂O (200 mL), washed with water (2×) and brine. The combined aqueous layers were extracted with ether, and the combined organic solutions

were dried (MgSO₄). After evaporation of solvents, the residue was purified by column chromatography (Et₂O/*n*-hexane, 2/1 → 4/1). Phenol **288-H** (*R*_f = 0.07 in *n*-hexane/Et₂O, 1/5) was isolated in 99% yield (12.15 g). ¹H NMR (400 MHz, CDCl₃): δ = 1.27 (s, 6 H, 2×Me), 1.28 (t, *J* = 7.2 Hz, 3 H, Et), 1.92 (m, 2 H, CH₂), 1.93 (d, *J* = 1.2 Hz, 3 H, Me), 2.39 (m, 2 H, CH₂), 3.20 (m, 2 H, NCH₂), 4.18 (q, *J* = 7.2 Hz, 2 H, Et), 5.08 (q, *J* = 1.2 Hz, 1 H), 6.13 (m, 2 H, Ar), 6.54 (br. s, 1 H, OH), 6.90 (d, *J* = 8.6 Hz, 1 H, Ar) ppm. ¹³C NMR (100.7 MHz, CDCl₃): δ = 14.2, 18.7, 23.4, 28.3, 31.6, 43.4, 56.8, 60.8, 98.3, 102.4, 116.2, 124.8, 126.5, 127.6, 145.3, 156.9, 174.0 ppm.



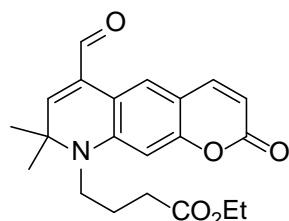
1-[3-(Ethoxycarbonyl)propyl]-1,2-dihydro-6-formyl-7-hydroxy-2,2,4-trimethylquinoline (289)

POCl₃ (3.90 g, 25.5 mmol) was added to DMF (30 mL) at 5 °C, and the mixture was allowed to warm to room temperature. After stirring for 15 min at room temperature, it was cooled down (5 °C), and a solution of phenol **288-Et** (5.15 g, 17.0 mmol) in DMF (15 mL) was added slowly. The cooling bath was removed, and the reaction mixture was allowed to warm up to room temperature, stirred for 0.5 h, and finally heated at 50 °C for 15 min. The TLC control of this reaction is difficult, because the product was found to have the same *R*_f value, as the starting material (in most solvents). After cooling, the reaction was “quenched” by adding 1 mL of sat. aq. NaHCO₃, and the product **289** was extracted with dichloromethane. The organic layer was dried (MgSO₄), and, after evaporation of solvents, the residue was purified by column chromatography (gradient elution with hexane/ether mixture, 1/1 to 1/4). Yield 3.59 g (64%). ¹H NMR (400 MHz, CDCl₃): δ = 1.29 (t, *J* = 7.2 Hz, 3 H, Et), 1.31 (s, 6 H, 2×Me), 1.93 (m, 2 H, CH₂), 1.96 (d, *J* = 1.2 Hz, 3 H, Me), 2.40 (m, 2 H, CH₂), 3.33 (m, 2 H, NCH₂), 4.18 (q, *J* = 7.2 Hz, 2 H, Et), 5.19 (q, *J* = 1.2 Hz, 1 H), 5.98 (s, 1 H_{ar}), 7.03 (s, 1 H, Ar), 9.48 (s, 1 H), 11.76 (s, 1 H) ppm. ¹³C NMR (100.7 MHz, CDCl₃): δ = 14.2(+), 18.6(+), 22.8(-), 29.3(+), 31.4(-), 44.0(-), 58.3(q), 60.7(-), 96.4(+), 110.9(-), 115.9(-), 126.1(-), 127.4(+), 128.1(+), 151.1(-), 164.7(-), 172.7(-), 191.9(+) ppm. HRMS (ESI, C₁₉H₂₅NO₄): 330.1715 (found [M-H]⁻), 330.1711 (calc.); HRMS (ESI, C₁₉H₂₅NO₄): 354.1671 (found [M+Na]⁺), 354.1676 (calc.); 332.1859 (found [M+H]⁺), 332.1856 (calc.).



Ethyl 4-(6,8,8-trimethyl-2-oxo-1,2,8,9-tetrahydropyrano[3,2-g]quinolin-9-yl)butanoate (290)

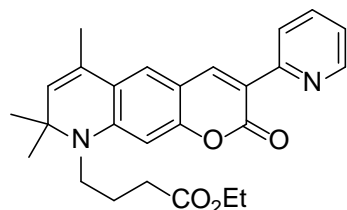
Compound **289** and (ethoxycarbonylmethylene)triphenylphosphorane were dissolved in *p*-xylene, and refluxed for 3 h under argon. After cooling to r.t., the reaction mixture was filtered to remove triphenylphosphine oxide; afterwards the solvent was evaporated *in vacuo*. The residue was subjected to a column chromatography (100 g SiO₂; hexane/EtOAc, 4:1 → 2:1) to furnish 2.4 g (73%) of the titled product. ¹H NMR (300 MHz, CDCl₃): δ = 1.28 (t, *J* = 7.1 Hz, 3 H, Et), 1.35 (s, 6 H, 2×Me), 1.80–1.95 (m, 2 H, CH₂), 1.96 (d, *J* = 1.4 Hz, 3 H, Me), 2.39 (t, *J* = 6.9 Hz, 2 H, CH₂), 3.25–3.35 (m, 2 H, NCH₂), 4.17 (q, *J* = 7.1 Hz, 2 H, CH₂), 5.26 (q, *J* = 1.4 Hz, 1 H), 6.01 (d, *J* = 9.3 Hz, 1 H, Ar), 6.34 (s, 1 H, Ar), 6.99 (s, 1H, Ar), 7.49 (d, *J* = 9.3 Hz, 1 H, Ar) ppm. ¹³C NMR (125 MHz, CDCl₃): δ = 14.2(+), 18.6 (+), 22.6(–), 29.0(+), 31.3(–), 43.8(–), 57.8(–), 60.6(–), 97.1(+), 108.3(–), 109.4(+), 120.1(–), 122.2(+), 126.3(–), 129.8(+), 143.8(+), 147.5(–), 156.6(–), 162.2(–), 172.8(–) ppm. HRMS (ESI): calc. for C₂₁H₂₄NO₄ [M+H]⁺ 356.1856; found 356.1852.



Ethyl 4-(6-formyl-8,8-dimethyl-2-oxo-1,2,8,9-tetrahydropyrano[3,2-g]quinolin-9-yl)butanoate (291)

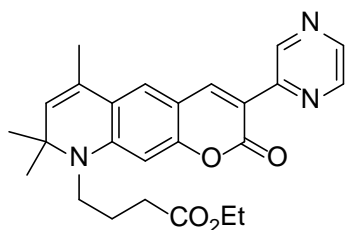
In a typical experiment, a 10 mL flask was charged with solution of compound **290** (300 mg, 0.845 mmol) in dioxane (4 mL) and finely powdered SeO₂ (117 mg, 1.06 mmol). The resulted suspension refluxed for 3.5 h, then, water (0.5 mL) was added, and the reaction mixture was allowed to cool to r.t. All volatile materials were evaporated *in vacuo*, the residue was dissolved in CH₂Cl₂ and washed with sat. aq. NaHCO₃. Organic layer was dried with Na₂SO₄ and evaporated to give a crude product. The title compound was isolated as a yellow powder (235 mg; 75%) by means of column chromatography (30 g SiO₂, hexane/EtOAc, 1:1). ¹H NMR (300 MHz, CDCl₃): δ = 1.28 (t, *J* = 7.1 Hz, 3

H, Et), 1.50 (s, 6 H, 2×Me), 1.85–1.97 (m, 2 H, CH₂), 2.40 (t, $J = 6.8$ Hz, 2 H, CH₂), 3.29–3.37 (m, 2 H, NCH₂), 4.16 (q, $J = 7.1$ Hz, 2 H, Et), 6.07 (d, $J = 9.3$ Hz, 1 H, Ar), 6.21 (s, 1 H), 6.44 (s, 1H, Ar), 7.56 (d, $J = 9.3$ Hz, 1 H, Ar), 8.39 (s, 1 H, Ar), 9.56 (s, 1 H, CHO) ppm. ¹³C NMR (125 MHz, CDCl₃): $\delta = 14.3(+)$, 22.9(-), 28.0(+), 31.3(-), 44.0(-), 58.1(-), 60.8(-), 98.3(+), 109.0(-), 110.5(+), 113.5(-), 125.4(+), 130.6(-), 143.9(+), 147.0(-), 151.9(+), 156.6(-), 161.6(-), 172.6(-), 191.6(+)) ppm. HRMS (ESI): calc. for C₂₁H₂₃NO₅ [M+H]⁺ 370.1649; found 370.1640.



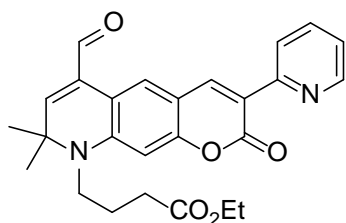
Ethyl 4-(6,8,8-trimethyl-2-oxo-3-(pyridin-2-yl)-1,2,8,9-tetrahydropyrano[3,2-g]quinolin-9-yl)butanoate (292)

To a suspension of 2-pyridylacetic acid (394 mg, 2.27 mmol) in DMF (5 mL) NEt₃ (400 μ L) was added. The resulted mixture was stirred for 5 min, then subsequently solution of aldehyde **289** (500 mg, 1.51 mmol) in CH₂Cl₂ (10 mL), EDC·HCl (436 mg, 2.27 mmol), NEt₃ (800 μ L), 4-DMAP (18.3 mg, 0.15 mmol) were added. The reaction mixture was stirred overnight at r.t. Afterwards, water (15 mL) was added, organic phase was separated, and the aq. phase was extracted with CH₂Cl₂. The combined organic extracts were dried with Na₂SO₄ and evaporated. After a column chromatography (100 g SiO₂, *n*-hexane/EtOAc, 2:1), the titled product was isolated in 35% yield (227 mg) as an orange solid. ¹H NMR (400 MHz, CDCl₃): $\delta = 1.29$ (t, $J = 7.1$ Hz, 3 H, Me), 1.38 (s, 6 H, 2×Me), 1.89–1.97 (m, 2 H, CH₂, overlapped), 1.97 (d, $J = 1.3$ Hz, 3 H, Me), 2.40 (t, $J = 6.9$ Hz, 2 H, CH₂), 3.29–3.37 (m, 2 H, NCH₂), 4.18 (q, $J = 7.1$ Hz, 2 H, CH₂), 5.28 (q, $J = 1.3$ Hz, 1 H), 6.37 (s, 1 H, Ar), 7.16 (s, 1 H, Ar), 7.17 (ddd, $J = 7.8, 4.8$ and 1.0 Hz, 1 H, Ar, overlapped), 7.70 (ddd, $J = 8.1, 7.8$ and 1.9 Hz, 1 H, Ar), 8.40 (dt, $J = 8.1$ and 1.0 Hz, 1 H, Ar), 8.60 (ddd, $J = 4.8, 1.9$ and 1.0 Hz, 1 H, Ar), 8.64 (s, 1 H, Ar) ppm. ¹³C NMR (100.7 MHz, CDCl₃): $\delta = 14.2(+)$, 18.7(+), 22.7(-), 29.2(+), 31.4(+), 44.0(-), 58.1(-), 60.7(-), 96.3(+), 109.1(-), 117.8(-), 120.4(-), 122.1(+), 123.2(+), 126.2(-), 129.6(+), 136.4(+), 142.9(+), 148.0(-), 149.0(+), 152.5(-), 156.7(-), 161.3(-), 172.7(-)) ppm. HRMS (ESI): calc. for C₂₆H₂₈N₂O₄ [M+H]⁺ 433.2122; found 433.2123.



Ethyl 4-(6,8,8-trimethyl-2-oxo-3-(pyrazin-2-yl)-1,2,8,9-tetrahydropyrano[3,2-g]quinolin-9-yl)butanoate (293)

To a solution of **289** (166 mg, 0.5 mmol) in CH_2Cl_2 (3 mL) 2-(pyrazin-2-yl)acetic acid (69 mg, 0.5 mmol), NEt_3 (106 mg, 1.05 mmol), DCC (103 mg, 0.5 mmol) and DMAP (6 mg, 10 mol%) were added. The resulting mixture was allowed to stir overnight. The precipitated urea was filtered; the filtrate was evaporated under reduced pressure. The residue was subjected to a column chromatography (25 g of SiO_2 , $\text{CH}_2\text{Cl}_2/\text{MeOH}$, 30:1) to furnish 100 mg (46%) of a title product as an orange powder. ^1H NMR (300 MHz, CDCl_3): δ = 1.29 (t, J = 7.1 Hz, 3 H, Me), 1.39 (s, 6 H, 2 \times Me), 1.89–1.97 (m, 2 H, CH_2), 1.98 (d, J = 1.4 Hz, 3 H, Me), 2.41 (t, J = 6.9 Hz, 2 H, CH_2), 3.30–3.39 (m, 2 H, CH_2), 4.18 (q, J = 7.1 Hz, 2 H, CH_2), 5.30 (q, J = 1.4 Hz, 1 H), 6.39 (s, 1 H, Ar), 7.15 (s, 1 H, Ar), 8.45 (d, J = 2.5 Hz, 1 H, Ar), 8.54 (dd, J = 2.5 and 1.5 Hz, 1 H, Ar), 8.64 (s, 1 H, Ar), 9.66 (d, J = 1.5 Hz, 1 H, Ar) ppm. ^{13}C NMR (125.7 MHz, CDCl_3): δ = 14.2(+), 18.6(+), 22.5(-), 29.2(+), 19.6(q), 31.3(-), 44.1(-), 58.3(-), 60.7(-), 96.3(+), 109.1(-), 114.9 (-), 120.6(-), 123.4(+), 126.1(-), 129.9(+), 142.3(+), 143.6(+), 144.0(+), 144.4(+), 148.8(-), 157.3(-), 160.8(-), 172.8 (-) ppm. HRMS (ESI): calc. for $\text{C}_{25}\text{H}_{27}\text{N}_3\text{O}_4$ $[\text{M}+\text{H}]^+$ 456.1894; found 456.1878. UV-Vis spectral data in CH_2Cl_2 : $\lambda_{\text{abs,max}}$ = 451 nm; ϵ = 39200 $\text{M}^{-1}\text{cm}^{-1}$, $\lambda_{\text{em,max}}$ = 506 nm, Φ_{fl} = 0.74 (standard: Lucifer Yellow, Φ_{fl} = 0.21 in H_2O). UV-Vis spectral data in MeOH: $\lambda_{\text{abs,max}}$ = 451 nm; ϵ = 39600 $\text{M}^{-1}\text{cm}^{-1}$, $\lambda_{\text{em,max}}$ = 535 nm, Φ_{fl} = 0.08 (standard: Lucifer Yellow, Φ_{fl} = 0.21 in H_2O).

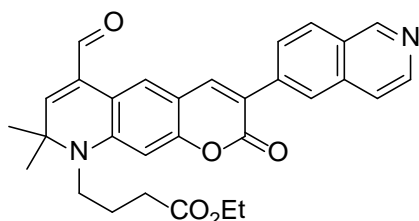


Ethyl 4-(6-formyl-8,8-dimethyl-2-oxo-3-(pyridin-2-yl)-1,2,8,9-tetrahydropyrano[3,2-g]quinolin-9-yl)butanoate (294)

From compound **292**: A round-bottomed flask was charged with solution of compound **292** (208 mg, 0.48 mmol) in dioxane (5 mL) and finely powdered SeO_2 (67 mg,

0.60 mmol). The resulted suspension refluxed for 3.5 h, then water (1 mL) was added, and the reaction mixture was allowed to cool to r.t. All volatile materials were evaporated; the residue was dissolved in CH₂Cl₂, washed with saturated aq. NaHCO₃, dried, and evaporated *in vacuo*. The title compound was isolated as a yellow solid (183 mg, 85%) by means of column chromatography (40 g SiO₂, CH₂Cl₂/Et₂O, 10:1). ¹H NMR (300 MHz, CDCl₃): δ = 1.29 (t, *J* = 7.1 Hz, 3 H, Et), 1.52 (s, 6 H, 2×Me), 1.88–1.99 (m, 2 H, CH₂), 2.42 (t, *J* = 6.8 Hz, 2 H, CH₂), 3.32–3.40 (m, 2 H, NCH₂), 4.18 (q, *J* = 7.1 Hz, 2 H, Et), 6.22 (s, 1 H), 6.47 (s, 1 H, Ar), 7.22 (ddd, *J* = 7.5, 4.8 and 1.0 Hz, 1 H, Ar), 7.74 (ddd, *J* = 8.1, 7.5 and 1.9 Hz, 1 H, Ar), 8.37 (dt, *J* = 8.1 and 1.0 Hz, 1 H, Ar), 8.58 (s, 1 H, Ar), 8.63 (ddd, *J* = 4.8, 1.9 and 1.0 Hz, 1 H, Ar), 8.71 (s, 1 H, Ar) 9.58 (s, 1 H, CHO) ppm. ¹³C NMR (125 MHz, CDCl₃): δ = 14.3(+), 22.9(-), 28.2(+), 31.3(-), 44.2(-), 58.4(-), 60.8(-), 97.5(+), 109.7(-), 113.9(-), 122.3(+), 123.4(+), 126.6(+), 130.5(-), 136.7(+), 143.5(+), 147.6(-), 148.7(+), 151.4(+), 151.9(-), 156.8(-), 160.8(-), 172.6(-), 191.3(+) ppm. HRMS (ESI): calc. for C₂₆H₂₆NO₅ [M+H]⁺ 447.1914; found 447.1906.

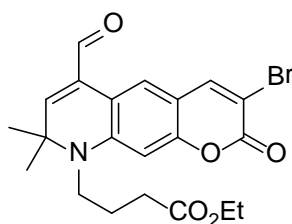
From compound **297**: In a screw-cap tube compound **297** (50 mg, 0.11 mmol), 2-(tributylstannyl)pyridine (43 mg, 0.12 mmol), and Pd(PPh₃)₄ (6.3 mg, 5 mol%) in dioxane (1 mL) were placed under argon. The mixture was heated to 110 °C and left overnight at this temperature with stirring. Afterwards, the reaction mixture was allowed to cool to r.t., diluted with CH₂Cl₂ (10 mL), and water (5 mL) was added. The organic layer was separated; the aqueous phase was extracted with CH₂Cl₂ (3×10 mL). The combined organic extracts were dried and concentrated *in vacuo* to give a crude product. Column chromatography (25 g SiO₂, hexane/EtOAc, 1:1) furnished the desired product as a yellow solid (22 mg, 45 %).



Ethyl 4-(6-formyl-3-(isoquinolin-6-yl)-8,8-dimethyl-2-oxo-1,2,8,9-tetrahydropyrano[3,2-g]quinolin-9-yl)butanoate (295)

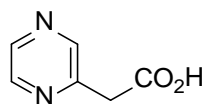
In a screw-cap tube compound **297** (50 mg, 0.11 mmol), boronic ester **301** (34 mg, 0.13 mmol), Pd(PPh₃)₄ (6.5 mg, 5 mol%) and 2 M Na₂CO₃ (224 μL, 0.45 mmol) in toluene (1 mL) were placed under argon. The mixture was heated to 110 °C and left

overnight at this temperature with stirring. Afterwards, the reaction mixture was allowed to cool to r.t., diluted with CH₂Cl₂ (10 mL), passed through a plug of Celite (eluting with CH₂Cl₂), and the filtrate evaporated *in vacuo*. Column chromatography (30 g of SiO₂, CH₂Cl₂/MeOH, 30:1) furnished the title product as a yellow solid (31 mg, 56%). ¹H NMR (400 MHz, CDCl₃): δ = 1.31 (t, *J* = 7.1 Hz, 3 H, Et), 1.55 (s, 6 H, 2×Me), 1.91–2.01 (m, 2 H, CH₂), 2.44 (m, 2 H, CH₂), 3.36–3.43 (m, 2 H, NCH₂), 4.21 (q, *J* = 7.1 Hz, 2 H, Et), 6.26 (s, 1 H), 6.53 (s, 1 H, Ar), 7.68–7.71 (m, 1 H, Ar), 7.93 (dd, *J* = 8.6 Hz and 1.7 Hz, 1 H, Ar), 7.93 (s, 1 H, Ar), 8.01 (d, *J* = 8.6 Hz, 1 H, Ar), 8.22 (br. s, 1 H, Ar), 8.54 (d, *J* = 5.8 Hz, 1 H, Ar), 9.25 (s, 1 H, Ar), 9.61 (s, 1 H, CHO) ppm. ¹³C NMR (100 MHz, CDCl₃): δ = 14.3(+), 22.8(-), 28.1(+), 31.2(-), 44.1(-), 58.3(-), 60.8(-), 97.8(+), 109.7(-), 113.9(-), 120.7(+), 120.9(-), 125.9(+), 127.4(+), 127.5(+), 130.5(-), 135.8(-), 137.4(-), 142.0(+), 143.4(+), 147.5(-), 152.0(+), 156.5(-), 161.0(-), 172.7(-), 191.8(+) ppm. HRMS (ESI): calc. for C₃₀H₂₈N₂O₅ [M+H]⁺ 497.2071; found 497.2059.



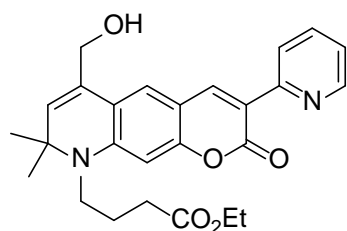
Ethyl 4-(3-bromo-6-formyl-8,8-dimethyl-2-oxo-1,2,8,9-tetrahydropyrano[3,2-g]quinolin-9-yl)butanoate (297)

To a solution of compound **291** (1032 mg, 2.8 mmol) in AcOH (10 mL) bromine solution (537 mg, 3.36 mmol in 5 mL of AcOH) was added dropwise under stirring. After 1 h stirring, the reaction mixture was poured onto water; the resulting slurry was extracted with CH₂Cl₂ (3×20 mL). Combined organic extracts were dried with Na₂SO₄ and evaporated. The crude product was purified by column chromatography (100 g SiO₂, hexane/EtOAc, 1:1) to yield 1240 mg (99%) of title compound as a yellow powder. ¹H NMR (300 MHz, CDCl₃, ppm): δ = 1.28 (t, *J* = 7.1 Hz, 3 H, Et), 1.51 (s, 6 H, 2×Me), 1.85–1.95 (m, 2 H, CH₂), 2.40 (t, *J* = 6.8 Hz, 2 H, CH₂), 3.29–3.37 (m, 2 H, NCH₂), 4.17 (q, *J* = 7.1 Hz, 2 H, Et), 6.23 (s, 1 H), 6.44 (s, 1 H, Ar), 7.92 (s, 1 H, Ar), 8.38 (s, 1 H, Ar), 9.56 (s, 1 H, CHO) ppm. ¹³C NMR (125.7 MHz, CDCl₃): δ = 14.3(+), 22.8(-), 28.1(+), 31.2(-), 44.1(-), 58.3(-), 60.8(-), 98.0(+), 104.4(-), 109.5(-), 113.9(-), 124.7(+), 130.3(-), 144.9(+), 147.2(-), 152.0(+), 155.9(-), 157.8(-), 172.5(-), 191.4(+) ppm. HRMS (ESI): calc. for C₂₁H₂₂BrNO₅ [M+H]⁺ 448.0754; found 448.0741.



2-(Pyrazin-2-yl)acetic acid (299)

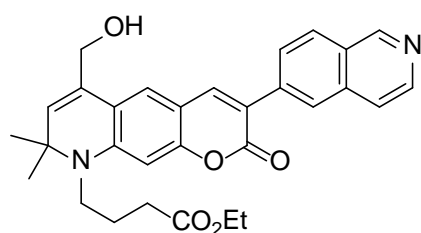
A 100 mL Schlenk flask was charged with a solution of *i*Pr₂NH (1290 mg, 12.8 mmol) in THF (15 mL), cooled to -78 °C, and 1.6M solution of BuLi in hexanes (8 mL, 12.8 mmol) was injected. After 30 min of stirring at this temperature pyrazine (1 g, 10.6 mmol) was added. The reaction mixture was allowed to stir for 1 h and then was quenched with an excess of solid CO₂. After the mixture warmed to r.t., water was added until clear phases formed. A pH was adjusted to 3 with conc. HCl with stirring under ice-cooling. Further extraction with EtOAc (8×50 mL) gave organic solution, which was dried with Na₂SO₄ and evaporated at r.t. to furnish 915 mg (62%) of orange powder. This crude product was used directly without further purification. ¹H NMR (400 MHz, CD₃OD): δ = 3.89 (s, 2 H, CH₂), 8.49 (d, *J* = 2.64 Hz, 1 H, Ar), 8.54 (dd, *J* = 2.64 and 1.52 Hz, 1 H, Ar), 8.62 (d, *J* = 1.52 Hz, 1 H, Ar) ppm. HRMS (ESI): found 137.0354; calc. for C₆H₆N₂O₂ [M-H]⁻ 137.0357.



Ethyl 4-(6-(hydroxymethyl)-8,8-dimethyl-2-oxo-3-(pyridin-2-yl)-1,2,8,9-tetrahydro pyrano[3,2-g]quinolin-9-yl)butanoate (282)

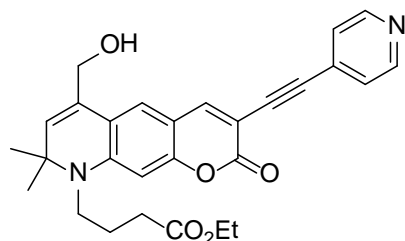
To a cooled solution (0 °C) of compound **294** (67 mg, 0.15 mmol) in the solvent mixture (THF/MeOH, 1:1, 5 mL) powder of CeCl₃ (37 mg, 0.15 mmol) was added. The resulting mixture was stirred until CeCl₃ dissolved, and NaBH₄ (6 mg, 0.15 mmol) was added in one portion. Bright green fluorescence appeared immediately, and after 5 min sat. aq. NH₄Cl (5 mL) and water (5 mL) were added. The reaction mixture was extracted with CH₂Cl₂ (4×10 mL), the combined organic extracts were dried with Na₂SO₄ and evaporated. The residue was purified by column chromatography (30 g of SiO₂, CH₂Cl₂/MeOH, 25:1) to furnish an orange solid (27 mg; 85%). ¹H NMR (300 MHz, CDCl₃): δ = 1.29 (t, *J* = 7.1 Hz, 3 H, Et), 1.36 (s, 6 H, 2×Me), 1.87–1.99 (m, 2 H, CH₂), 2.41 (t, *J* = 6.9 Hz, 2 H, CH₂), 3.27–3.36 (m, 2 H, NCH₂), 4.20 (q, *J* = 7.1 Hz, 2 H, Et), 4.45 (d, *J* = 1.2 Hz, 2 H, CH₂), 5.47 (t, *J* = 1.2 Hz, 1 H), 6.37 (s, 1 H, Ar), 7.18 (ddd, *J* = 7.5, 4.8 and 1.0 Hz,

1 H, Ar), 7.25 (s, 1 H, Ar), 7.71 (ddd, $J = 8.1, 7.5$ and 1.9 Hz, 1 H, Ar), 8.37 (dt, $J = 8.1$ and 1.0 Hz, 1 H, Ar), 8.56 (s, 1 H, Ar), 8.59 (ddd, $J = 4.8, 1.9$ and 1.0 Hz, 1 H, Ar) ppm. ^{13}C NMR (125.7 MHz, CDCl_3): $\delta = 14.4(+), 22.7(-), 29.1(+), 31.4(-), 44.2(-), 58.0(-), 60.7(-), 62.8(-), 96.7(+), 109.1(-), 117.6(-), 117.9(-), 122.1(+), 123.0(+), 123.3(+), 129.3(+), 129.5(-), 136.4(+), 142.9(+), 148.0(-), 148.8(+), 152.3(-), 156.6(-), 161.1(-), 172.6(-)$ ppm. HRMS (ESI): calc. for $\text{C}_{26}\text{H}_{28}\text{NO}_5$ $[\text{M}+\text{H}]^+$ 449.2071; found 449.2071. UV-Vis spectral data in MeOH: $\lambda_{\text{abs,max}} = 431$ nm; $\epsilon = 32100 \text{ M}^{-1}\text{cm}^{-1}$, $\lambda_{\text{em,max}} = 498$ nm, $\Phi_{\text{fl}} = 0.67$ (standard: Coumarin 334, $\Phi_{\text{fl}} = 0.69$ in EtOH).



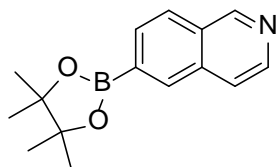
Ethyl 4-(6-(hydroxymethyl)-3-(isoquinolin-6-yl)-8,8-dimethyl-2-oxo-1,2,8,9-tetrahydropyrano[3,2-g]quinolin-9-yl)butanoate (284)

To a cooled solution ($0\text{ }^\circ\text{C}$) of compound **295** (31 mg, 0.06 mmol) in the solvent mixture (THF/MeOH, 1:1, 5 mL) powder of CeCl_3 (15 mg, 0.06 mmol) was added. The resulting mixture was stirred until CeCl_3 dissolved, and NaBH_4 (2.5 mg, 0.06 mmol) was added in one portion. Bright green fluorescence appeared immediately, and after 5 min, sat. aq. NH_4Cl (2 mL) and water (2 mL) were added. The reaction mixture was extracted with CH_2Cl_2 (3×15 mL); combined organic extracts were dried with Na_2SO_4 and evaporated. The residue was purified by column chromatography (30 g of SiO_2 , $\text{CH}_2\text{Cl}_2/\text{MeOH}$, 25:1) to furnish an orange solid (14 mg, 45%). ^1H NMR (400 MHz, CDCl_3): $\delta = 1.32$ (t, $J = 7.1$ Hz, 3 H, Et), 1.44 (s, 6 H, $2 \times \text{Me}$), 1.91–2.02 (m, 2 H, CH_2), 2.44 (m, 2 H, CH_2), 3.37 (m, 2 H, NCH_2), 4.21 (q, $J = 7.1$ Hz, 2 H, Et), 4.51 (s, 2 H, CH_2), 5.58 (s, 1 H), 6.46 (s, 1 H, Ar), 7.31 (s, 1 H, Ar), 7.69 (d, $J = 5.8$ Hz, 1 H, Ar), 7.85 (s, 1 H, Ar), 7.92 (dd, $J = 8.6$ and 1.7 Hz, 1 H, Ar), 7.99 (d, $J = 8.6$ Hz, 1 H, Ar), 8.22 (br. s, 1 H, Ar), 8.53 (d, $J = 5.8$ Hz, 1 H, Ar), 9.24 (s, 1 H, Ar) ppm. ^{13}C NMR (100 MHz, CDCl_3): $\delta = 14.3, 22.7, 29.0, 31.3, 44.0, 58.0, 60.7, 63.0, 97.0, 109.2, 117.7, 119.9, 120.8, 122.6, 125.6, 127.4, 127.5, 127.8, 129.7, 130.1, 135.8, 137.7, 141.8, 143.2, 148.0, 152.0, 156.4, 161.2, 172.7$ ppm. MS (ESI): m/z (positive mode, rel. int., %) = 499 (100) $[\text{M}+\text{H}]^+$. UV-Vis spectral data in MeOH: $\lambda_{\text{abs,max}} = 431$ nm; $\epsilon = 41100 \text{ M}^{-1}\text{cm}^{-1}$, $\lambda_{\text{em,max}} = 511$ nm, $\Phi_{\text{fl}} = 0.72$ (standard: Coumarin 522, $\Phi_{\text{fl}} = 0.65$ in EtOH).



Ethyl 4-(6-(hydroxymethyl)-8,8-dimethyl-2-oxo-3-(pyridin-4-ylethynyl)-1,2,8,9-tetrahydropyrano[3,2-g]quinolin-9-yl)butanoate (285)

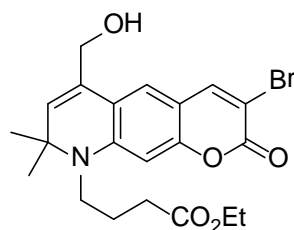
To a cooled solution (0 °C) of compound **296** (80 mg, 0.17 mmol) in the solvent mixture (THF/MeOH, 2:1, 7 mL) powder of CeCl₃ (42 mg, 0.17 mmol) was added. The resulting mixture was stirred until CeCl₃ dissolved, and NaBH₄ (6.5 mg, 0.17 mmol) was added in one portion. Bright green fluorescence appeared immediately, and after 5 min, an excess of acetone was added. The reaction mixture was evaporated, and the residue was taken in water (~15 mL) and extracted with CH₂Cl₂ (3×20 mL). Combined organic extracts were dried with Na₂SO₄ and evaporated. Purification by column chromatography (30 g SiO₂, CH₂Cl₂/MeOH, 25:1) furnished the title product as an orange solid (14 mg, 45%). ¹H NMR (300 MHz, CDCl₃): δ = 1.29 (t, *J* = 7.1 Hz, 3 H, Et), 1.42 (s, 6 H, 2×Me), 1.85–1.97 (m, 2 H, CH₂), 2.40 (m, 2 H, CH₂), 3.34 (m, 2 H, NCH₂), 4.18 (q, *J* = 7.1 Hz, 2 H, Et), 4.45 (br. s, 2 H, CH₂), 5.55 (s, 1 H), 6.38 (s, 1 H, Ar), 7.16 (s, 1 H, Ar), 7.35–7.39 (m, 2 H, Ar), 7.79 (s, 1 H, Ar), 8.54–8.57 (m, 2 H, Ar) ppm. ¹³C NMR (125.7 MHz, CDCl₃): δ = 14.3(+), 22.7(-), 29.2(+), 31.3(-), 44.2(-), 58.3(-), 60.8(-), 62.9(-), 89.4(-), 90.5(-), 97.2(+), 103.7(-), 108.4(-), 117.8(-), 122.3(+), 125.4(+), 129.3(-), 130.0(+), 131.2(-), 146.6(+), 148.5(-), 149.5(+), 156.4(-), 160.3(-), 172.5(-) ppm. HRMS (ESI): calc. for C₂₈H₂₈N₂O₅ [M+H]⁺ 473.2071; found 473.2054. UV-Vis spectral data in MeOH: λ_{abs,max} = 457 nm; ε = 44200 M⁻¹cm⁻¹, λ_{em,max} = 511 nm, Φ_{fl} = 0.62 (standard: Coumarin 334, Φ_{fl} = 0.69 in EtOH).



6-(4,4,5,5-Tetramethyl-1,3,2-dioxaborolan-2-yl)isoquinoline (301)

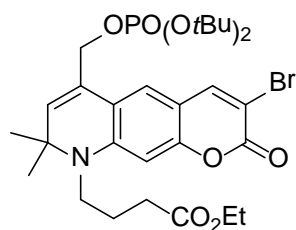
A dried 25 mL Schlenk flask was charged with a solution of 6-bromoisquinoline (200 mg, 0.96 mmol) in THF (7 mL) and cooled down to -78 °C. Afterwards, a solution of *t*BuLi (0.68 mL, 1.7 M, 1.15 mmol) was injected. The resulting reaction mixture was stirred for 20 min at -78 °C, and B(O*i*Pr₃) (218 mg, 1.15 mmol) was added. After over-

night stirring at r.t., AcOH (86 mg, 1.44 mmol) and pinacol (226 mg, 1.92 mmol) were added. The reaction mixture was stirred for additional 2 h at r.t., and sat. aq. NaCl was added (~25 mL). The resulted mixture was extracted with EtOAc (3×25 mL). Combined organic extracts were dried with Na₂SO₄ and evaporated. The residue was subjected to column chromatography to afford 147 mg (60%) of a clear oil. ¹H NMR (400 MHz, CDCl₃): δ = 1.40 (s, 12 H, 4×Me), 7.68 (d, *J* = 5.7 Hz, 1 H, Ar), 7.93–7.99 (m, 2 H, Ar), 8.34 (s, 1 H, Ar), 8.54 (d, *J* = 5.7 Hz, 1 H, Ar), 9.27 (s, 1 H, Ar) ppm. MS (ESI): *m/z* (positive mode, rel. int., %) = 256 (100) [M+H]⁺.



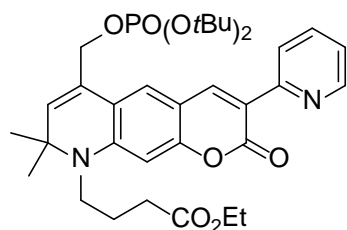
Ethyl 4-(3-bromo-6-(hydroxymethyl)-8,8-dimethyl-2-oxo-1,2,8,9-tetrahydro-pyrano[3,2-g]quinolin-9-yl)butanoate (302)

To an ice cooled solution of compound **297** (100 mg; 0.22 mmol) in a solvent mixture (5 mL, THF/MeOH, 1:1) powder of CeCl₃ (54 mg; 0.22 mmol) was added under stirring. After its dissolution, NaBH₄ (8.5 mg; 0.22 mmol) was added in one portion. The reaction mixture was stirred for 5 min, acetone (5 mL) was added, and reaction mixture was allowed to warm up to r.t. All volatile materials were evaporated *in vacuo*, the residue was taken up in water (10 mL) and extracted with CHCl₃ (3×10 mL). The combined organic liquids were dried and concentrated to give crude product. The title compound was purified by means of column chromatography (25 g of SiO₂, CH₂Cl₂/MeOH, 25:1) as a yellow amorphous solid (96 mg; 95%). ¹H NMR (400 MHz, CDCl₃): δ = 1.30 (t, *J* = 7.1 Hz, 3 H, Et), 1.42 (s, 6 H, 2×Me), 1.87–1.96 (m, 2 H, CH₂), 2.41 (t, *J* = 6.9 Hz, 2 H, CH₂), 3.29–3.35 (m, 2 H, NCH₂), 4.19 (q, *J* = 7.1 Hz, 2 H, Et), 4.45 (br. s, 2 H, CH₂), 5.55 (t, *J* = 1.2 Hz, 1 H), 7.1 (s, 1 H, Ar), 7.87 (s, 1 H, Ar) ppm. ¹³C NMR (100 MHz, CDCl₃): δ = 14.2(+), 22.6(-), 29.0(+), 31.3(-), 44.0(-), 57.9(-), 60.7(-), 63.0(-), 97.2(+), 103.4(-), 109.1(-), 117.8(-), 121.5(+), 129.5(-), 130.2(+), 144.7(+), 147.8(-), 155.9(-), 172.7(-) ppm. HRMS (ESI): calc. for C₂₆H₂₈N₂O₅ [M+H]⁺ 449.2071; found 449.2071.



Ethyl 4-(3-bromo-6-((di-*tert*-butoxyphosphoryloxy)methyl)-8,8-dimethyl-2-oxo-1,2,8,9-tetrahydropyrano[3,2-*g*]quinolin-9-yl)butanoate (303)

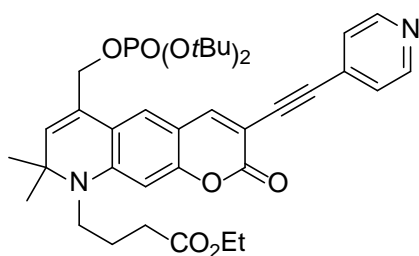
To a stirred and preheated (40 °C) solution of compound **302** (130 mg, 0.29 mmol) in CH₂Cl₂ (10 mL) di-*t*-butyl *N,N*-diisopropylphosphoramidite (240 mg, 0.87 mmol) and 1*H*-tetrazole (65 mg, 0.93 mmol) were added in two equal portions at interval of 20 min under Ar. After further 20 min the reaction mixture was cooled with ice bath (0 °C) and solution of *m*CPBA (214 mg, 70% purity, 0.87 mmol) in CH₂Cl₂ was added. After stirring for additional 30 min aqueous solutions of Na₂SO₃ (4 mL, 10%) and NaHCO₃ (5 mL, saturated) were added, and the reaction mixture was allowed to warm up to r.t. The organic layer was separated and the aqueous phase was extracted with CH₂Cl₂ (3×20 mL). The combined organic extracts were dried, the solvents were evaporated, and the titled compound was isolated by column chromatography (30 g of SiO₂, *n*-hexane/EtOAc, 1:1) as a yellow amorphous solid (162 mg, 87%). ¹H NMR (400 MHz, CDCl₃): δ = 1.29 (t, *J* = 7.1 Hz, 3 H, Et), 1.41 (s, 6 H, 2×Me), 1.48 (s, 18 H, 2×*t*Bu), 1.86–1.95 (m, 2 H, CH₂), 2.40 (t, *J* = 6.8 Hz, 2 H, CH₂), 3.28–3.34 (m, 2H, NCH₂), 4.18 (q, *J* = 7.1 Hz, 2 H, Et), 4.72 (d, ³*J*_{HP} = 7.4 Hz, 2 H, CH₂), 5.61 (s, 1H), 6.38 (s, 1 H, Ar), 7.13 (s, 1 H, Ar), 7.86 (s, 1 H, Ar) ppm. ¹³C NMR (100.7 MHz, CDCl₃): δ = 14.2(+), 22.6(+), 28.9(+), 29.9(+, d, ³*J*_{CP} = 4.3 Hz), 31.3(-), 44.0(-), 58.0(-), 60.7(-), 66.0(-, d, ²*J*_{CP} = 5.5 Hz), 82.7 (-, d, ²*J*_{CP} = 7.4 Hz), 97.2(+), 103.5(-), 109.1(-), 117.4(-), 121.6(+), 126.1(-, d, ³*J*_{CP} = 7.8 Hz), 132.0(+), 144.7(+), 147.6(-), 155.9(-), 158.1(-), 172.7(-) ppm. HRMS (ESI): calc. for C₂₉H₄₁BrNO₈P [M+H]⁺ 642.1826; found 642.1818.



Ethyl 4-(6-((di-*tert*-butoxyphosphoryloxy)methyl)-8,8-dimethyl-2-oxo-3-(pyridin-2-yl)-1,2,8,9-tetrahydropyrano[3,2-*g*]quinolin-9-yl)butanoate (304)

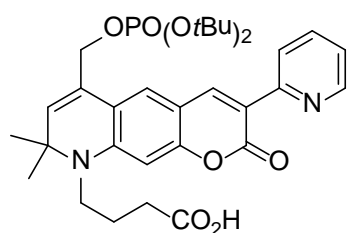
From compound **282**: To a stirred and preheated (40 °C) solution of compound **282** (70 mg, 0.16 mmol) in CH₂Cl₂ (10 mL) di-*t*-butyl *N,N*-diisopropylphosphoramidite (130 mg, 0.47 mmol) and 1*H*-tetrazole (35 mg, 0.5 mmol) were added in two equal portions at interval of 20 min under argon. After further 20 min the reaction mixture was cooled with ice bath (0 °C), and solution of *m*CPBA (115 mg, 70 % purity, 0.47 mmol) in CH₂Cl₂ was added. After stirring for additional 30 min aqueous solutions of Na₂SO₃ (2 mL, 10%) and NaHCO₃ (2 mL, saturated) were added, and the reaction mixture was allowed to warm up to r.t. The organic layer was separated and the aqueous phase was extracted with CH₂Cl₂ (3×10 mL). The combined organic extracts were dried, the solvents were evaporated, and the titled compound was isolated by column chromatography (30 g of SiO₂, CH₂Cl₂/MeOH, 25:1) as an orange amorphous solid (88 mg, 88%). ¹H NMR (400 MHz, CDCl₃): δ = 1.31 (t, *J* = 7.1 Hz, 3 H, Et), 1.43 (s, 6 H, 2×Me), 1.50 (s, 18 H, 2×*t*Bu), 1.90–1.99 (m, 2 H, CH₂), 2.42 (t, *J* = 6.9 Hz, 2 H, CH₂), 3.33–3.38 (m, 2 H, NCH₂), 4.20 (q, *J* = 7.1 Hz, 2 H, Et), 4.75 (dd, ³*J*_{HP} = 7.3 Hz, ⁴*J*_{HH} = 1.2 Hz, 2 H, CH₂), 5.64 (t, *J* = 1.2 Hz, 1 H), 6.42 (s, 1 H, Ar), 7.19 (ddd, *J* = 7.5, 4.8 and 1.0 Hz, 1 H, Ar), 7.26 (s, 1 H, Ar), 7.72 (ddd, *J* = 8.1, 7.5 and 1.9 Hz, 1 H, Ar), 8.39 (dt, *J* = 8.1 and 1.0 Hz, 1 H, Ar), 8.62 (ddd, *J* = 4.8, 1.9 and 1.0 Hz, 1 H, Ar), 8.65 (s, 1 H, Ar) ppm. ¹³C NMR (100.7 MHz, CDCl₃): δ = 14.3(+), 22.7(–), 28.9(+), 29.9 (+, d, ³*J*_{CP} = 4.3 Hz), 31.3(–), 44.1(–), 58.0(–), 60.7(–), 65.8(–, d, ²*J*_{CP} = 5.5 Hz), 82.6 (–, d, ²*J*_{CP} = 7.4 Hz), 96.7(+), 109.3(–), 117.4(–), 118.4(–), 122.2(+), 123.1(+), 123.2(+), 126.2(–, d, ³*J*_{CP} = 7.8 Hz), 131.1(+), 136.4(+), 142.9(+), 147.9(–), 149.1(+), 152.4(–), 156.7(–), 161.2(–), 172.7(–) ppm. HRMS (ESI): calc. for C₃₄H₄₅N₂O₈P [M+H]⁺ 641.2986; found 641.2986.

From compound **303**: A 10 mL Schlenk flask was flushed with Ar and charged consequently with toluene (0.5 mL), Pd(OAc)₂ (1 mg; 4.5·10^{–3} mmol), the solution of P(*t*-Bu)₃ in dioxane (0.395 M, 23 μl, 9·10^{–3} mmol), the solution of bromide **303** (48 mg; 0.075 mmol) in toluene (1 mL) and 2-(tributylstannyl)pyridine (30 mg; 0.082 mmol). The reaction mixture was stirred at 110 °C for 2 h, cooled to r.t., and water (5 mL) and CH₂Cl₂ were added. The organic phase was separated; aqueous layer was extracted with CH₂Cl₂ (3×10 mL). The combined organic extracts were dried with Na₂SO₄ and evaporated. A purification of the crude product by chromatography (30 g of SiO₂, CH₂Cl₂/MeOH, 25:1) gave 27 mg (56 %) of a red solid.



Ethyl 4-(6-((di-*tert*-butoxyphosphoryloxy)methyl)-8,8-dimethyl-2-oxo-3-(pyridin-4-ylethynyl)-1,2,8,9-tetrahydropyrano[3,2-*g*]quinolin-9-yl)butanoate (305)

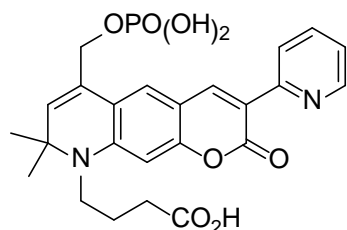
To a stirred and preheated (40 °C) solution of compound **285** (20 mg, 0.04 mmol) in CH₂Cl₂ (4 mL) di-*t*-butyl *N,N*-diisopropylphosphoramidite (16 mg, 0.06 mmol) and 1*H*-tetrazole (5 mg, 0.07 mmol) were added in two equal portions at interval of 20 min under argon. After further 20 min the reaction mixture was cooled down with ice bath (0 °C), and solution of *m*CPBA (15.5 mg, 70 % purity, 0.06 mmol) in CH₂Cl₂ (2 mL) was added. After stirring for additional 15 min, aqueous solutions of Na₂SO₃ (2 mL, 10%) and NaHCO₃ (2 mL, saturated) were added, and the reaction mixture was allowed to warm up to r.t. The organic layer was separated, and the aqueous phase was extracted with CH₂Cl₂ (2×10 mL). The combined organic extracts were dried, the solvents were evaporated, and the titled compound was isolated by column chromatography (25 g of SiO₂, CH₂Cl₂/MeOH, 25:1) as an orange amorphous solid (23 mg; 82%). ¹H NMR (400 MHz, CDCl₃): δ = 1.19 (t, *J* = 7.1 Hz, 3 H, Et), 1.42 (s, 6 H, 2×Me), 1.48 (br. s, 18 H, 2×*t*Bu), 1.87–1.95 (m, 2 H, CH₂), 2.40 (t, *J* = 6.8 Hz, 2 H, CH₂), 3.30–3.38 (m, 2 H, NCH₂), 4.18 (q, *J* = 7.1 Hz, 2 H, Et), 4.75 (d, ³*J*_{HP} = 7.0 Hz, 2 H, CH₂), 5.61 (s, 1 H), 6.38 (s, 1 H, Ar), 7.18 (s, 1 H, Ar), 7.36–7.39 (m, 2 H, Ar), 7.79 (s, 1 H, Ar), 8.55–8.58 (m, 2 H, Ar) ppm. HRMS (ESI): calc. for C₃₆H₄₅N₂O₈P [M+H]⁺ 665.2986; found 665.2984.



4-(6-((Di-*tert*-butoxyphosphoryloxy)methyl)-8,8-dimethyl-2-oxo-3-(pyridin-2-yl)-1,2,8,9-tetrahydropyrano[3,2-*g*]quinolin-9-yl)butanoic acid (306)

To a solution of **304** (98 mg, 0.15 mmol) in the solvent mixture (20 mL, THF/water, 3:2) 1 M solution of NaOH (0.6 mL, 0.6 mmol) was added. The reaction mixture was stirred overnight at r.t., then its acidity was adjusted to pH 4 with sat. aq. KHSO₄. The resulted solution was extracted with EtOAc (5×25 mL), the combined organic extracts were dried

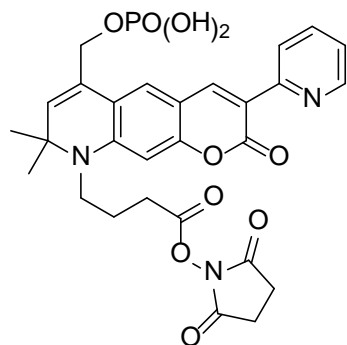
and concentrated *in vacuo*. The titled compound was isolated by column chromatography (30 g of SiO₂, CH₂Cl₂/MeOH, 15:1) as a red solid (60 mg; 65%). ¹H NMR (400 MHz, CDCl₃): δ = 1.40 (s, 6 H, 2×Me), 1.50 (s, 18 H, 2×*t*Bu), 1.90–2.00 (m, 2 H, CH₂), 2.47 (t, *J* = 6.8 Hz, 2 H, CH₂), 3.33–3.39 (m, 2 H, CH₂), 4.78 (dd, *J*_{HP} = 7.5 Hz, *J*_{HH} = 1.1 Hz, 2 H, CH₂), 5.64 (d, *J* = 1.1 Hz, 1 H), 6.43 (s, 1 H, Ar), 7.21 (ddd, *J* = 7.5, 4.9 and 1.1 Hz, 1 H, Ar), 7.73 (ddd, *J* = 8.0, 7.5 and 1.9 Hz, 1 H, Ar), 8.35 (dt, *J* = 8.0 and 1.1 Hz, 1 H, Ar), 8.59 (s, 1 H, Ar), 8.64 (ddd, *J* = 4.9, 1.9 and 1.1 Hz, 1 H, Ar) ppm. ¹³C NMR (100 MHz, CDCl₃): δ = 14.1(+), 22.7(-), 28.8(+), 29.9 (+, d, *J*_{CP} = 4.3 Hz), 31.1(-), 43.9(-), 58.0(-), 66.0(-, d, *J*_{CP} = 5.5 Hz), 83.1(-, d, *J*_{CP} = 7.6 Hz), 96.9(+), 109.3(-), 117.5(-), 118.2(-), 122.3(+), 123.1(+), 123.4(+), 126.2(-, d, *J*_{CP} = 7.7 Hz), 131.4(+), 136.6(+), 143.1(+), 148.0(-), 148.9(+), 152.4(-), 156.7(-), 161.2(-), 176.7(-) ppm. HRMS (ESI): calc. for C₃₂H₄₁N₂O₈P [M-H]⁻ 611.2528; found 611.2517.



4-(8,8-Dimethyl-2-oxo-6-(phosphonomoxymethyl)-3-(pyridin-2-yl)-1,2,8,9-tetrahydropyrano[3,2-*g*]quinolin-9-yl)butanoic acid (308)

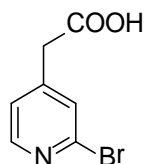
To a solution of **307** (60 mg, 0.10 mmol) in CH₂Cl₂ (5 mL) trifluoroacetic acid (0.3 mL) was added. The resulted mixture was stirred for 30 min. Then all volatile substances were evaporated *in vacuo*, and the residue was subjected to a column chromatography (20 g of SiO₂, MeCN/water, 2:1 + 0.1% NEt₃) to furnish 56 mg of red amorphous solid (as **308**·3NEt₃, 78%). ¹H NMR (400 MHz, CD₃OD): δ = 1.29 (t, *J* = 7.3 Hz, 27 H, 9×Et), 1.41 (s, 6 H, 2×Me), 1.84–1.93 (m, 2 H, CH₂), 2.44 (t, *J* = 6.7 Hz, 2 H, CH₂), 3.17 (q, *J* = 7.3 Hz, 18 H, 9×CH₂), 3.37–3.44 (m, 2 H, CH₂), 4.69 (d, *J*_{HP} = 4.8 Hz, 2 H, CH₂), 5.71 (s, 1 H), 6.58 (s, 1 H, Ar), 7.28 (ddd, *J* = 7.5, 4.9 and 1.1 Hz, 1 H, Ar), 7.48 (s, 1 H, Ar), 7.81 (ddd, *J* = 8.0, 7.5 and 1.9 Hz, 1 H, Ar), 8.15–8.20 (m, 1 H, Ar), 8.52 (s, 1 H, Ar), 8.53–8.57 (m, 1 H, Ar) ppm. ¹³C NMR (100.7 MHz, CD₃OD): δ = 22.6(-), 27.7(+), 30.4(-), 43.7(-), 58.0(-), 64.4(-, d, *J*_{CP} = 5.5 Hz), 96.2(+), 108.9(-), 110.0(-), 116.7(-), 118.1(-), 122.2(+), 123.2(+), 123.5(+), 127.3(-, d, *J*_{CP} = 7.7 Hz), 131.1(+), 136.8(+), 143.8(+), 148.3(+), 148.7(-), 152.5(-), 156.6(-), 161.6(-), 175.4(-) ppm. HRMS (ESI): calc. for C₂₄H₂₅N₂O₈P [M-H]⁻ 499.1276; found 499.1266. UV-Vis spectral data in PBS

7.4: $\lambda_{\text{abs,max}} = 432 \text{ nm}$; $\epsilon = 20417 \text{ M}^{-1}\text{cm}^{-1}$, $\lambda_{\text{em,max}} = 512 \text{ nm}$, $\Phi_{\text{fl}} = 0.81$ (standard: Coumarin 522, $\Phi_{\text{fl}} = 0.65$ in EtOH).



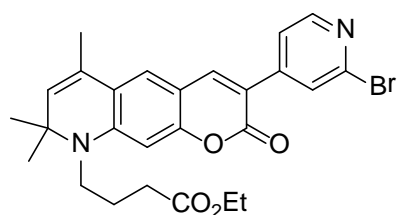
2,5-Dioxopyrrolidin-1-yl 4-(8,8-dimethyl-2-oxo-6-(phosphonooxymethyl)-3-(pyridin-2-yl)-1,2,8,9-tetrahydropyrano[3,2-g]quinolin-9-yl)butanoate (309)

Solution of **308**·3NEt₃ (10 mg, 0.012 mmol), N-hydroxysuccinimide (2.8 mg; 0.024 mmol), HATU (11.4 mg, 0.030 mmol) and NEt₃ (12 mg, 0.120 mmol) in DMF (1.5 mL) was stirred overnight at r.t. Afterwards, DMF was evaporated at r.t., and the residue was subjected to column chromatography (15 g of SiO₂, MeCN/water, 4:1) to give 3 mg of red solid (42%). HPLC: B/A = 20/80 to 50/50 in 25 min, detection at 433 nm, $t_{\text{R}} = 12.6$ min (100%). HRMS (ESI): calc. for C₂₈H₂₈N₃O₁₀P [M-H]⁻ 596.1440; found 596.1428.



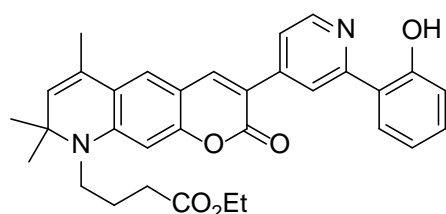
2-(2-bromopyridin-4-yl)acetic acid (316)

A dried Schlenk flask was charged with a solution of *i*Pr₂NH (704 mg, 7.0 mmol) in THF (10 mL), cooled to -78 °C, and 1.6M solution of BuLi in hexanes (4.4 mL, 7.0 mmol) was injected. After 15 min stirring at this temperature, 2-bromo-4-picoline (1 g, 5.8 mmol) was added. The reaction mixture was allowed to stir for 1.5 h and then was quenched with an excess of solid CO₂. After the reaction mixture had warmed to r.t., water was added until clear phases formed. pH was adjusted to 14 with KOH under ice-cooling. The resulting mixture was extracted with CH₂Cl₂ (3×). The aq. layer was separated and acidified to pH 3 with conc. HCl. Further extraction with CH₂Cl₂ (4×) gave organic solution, which was dried with Na₂SO₄ and evaporated at r.t. to furnish 1170 mg (80%) of the crude product as a hydrochloride. ¹H NMR (400 MHz, CD₃OD): $\delta = 3.69$ (s, 2 H, CH₂), 7.34 (d, $J = 5.1$ Hz, 1 H, Ar), 7.58 (s, 1 H, Ar), 8.25 (d, $J = 5.1$ Hz, 1 H, Ar) ppm. MS (ESI): m/z (positive mode, rel. int., %) = 216 (100) [M+H]⁺.



Ethyl 4-(3-(2-bromopyridin-4-yl)-6,8,8-trimethyl-2-oxo-1,2,8,9-tetrahydropyrano[3,2-g]quinolin-9-yl)butanoate (317)

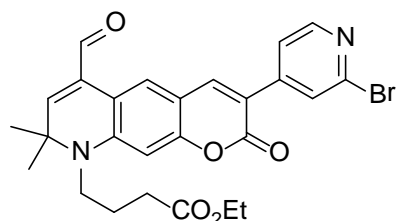
To a solution of **289** (1280 mg, 3.9 mmol) in CH₂Cl₂ (50 mL) compound **316**·HCl (1170 mg, 4.6 mmol), NEt₃ (1580 mg, 15.6 mmol), DCC (1200 mg, 5.8 mmol) and DMAP (47 mg, 0.39 mmol, 10 mol%) were added. The resulting mixture was stirred overnight. Afterwards, an additional amount of DCC (1200 mg, 5.8 mmol) was added, and the reaction mixture was heated under reflux for 6 h. After cooling down, the precipitated urea was filtered, and the filtrate was evaporated under reduced pressure. The residue was subjected to column chromatography (150 g of SiO₂, *n*-hexane/EtOAc, 2:1) to furnish 1320 mg (66%) of a title product as a yellow-orange powder. ¹H NMR (400 MHz, CDCl₃): δ = 1.31 (t, *J* = 7.1 Hz, 3 H, Et), 1.41 (s, 3 H, 2×Me), 1.89–1.98 (m, 2 H, CH₂), 2.00 (s, 3 H, Me), 2.43 (t, *J* = 6.8 Hz, 2 H, CH₂), 3.31–3.40 (m, 2 H, NCH₂), 4.20 (q, *J* = 7.1 Hz, 2 H, Et), 5.33 (s, 1 H, Ar), 6.38 (s, 1 H, Ar), 7.10 (s, 1 H, Ar), 7.68 (dd, *J* = 5.3 and 1.5 Hz, 1 H, Ar), 7.85 (s, 1 H, Ar), 7.88 (d, *J* = 1.5 Hz, 1 H, Ar), 8.34 (d, *J* = 5.3 Hz, 1 H, Ar) ppm. HRMS (ESI): calc. for C₂₆H₂₅N₂O₅Br [M+H]⁺ 511.1227; found 511.1202.



Ethyl 4-(3-(2-(2-hydroxyphenyl)pyridin-4-yl)-6,8,8-trimethyl-2-oxo-1,2,8,9-tetrahydropyrano[3,2-g]quinolin-9-yl)butanoate (318)

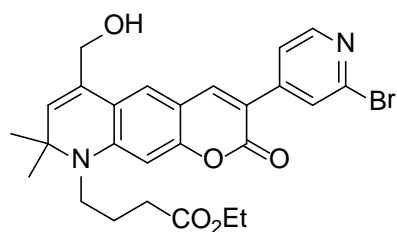
In a screw-cap tube compound **317** (20 mg, 0.04 mmol), 2-hydroxyphenylboronic acid (5.5 mg, 0.04 mmol), Pd(PPh₃)₄ (2.3 mg, 0.002 mmol, 5 mol%), sat. aq. solution of Na₂CO₃ (80 μL, 2 M, 0.16 mmol), EtOH (80 μL) and toluene (1 mL) were placed under argon. The mixture was heated to 110 °C and left stirred overnight at this temperature. Afterwards, the reaction mixture was allowed to cool to r.t., diluted with CH₂Cl₂ (10 mL), passed through a plug of Celite (eluting with CH₂Cl₂), and the filtrate evaporated *in vacuo*. Column chromatography (25 g of SiO₂, *n*-hexane/EtOAc, 3:1) furnished the title

product as a yellow solid (17 mg; 81%). ^1H NMR (400 MHz, CDCl_3): δ = 1.33 (t, J = 7.1 Hz, 3 H, Et), 1.43 (s, 6 H, 2 \times Me), 1.92–2.01 (m, 2 H, CH_2), 2.03 (s, 3 H, Me), 2.45 (t, J = 6.9 Hz, 2 H, CH_2), 3.34–3.42 (m, 2 H, CH_2), 4.22 (q, J = 7.1 Hz, 2 H, Et), 5.34 (s, 1 H), 6.43 (s, 1 H, Ar), 6.89–6.96 (m, 1 H, Ar), 7.02–7.07 (m, 1 H, Ar), 7.14 (s, 1 H, Ar), 7.28–7.35 (m, 1 H, Ar), 7.63–7.67 (m, 1 H, Ar), 7.88–7.94 (m, 2 H, Ar), 8.34 (s, 1 H, Ar), 8.49–8.53 (m, 1 H, Ar) ppm. MS (ESI): m/z (positive mode, rel. int., %) = 525 (100) $[\text{M}+\text{H}]^+$.



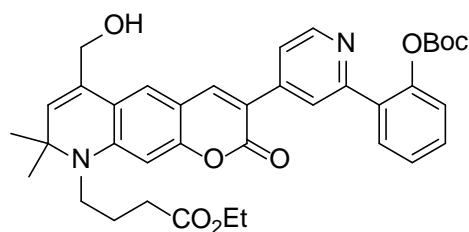
Ethyl 4-(3-(2-bromopyridin-4-yl)-6-formyl-8,8-dimethyl-2-oxo-1,2,8,9-tetrahydropyrano[3,2-g]quinolin-9-yl)butanoate (320)

A round-bottomed flask was charged with solution of compound **317** (600 mg, 1.17 mmol) in dioxane (10 mL) and finely powdered SeO_2 (162 mg, 1.46 mmol). The resulted suspension was heated under reflux for 3.5 h, then water (10 mL) was added, and the reaction mixture was allowed to cool to r.t. All volatile materials were evaporated; the residue was dissolved in CH_2Cl_2 , washed with saturated aq. NaHCO_3 , dried, and evaporated *in vacuo*. The title compound was isolated as a yellow solid (320 mg, 52%) by means of column chromatography (100 g of SiO_2 , $\text{CH}_2\text{Cl}_2/\text{Et}_2\text{O}$, 10:1). ^1H NMR (400 MHz, CDCl_3): δ = 1.31 (t, J = 7.1 Hz, 3 H, Et), 1.56 (s, 6 H, 2 \times Me), 1.90–2.00 (m, 2 H, CH_2), 2.44 (t, J = 6.7 Hz, 2 H, CH_2), 3.40 (m, 2 H, CH_2), 4.20 (q, J = 7.1 Hz, 2 H, Et), 6.27 (s, 1 H), 6.50 (s, 1 H, Ar), 7.66 (dd, J = 5.3 and 1.6 Hz, 1 H, Ar), 7.90 (dd, J = 1.6 and 0.6 Hz, 1 H, Ar), 7.92 (s, 1 H, Ar), 8.38 (dd, J = 5.3 and 0.6 Hz, 1 H, Ar), 8.55 (s, 1 H, Ar), 9.60 (s, 1 H, CHO) ppm. ^{13}C NMR (100 MHz, CDCl_3): δ = 14.3(+), 22.7(-), 28.2(+), 31.1(-), 44.2(-), 58.6(-), 60.8(-), 97.7(+), 109.1(-), 114.1(-), 116.9(-), 121.3(+), 126.3(+), 126.3(+), 130.2(-), 142.6(-), 142.7(+), 145.7(-), 148.2(-), 150.0(+), 152.0(+), 156.9(-), 160.0(-), 172.6(-), 191.6(+) ppm. HRMS (ESI): calc. for $\text{C}_{26}\text{H}_{25}\text{N}_2\text{O}_5\text{Br}$ $[\text{M}+\text{H}]^+$ 525.1020; found 525.1006.



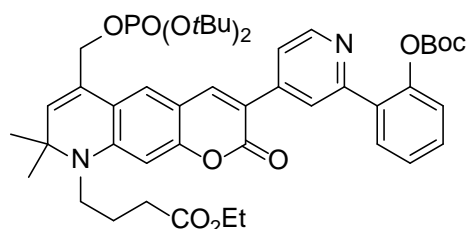
Ethyl 4-(3-(2-bromopyridin-4-yl)-6-(hydroxymethyl)-8,8-dimethyl-2-oxo-1,2,8,9-tetrahydropyrano[3,2-g]quinolin-9-yl)butanoate (321)

To an ice cooled solution of compound **320** (200 mg, 0.38 mmol) in a solvent mixture (10 mL, THF/MeOH, 1:1) powder of CeCl₃ (93 mg, 0.38 mmol) was added under stirring. After its dissolution, NaBH₄ (14.5 mg, 0.38 mmol) was added in one portion. The reaction mixture was stirred for 5 min, acetone (5 mL) was added, and the reaction mixture was allowed to warm up to r.t. All volatile materials were evaporated *in vacuo*, the residue was taken up in water (10 mL) and extracted with CHCl₃ (3×10 mL). The combined organic liquids were dried and concentrated to give a crude product. The title compound was purified by means of column chromatography (25 g of SiO₂, CH₂Cl₂/MeOH, 25:1) as an orange solid (195 mg, 97%). ¹H NMR (400 MHz, CDCl₃): δ = 1.31 (t, *J* = 7.1 Hz, 3 H, Et), 1.44 (s, 6 H, 2×Me), 1.88–1.98 (m, 2 H, CH₂), 2.42 (t, *J* = 6.8 Hz, 2 H, CH₂), 3.32–3.39 (m, 2 H, NCH₂), 4.20 (q, *J* = 7.1 Hz, 2 H, Et), 4.48 (s, 2 H, CH₂OH), 5.58 (s, 1 H), 6.42 (s, 1 H, Ar), 7.28 (s, 1 H, Ar), 7.66 (dd, *J* = 5.3 and 1.6 Hz, 1 H, Ar), 7.85 (s, 1 H, Ar), 7.88 (dd, *J* = 1.6 and 0.6 Hz, 1 H, Ar), 8.34 (dd, *J* = 5.3 and 0.6 Hz, 1 H, Ar) ppm. ¹³C NMR (100 MHz, CDCl₃): δ = 14.3(+), 22.6(-), 29.2(+), 31.3(-), 44.1(-), 58.2(-), 60.8(-), 62.9(-), 96.8(+), 108.6(-), 115.6(-), 117.9(-), 121.5(+), 123.0(+), 126.1(+), 129.4(-), 130.1(+), 142.4(+), 142.5(-), 146.0(-), 148.8(-), 149.9(+), 156.8(-), 160.2(-), 172.7(-) ppm. HRMS (ESI): calc. for C₂₆H₂₇N₂O₅Br [M+H]⁺ 527.1176; found 527.1181.



Ethyl 4-(3-(2-(2-(tert-butoxycarbonyloxy)phenyl)pyridin-4-yl)-6-(hydroxymethyl)-8,8-dimethyl-2-oxo-1,2,8,9-tetrahydropyrano[3,2-g]quinolin-9-yl)butanoate (322-H,Boc,Et)

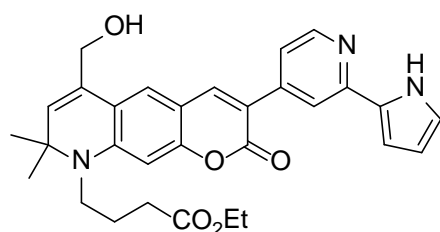
In a screw-cap tube, compound **321** (50 mg, 0.095 mmol), compound **323** (36 mg, 0.113 mmol), Pd(PPh₃)₄ (5.5 mg, 0.005 mmol, 5 mol%), 2 M Na₂CO₃ (190 μL, 0.38 mmol), EtOH (190 μL) and toluene (2 mL) were placed under argon. The mixture was heated to 110 °C and left stirred overnight at this temperature. Afterwards, the reaction mixture was allowed to cool to r.t., diluted with CH₂Cl₂ (10 mL), passed through a plug of Celite (eluting with CH₂Cl₂), and the filtrate evaporated *in vacuo*. Column chromatography (60 g of SiO₂, CH₂Cl₂/MeOH, 25:1) furnished the title product as a yellow solid (26 mg, 43%). ¹H NMR (400 MHz, CDCl₃): δ = 1.32 (t, *J* = 7.1 Hz, 3 H, Et), 1.38 (s, 9 H, *t*Bu), 1.44 (s, 6 H, 2×Me), 1.91–2.00 (m, 2 H, CH₂), 2.43 (t, *J* = 6.9 Hz, 2 H, CH₂), 3.33–3.40 (m, 2 H, CH₂), 4.21 (q, *J* = 7.1 Hz, 2 H, Et), 4.47 (br s., 2 H, CH₂OH), 1.21 (s, 1 H), 6.44 (s, 1 H, Ar), 7.23–7.26 (m, 1 H, Ar), 7.27 (s, 1 H, Ar), 7.34–7.39 (m, 1 H, Ar), 7.41–7.45 (m, 1 H, Ar), 7.76 (dd, *J* = 5.3 and 1.8 Hz, 1 H, Ar), 7.78–7.81 (m, 1 H, Ar), 7.89 (dd, *J* = 1.8 and 0.8 Hz, 1 H, Ar), 7.92 (s, 1 H, Ar), 8.71 (dd, *J* = 5.3 and 0.8 Hz, 1 H, Ar) ppm. ¹³C NMR (100 MHz, CDCl₃): δ = 14.3(+), 22.7(-), 27.5(+), 29.1(+), 31.3(-), 44.1(-), 58.1(-), 60.8(-), 62.9(-), 83.3(-), 97.0(+), 108.9(-), 117.7(-), 121.1(+), 121.9(+), 122.7(+), 122.8(+), 126.4(+), 129.5(-), 129.7(+), 130.0(+), 130.9(+), 133.2(-), 141.9(+), 143.6(-), 148.3(-), 148.5(-), 149.7(+), 151.4(-), 156.6(-), 160.5(-), 172.7(-) ppm. HRMS (ESI): calc. for C₃₇H₄₀N₂O₈ [M+H]⁺ 641.2857; found 641.2855.



Ethyl 4-(3-(2-(2-(tert-butoxycarbonyloxy)phenyl)pyridin-4-yl)-6-((di-tert-butoxyphosphoryloxy)methyl)-8,8-dimethyl-2-oxo-1,2,8,9-tetrahydropyrano[3,2-*g*]quinolin-9-yl)butanoate (322-OPO(*t*Bu)₂,Boc,Et)

To a stirred and preheated (40 °C) solution of compound **322-H,Boc,Et** (21 mg, 0.033 mmol) in CH₂Cl₂ (5 mL) di-*t*-butyl *N,N*-diisopropylphosphoramidite (27 mg, 0.100 mmol) and 1*H*-tetrazole (7.4 mg, 0.107 mmol) were added in two equal portions at interval of 20 min under argon. After further 20 min the reaction mixture was cooled with ice bath (0 °C), and solution of *m*CPBA (24 mg, 70% purity, 0.100 mmol) in CH₂Cl₂ was added. After stirring for additional 30 min aqueous solutions of Na₂SO₃ (2 mL, 10%) and NaHCO₃ (1 mL, saturated) were added, and the reaction mixture was allowed to warm up to r.t. The organic layer was separated and the aqueous phase was extracted with CH₂Cl₂

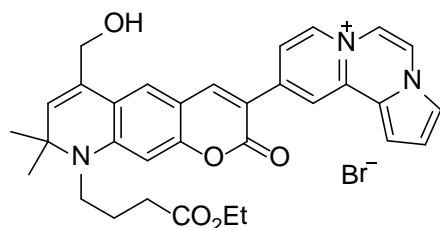
(3×10 mL). The combined organic extracts were dried, the solvents were evaporated, and the titled compound was isolated by column chromatography (30 g of SiO₂, CH₂Cl₂/MeOH, 25:1) as a yellow amorphous solid (12 mg; 44%). ¹H NMR (400 MHz, CDCl₃): δ = 1.31 (t, *J* = 7.1 Hz, 3 H, Et), 1.39 (s, 9 H, *t*Bu), 1.44 (s, 6 H, 2×Me), 1.50 (d, *J*_{CP} = 0.5 Hz, 18 H, 2×*t*Bu), 1.90–1.99 (m, 2 H, CH₂), 2.43 (t, *J* = 6.9 Hz, 2 H, CH₂), 3.33–3.39 (m, 2 H, NCH₂), 4.20 (q, *J* = 7.1 Hz, 2 H, Et), 4.75 (d, *J*_{CP} = 6.6 Hz, 2 H, CH₂), 5.65 (s, 1 H), 6.44 (s, 1 H), 7.23–7.26 (m, 2 H, Ar), 7.34–7.39 (m, 1 H, Ar), 7.40–7.45 (m, 1 H, Ar), 7.72 (dd, *J* = 5.2 and 1.7 Hz, 1 H, Ar), 7.77–7.82 (m, 1 H, Ar), 7.89–7.91 (m, 2 H, Ar), 8.71 (dd, *J* = 5.3 and 0.8 Hz, 1 H, Ar) ppm. MS (ESI): *m/z* (positive mode, rel. int., %) = 833 (100) [M+H]⁺.



Ethyl 4-(3-(2-(1*H*-pyrrol-2-yl)pyridin-4-yl)-6-(hydroxymethyl)-8,8-dimethyl-2-oxo-1,2,8,9-tetrahydropyrano[3,2-*g*]quinolin-9-yl)butanoate (325)

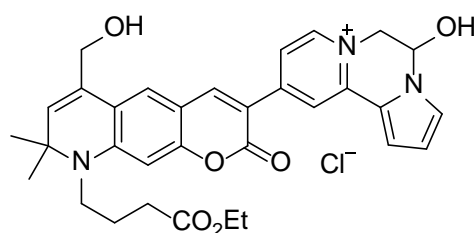
In a screw-cap tube, compound **321** (20 mg, 0.038 mmol), compound **326** (10 mg, 0.046 mmol), Pd(PPh₃)₄ (2.2 mg, 0.002 mmol, 5 mol%), sat. aq. solution of Na₂CO₃ (76 μL, 2 M, 0.152 mmol), EtOH (76 μL) and toluene (1.5 mL) were placed under argon. The mixture was stirred for 15 h at 110 °C and for 10 min at 150 °C. Afterwards, the reaction mixture was allowed to cool to r.t., diluted with CH₂Cl₂ (10 mL), passed through a plug of Celite (eluting with CH₂Cl₂), and the filtrate evaporated *in vacuo*. Column chromatography (60 g of SiO₂; CH₂Cl₂/MeOH, 25:1) furnished the title product as an orange solid (12 mg, 61%). ¹H NMR (400 MHz, CDCl₃): δ = 1.32 (t, *J* = 7.1 Hz, 3 H, Et), 1.43 (s, 6 H, 2×Me), 1.90–1.99 (m, 2 H, CH₂), 2.43 (t, *J* = 6.9 Hz, 2 H, CH₂), 3.31–3.38 (m, 2 H, NCH₂), 4.20 (q, *J* = 7.1 Hz, 2 H, Et), 4.49 (d, *J* = 0.9 Hz, 2 H, CH₂), 5.56 (s, 1 H), 6.30 (m, 1 H, Ar), 6.42 (s, 1 H, Ar), 6.79 (m, 1 H, Ar), 6.90 (m, 1 H, Ar), 7.28 (s, 1 H, Ar), 7.43 (dd, *J* = 5.3 and 1.7 Hz, 1 H, Ar), 7.82 (s, 1 H, Ar), 7.88 (dd, *J* = 1.7 and 0.8 Hz, 1 H, Ar), 8.44 (dd, *J* = 5.3 and 0.8 Hz, 1 H, Ar), 9.77 (br. s, 1 H, Ar) ppm. ¹³C NMR (100 MHz, CDCl₃): δ = 14.3(+), 22.7(–), 29.1(+), 31.3(–), 44.1(–), 58.1(–), 60.8(–), 63.0(–), 96.9(+), 107.5(+), 108.8(–), 110.2(+), 116.6(+), 117.7(–), 119.3(+), 119.9(+), 122.8(+), 129.6(–), 130.1(+), 131.5(–), 141.7(+), 143.8(–), 148.3(–), 148.7(+), 150.7(–), 156.6(–), 160.6(–), 172.7(–) ppm. MS (ESI): *m/z* (positive mode, rel. int., %) = 514 (100)

$[M+H]^+$. UV-Vis spectral data in MeOH: $\lambda_{\text{abs,max}} = 432 \text{ nm}$; $\epsilon = 33650 \text{ M}^{-1}\text{cm}^{-1}$, $\lambda_{\text{em,max}} = 432 \text{ nm}$, $\Phi_{\text{fl}} = 0.50$ (standard: Coumarin 510, $\Phi_{\text{fl}} = 0.85$ in EtOH).



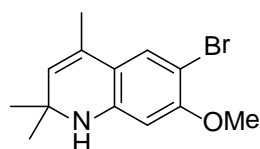
10-(9-(4-Ethoxy-4-oxobutyl)-6-(hydroxymethyl)-8,8-dimethyl-2-oxo-1,2,8,9-tetrahydropyrano[3,2-g]quinolin-3-yl)pyrido[1,2-a]pyrrolo[2,1-c]pyrazin-7-ium bromide (328)

In a screw-cap tube a solution of compound **325** (33 mg, 0.064 mmol) in dibromoethane (1 mL) was stirred at 130 °C for 3 days. Afterwards, all volatiles were evaporated *in vacuo*, and the residue was subjected to column chromatography (35 g of SiO₂, CH₂Cl₂/MeOH, 12:1 → 5:1) to furnish 1 mg (2.5%) of the title compound. ¹H NMR (400 MHz, DMSO-*d*₆): $\delta = 1.22$ (t, $J = 7.1$ Hz, 3 H, Et), 1.41 (s, 6 H, 2×Me), 1.74–1.84 (m, 2 H, CH₂), 2.51 (t, $J = 6.8$ Hz, 2 H, CH₂), 3.40–3.48 (m, 2 H, NCH₂), 4.11 (q, $J = 7.1$ Hz, 2 H, Et), 4.28 (s, 2 H, CH₂OH), 5.68 (s, 1 H), 6.68 (s, 1 H, Ar), 7.12 (dd, $J = 4.1$ and 2.6 Hz, 1 H, Ar), 7.43 (s, 1 H, Ar), 7.88 (d, $J = 4.1$ Hz, 1 H, Ar), 8.03–8.06 (m, 2 H, Ar), 8.36 (dd, $J = 7.2$ and 2.1 Hz, 1 H, Ar), 8.56 (d, $J = 5.9$ Hz, 1 H, Ar), 8.83 (s, 1 H, Ar), 8.93 (d, $J = 7.3$ Hz, 1 H, Ar), 9.04 (d, $J = 2.0$ Hz, 1 H, Ar) ppm. ¹³C NMR (100.5 MHz, DMSO-*d*₆): $\delta = 14.6(+)$, 22.7(-), 29.3(+), 30.8(-), 44.0(-), 59.2(-), 60.5(-), 61.0(-), 96.4(+), 109.0(-), 110.0(+), 111.4(-), 116.5(+), 116.7(+), 116.8(+), 118.6(-), 119.7(+), 121.4(+), 122.2(-), 122.6(+), 124.1(+), 129.4(-), 129.7(+), 137.4(+), 137.8(-), 146.2(+), 147.7(-), 150.4(-), 157.7(-), 159.8(-), 173.2(-) ppm. HRMS (ESI): calc. for C₃₂H₃₂N₃O₅ M⁺ 538.2336; found 538.2326. UV-Vis spectral data in MeOH: $\lambda_{\text{abs,max}} = 489 \text{ nm}$, $\lambda_{\text{em,max}} = 587 \text{ nm}$, $\Phi_{\text{fl}} = 0.56$ (standard: Rhodamine B, $\Phi_{\text{fl}} = 0.69$ in EtOH).



10-(9-(4-Ethoxy-4-oxobutyl)-6-(hydroxymethyl)-8,8-dimethyl-2-oxo-1,2,8,9-tetrahydropyrano[3,2-g]quinolin-3-yl)-5-hydroxy-5,6-dihydropyrido[1,2-a]pyrrolo[2,1-c]pyrazin-7-ium chloride (329)

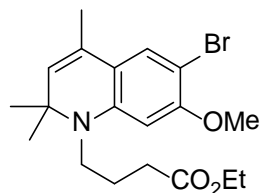
In a screw-cap tube, a mixture of compound **325** (17 mg, 0.033 mmol), chloroacetaldehyde diethyl acetal (1 mL) and NaI (100 mg, 0.66 mmol) in DMF (1 mL) was stirred for 5 h at 100 °C. Afterwards, the reaction mixture was diluted with water (~20 mL), and sat. aq. Na₂S₂O₃ was added (~5 mL). The resulting slurry was extracted with CHCl₃ (3×25 mL), and combined organic extracts were washed with sat. aq. NaCl, dried with Na₂SO₄ and evaporated. The residue was subjected to column chromatography (30 g of SiO₂, CH₂Cl₂/MeOH, 5:1 → 2.5:1) to give 12 mg (67%) of a purple solid. ¹H NMR (400 MHz, DMSO-*d*₆): δ = 1.21 (t, *J* = 7.1 Hz, 3 H, Et), 1.40 (s, 6 H, 2×Me), 1.73–1.83 (m, 2 H, CH₂), 2.50 (t, *J* = 6.7 Hz, 2 H, CH₂), 3.39–3.45 (m, 2 H, NCH₂), 4.11 (q, *J* = 7.1 Hz, 2 H, Et), 4.27 (br. s, 2 H, CH₂OH), 4.79–4.84 (m, 2 H, CH₂), 5.67 (s, 1 H), 6.08–6.12 (m, 1 H), 6.47 (dd, *J* = 3.4 and 2.6 Hz, 1 H, Ar), 6.66 (s, 1 H, Ar), 7.40–7.45 (m, 3 H, Ar), 8.17 (dd, *J* = 7.0 and 2.1 Hz, 1 H, Ar), 8.65 (d, *J* = 2.1 Hz, 1 H, Ar), 8.70 (d, *J* = 7.0 Hz, 1 H, Ar), 8.81 (s, 1 H, Ar) ppm. ¹³C NMR (100.5 MHz, DMSO-*d*₆): δ = 14.6(+), 22.7(–), 29.3(+), 30.8(–), 44.0(–), 58.8(–), 59.1(–), 60.5(–), 60.9(–), 73.8(+), 96.4(+), 108.9(–), 111.2(–), 112.6(+), 115.6(+), 117.8(+), 118.6(–), 119.7(+), 120.6(–), 124.1(+), 127.2(+), 129.4(–), 129.6(+), 142.2(–), 143.3(+), 146.4(+), 150.4(–), 150.8(–), 157.8(–), 159.8(–), 173.2(–) ppm. HRMS (ESI): calc. for C₃₂H₃₄N₃O₆ [M]⁺ 556.2442; found 556.2439.



6-Bromo-7-methoxy-2,2,4-trimethyl-1,2-dihydroquinoline (335)

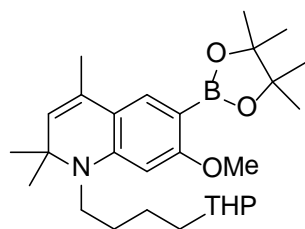
Anhydrous ytterbium(III) triflate (1.0 g, 1.63 mmol, 6.5 mol%, freshly dried *in vacuo* at 130 °C for 4 h) was added in one portion to a solution of compound **334** (5.0 g, 25 mmol) in dry acetone (75 mL). The reaction mixture was stirred at r.t. for 16 h. Acetone was evaporated *in vacuo*, the residue was dissolved in EtOAc, washed with sat. aq. NaHCO₃ (twice), water, brine and dried over MgSO₄. After evaporation of solvents, the oily residue was dried *in vacuo* (0.5 Torr) to a constant weight. Purification by column chromatography (100 g of SiO₂, *n*-hexane/Et₂O, 4:1) afforded the title compound a white powder (5.6 g, 80% yield). ¹H NMR (300 MHz, CDCl₃): δ = 1.25 (s, 6 H, 2×Me), 1.91 (d, *J* = 1.31 Hz, 3 H, Me), 3.80 (s, 3 H, OMe), 5.18 (br. s, 1 H), 6.02 (s, 1 H, Ar), 7.13 (s, 1 H,

Ar) ppm. ^{13}C NMR (75 MHz, CDCl_3): $\delta = 18.5(+)$, $31.0(+)$, $52.1(-)$, $56.1(+)$, $97.2(+)$, $97.8(-)$, $116.2(-)$, $126.5(+)$, $127.4(-)$, $128.0(+)$, $143.8(-)$, $155.7(-)$ ppm. HRMS (ESI): found 304.0304; calc. for $\text{C}_{13}\text{H}_{16}\text{NOBr}$ $[\text{M}+\text{Na}]^+$ 304.0307.



Ethyl 4-(6-bromo-7-methoxy-2,2,4-trimethylquinolin-1(2H)-yl)butanoate (336)

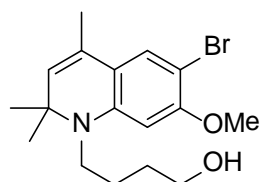
DIEA (3.4 g, 26.0 mmol) was added to a mixture of compound **335** (5.6 g, 20.0 mmol) and ethyl 3-iodobutyrates (6.3 g, 26.0 mmol) in a screw-cup bottle, and the reaction mixture was stirred with heating (110 °C) for 64 h. After cooling down, the reaction mixture was distributed between EtOAc (70 mL) and water (70 mL). The organic layer was washed with brine (70 mL) and water (70 mL), dried with Na_2SO_4 and evaporated. The residue was subjected to column chromatography (150 g of SiO_2 , n -hexane/ CH_2Cl_2 , 3:5) to furnish 6.5 g (82%) of the title compound. ^1H NMR (300 MHz, CDCl_3): $\delta = 1.25$ (t, $J = 7.1$ Hz, 3 H, Et), 1.27 (s, 6 H, 2×Me), 1.84–1.95 (m, 2 H, CH_2), 1.89 (d, $J = 1.4$ Hz, 3 H, Me), 2.37 (t, $J = 6.7$ Hz, 2 H, CH_2), 3.19–3.26 (m, 2 H, NCH_2), 3.91 (s, 3 H, OMe), 4.13 (q, $J = 7.1$ Hz, 2 H, Et), 5.09 (q, $J = 1.3$ Hz, 1 H), 6.28 (s, 1 H, Ar), 7.10 (s, 1 H, Ar) ppm. ^{13}C NMR (75 MHz, CDCl_3): $\delta = 14.2(+)$, $18.6(+)$, $23.2(-)$, $28.3(+)$, $31.3(-)$, $43.5(-)$, $56.4(+)$, $57.0(-)$, $60.5(-)$, $96.3(+)$, $96.6(-)$, $117.7(-)$, $126.8(-)$, $127.6(+)$, $127.7(+)$, $144.5(-)$, $156.1(-)$, $173.1(-)$ ppm. HRMS (ESI): found 396.1165; calc. for $\text{C}_{19}\text{H}_{26}\text{NO}_3\text{Br}$ $[\text{M}+\text{H}]^+$ 396.1169.



7-Methoxy-2,2,4-trimethyl-1-(4-(tetrahydro-2H-pyran-2-yloxy)butyl)-6-(4,4,5,5-tetramethyl-1,3,2-dioxaborolan-2-yl)-1,2-dihydroquinoline (338)

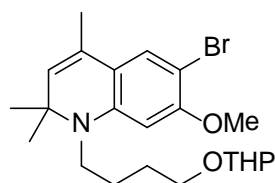
In a dried Schlenk flask a solution of compound **339**-THP (500 mg, 1.14 mmol) in THF (20 mL) was placed under argon. The flask was cooled down to -78 °C, and a solution of $t\text{BuLi}$ (740 μL , 1.7 M, 1.26 mmol) was injected with stirring. After 45 min stirring at -78 °C, $\text{B}(\text{O}i\text{Pr})_3$ (237 mg, 1.26 mmol) was added. The resulting mixture was stirred over-

night at r.t., and then AcOH (76 mg, 1.26 mmol) and pinacol (297 mg, 2.52 mmol) were added. After 1 h stirring, brine (20 mL) was added thereto, the organic layer was separated, and the aq. layer was extracted with EtOAc (2×20 mL). Combined organic solutions were dried with Na₂SO₄ and evaporated. The residue was purified by column chromatography (50 g of SiO₂, *n*-hexane/EtOAc, 2:1) to yield 490 mg (89%) of a yellow oil. ¹H NMR (300 MHz, CDCl₃): δ = 1.28 (s, 6 H, 2×Me), 1.29 (s, 12 H, 4×Me), 1.44–1.58 (m, 4 H, 2×CH₂), 1.59–1.82 (m, 6 H, 3×CH₂), 1.97 (s, 3 H, Me), 3.21–3.29 (m, 2 H, CH₂), 3.35–3.52 (m, 2 H, OCH₂), 3.72–3.78 (m, 2 H, NCH₂), 3.80 (s, 3 H, OMe), 4.52–4.58 (m, 1 H), 5.03 (br. s, 1 H), 5.95 (s, 1 H, Ar), 7.35 (s, 1 H, Ar) ppm. ¹³C NMR (75 MHz, CDCl₃): δ = 18.3(+), 19.6(-), 24.8(+), 25.4(-), 25.5(-), 27.5(-), 28.9(+), 30.7(-), 44.1(-), 56.1(+), 57.1(-), 62.4(-), 67.2(-), 82.6(-), 98.9(+), 115.5(-), 125.9(+), 127.7(-), 132.5(+), 148.0(-), 166.2(-) ppm. HRMS (ESI): found 508.3212; calc. for C₂₈H₄₄NO₅B [M+Na]⁺ 508.3210.



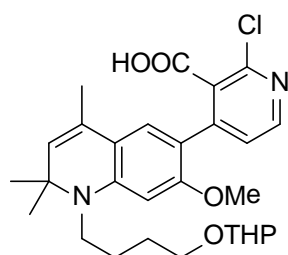
4-(6-Bromo-7-methoxy-2,2,4-trimethylquinolin-1(2H)-yl)butan-1-ol (339-H)

To a suspension of LiAlH₄ (38 mg, 1 mmol) in THF (5 mL) a solution of compound **336** (500 mg, 1.26 mmol) in THF (5 mL) was added dropwise at 0 °C. The resulting mixture was stirred for 1.5 h at 0 °C and for 1 h at r.t. Afterwards, the reaction mixture was quenched with 1 M KHSO₄ (5 mL), brine (5 mL) was added, and the organic layer was separated. The aq. layer was extracted with EtOAc (3×10 mL), and the combined organic solutions were dried with Na₂SO₄ and evaporated. The residue was subjected to column chromatography (50 g of SiO₂, *n*-hexane/EtOAc, 1:1) to afford 440 mg (98%) of a yellow oil. ¹H NMR (300 MHz, CDCl₃): δ = 1.27 (s, 6 H, 2×Me), 1.57–1.73 (m, 4 H, 2×CH₂), 1.89 (d, *J* = 1.2 Hz, 3 H, Me), 3.18–3.25 (m, 2 H, OCH₂), 3.65–3.71 (m, 2 H, NCH₂), 3.85 (s, 3 H, OMe), 5.10 (br. s, 1 H), 6.05 (s, 1 H, Ar), 7.10 (s, 1 H, Ar) ppm. ¹³C NMR (75 MHz, CDCl₃): δ = 18.6(+), 24.7(-), 28.4(+), 30.2(-), 44.0(-), 56.1(+), 60.4(-), 62.5(-), 96.0(+), 96.4(-), 117.8(-), 126.7(-), 127.7(+), 127.7(+), 144.4(-), 155.9(-) ppm. HRMS (ESI): found 376.0881; calc. for C₁₇H₂₄NO₂Br [M+Na]⁺ 376.0883.



6-Bromo-7-methoxy-2,2,4-trimethyl-1-(4-(tetrahydro-2H-pyran-2-yloxy)butyl)-1,2-dihydroquinoline (339-THP)

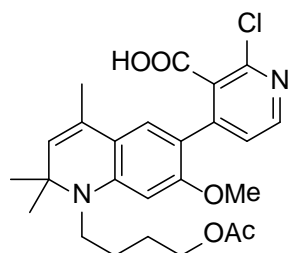
To a solution of compound **339-H** (100 mg, 0.28 mmol) in CH_2Cl_2 (2 mL) 3,4-dihydro-2H-pyran (105 mg, 1.25 mmol) and $\text{TsOH}\cdot\text{H}_2\text{O}$ (0.5 mg, 0.025 mmol) were added at 0 °C. The resulting mixture was stirred overnight at r.t. Afterwards, additional amounts of 3,4-dihydro-2H-pyran (105 mg, 1.25 mmol) and $\text{TsOH}\cdot\text{H}_2\text{O}$ (5 mg, 0.25 mmol) were added, and the reaction mixture was heated to 40 °C and stirred for 20 min at this temperature. After cooling down, the reaction mixture was diluted to 5 mL with CH_2Cl_2 , and sat. aq. NaHCO_3 (5 mL) was added. The organic layer was separated, and the aq. layer was extracted with CH_2Cl_2 (2×5 mL). Combined organic solutions were dried with Na_2SO_4 and evaporated. The residue was subjected to column chromatography (20 g of SiO_2 , *n*-hexane/EtOAc, 5:1) to give 102 mg (82%) of a colorless oil. ^1H NMR (300 MHz, CDCl_3): δ = 1.27 (s, 6 H, 2×Me), 1.44–1.58 (m, 4 H, 2× CH_2), 1.61–1.74 (m, 6 H, 3× CH_2), 1.89 (br. s, 3 H, Me), 3.16–3.25 (m, 2 H, CH_2), 3.36–3.52 (m, 2 H, CH_2), 3.74–3.82 (m, 2 H, CH_2), 3.85 (s, 3 H, OMe), 4.55 (t, J = 3.4 Hz, 1 H), 5.09 (br. s, 1 H), 6.02 (s, 1 H, Ar), 7.09 (s, 1 H, Ar) ppm. ^{13}C NMR (125.7 MHz, CDCl_3): δ = 18.5(+), 19.6(-), 25.2(-), 25.3(-), 27.4(-), 28.4(+), 30.7(-), 44.2(-), 56.1(+), 57.0(-), 62.5(-), 67.2(-), 96.0(+), 96.3(-), 99.0(+), 117.9(-), 126.8(-), 127.8(+), 144.6(-), 156.0(-) ppm. HRMS (ESI): found 460.1451; calc. for $\text{C}_{22}\text{H}_{32}\text{NO}_3\text{Br}$ $[\text{M}+\text{Na}]^+$ 460.1458.



2-Chloro-4-(7-methoxy-2,2,4-trimethyl-1-(4-(tetrahydro-2H-pyran-2-yloxy)butyl)-1,2-dihydroquinolin-6-yl)nicotinic acid (342-THP)

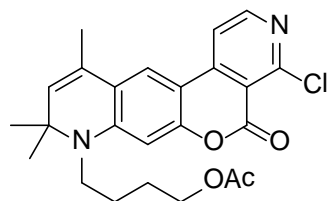
In a screw-cap tube, compound **339-THP** (490 mg, 1.01 mmol), 2-chloro-4-iodonicotinic acid (314 mg, 1.11 mmol), $\text{Pd}(\text{PPh}_3)_4$ (58 mg, 0.05 mmol, 5 mol%), sat. aq. solution of Na_2CO_3 (2 mL, 2 M, 4.04 mmol), EtOH (2 mL) and toluene (10 mL) were placed under argon. The mixture was heated to 110 °C and left stirred overnight at this temperature.

After cooling down, sat. aq. KHSO_4 (5 mL) and water (5 mL) were added. The organic layer was separated, and the aq. layer was extracted with CHCl_3 (2×10 mL). Combined organic solutions were dried with Na_2SO_4 and evaporated. Column chromatography (100 g of SiO_2 , $\text{CHCl}_3/\text{MeOH}$, 7:1) furnished the title product as a yellow solid (440 mg, 85%). ^1H NMR (300 MHz, CDCl_3): δ = 1.27 (s, 6 H, 2×Me), 1.43–1.57 (m, 4 H, 2× CH_2), 1.60–1.80 (m, 6 H, 3× CH_2), 1.83 (s, 3 H, Me), 3.17–3.27 (m, 2 H, CH_2), 3.35–3.53 (m, 2 H, OCH_2), 3.66 (s, 3 H, OMe), 3.72–3.87 (m, 2 H, NCH_2), 4.54 (br. s, 1 H), 5.02 (s, 1 H), 5.98 (s, 1 H, Ar), 7.12 (s, 1 H, Ar), 7.17 (d, J = 5.1 Hz, 1 H, Ar), 8.15 (d, J = 5.1 Hz, 1 H, Ar) ppm. ^{13}C NMR (125.7 MHz, CDCl_3): δ = 18.7(+), 19.7(-), 25.3(-), 25.4(-), 27.4(-), 29.1(+), 30.8(-), 31.9(-), 44.1(-), 55.9(+), 57.2(-), 62.5(-), 67.2(-), 99.0(+), 113.2(-), 115.6(-), 125.20(+), 126.3(+), 126.6(+), 127.2(-), 145.6(-), 146.1(-), 146.5(+), 146.8(-), 157.0(-), 172.9(-) ppm. HRMS (ESI): found 515.2300; calc. for $\text{C}_{28}\text{H}_{35}\text{N}_2\text{O}_5\text{Cl}$ $[\text{M}+\text{H}]^+$ 515.2307.



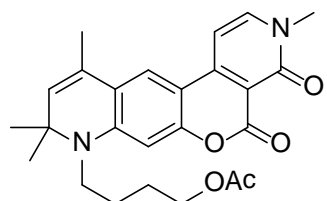
4-(1-(4-Acetoxybutyl)-7-methoxy-2,2,4-trimethyl-1,2-dihydroquinolin-6-yl)-2-chloronicotinic acid (342-Ac)

Compound **324**-Ac was prepared according to the known procedure.^[149] In a screw-cap tube a solution of compound **342**-THP (207 mg, 0.4 mmol) in a mixture of AcOH (4 mL) and AcCl (4 mL) was placed. This solution was stirred with heating at 80 °C for 1 h. Afterwards, the reaction mixture was diluted with H_2O , neutralized with sat. aq. NaHCO_3 and extracted with CHCl_3 (3×40 mL). Combined organic solutions were dried with Na_2SO_4 and evaporated *in vacuo*. The residue was purified by column chromatography (40 g of SiO_2 , $\text{CHCl}_3/\text{MeOH}$, 7:1) to yield 125 mg (66%) of the title compound as an orange powder. ^1H NMR (300 MHz, CDCl_3): δ = 1.26 (s, 6 H, 2×Me), 1.58–1.72 (m, 4 H, 2× CH_2), 1.81 (s, 3 H, Me), 1.99 (s, 3 H, Me), 3.15–3.29 (m, 2 H, CH_2), 3.64 (s, 3 H, OMe), 4.00–4.14 (m, 2 H, CH_2), 5.03 (s, 1 H), 5.92 (s, 1 H, Ar), 6.97 (s, 1 H, Ar), 7.21 (d, J = 4.5 Hz, 1 H, Ar), 8.22 (br. s, 1 H, Ar) ppm. HRMS (ESI): found 473.1837; calc. for $\text{C}_{25}\text{H}_{29}\text{N}_2\text{O}_5\text{Cl}$ $[\text{M}+\text{H}]^+$ 473.1838.



4-(4-Chloro-9,9,11-trimethyl-5-oxo-6,7,8,9-tetrahydropyrido[4',3':4,5]pyrano[3,2-g]quinolin-8-yl)butyl acetate (343-OAc)

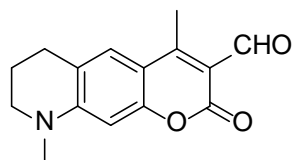
To a solution of compound **342**-Ac (10 mg, 0.02 mmol) in CH₂Cl₂ (1 mL) 2 M solution of BBr₃ (130 μL, 0.13 mmol) in CH₂Cl₂ was added at 0 °C under Ar. The resulting mixture was stirred overnight at r.t. Afterwards, the reaction mixture was quenched with sat. aq. NaHCO₃ (5 mL) and extracted with CH₂Cl₂ (3×5 mL). Combined organic extracts were dried with Na₂SO₄ and evaporated. Column chromatography (15 g of SiO₂, *n*-hexane/EtOAc, 2:1) provided 4 mg (36%) of the title compound. ¹H NMR (600 MHz, CDCl₃): δ = 1.37 (s, 6 H, 2×Me), 1.65–1.75 (m, 4 H, 2×CH₂), 2.04 (d, *J* = 1.02 Hz, 3 H, Me), 2.07 (s, 3 H, Me), 3.28 (m, 2 H, CH₂), 4.12 (t, *J* = 6.0 Hz, 2 H, CH₂), 5.32 (m, 1 H), 6.25 (s, 1 H, Ar), 7.43 (s, 1 H, Ar), 7.61 (d, *J* = 5.5 Hz, 1 H, Ar), 8.43 (d, *J* = 5.5 Hz, 1 H, Ar) ppm. HRMS (ESI): found 463.1386; calc. for C₂₄H₂₅N₂O₄Cl [M+Na]⁺ 463.1395.



4-(3,9,9,11-tetramethyl-4,5-dioxo-3,4,6,7,8,9-hexahydropyrido[4',3':4,5]pyrano[3,2-g]quinolin-8-yl)butyl acetate (344)

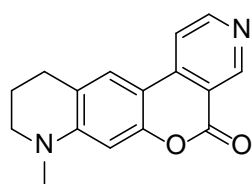
A solution of compound **343**-OAc (15 mg, 0.034 mmol) and MeI (100 μL) in MeCN (1 mL) stirred at 75 °C for 2 days under Ar. After cooling down, the reaction mixture was directly subjected to column chromatography (15 g of SiO₂, CH₂Cl₂/MeOH, 12:1) to afford 4 mg (27%) of the title compound as a yellow powder. ¹H NMR (300 MHz, CDCl₃): δ = 1.31 (s, 6 H, 2×Me), 1.61–1.75 (m, 4 H, 2×CH₂), 2.02 (s, 3 H, Me), 2.05 (s, 3 H, Me), 3.22–3.32 (m, 2 H, CH₂), 3.55 (s, 3 H, NMe), 4.10 (m, 2 H, OCH₂), 5.30 (s, 1 H), 6.19 (s, 1 H, Ar), 6.69 (d, *J* = 7.5 Hz, 1 H, Ar), 7.30 (s, 1 H, Ar), 7.73 (d, *J* = 7.5 Hz, 1 H, Ar) ppm. ¹³C NMR (125.7 MHz, CDCl₃): δ = 18.8(+), 20.9(+), 26.0(-), 29.3(+), 29.6(-), 38.0(+), 44.4(-), 58.1(-), 63.7(-), 96.7(+), 99.10(+), 103.8(-), 119.0(+), 120.6(-), 126.2(-), 130.1(+), 143.9(+), 149.2(-), 150.1(-), 156.1(-), 161.1(-), 171.3(-) ppm. HRMS (ESI): found 437.2067; calc. for C₂₅H₂₈N₂O₅ [M+H]⁺ 437.2071. HPLC: B/A = 50/50 to 100/0 in

25 min, detection at 254 nm, $t_R = 12.2$ min (99 %). UV-Vis spectral data in CH_2Cl_2 : $\lambda_{\text{abs,max}} = 422$ nm; $\epsilon = 11500 \text{ M}^{-1}\text{cm}^{-1}$, $\lambda_{\text{em,max}} = 497$ nm, $\Phi_{\text{fl}} = 0.56$ (standard: Lucifer Yellow, $\Phi_{\text{fl}} = 0.21$ in H_2O). UV-Vis spectral data in MeOH: $\lambda_{\text{abs,max}} = 427$ nm; $\epsilon = 18800 \text{ M}^{-1}\text{cm}^{-1}$, $\lambda_{\text{em,max}} = 524$ nm, $\Phi_{\text{fl}} = 0.46$ (standard: Lucifer Yellow, $\Phi_{\text{fl}} = 0.21$ in H_2O).



4,9-Dimethyl-2-oxo-1,2,6,7,8,9-hexahydropyrano[3,2-*g*]quinoline-3-carbaldehyde (348)

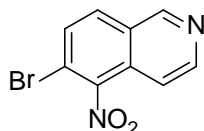
In a Schlenk flask POCl_3 (675 mg, 4.4 mmol) and DMF (642 mg, 8.8 mmol) were placed under Ar. The resulting solution was warmed up to 50 °C and stirred for 30 min at this temperature. Afterwards, a solution of coumarin **347** (100 mg, 0.44 mmol) in DMF (2 mL) was added dropwise. The reaction mixture was stirred for 10 min, and then poured onto ice. Acidity of the resulting slurry was adjusted with 1 M NaOH to pH 12, and the mixture was extracted with CH_2Cl_2 (3×20 mL). Combined organic solutions were dried with Na_2SO_4 and evaporated. The crude product was subjected to column chromatography (30 g of SiO_2 , *n*-hexane/EtOAc, 1:1) to furnish 28 mg (25%) of the title compound as an orange powder. ^1H NMR (300 MHz, CDCl_3): $\delta = 1.98$ (m, 2 H, CH_2), 2.74–2.80 (m, 2 H, CH_2), 2.75 (s, 3 H, Me), 3.01 (s, 3 H, NMe), 3.42 (m, 2 H, NCH_2), 6.30 (s, 1 H, Ar), 7.29 (m, 1 H, Ar), 10.34 (s, 1 H, CHO) ppm.



8-Methyl-8,9,10,11-tetrahydropyrido[4',3':4,5]-5H-pyrano[3,2-*g*]quinolin-5-one (349)

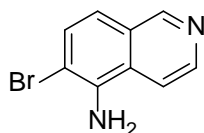
To a solution of compound **348** (28 mg, 0.11 mmol) in formamide (1 mL) conc. H_2SO_4 (1 mL) was added dropwise at 0 °C. The resulting mixture was heated to 90 °C and left stirred overnight at this temperature. Afterwards, the solid reaction mixture was cooled down to 0 °C, and water (20 mL) was added. Acidity of the resulting slurry was adjusted with 1 M NaOH to pH 10, and the mixture was extracted with CH_2Cl_2 (3×30 mL). Combined organic extracts were dried with Na_2SO_4 and evaporated. The residue was subjected

to column chromatography (30 g of SiO₂, CH₂Cl₂/MeOH, 20:1) to afford 8 mg (27%) of the title compound. ¹H NMR (300 MHz, CDCl₃): δ = 2.00 (m, 2 H, CH₂), 2.82 (m, 2 H, CH₂), 2.99 (s, 3 H, NMe), 3.39 (m, 2 H, NCH₂), 6.38 (s, 1 H, Ar), 7.47 (m, 1 H, Ar), 7.61 (m, *J* = 5.6 Hz, 1 H, Ar), 8.71 (d, *J* = 5.6 Hz, 1 H, Ar), 9.37 (d, *J* = 0.8 Hz, 1 H, Ar) ppm. MS (ESI): *m/z* (positive mode, rel. int., %) = 267 (100) [M+H]⁺. UV-Vis spectral data in MeOH: λ_{abs,max} = 377 nm; ε = 14200 M⁻¹cm⁻¹, λ_{em,max} = 500 nm, Φ_{fl} = 0.02 (standard: Coumarin 153, Φ_{fl} = 0.69 in EtOH).



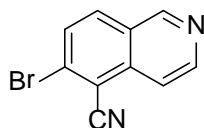
6-Bromo-5-nitroisoquinoline (350)

A solution of 6-bromoisoquinoline (2080 mg; 10 mmol) in a H₂SO₄/HNO₃ mixture (1:1, 10 mL) was stirred for 2 h at r.t. Afterwards, the reaction mixture was poured onto ice, pH was adjusted to 9 using 22% aq. ammonia, and the white precipitate was filtered out, washed and dried. This crude product (2070 mg; 93%) was used without further purification. ¹H NMR (400 MHz, CDCl₃): δ = 7.54 (d, *J* = 6.0 Hz, 1H_{ar}), 7.86 (d, *J* = 8.8 Hz, 1H_{ar}), 8.03 (d, *J* = 8.8 Hz, 1H_{ar}), 8.73 (d, *J* = 6.0 Hz, 1H_{ar}), 9.36 (s, 1H_{ar}) ppm.



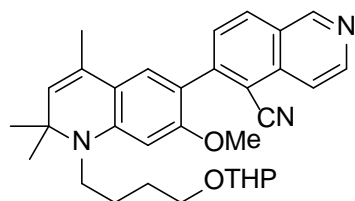
5-Amino-6-bromoisoquinoline (351)

NH₄Cl (4066 mg, 76 mmol) was dissolved in 40% aq. EtOH (50 mL). To this solution iron powder (2128 mg, 38 mmol) was added, and the resulting suspension was stirred for 10 min at r.t. Afterwards, compound **350** (1690 mg, 7.6 mmol) was added thereto. The reaction mixture was stirred for 1 h at r.t., and then filtered through a plug of Celite washing with EtOH. The filtrate was partially evaporated; the precipitated crude product was filtered out using a glass filter and dried. ¹H NMR (400 MHz, CDCl₃): δ = 4.73 (br. s, 2 H, NH₂), 7.28 (d, *J* = 8.8 Hz, 1 H, Ar), 7.57 (d, *J* = 6.0 Hz, 1 H, Ar), 7.63 (d, *J* = 8.8 Hz, 1 H, Ar), 8.54 (d, *J* = 5.9 Hz, 1 H, Ar), 9.16 (s, 1 H, Ar) ppm. MS (ESI): *m/z* (positive mode, rel. int., %) = 223 (100) [M+H, ⁷⁹Br]⁺, 225 (95) [M+H, ⁸¹Br]⁺.



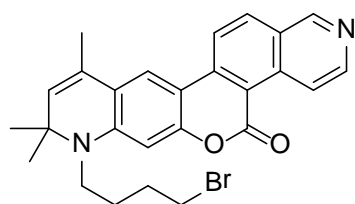
5-Cyano-6-bromoisoquinoline (352-CN)

A Schlenk flask was charged with a solution of compound **351** (100 mg, 0.52 mmol) in DMSO (3 mL) and CuCN (61 mg, 0.68 mmol). The resulting mixture was heated to 50 °C with stirring, and *t*BuONO (206 μ L, 1.56 mmol) was injected. The reaction mixture was stirred for 2 h at 50 °C, then cooled down to r.t. and poured in 0.1 M HCl (~20 mL). The resulted slurry was extracted with CH₂Cl₂ (4 \times 20 mL). Combined organic solutions were dried with Na₂SO₄ and evaporated. The residue was subjected to column chromatography (40 g of SiO₂, *n*-hexane/EtOAc, 1:1) to afford 13 mg (11%) of a yellowish crystalline solid. ¹H NMR (400 MHz, CDCl₃): δ = 7.86 (d, *J* = 8.8 Hz, 1 H, Ar), 7.99 (dt, *J* = 5.9 and 0.9 Hz, 1 H, Ar), 8.08 (dd, *J* = 8.8 and 0.8 Hz, 1 H, Ar), 8.77 (d, *J* = 5.9 Hz, 1 H, Ar), 9.34 (d, *J* = 0.9 Hz, 1 H, Ar) ppm. ¹³C NMR (100 MHz, CDCl₃): δ = 112.4, 115.1, 117.4, 126.2, 131.2, 131.5, 133.3, 136.8, 146.4, 152.8 ppm. MS (ESI): *m/z* (positive mode, rel. int., %) = 233 (100) [M+H, ⁷⁹Br]⁺, 235 (96) [M+H, ⁸¹Br]⁺.



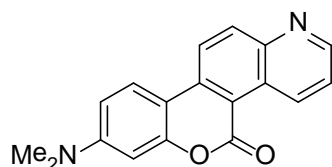
6-(7-Methoxy-2,2,4-trimethyl-1-(4-(tetrahydro-2H-pyran-2-yloxy)butyl)-1,2-dihydroquinolin-6-yl)isoquinoline-5-carbonitrile (353)

In a screw-cap tube, compound **338** (105 mg, 0.215 mmol), compound **352-CN** (50 mg, 0.215 mmol), Pd(PPh₃)₄ (12.5 mg, 0.011 mmol, 5 mol%), sat. aq. solution of Na₂CO₃ (430 μ L, 2 M, 0.86 mmol) and toluene (3 mL) were placed under argon. The mixture was heated to 110 °C and left stirred overnight at this temperature. After cooling, the reaction mixture was filtered through a plug of Celite eluting with CH₂Cl₂, and the filtrate was evaporated. Column chromatography (30 g of SiO₂, cyclohexane/EtOAc, 1:2) furnished the title product as an orange oil (86 mg, 78%). ¹H NMR (400 MHz, CDCl₃): δ = 1.24 (s, 6 H, 2 \times Me), 1.47–1.60 (m, 4 H, 2 \times CH₂), 1.67–1.85 (m, 6 H, 3 \times CH₂), 1.97 (s, 3 H, Me), 3.30–3.37 (m, 2 H, CH₂), 3.43–3.53 (m, 2 H, CH₂), 3.80–3.90 (m, 2 H, CH₂), 3.85 (s, 3 H, OMe), 4.59 (m, 1 H), 5.15 (s, 1 H), 6.12 (s, 1 H, Ar), 7.10 (s, 1 H, Ar), 7.77 (d, *J* = 8.6 Hz, 1 H, Ar), 8.06 (d, *J* = 5.9 Hz, 1 H, Ar), 8.11 (d, *J* = 8.8 Hz, 1 H, Ar), 8.67 (d, *J* = 5.9 Hz, 1 H, Ar), 9.27 (s, 1 H, Ar) ppm. MS (ESI): *m/z* (positive mode, rel. int., %) = 512 (100) [M+H]⁺.



8-(4-Bromobutyl)-9,9,11-trimethyl-5-oxo-5,6,8,9-tetrahydroisoquinolino[6',5':4,5]pyrano[3,2-g]quinoline (354)

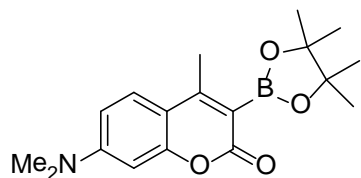
In a screw-cap tube a solution of compound **353** (10 mg, 0.019 mmol) in conc. aq. HBr (1 mL) was stirred for 3 h at 130 °C. After cooling, the reaction mixture was diluted with water (~5 mL), quenched with NaHCO₃ and extracted with CH₂Cl₂ (3×10 mL). Combined organic solutions were dried with Na₂SO₄ and evaporated. The crude product was purified by column chromatography (15 g of SiO₂, cyclohexane/EtOAc, 1:2) to furnish 6 mg (66%) of the title compound as a red solid. ¹H NMR (400 MHz, CDCl₃): δ = 1.43 (s, 6 H, 2×Me), 1.80–1.90 (m, 2 H, CH₂), 1.95–2.04 (m, 2 H, CH₂), 2.12 (s, 3 H, Me), 3.31–3.38 (m, 2 H, CH₂), 3.49 (t, *J* = 6.6 Hz, 2 H, CH₂), 5.38 (s, 1 H), 6.38 (s, 1 H, Ar), 7.66 (s, 1 H, Ar), 8.19 (d, *J* = 8.9 Hz, 1 H, Ar), 8.25 (d, *J* = 8.9 Hz, 1 H, Ar), 8.67 (d, *J* = 6.3 Hz, 1 H, Ar), 9.25 (s, 1 H, Ar), 9.58 (d, *J* = 6.2 Hz, 1 H, Ar) ppm. MS (ESI): *m/z* (positive mode, rel. int., %) = 477 (91) [M+H, ⁷⁹Br]⁺, 479 (100) [M+H, ⁸¹Br]⁺.



8-*N,N*-dimethylamino-5*H*-chromeno[3,4-*f*]quinolin-5-one (356)

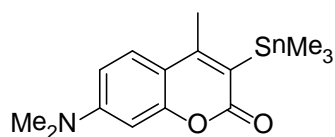
The synthesis was carried out analogously to known procedure.^[152] LiCl (12 mg, 0.275 mmol) was placed in a Schlenk flask. This flask was evacuated and dried with a heatgun. After cooling, the flask was flushed with Ar, and compound **358** (20 mg, 0.055 mmol), 3-bromopyridine-2-carbaldehyde (10 mg, 0.055 mmol), CuCl (23 mg, 0.231 mmol), Pd(PPh₃)₄ (6.3 mg, 0.005 mmol, 10 mol%) and DMSO (1 mL) were added. The resulting mixture was stirred for 15 h at 90 °C. Afterwards, the reaction mixture was left to cool down, diluted with CH₂Cl₂ and filtered through a plug of SiO₂ eluting with CH₂Cl₂. The filtrate was washed with brine, dried with Na₂SO₄ and evaporated. Purification of the crude product by column chromatography (35 g of SiO₂, *n*-hexane/EtOAc, 1:1) gave 7 mg (44%) of the title product. ¹H NMR (400 MHz, CDCl₃): δ = 3.06 (s, 6 H, NMe₂), 6.57 (d, *J* = 2.6 Hz, 1 H, Ar), 6.71 (dd, *J* = 9.0 and 2.6 Hz, 1 H, Ar), 7.60 (dd, *J* = 8.7 and 3.9 Hz, 1 H, Ar), 7.94 (d, *J* = 9.2 Hz, 1 H, Ar), 8.26 (d, *J* = 9.2 Hz, 1 H, Ar), 8.37 (d, *J* = 9.1

Hz, 1 H, Ar), 8.91 (br. s, 1 H, Ar), 10.04 (dd, $J = 8.8$ and 1.1 Hz, 1 H, Ar) ppm. UV-Vis spectral data in MeOH: $\lambda_{\text{abs,max}} = 411$ nm; $\epsilon = 16700$ M⁻¹cm⁻¹, $\lambda_{\text{em,max}} = 577$ nm, $\Phi_{\text{fl}} = 0.11$ (standard: Coumarin 153, $\Phi_{\text{fl}} = 0.54$ in EtOH).



7-*N,N*-Dimethylamino-4-methyl-3-(4,4,5,5-tetramethyl-1,3,2-dioxaborolan-2-yl)coumarin (357)

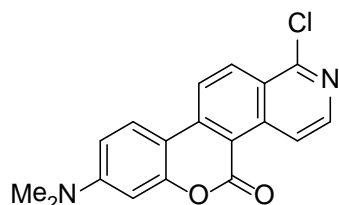
A Schlenk flask was charged with dried AcOK (103 mg, 1.05 mmol), compound **355-Br** (100 mg, 0.35 mmol), bis(pinacolato)diboron (108 mg, 0.42 mmol), PdCl₂(dppf) (15.4 mg, 0.02 mmol, 6 mol%) and dioxane (3 mL). The resulting mixture was stirred overnight at 80 °C. After cooling, water (~10 mL) and CH₂Cl₂ (~10 mL) were added, the organic layer was separated, and the aq. phase was extracted with CH₂Cl₂ (3×20 mL). Combined organic solutions were dried with Na₂SO₄ and evaporated. The crude product was purified by column chromatography (40 g of SiO₂, *n*-hexane/EtOAc, 2:1) to yield 40 mg (35%) of the title compound. ¹H NMR (400 MHz, CDCl₃): $\delta = 1.39$ (s, 12 H, 4×Me), 2.46 (s, 3 H, Me), 3.04 (s, 6 H, 2Me), 6.50 (d, $J = 2.6$ Hz, 1 H, Ar), 6.60 (dd, $J = 9.0$ and 2.6 Hz, 1 H, Ar), 7.44 (d, $J = 9.0$ Hz, 1 H, Ar) ppm. ¹³C NMR (100 MHz, CDCl₃): $\delta = 18.1(+)$, 24.8(+), 40.2(+), 84.0(-), 98.2(+), 108.6(+), 125.7(+), 152.8(-), 155.9(-), 158.9(-), 163.2(-) ppm. MS (ESI): m/z (positive mode, rel. int., %) = 330 (42) [M+H]⁺, 352 (38) [M+Na]⁺, 681 (100) [2M+Na]⁺.



7-*N,N*-Dimethylamino-4-methyl-3-trimethylstannylcoumarin (358)

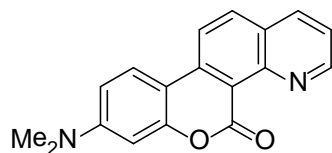
A screw-cap tube was charged with coumarin **355-Br** (100 mg, 0.35 mmol), hexamethylditin (151 mg, 0.46 mmol), Pd(PPh₃)₄ (20 mg, 0.017 mmol, 5 mol%) and toluene (2 mL). The resulting mixture was stirred overnight at 120 °C under Ar. After cooling, the reaction mixture was filtered through a pad of Celite eluting with CH₂Cl₂. The filtrate was evaporated, and the residue was subjected to column chromatography (30 g of SiO₂, *n*-hexane/EtOAc, 2:1) to afford 63 mg (49%) of the title compound. ¹H NMR (300 MHz, CDCl₃): $\delta = 0.35$ (s, 9 H, SnMe₃), 2.38 (s, 3 H, Me), 3.02 (s, 6 H, NMe₂), 6.46 (d, $J = 2.6$

Hz, 1 H, Ar), 6.55 (dd, $J = 8.9$ and 2.6 Hz, 1 H, Ar), 7.39 (d, $J = 8.9$ Hz, 1 H, Ar) ppm. ^{13}C NMR (125.7 MHz, CDCl_3): $\delta = -6.6(+)$, $20.3(+)$, $40.0(+)$, $98.1(+)$, $108.3(+)$, $110.7(+)$, $122.8(-)$, $125.1(+)$, $152.6(-)$, $156.0(-)$, $160.2(-)$, $165.3(-)$ ppm. HRMS (ESI): found 368.0663; calc. for $\text{C}_{15}\text{H}_{21}\text{NO}_2\text{Sn}$ $[\text{M}+\text{H}]^+$ 368.0669.



1-Chloro-8-*N,N*-dimethylamino-5*H*-chromeno[3,4-*f*]isoquinolin-5-one (359)

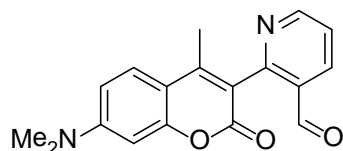
Compound **359** was prepared from compound **358** and 2-chloro-4-iodopyridine-3-carbaldehyde using the procedure described for compound **356**. Yield: 10 mg (56%) as an orange powder. ^1H NMR (300 MHz, CDCl_3): $\delta = 3.12$ (s, 6 H, NMe_2), 6.60 (d, $J = 2.6$ Hz, 1 H, Ar), 6.76 (dd, $J = 9.1$ and 2.6 Hz, 1 H, Ar), 7.97 (d, $J = 9.2$ Hz, 1 H, Ar), 8.20 (d, $J = 9.3$ Hz, 1 H, Ar), 8.46 (d, $J = 6.1$ Hz, 1 H, Ar), 8.65 (dd, $J = 9.2$ and 0.9 Hz, 1 H, Ar), 9.48 (dd, $J = 6.1$ and 0.8 Hz, 1 H, Ar) ppm. MS (ESI): m/z (positive mode, rel. int., %) = 325 (100) $[\text{M}+\text{H}, ^{35}\text{Cl}]^+$, 327 (30) $[\text{M}+\text{H}, ^{37}\text{Cl}]^+$.



8-*N,N*-Dimethylamino-5*H*-chromeno[4,3-*h*]quinolin-5-one (360)

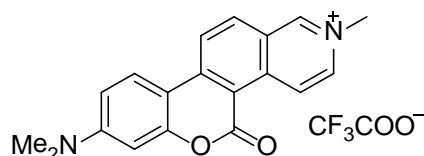
From boronic ester **357**: A screw-cap tube was charged with compound **357** (20 mg, 0.061 mmol), 2-bromopyridine-3-carbaldehyde (13.6 mg, 0.073 mmol), $\text{Pd}(\text{PPh}_3)_4$ (3.5 mg, 0.003 mmol, 5 mol%), 2 M sat. aq. NaHCO_3 (122 μL , 0.244 mmol) and toluene (1 mL). The resulting mixture was stirred overnight at 120°C under Ar. After cooling, the reaction mixture was filtered through a plug of Celite eluting with CH_2Cl_2 . The filtrate was evaporated, and the residue was subjected to column chromatography (30 g of SiO_2 , $\text{CH}_2\text{Cl}_2/\text{MeOH}$, 20:1) to afford 9 mg (51%) of the title compound. ^1H NMR (400 MHz, $\text{DMSO}-d_6$): $\delta = 3.03$ (s, 6 H, NMe_2), 6.58 (d, $J = 2.5$ Hz, 1 H, Ar), 6.79 (dd, $J = 9.0$ and 2.5 Hz, 1 H, Ar), 7.57 (dd, $J = 8.1$ and 4.2 Hz, 1 H, Ar), 8.19 (d, $J = 9.2$ Hz, 1 H, Ar), 8.31 (d, $J = 8.9$ Hz, 1 H, Ar), 8.39 (d, $J = 8.6$ Hz, 1 H, Ar), 8.40 (d, $J = 8.1$ Hz, 1 H, Ar), 9.03 (m, 1 H, Ar) ppm. ^{13}C NMR (100 MHz, $\text{DMSO}-d_6$): $\delta = 97.9(+)$, $106.3(-)$, $109.8(+)$, $111.9(-)$, $120.8(+)$, $121.7(+)$, $125.9(+)$, $126.9(-)$, $136.1(+)$, $136.9(+)$, $141.0(-)$, $147.6(-)$,

152.3(+), 153.2(-), 154.4(-), 157.2(-) ppm. HRMS (ESI): found 291.1128; calc. for $C_{18}H_{14}N_2O_2$ $[M+H]^+$ 291.1128. UV-Vis spectral data in MeOH: $\lambda_{abs,max} = 420$ nm; $\epsilon = 13200$ $M^{-1}cm^{-1}$, $\lambda_{em,max} = 560$ nm, $\Phi_{fl} = 0.29$ (standard: Coumarin 153, $\Phi_{fl} = 0.54$ in EtOH).



2-(7-*N,N*-Dimethylamino-4-methyl-2-oxo-1,2-dihydrochromen-3-yl)nicotinaldehyde (361)

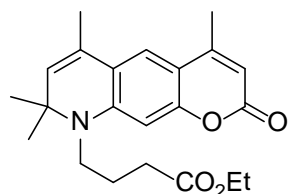
Compound **361** was prepared from compound **358** and 2-bromopyridine-3-carbaldehyde using the procedure described for compound **356**. Column chromatography (30 g of SiO_2 , $CH_2Cl_2/MeOH$, 20:1) yielded 14 mg (82%) of the title compound as a yellow powder. 1H NMR (300 MHz, $CDCl_3$): $\delta = 2.22$ (s, 3 H, Me), 3.07 (s, 6 H, NMe_2), 6.55 (d, $J = 2.5$ Hz, 1 H, Ar), 6.66 (dd, $J = 9.0$ and 2.5 Hz, 1 H, Ar), 7.42–7.54 (m, 1 H, Ar), 7.51 (d, $J = 9.0$ Hz, 1 H, Ar), 8.30 (d, $J = 7.8$ Hz, 1 H, Ar), 8.89 (br. s, 1 H, Ar), 10.01 (s, 1 H, CHO) ppm. HRMS (ESI): calc. for $C_{18}H_{16}N_2O_3$ $[M+H]^+$ 309.1234; found 309.1230.



8-*N,N*-dimethylamino-2-methyl-5-oxo-5*H*-chromeno[3,4-*f*]isoquinolin-2-ium trifluoroacetate (362)

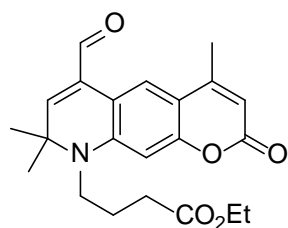
In a screw-cap tube, a solution of compound **359** (7 mg, 0.021 mmol) and MeI (4.6 mg, 0.032 mmol) in DMF (2 mL) was stirred overnight at 100 °C. After cooling, the reaction mixture was diluted with water (~10 mL) and extracted with CH_2Cl_2 (3×20 mL). Combined organic solutions were dried with Na_2SO_4 and evaporated *in vacuo*. The crude product was purified by column chromatography (30 g of SiO_2 , $MeCN/H_2O$, 5:1 + 0.1 v/v% TFA) to afford 3 mg (44%) of the title compound as an orange powder. 1H NMR (300 MHz, $DMSO-d_6$): $\delta = 3.11$ (s, 6 H, NMe_2), 4.41 (s, 3 H, Me), 6.68 (d, $J = 2.5$ Hz, 1 H, Ar), 6.90 (dd, $J = 9.2$ and 2.6 Hz, 1 H, Ar), 8.30 (d, $J = 9.4$ Hz, 1 H, Ar), 8.57 (d, $J = 8.9$ Hz, 1 H, Ar), 8.74 (d, $J = 9.3$ Hz, 1 H, Ar), 8.78 (dd, $J = 7.2$ and 1.5 Hz, 1 H, Ar), 9.64 (d, $J = 7.2$ Hz, 1 H, Ar), 9.81 (s, 1 H, Ar) ppm. MS (ESI): m/z (positive mode, rel.

int., %) = 305 (100) M^+ . UV-Vis spectral data in MeOH: $\lambda_{\text{abs,max}} = 467 \text{ nm}$; $\epsilon = 13400 \text{ M}^{-1} \text{ cm}^{-1}$, $\lambda_{\text{em,max}} = 608 \text{ nm}$, $\Phi_{\text{fl}} = 0.26$ (standard: Coumarin 153, $\Phi_{\text{fl}} = 0.54$ in EtOH).



9-(Ethoxycarbonylpropyl)-8,9-dihydro-4,6,8,8-tetramethyl-2H-pyrano[3,2-g]quinolin-2-one (362)

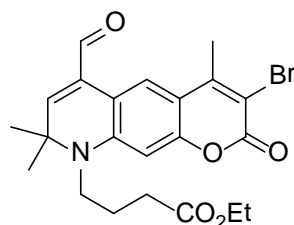
Ethyl acetoacetate (1.50 g, 11.5 mmol) was added to a solution of phenol **288-H** (1.95 g, 6.44 mmol) in ethanol (4 mL) followed by addition of dry ZnCl_2 (1.3 g, 9.6 mmol). The reaction mixture was heated in an open flask (90 °C) for 20 h. The obtained green-grey slurry was cooled, dissolved in dichloromethane (50 mL) and shaken with 2% aq. ammonia solution (50 mL). The organic layer was separated and passed through a plug of SiO_2 eluting with $\text{CH}_2\text{Cl}_2/\text{Et}_2\text{O}$ (1:1). After evaporation of solvents, the oily residue was purified by column chromatography (cyclohexane/ $\text{CH}_2\text{Cl}_2/\text{Et}_2\text{O}$, 4:4:1) to give 1.52 g (64%) of a pale-yellow solid. ^1H NMR (400 MHz, CDCl_3): $\delta = 1.28$ (t, $J = 7.2$, 3 H, Et), 1.35 (s, 6 H, 2×Me), 1.90 (m, 2 H, CH_2), 1.98 (d, $J = 0.8$ Hz, 3 H, Me), 2.31 (d, $J = 0.8$ Hz, 3 H, Me), 2.38 (m, 2 H, CH_2), 3.29 (m, 2 H, NCH_2), 4.16 (q, $J = 7.2$ Hz, 2 H, Et), 5.28 (q, $J = 0.8$ Hz, 1 H), 5.91 (q, $J = 0.8$ Hz, 1 H), 6.34 (s, 1 H, Ar), 7.09 (s, 1 H, Ar) ppm. ^{13}C NMR (100.7 MHz, CDCl_3): $\delta = 14.2$, 18.5, 18.7, 22.7, 29.0, 31.4, 43.8, 57.7, 60.6, 97.2, 108.8, 109.0, 118.8, 119.8, 126.3, 129.8, 147.3, 152.9, 155.8, 162.0, 172.8 ppm. MS (ESI): m/z (positive mode, rel. int., %) = 761.4 (100) $[2\text{M}+\text{Na}]^+$, 392.3 (70) $[\text{M}+\text{Na}]^+$, 370.3 (18) $[\text{M}+\text{H}]^+$.



8,9-Dihydro-9-ethoxycarbonylpropyl-6-formyl-4,8,8-trimethyl-2H-pyrano[3,2-g]quinolin-2-one (363)

Finely powdered SeO_2 (676 mg, 6.09 mmol) was added to a hot (90 °C) solution of **362** (1.50 g, 4.06 mmol) in dioxane (30 mL). Then the reaction mixture was stirred at 100 °C for 1 h. After cooling, dioxane was evaporated *in vacuo*, the residue was diluted with

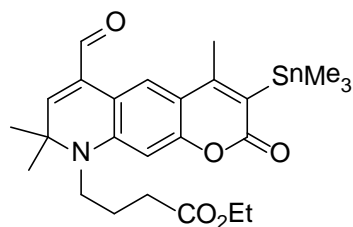
dichloromethane (50 mL) and the organic layer was washed with sat. aq. NaHCO₃ and dried with MgSO₄. All volatiles were evaporated, and the residue was purified by column chromatography (cyclohexane/CH₂Cl₂/Et₂O, 2:2:0.6). Fractions containing the product were collected and, after evaporation of solvents, the residue was triturated with Et₂O to afford 794 mg (51%) of a yellow solid. ¹H NMR (300 MHz, CDCl₃): δ = 1.28 (t, *J* = 7.2 Hz, 3 H, Et), 1.50 (s, 6 H, 2×Me), 1.90 (m, 2 H, CH₂), 2.37 (d, *J* = 0.8 Hz, 3H, Me), 2.39 (m, 2 H, CH₂), 3.32 (m, 2 H, NCH₂), 4.17 (q, *J* = 7.2 Hz, 2 H, Et), 5.97 (q, *J* = 0.8 Hz, 1 H), 6.21 (s, 1 H, Ar), 6.43 (s, 1 H, Ar), 8.54 (s, 1 H, Ar), 9.58 (s, 1 H, CHO) ppm. ¹³C NMR (125.7 MHz, CDCl₃): δ = 14.3(+), 18.6(+), 22.9(-), 27.9(+), 31.3(-), 43.9(-), 58.0(-), 60.7(-), 98.3(+), 109.7(+), 109.9(-), 113.4(-), 122.3(+), 130.8(-), 146.9(-), 152.0(+), 153.4(-), 156.0(-), 161.6(-), 172.6(-), 191.8(+) ppm. MS (ESI): *m/z* (positive mode, rel. int., %) = 761.4 (100) [2M+Na]⁺, 392.3 (70) [M+Na]⁺, 370.3 (18) [M+H]⁺.



Ethyl (3-bromo-6-formyl-8,9-dihydro-4,8,8-trimethyl-2H-pyrano[3,2-g]quinolin-2-one)-9-butanoate (364)

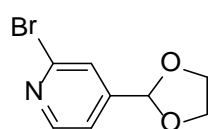
A solution of bromine (184 mg, 1.15 mmol) in AcOH (1 mL) was added to a solution of **363** (421 mg, 1.09 mmol) in AcOH (8 mL). The reaction mixture was stirred at room temperature for 10 min and left in refrigerator (5 °C) for 1 h. The precipitate was filtered, washed with cold ether and dried. Afterwards, this crude product was dissolved in dichloromethane, washed with sat. aq. NaHCO₃ and passed through a plug of SiO₂ eluting with CH₂Cl₂/Et₂O (1:1). After evaporation of solvents, the title compound was precipitated from Et₂O with *n*-hexane; yield 530 mg (96%) as a solvate with CH₂Cl₂ according to ¹H NMR (**364**·1/2CH₂Cl₂). ¹H NMR (300 MHz, CDCl₃): δ = 1.28 (t, *J* = 7.2 Hz, 3 H, Et), 1.50 (s, 6 H, 2×Me), 1.90 (m, 2 H, CH₂), 2.40 (m, 2 H, CH₂), 2.55 (s, 3 H, Me), 3.32 (m, 2 H, NCH₂), 4.17 (q, *J* = 7.2 Hz, 2 H, Et), 5.27 (1 H, 1/2·CH₂Cl₂), 6.23 (s, 1 H), 6.44 (s, 1 H, Ar), 8.62 (s, 1 H, Ar), 9.49 (s, 1 H, CHO) ppm. ¹³C NMR (125.7 MHz, CDCl₃): δ = 14.3(+), 19.4(+), 22.8(-), 28.1(+), 31.2(-), 44.0(-), 58.2(-), 60.8(-), 98.0(+), 106.7(-), 109.8(-), 113.8(-), 122.8(+), 130.5(-), 147.0(-), 151.9(-), 152.3(+), 154.4(-), 157.6(-), 172.6(-), 191.7(+) ppm. HRMS (ESI, C₂₂H₂₄NO₃Br): 462.0754/460.0752 (found

[M-H]⁻), 462.0746/460.0765 (calc.); HRMS (ESI, C₂₂H₂₄NO₅Br): 486.0697/484.0725 (found [M+Na]⁻), 486.0711/484.0730 (calc.); 464.0888/462.0897 (found [M+H]⁻), 464.0891/464.0911 (calc.).



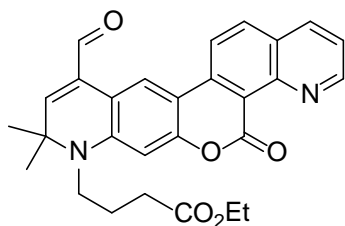
Ethyl 4-(6-formyl-4,8,8-trimethyl-2-oxo-3-(trimethylstannyl)-1,2,8,9-tetrahydro pyrano[3,2-g]quinolin-9-yl)butanoate (368)

A screw-cap tube was charged with coumarin **364** (631 mg, 1.36 mmol), hexamethylditin (538 mg, 1.64 mmol), Pd(PPh₃)₄ (161 mg, 0.14 mmol, 10 mol%) and toluene (10 mL). The resulting mixture was stirred overnight at 120 °C under Ar. After cooling, the reaction mixture was filtered through a pad of Celite eluting with CH₂Cl₂. The filtrate was evaporated, and the residue was subjected to column chromatography (30 g of SiO₂, *n*-hexane/EtOAc, 2:1) to afford 364 mg (49%) of the title compound. ¹H NMR (400 MHz, CDCl₃): δ = 0.37 (s, 9 H, SnMe₃), 1.30 (t, *J* = 7.1 Hz, 3 H, Et), 1.50 (s, 6 H, 2×Me), 1.59 (s, 3 H, Me), 1.88–1.97 (m, 2 H, CH₂), 2.38–2.45 (m, 2 H, CH₂), 2.44 (s, 3 H, Me), 3.30–3.36 (m, 2 H, NCH₂), 4.18 (q, *J* = 7.1 Hz, 2 H, Et), 6.21 (s, 1 H), 6.41 (s, 1 H, Ar), 7.26 (s, 1 H, Ar), 8.58 (s, 1 H, Ar), 9.60 (s, 1 H, CHO) ppm. HRMS (ESI): calc. for C₂₅H₃₃NO₅Sn [M+H]⁺ 548.1458; found 548.1446.



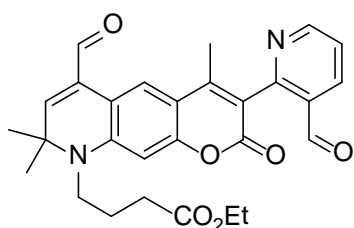
2-Bromo-4-(1,3-dioxolan-2-yl)pyridine (369)

A mixture of 2-bromopyridine-3-carbaldehyde (500 mg, 2.69 mmol), ethylene glycol (0.6 mL), TsOH·H₂O (204 mg, 1.08 mmol) and toluene (50 mL) was refluxed with a Dean-Stark trap for 5 h. After cooling, the reaction mixture was diluted with EtOAc (50 mL), washed with water (50 mL), aq. NaHCO₃ (50 mL), and again with water (50 mL). The organic layer was dried with MgSO₄ and evaporated to give 577 mg (93%) of the crude product which was used without further purification. ¹H NMR (400 MHz, CDCl₃): δ = 4.06–4.19 (m, 4 H, 2×CH₂), 6.04 (s, 1 H, Ar), 7.31 (dd, *J* = 7.6 and 4.7 Hz, 1 H, Ar), 7.89 (dd, *J* = 7.6 and 2.0 Hz, 1 H, Ar), 8.37 (dd, *J* = 4.7 and 2.0 Hz, 1 H, Ar) ppm.



Ethyl 4-(11-formyl-9,9-dimethyl-5,6,8,9-tetrahydroquinolino[7',8':4,5]pyrano[3,2-g]quinolin-8-yl)butanoate (370)

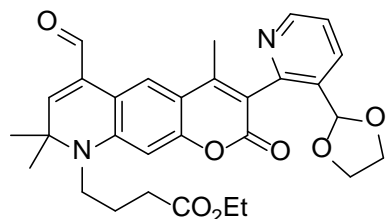
To a solution of compound **371** (30 mg, 0.06 mmol) in CH₂Cl₂/MeOH (1:2, 3 mL) Cs₂CO₃ (4 mg, 0.012 mmol) was added, and the resulting mixture left stirred for 2.5 h at r.t. Afterwards, water (15 mL) was added, and the resulting slurry was extracted with CH₂Cl₂ (3×15 mL). Combined organic solutions were dried with Na₂SO₄ and evaporated. The crude product was purified by column chromatography (30 g of SiO₂, CH₂Cl₂/MeOH, 20:1) to provide 20 mg (71%) of the title product. ¹H NMR (400 MHz, CDCl₃): δ = 1.29 (t, *J* = 7.1 Hz, 3 H, Et), 1.54 (s, 6 H, 2×Me), 1.91–2.01 (m, 2 H, CH₂), 2.45 (t, *J* = 6.9 Hz, 2 H, CH₂), 3.33–3.40 (m, 2 H, NCH₂), 4.18 (q, *J* = 7.1 Hz, 2 H, Et), 6.26 (s, 1 H), 6.53 (s, 1 H, Ar), 7.48 (dd, *J* = 8.1 and 4.3 Hz, 1 H, Ar), 8.10 (d, *J* = 8.9 Hz, 1 H, Ar), 8.18 (dd, *J* = 8.2 and 1.9 Hz, 1 H, Ar), 8.20 (d, *J* = 9.0 Hz, 1 H, Ar), 9.16 (s, 1 H, Ar), 9.24 (dd, *J* = 4.3 and 1.9 Hz, 1 H, Ar), 9.64 (s, 1 H, CHO) ppm. ¹³C NMR (100 MHz, CDCl₃): δ = 14.3(+), 22.8(-), 28.0(+), 31.0(-), 43.9(-), 58.1(-), 60.8(-), 98.4(+), 107.0(-), 112.8(-), 113.7(-), 120.3(+), 121.1(+), 121.6(+), 127.1(-), 130.8(-), 135.3(+), 136.5(+), 140.8(-), 146.9(-), 147.9(-), 152.5(+), 154.9(-), 158.5(-), 173.3(-), 192.2(+ ppm. HRMS (ESI): calc. for C₂₈H₂₆N₂O₅ [M+H]⁺ 471.1914; found 471.1897.



Ethyl 4-(6-formyl-3-(3-formylpyridin-2-yl)-4,8,8-trimethyl-2-oxo-1,2,8,9-tetrahydropyrano[3,2-g]quinolin-9-yl)butanoate (371)

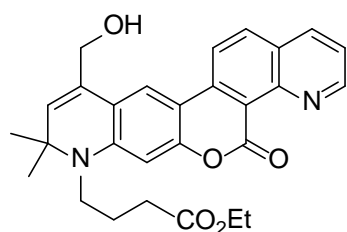
Compound **371** was prepared from compound **368** and 2-bromopyridine-3-carbaldehyde using the procedure described for compound **356**. Column chromatography (40 g of SiO₂, CH₂Cl₂/MeOH, 30:1) yielded 44 mg (91%) of the title compound as a yellow powder. ¹H NMR (400 MHz, CDCl₃): δ = 1.30 (t, *J* = 7.1 Hz, 3 H, Et), 1.55 (s, 6 H, 2×Me), 1.90–2.01 (m, 2 H, CH₂), 2.26 (s, 3 H, Me), 2.43 (t, *J* = 6.8 Hz, 2 H, CH₂), 3.35–3.42 (m, 2 H,

NCH₂), 4.19 (q, $J = 7.1$ Hz, 2 H, Et), 6.26 (s, 1 H, Ar), 6.52 (s, 1 H, Ar), 7.42–7.49 (m, 1 H, Ar), 7.51–7.57 (m, 1 H, Ar), 7.63–7.70 (m, 1 H, Ar), 8.73 (s, 1 H, Ar), 9.61 (s, 1 H, CHO), 10.02 (s, 1 H, CHO) ppm. ¹³C NMR (100 MHz, CDCl₃): $\delta = 14.2(+)$, 16.3(+), 22.8(-), 28.1(+), 31.2(-), 44.0(-), 58.3(-), 60.7(-), 98.1(+), 109.9(-), 113.8(-), 117.9(-), 123.2(+), 123.4(+), 130.6(-), 131.4(-), 136.1(+), 147.5(-), 152.2(+), 152.6(-), 153.9(+), 155.9(-), 156.6(-), 161.2(-), 172.7(-), 190.2(+), 191.9(+) ppm. HRMS (ESI): calc. for C₂₈H₂₈N₂O₆ [M+H]⁺ 489.2020; found 489.2019.



Ethyl 4-(3-(3-(1,3-dioxolan-2-yl)pyridin-2-yl)-6-formyl-4,8,8-trimethyl-2-oxo-1,2,8,9-tetrahydropyrano[3,2-g]quinolin-9-yl)butanoate (372)

Compound **372** was prepared from compound **368** and compound **369** using the procedure described for compound **356**. Column chromatography (35 g of SiO₂, CH₂Cl₂/MeOH, 40:1) yielded 77 mg (80%) of the title compound as a yellow powder. ¹H NMR (400 MHz, CDCl₃): $\delta = 1.30$ (t, $J = 7.1$ Hz, 3 H, Et), 1.53 (s, 3 H, Me), 1.54 (s, 3 H, Me), 1.90–2.00 (m, 2 H, CH₂), 2.16 (s, 3 H, Me), 2.42 (t, $J = 6.8$ Hz, 2 H, CH₂), 3.31–3.41 (m, 2 H, NCH₂), 3.83–3.90 (m, 1 H), 3.90–3.99 (m, 2 H), 4.04–4.09 (m, 1 H), 4.19 (q, $J = 7.1$ Hz, 2 H, Et), 5.74 (s, 1 H), 6.24 (s, 1 H), 6.49 (s, 1 H, Ar), 7.42–7.49 (m, 1 H, Ar), 7.51–7.57 (m, 1 H, Ar), 7.63–7.70 (m, 1 H, Ar), 8.68 (s, 1 H, Ar), 9.60 (s, 1 H, CHO) ppm. HRMS (ESI): calc. for C₃₀H₃₂N₂O₇ [M+H]⁺ 533.2282; found 533.2279.

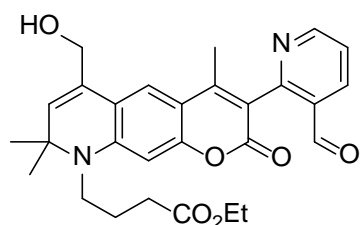


Ethyl 4-(11-hydroxymethyl-9,9-dimethyl-5,6,8,9-tetrahydroquinolino[7',8':4,5]pyrano[3,2-g]quinolin-8-yl)butanoate (373)

From aldehyde **370**: To a solution of compound **370** (32 mg, 0.068 mmol) in THF/EtOH (3:1, 4 mL) NaBH₄ (3 mg, 0.068 mmol) was added at 0 °C with stirring. After 5 min, 3 drops of 70% aq. HClO₄ and Bu₄NIO₄ (4.3 mg, 0.01 mmol) were added. After 5 min stirring, the reaction mixture was neutralized with sat. aq. NaHCO₃. The resulting mixture

was diluted with water (10 mL) and extracted with CH₂Cl₂ (3×10 mL). Combined organic solutions were dried with Na₂SO₄ and evaporated *in vacuo*. The residue was subjected to column chromatography (40 g of SiO₂, CH₂Cl₂/MeOH, 8:1) to furnish 10 mg (31%) of the title product.

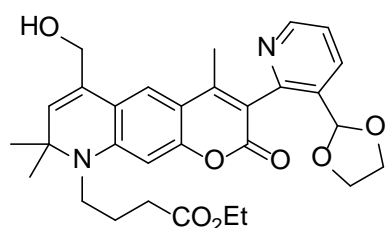
From aldehyde **374**: To a solution of compound **374** (30 mg, 0.061 mmol) in EtOH (1 mL) Cs₂CO₃ (2 mg, 0.006 mmol, 10 mol%) was added. The resulting mixture was stirred for 1.5 h at r.t. Afterwards, sat. aq. NH₄Cl (5 mL) and water (5 mL) were added, and the reaction mixture was extracted with CH₂Cl₂ (3×10 mL). Combined organic solutions were dried with Na₂SO₄ and evaporated. The residue was subjected to column chromatography (30 g of SiO₂, CH₂Cl₂/MeOH, 20:1) to give 24 mg (83%) of the title product. ¹H NMR (400 MHz, CDCl₃): δ = 1.30 (t, *J* = 6.8 Hz, 3 H, Et), 1.41 (s, 6 H, 2×Me), 1.88–2.00 (m, 2 H, CH₂), 2.37–2.46 (m, 2 H, CH₂), 3.28–3.38 (m, 2 H, NCH₂), 4.18 (q, *J* = 6.8 Hz, 2 H, Et), 4.59 (s, 2 H, OCH₂), 5.57 (s, 1 H), 6.42 (s, 1 H, Ar), 7.40–7.49 (m, 1 H, Ar), 7.86 (s, 1 H, Ar), 8.2 (d, *J* = 8.5 Hz, 1 H, Ar), 8.12 (d, *J* = 8.1 Hz, 1 H, Ar), 9.19 (s, 1 H, Ar) ppm. MS (ESI): *m/z* (positive mode, rel. int., %) = 473 (100) [M+H]⁺. UV-Vis spectral data in MeOH: λ_{abs,max} = 438 nm; ε = 19300 M⁻¹cm⁻¹, λ_{em,max} = 574 nm, Φ_{fl} = 0.27 (standard: Coumarin 153, Φ_{fl} = 0.54 in EtOH).



Ethyl 4-(3-(3-formylpyridin-2-yl)-6-hydroxymethyl-4,8,8-trimethyl-2-oxo-1,2,8,9-tetrahydropyrano[3,2-g]quinolin-9-yl)butanoate (374)

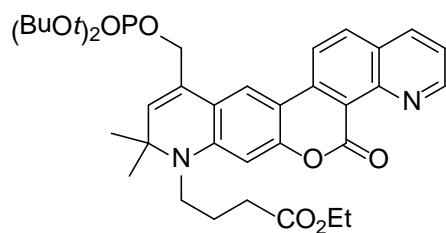
To a solution of compound **375** (46 mg, 0.086 mmol) acetone/water (4:1, 3 mL) TsOH·H₂O (16 mg, 0.086 mmol) was added. The resulting reaction mixture was stirred overnight at reflux. After cooling, sat. aq. NaHCO₃ (4 mL) and brine (5 mL) were added, and the reaction mixture was extracted with CH₂Cl₂ (3×30 mL). Combined organic solutions were dried with Na₂SO₄ and evaporated. The crude product was purified by column chromatography (30 g of SiO₂, CH₂Cl₂/MeOH, 20:1 → 10:1) to give 30 mg (71%) of the title compound. ¹H NMR (400 MHz, CDCl₃): δ = 1.29 (t, *J* = 7.1 Hz, 3 H, Et), 1.40 (s, 3 H, Me), 1.41 (s, 3 H, Me), 1.89–1.99 (m, 2 H, CH₂), 2.19 (s, 3 H, Me), 2.41 (t, *J* = 6.9 Hz, 2 H, CH₂), 3.30–3.37 (m, 2 H, NCH₂), 4.18 (q, *J* = 7.1 Hz, 2 H, Et), 4.46 (s, 2 H, OCH₂), 5.55 (s, 1 H), 6.43 (s, 1 H, Ar), 7.36 (s, 1 H, Ar), 7.48 (dd, *J* = 7.9 and 4.8 Hz, 1 H, Ar),

8.30 (dd, $J = 7.9$ and 1.8 Hz, 1 H, Ar), 8.88 (dd, $J = 4.8$ and 1.8 Hz, 1 H, Ar), 9.98 (s, 1 H, CHO) ppm. ^{13}C NMR (100 MHz, CDCl_3): $\delta = 14.3(+)$, $16.2(+)$, $22.7(-)$, $29.0(+)$, $31.3(-)$, $44.0(-)$, $57.8(-)$, $60.7(-)$, $62.8(-)$, $97.3(+)$, $109.1(-)$, $116.9(-)$, $117.6(-)$, $119.6(+)$, $123.4(+)$, $129.8(-)$, $129.9(+)$, $131.5(-)$, $136.1(+)$, $148.0(-)$, $152.2(-)$, $153.7(+)$, $155.6(-)$, $156.8(-)$, $161.4(-)$, $172.8(-)$, $190.3(+)$ ppm. HRMS (ESI): calc. for $\text{C}_{28}\text{H}_{30}\text{N}_2\text{O}_6$ $[\text{M}+\text{H}]^+$ 491.2177; found 491.2181.



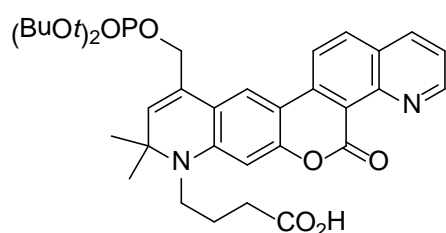
Ethyl 4-(3-(3-(1,3-dioxolan-2-yl)pyridin-2-yl)-6-hydroxymethyl-4,8,8-trimethyl-2-oxo-1,2,8,9-tetrahydropyrano[3,2-g]quinolin-9-yl)butanoate (375)

To a solution of compound **372** (77 mg, 0.145 mmol) in THF/EtOH (3:1, 4 mL) NaBH_4 (5.5 mg, 0.145 mmol) was added at 0°C with stirring. After 5 min, the reaction mixture was quenched with sat. aq. NH_4Cl , diluted with water (2 mL), and extracted with CH_2Cl_2 (3×10 mL). Combined organic extracts were dried with Na_2SO_4 and evaporated. The residue was subjected to column chromatography (30 g of SiO_2 , $\text{CH}_2\text{Cl}_2/\text{MeOH}$, 20:1) to yield 62 mg (80%) of the title compound as a yellow solid. ^1H NMR (400 MHz, CDCl_3): $\delta = 1.29$ (t, $J = 1.29$ Hz, 3 H, Et), 1.39 (s, 6 H, $2 \times \text{Me}$), 1.88 – 1.98 (m, 2 H, CH_2), 2.04 (s, 3 H, Me), 2.41 (t, $J = 6.9$ Hz, 2 H, CH_2), 3.28 – 3.36 (m, 2 H, NCH_2), 3.81 – 3.89 (m, 1 H, OCH_2), 3.89 – 3.97 (m, 2 H, OCH_2), 4.02 – 4.10 (m, 1 H, OCH_2), 4.18 (q, $J = 7.1$ Hz, 2 H, Et), 4.36 – 4.40 (m, 1 H, OCH_2), 4.41 – 4.46 (m, 1 H, OCH_2), 5.56 (s, 1 H), 5.71 (s, 1 H), 6.39 (s, 1 H, Ar), 7.23 (s, 1 H, Ar), 7.38 (dd, $J = 7.9$ and 4.9 Hz, 1 H, Ar), 8.04 (dd, $J = 7.9$ and 1.6 Hz, 1 H, Ar), 8.69 (dd, $J = 4.9$ and 1.7 Hz, 1 H, Ar) ppm. ^{13}C NMR (100 MHz, CDCl_3): $\delta = 14.3(+)$, $16.1(+)$, $22.7(-)$, $28.9(+)$, $29.0(+)$, $31.4(-)$, $43.9(-)$, $57.7(-)$, $60.7(-)$, $62.4(-)$, $65.3(-)$, $65.4(-)$, $97.3(+)$, $100.7(+)$, $109.1(-)$, $110.0(+)$, $117.4(-)$, $119.2(+)$, $123.1(+)$, $129.2(+)$, $129.8(-)$, $134.1(-)$, $135.2(+)$, $147.4(-)$, $149.7(+)$, $151.2(-)$, $153.4(-)$, $155.5(-)$, $160.8(-)$, $172.8(-)$ ppm. HRMS (ESI): calc. for $\text{C}_{30}\text{H}_{34}\text{N}_2\text{O}_7$ $[\text{M}+\text{H}]^+$ 535.2439; found 535.2433.



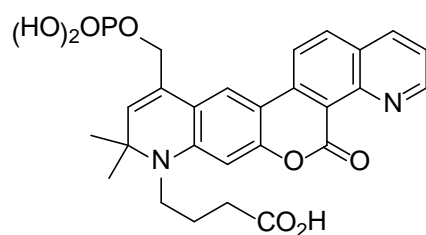
Ethyl 4-(11-(di-*tert*-butoxyphosphoryloxy)methyl-9,9-dimethyl-5,6,8,9-tetrahydroquinolino[7',8':4,5]pyrano[3,2-*g*]quinolin-8-yl)butanoate (376)

To a stirred and preheated (40 °C) solution of compound **373** (10 mg, 0.021 mmol) in CH₂Cl₂ (1 mL) di-*t*-butyl *N,N*-diisopropylphosphoramidite (18 mg, 0.063 mmol) and 1*H*-tetrazole (4.7 mg, 0.063 mmol) were added in two equal portions at interval of 20 min under argon. After further 20 min, the reaction mixture was cooled with dry ice bath (−78 °C), and solution of *m*CPBA (15.5 mg, 70% purity, 0.063 mmol) in CH₂Cl₂ (1 mL) was injected. After 1 h stirring at −78 °C, the reaction mixture was allowed to warm to 0 °C, and aqueous solutions of Na₂SO₃ (2 mL, 10%) and NaHCO₃ (1 mL, saturated) were added, and the reaction mixture was allowed to warm up to r.t. The organic layer was separated and the aqueous phase was extracted with CH₂Cl₂ (3×10 mL). The combined organic extracts were dried, the solvents were evaporated, and the titled compound was isolated by column chromatography (30 g of SiO₂, CH₂Cl₂/MeOH, 15:1) as a red solid (10 mg; 71%). ¹H NMR (300 MHz, CDCl₃): δ = 1.29 (t, *J* = 7.1 Hz, 3 H, Et), 1.43 (s, 6 H, 2×Me), 1.48 (d, *J*_{CP} = 1.5 Hz, 18 H, 2×*t*Bu), 1.95 (m, 2 H, CH₂), 2.42 (t, *J* = 6.9 Hz, 2 H, CH₂), 3.29–3.38 (m, 2 H, NCH₂), 4.18 (q, *J* = 7.1 Hz, 2 H, Et), 4.85 (d, *J*_{CP} = 6.2 Hz, 2 H, OCH₂), 5.61 (s, 1 H), 6.47 (s, 1 H, Ar), 7.49 (dd, *J* = 8.1 and 4.4 Hz, 1 H, Ar), 7.96 (s, 1 H, Ar), 8.09 (d, *J* = 9.0 Hz, 1 H, Ar), 8.18 (dd, *J* = 8.2 and 1.9 Hz, 1 H, Ar), 8.31 (d, *J* = 9.1 Hz, 1 H, Ar), 9.27 (dd, *J* = 4.4 and 1.9 Hz, 1 H, Ar) ppm. ¹³C NMR (125.7 MHz, CDCl₃): δ = 14.2(+), 29.8(+, d, *J*_{CP} = 4.3 Hz), 31.3(−), 43.9(−), 57.7(−), 60.7(−), 66.5 (−, *J*_{CP} = 5.6 Hz), 82.7(−), 82.8(−), 97.7(+), 106.4(−), 117.2(−), 119.3(+), 120.7(+), 121.1(+), 127.0(−), 132.7(+), 135.3(+), 136.8(+), 141.2(−), 147.4(−), 152.3(+), 154.8(−), 158.9(−), 173.0(−) ppm. HRMS (ESI): found 665.2984; calc. for C₃₆H₄₅N₂O₈P [M+H]⁺ 665.2986.



(11-(Di-*tert*-butoxyphosphoryloxy)methyl-9,9-dimethyl-5,6,8,9-tetrahydro-quinolino[7',8':4,5]pyrano[3,2-g]quinolin-8-yl)butanoic acid (377)

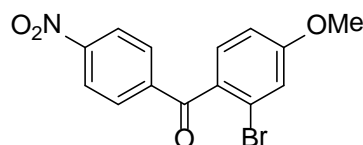
To a solution of compound **376** (10 mg, 0.015 mmol) in MeOH/H₂O (1:1, 2 mL) 1 M NaOH (150 μ L, 0.15 mmol) was added. The resulting mixture was stirred for 3 h at r.t., and then, citrate buffer (pH 3, 15 mL) was added. The aq. layer was saturated with NaCl and extracted with CH₂Cl₂ (3 \times 15 mL). Combined organic extracts were dried with Na₂SO₄ and evaporated. The residue was subjected with column chromatography (15 g of SiO₂, CH₂Cl₂/MeOH, 10:1 \rightarrow 5:1) to afford 7 mg (73%) of the title compound as a red solid. ¹H NMR (400 MHz, CDCl₃): δ = 1.41 (s, 6 H, 2 \times Me), 1.50 (br. s, 18 H, 2 \times *t*Bu), 1.91–2.02 (m, 2 H, CH₂), 2.43–2.52 (m, 2 H, CH₂), 3.27–3.37 (m, 2 H, NCH₂), 4.88 (br. s, 2 H, OCH₂), 5.62 (s, 1 H), 6.55 (s, 1 H, Ar), 7.50–7.60 (m, 1 H, Ar), 7.90 (s, 1 H, Ar), 8.08–8.16 (m, 1 H, Ar), 8.21–8.35 (m, 2 H, Ar), 9.24–9.34 (m, 1 H, Ar) ppm. MS (ESI): *m/z* (positive mode, rel. int., %) = 637 (100) [M+H]⁺.



(9,9-Dimethyl-11-phosphonooxymethyl-5,6,8,9-tetrahydro-quinolino[7',8':4,5]pyrano[3,2-g]quinolin-8-yl)butanoic acid (378)

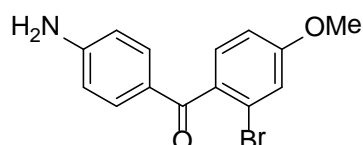
To a cooled (0 °C) solution of compound **377** (7 mg, 0.011 mmol) in CH₂Cl₂ (1 mL) TFA (100 μ L) was added. The resulting solution was stirred for 40 min at 0 °C, and then, all volatiles were evaporated *in vacuo*. The crude product was dissolved in water and freeze-dried. Yield: 6 mg (quantitative). ¹H NMR (300 MHz, CD₃OD): δ = 1.51 (s, 6 H, 2 \times Me), 1.89–2.02 (m, 2 H, CH₂), 2.51 (t, *J* = 6.5 Hz, 2 H, CH₂), 3.46–3.50 (m, 2 H, NCH₂), 4.85–4.89 (m, 2 H, OCH₂), 5.84 (s, 1 H), 6.77 (s, 1 H, Ar), 8.04–8.11 (m, 2 H, Ar), 8.47 (d, *J* = 9.1 Hz, 1 H, Ar), 8.63 (d, *J* = 9.1 Hz, 1 H, Ar), 9.08–9.18 (m, 2 H, Ar) ppm. ¹³C NMR (125.7 MHz, CD₃OD): δ = 23.8(-), 29.2(+), 31.4(-), 45.3(-), 60.1(-), 67.3(-, d, *J* = 4.6 Hz), 98.9(-), 104.3(-), 106.6(-), 115.9(-), 118.2(-), 119.9(-), 121.4(+), 123.1(+), 125.6(+), 129.5(-), 135.4(+), 136.8(+), 140.5(-), 145.6(+), 146.1(-), 148.3(+), 151.5(-), 157.0(-), 176.9(-) ppm. HRMS (ESI): found 525.1417; calc. for C₂₆H₂₅N₂O₈P [M+H]⁺ 513.2748; found 523.1274; calc. for C₂₆H₂₅N₂O₈P [M-H]⁻ 523.1276. UV-Vis spectral

data in PBS 7.4: $\lambda_{\text{abs,max}} = 453 \text{ nm}$; $\epsilon = 7740 \text{ M}^{-1}\text{cm}^{-1}$, $\lambda_{\text{em,max}} = 617 \text{ nm}$, $\Phi_{\text{fl}} = 0.44$ (standard: DCM, $\Phi_{\text{fl}} = 0.44$ in EtOH).



(2-Bromo-4-methoxyphenyl)-(4-nitrophenyl)methanone (400)

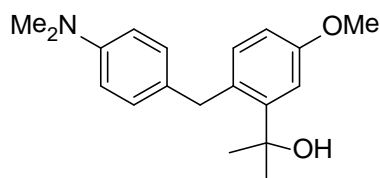
A dry 50 mL Schlenk flask was charged with AlCl_3 (1.73 g, 13 mmol) and CH_2Cl_2 (13 mL). To this suspension, 3-bromoanisole **399** (2.5 g, 13 mmol) was added under vigorous stirring at 0 °C. After warming up to r.t., a solution of *p*-nitrobenzoyl chloride (2.73 g, 15 mmol) in CH_2Cl_2 (20 mL) was introduced, and the reaction mixture refluxed for 3 h. After cooling down to r.t., the reaction mixture was poured into a mixture of ice and 1 M HCl. The organic layer was separated, the aqueous phase was extracted with CH_2Cl_2 (2 × 100 mL), and the combined organic solutions were washed with 1 M NaOH (3 × 50 mL) and dried with Na_2SO_4 . Evaporation of volatile solvents *in vacuo* gave a residue which was recrystallized from ethanol to yield 3.05 g (71%) of the title compound as a yellowish powder. ^1H NMR (300 MHz, CDCl_3): $\delta = 3.90$ (s, 3 H, OMe), 6.97 (dd, $J = 8.6$ and 2.4 Hz, 1 H, Ar), 7.21 (d, $J = 2.4$ Hz, 1 H, Ar), 7.39 (d, $J = 8.6$, 1 H, Ar), 7.93 (m, 2 H, Ar), 8.30 (m, 2 H, Ar) ppm. ^{13}C NMR (100.7 MHz, CDCl_3): $\delta = 55.8(+)$, 113.4(+), 119.1(+), 121.5(-), 123.7(+), 130.8(+), 131.2(-), 131.7(+), 142.0(-), 150.3(-), 162.1(-), 193.8(-) ppm. HRMS (ESI): found 335.9863; calc for $\text{C}_{14}\text{H}_{10}\text{NO}_4\text{Br}$ $[\text{M} + \text{H}]^+$ 335.9866.



(4-Aminophenyl)(2-bromo-4-methoxyphenyl)methanone (401)

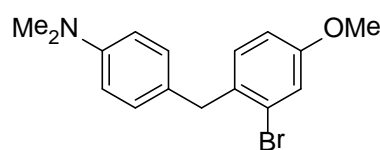
To 1.0 g (3.0 mmol) of compound **400** in a mixture of 1,2-dimethoxyethane and ethanol (9 and 11 mL, respectively), a solution of $\text{SnCl}_2 \cdot 2\text{H}_2\text{O}$ (2.64 g, 11.7 mmol) in conc. aq HCl (20 mL) was added at such a rate that the temperature did not exceed 30 °C. After stirring overnight at r.t., the reaction mixture was poured into an excess of ice–water and CH_2Cl_2 . Then the aqueous layer was neutralized to pH 12 with solid NaOH, the organic layer was separated, and the aqueous solution was extracted with CH_2Cl_2 (50 mL). The combined organic solutions were dried with Na_2SO_4 and evaporated *in vacuo* to give a residue which was purified by column chromatography (100 g SiO_2 , $\text{CH}_2\text{Cl}_2/\text{MeOH}$, 20:1) to furnish 758 mg (82%) of the title compound. ^1H NMR (300 MHz, CDCl_3): $\delta =$

3.85 (s, 3 H, OMe), 6.62 (m, 2 H, Ar), 6.89 (dd, $J = 8.5$ and 2.4 Hz, 1 H, Ar), 7.15 (d, $J = 2.4$ Hz, 1 H, Ar), 7.39 (d, $J = 8.5$ Hz, 1 H, Ar), 7.64 (m, 2 H, Ar) ppm. ^{13}C NMR (100.7 MHz, CDCl_3): $\delta = 55.6(+)$, $113.0(+)$, $113.9(+)$, $118.4(+)$, $120.7(-)$, $127.2(-)$, $130.3(+)$, $132.9(+)$, $133.6(-)$, $151.2(-)$, $160.7(-)$, $193.9(-)$ ppm. HRMS (ESI): found 306.0126; calc for $\text{C}_{14}\text{H}_{12}\text{NO}_2\text{Br}$ $[\text{M} + \text{H}]^+$ 306.0124.



2-(2-(4-(Dimethylamino)benzyl)-5-methoxyphenyl)-propan-2-ol (402)

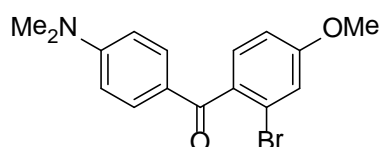
Into a Schlenk flask charged with a solution of compound **403** (516 mg, 1.6 mmol) in THF (10 mL), 2.2 M BuLi in hexanes (2.5 mL, 5.4 mmol) was added dropwise at -78 °C. After stirring for 40 min at -78 °C, acetone (1.30 g, 22.4 mmol) was slowly added, and the reaction mixture was allowed to warm up to r.t. An excess of sat. aq. NH_4Cl was added, and the mixture was extracted with EtOAc (3×50 mL). The combined organic solutions were dried with Na_2SO_4 and evaporated *in vacuo*. The title compound was isolated as a colorless oil (453 mg, 95%) by column chromatography (100 g SiO_2 , hexane/EtOAc, 2:1). ^1H NMR (300 MHz, CDCl_3): $\delta = 1.63$ (s, 6 H, CMe_2), 2.91 (s, 6 H, NMe_2), 3.81 (s, 3 H, OMe), 4.24 (s, 2 H, CH_2), 6.69 (m, 2 H, Ar), 6.73 (dd, $J = 8.5$ and 2.7 Hz, 1 H, Ar), 6.97 (m, 2 H, Ar), 7.05 (m, 2 H, Ar) ppm. ^{13}C NMR (125.7 MHz, CDCl_3): $\delta = 31.6(+)$, $37.9(-)$, $40.8(+)$, $55.2(+)$, $73.8(-)$, $111.3(+)$, $112.3(+)$, $113.0(+)$, $129.3(+)$, $130.9(-)$, $134.1(+)$, $147.5(-)$, $149.0(-)$, $157.6(-)$ ppm. HRMS (ESI): found 322.1778; calc for $\text{C}_{19}\text{H}_{25}\text{NO}_2$ $[\text{M} + \text{Na}]^+$ 322.1778.



4-(2-Bromo-4-methoxybenzyl)-N,N-dimethylaniline (403)

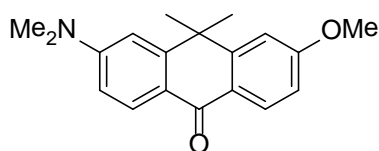
Compound **403** was prepared according to the published method.^[164] To a cooled (0 °C) solution of compound **4** (1.6 g, 4.8 mmol) in THF (45 mL), AlCl_3 (1.7 g, 13 mmol) was added in one portion, followed by NaBH_4 (890 mg, 23.5 mmol). The mixture was heated with reflux for 2 h, and then water (25 mL) was carefully added dropwise at 0 °C. The reaction mixture was extracted with CH_2Cl_2 (4×50 mL) and combined organic solutions were dried with Na_2SO_4 and evaporated *in vacuo*. Purification on SiO_2 (150 g;

hexane/EtOAc, 6:1) furnished 970 mg (65%) of the titled compound. ^1H NMR (300 MHz, CDCl_3): δ = 2.93 (s, 6 H, NMe_2), 3.78 (s, 3 H, OMe), 3.96 (s, 2 H, CH_2), 6.71 (m, 2 H, Ar), 6.78 (dd, J = 8.5 and 2.6 Hz, 1 H, Ar), 7.05 (m, 3 H, Ar), 7.12 (d, J = 2.6 Hz, 1 H, Ar) ppm. ^{13}C NMR (100.7 MHz, CDCl_3): δ = 39.8(-), 40.8(+), 55.5(+), 110.0(-), 113.0(+), 113.6(+), 117.8(+), 124.8(-), 129.5(+), 131.2(+), 133.3(-), 149.1(-), 158.3(-) ppm. HRMS (ESI): found 320.0648; calc for $\text{C}_{16}\text{H}_{18}\text{NOBr}$ $[\text{M} + \text{H}]^+$ 320.0645.



(2-Bromo-4-methoxyphenyl)(4-(dimethylamino)phenyl)-methanone (404)

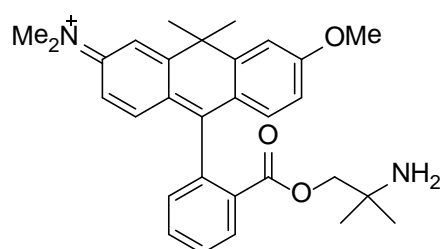
Compound **404** was prepared according to the known procedure.^[159] To a mixture of compound **401** (2.0 g, 6.5 mmol) and paraformaldehyde (1.96 g, 65 mmol) in AcOH (50 mL), NaBH_3CN (1.97 g, 31.3 mmol) was added in one portion at 0 °C. The reaction mixture was stirred overnight at r.t., and then an additional amount of NaBH_3CN (1.00 g, 15.9 mmol) was added. After stirring for 2 h at r.t., the reaction mixture was transferred into an excess of 15% NaOH with ice, pH was adjusted to 12 with solid NaOH, and the solution was extracted with CH_2Cl_2 (3 \times 100 mL). The combined organic solutions were dried with Na_2SO_4 and evaporated *in vacuo* to give 2.06 g (83%) of the title compound as a yellow oil. ^1H NMR (300 MHz, CDCl_3): δ = 3.08 (s, 6 H, NMe_2), 3.15 (s, 3 H, OMe), 6.64 (m, 2 H, Ar), 6.90 (dd, J = 8.5 and 2.4 Hz, 1 H, Ar), 7.16 (d, J = 2.4 Hz, 1 H, Ar), 7.26 (d, J = 8.5 Hz, 1 H, Ar), 7.71 (m, 2 H, Ar). ^{13}C NMR (100.7 MHz, CDCl_3): δ = 40.1(+), 55.6(+), 110.7(+), 113.0(+), 118.2(+), 120.6(-), 124.4(-), 130.1(+), 132.6(+), 134.0(-), 153.6(-), 160.6(-), 193.7(-). HRMS (ESI): found 320.0432; calc for $\text{C}_{16}\text{H}_{16}\text{NO}_2\text{Br}$ $[\text{M} + \text{H}]^+$ 334.0437.



3-(Dimethylamino)-6-methoxy-10,10-dimethylanthracen-9(10H)-one (405)

Cyclization of compound **402** to 1,2-dihydroanthracene derivative was performed according to the known method,^[165] and further oxidation to anthracenone **405** was carried out as described.^[156d] To a solution of compound **402** (100 mg, 0.33 mmol) in dry CH_2Cl_2 (4 mL), AlCl_3 (110 mg, 0.825 mmol) was added at 0 °C. The mixture was stirred for 6 h at 0 °C and for 10 h at r.t. After quenching with 1 M aq. NaOH (4 mL), the

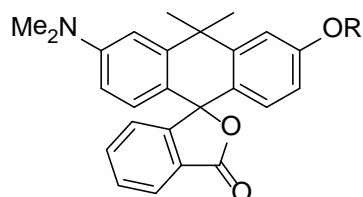
organic layer was separated and the aqueous solution was extracted with CH_2Cl_2 (3×10 mL). Combined organic solutions were dried with Na_2SO_4 and evaporated *in vacuo*. The residue was dissolved in acetone (4 mL), the solution was cooled down to -18 °C, and a powder of KMnO_4 (110 mg, 0.70 mmol) was added in small portions over 2 h. The reaction mixture was diluted with 2 volumes of CH_2Cl_2 ; MnO_2 was filtered off and washed with CH_2Cl_2 , and the filtrate was evaporated to dryness. The title compound was isolated by column chromatography (50 g SiO_2 ; hexane/EtOAc, 4:1) as a yellow solid (30 mg, 31%). ^1H NMR (300 MHz, CDCl_3): $\delta = 1.71$ (s, 6 H, CMe_2), 3.12 (s, 6 H, NMe_2), 3.91 (s, 3 H, OMe), 6.77 (m, 2 H, Ar), 6.95 (dd, $J = 2.5$ and 8.7 Hz, 1 H, Ar), 7.09 (d, $J = 2.5$ Hz, 1 H, Ar), 8.26 (d, $J = 8.40$ Hz, 1 H, Ar), 8.34 (d, $J = 8.7$ Hz, 1 H, Ar) ppm. ^{13}C NMR (125.7 MHz, CDCl_3): $\delta = 33.5(+)$, 38.2(-), 40.2(+), 55.4(+), 107.5(+), 110.9(+), 111.5(+), 112.2(+), 119.4(-), 124.3(-), 129.4(+), 129.5(+), 152.2(-), 152.5(-), 153.2(-), 162.9(-), 181.2(-) ppm. HRMS (ESI): found 296.1649; calc for $\text{C}_{19}\text{H}_{21}\text{NO}_2$ $[\text{M} + \text{H}]^+$ 296.1645.



***N*-(10-(2-((2-Amino-2-methylpropoxy)carbonyl)phenyl)-7-methoxy-9,9-dimethylanthracen-2(9*H*)-ylidene)-*N*-methyl methanaminium chloride (407)**

Into a Schlenk flask charged with a solution of 2-(2-bromophenyl)-4,4-dimethyl-4,5-dihydrooxazole (926 mg, 3.60 mmol) in THF (15 mL), 1.5 M *t*BuLi in pentane (2.6 mL, 3.9 mmol) was added dropwise at -78 °C to form the organolithium compound **406**. The mixture was stirred for 40 min at -78 °C, and a solution of ketone **405** (215 mg, 0.73 mmol) in THF (8 mL) was added dropwise. The reaction mixture was stirred at -78 °C for 1 h at r.t. and finally transferred into a cooled (0 °C) mixture of MeOH and AcOH (15 and 2 mL, respectively). The residue after complete evaporation of the reaction mixture was subjected to column chromatography (100 g SiO_2 , MeCN/ H_2O (both with 0.1% v/v TFA), 10:1 \rightarrow 10:1). Fractions containing the title compound were combined, evaporated *in vacuo*, and residue was dissolved in CH_2Cl_2 and washed with brine and sat. aq. NH_4Cl . Evaporation of CH_2Cl_2 gave 270 mg (73%) of the title compound. ^1H NMR (300 MHz, CDCl_3): $\delta = 1.36$ (s, 3 H, Me), 1.43 (s, 3 H, Me), 1.75 (s, 3 H, Me), 1.84 (s, 3 H, Me), 3.43 (s, 3 H, NMe), 3.53 (s, 3 H, NMe), 3.94 (s, 3 H, OMe), 4.05 (d, $J = 11.7$ Hz, 1 H),

4.22 (d, $J = 11.7$ Hz, 1 H), 5.82 (br. s, NH₂), 6.83 (m, 2 H, Ar), 7.17 (m, 2 H, Ar), 7.29 (d, $J = 2.4$ Hz, 1 H, Ar), 7.72 (m, 2 H, Ar), 8.69 (m, 1 H, Ar), 8.86 (m, 2 H, Ar) ppm. ¹³C NMR (75.5 MHz, CDCl₃): $\delta = 22.7(-)$, 22.8(+), 31.6(+), 31.9(-), 35.0(+), 41.9(+), 42.0(-), 53.3(-), 56.1(+), 69.7(-), 112.2(+), 113.6(+), 115.7(+), 122.7(-), 124.3(-), 129.5(-), 129.6(+), 130.4(+), 132.5(+), 132.6(+), 135.9(+), 136.8(-), 139.9(-), 154.3(-), 158.8(-), 160.1(-), 164.4(-), 166.0(-), 168.1(-) ppm. HRMS (ESI): found 471.2633; calc. for C₃₀H₃₅N₂O₃ [M⁺] 471.2642.



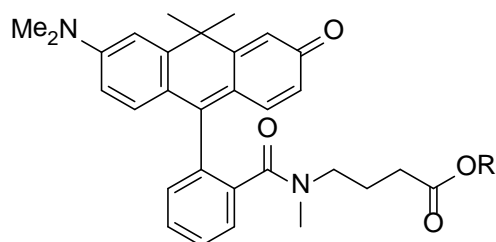
3-*N,N*-dimethylamino-6-methoxy-10,10-dimethyl-3'*H*,10*H*-spiro[anthracene-9,1'-isobenzofuran]-3'-one (408-Me) and 3-*N,N*-dimethylamino-6-hydroxy-10,10-dimethyl-3'*H*,10*H*-spiro[anthracene-9,1'-isobenzofuran]-3'-one (408-H)

A solution of compound **407** (200 mg, 0.40 mmol) in 20% aq HCl (30 mL) was stirred at 80 °C for 6.5 h. After cooling to r.t., the reaction mixture was neutralized with solid NaHCO₃ and extracted with CH₂Cl₂ (4 × 20 mL). Combined organic extracts were dried with Na₂SO₄ and evaporated. The residue was subjected to column chromatography (100 g SiO₂, hexane/EtOAc, 2:1) to furnish 68 mg (43%) of **408-Me** and 40 mg (26%) of **408-H** as colorless powders.

408-Me: ¹H NMR (300 MHz, CDCl₃): $\delta = 1.76$ (s, 3 H, Me), 1.87 (s, 3 H, Me), 2.99 (s, 6 H, NMe₂), 3.82 (s, 3 H, OMe), 6.50–6.65 (m, 2 H, Ar), 6.68 (m, 2 H, Ar), 6.92 (m, 1 H, Ar), 7.05 (m, 1 H, Ar), 7.15 (m, 1 H, Ar), 7.58 (m, 2 H, Ar), 8.00 (m, 1 H, Ar) ppm. ¹³C NMR (75.5 MHz, CDCl₃): $\delta = 32.4(+)$, 35.5(+), 38.6(-), 40.5(+), 55.3(+), 111.8(+), 112.3(+), 123.8(+), 124.4(-), 124.9(+), 126.9(-), 128.9(+), 129.3(+), 134.5(+), 146.4(-), 147.5(-), 155.3(-), 159.9(-), 170.6(-) ppm. HRMS (ESI): found 400.1898; calc. for C₂₆H₂₅NO₃ [M + H]⁺ 400.1907. Spectral data in MeOH with 0.1% v/v TFA: λ_{abs} , nm (ϵ , M⁻¹cm⁻¹) = 482 sh (10290), 513 (18250), 549 (18430), λ_{em} = 585 nm, Φ_{fl} = 0.01 (standard: RDC, Φ_{fl} = 0.33 in THF).

408-H: ¹H NMR (600 MHz, CDCl₃): $\delta = 1.56$ (s, 3 H, Me), 1.73 (s, 3 H, Me), 3.17 (s, 6 H, NMe₂), 6.64 (m, 2 H, Ar), 6.88 (m, 1 H, Ar), 7.03 (m, 2 H, Ar), 7.12 (m, 1 H, Ar), 7.61 (m, 2 H, Ar), 7.68 (m, 1 H, Ar), 8.05 (m, 1 H, Ar). HRMS (ESI): found 386.1747, calc. for C₂₅H₂₃NO₃ [M + H]⁺ 386.1751. Spectral data in MeOH: λ_{abs} (ϵ , M⁻¹cm⁻¹) = 561 (620),

$\lambda_{em} = 598$ nm, $\Phi_{fl} = 0.85$ (standard: rhodamine 630, $\Phi_{fl} = 0.97$ in ethanol). Low absorption in the visible range is explained by the fact that under neutral conditions, the equilibrium between the colorless “closed” form and the colored “open” form is shifted toward the former one (Scheme 28a). Spectral data in MeOH with 0.1% v/v TFA: λ_{abs} , nm (ϵ , $M^{-1}cm^{-1}$) = 483 sh (13500), 515(30000), 553 (37400), $\lambda_{em} = 585$ nm (broad), $\Phi_{fl} = 0.11$ (standard: perylene diimide KP174, $\Phi_{fl} = 0.58$ in water). Spectral data in MeOH with 0.1% v/v Et_3N : λ_{abs} , nm (ϵ , $M^{-1}cm^{-1}$) = 560 (34300), $\lambda_{em} = 598$ nm, $\Phi_{fl} = 0.94$ (standard: perylene diimide KP174, $\Phi_{fl} = 0.58$ in water).



Methyl 4-(2-(6-*N,N*-Dimethylamino-10,10-dimethyl-3-oxo-3,10-dihydroanthracen-9-yl)-*N'*-methylbenzamido)butanoate (409-Me) and 4-(2-(6-*N,N*-dimethylamino)-10,10-dimethyl-3-oxo-3,10-dihydroanthracen-9-yl)-*N'*-methylbenzamido)butanoic acid (409-H)

Into a Schlenk flask charged with a solution of compound **410** (36 mg, 0.065 mmol) in CH_2Cl_2 (5 mL), 1 M solution of BBr_3 in CH_2Cl_2 (400 μ L, 0.4 mmol) was added dropwise at r.t. The reaction mixture was stirred for 1 h and quenched with sat. aq. $NaHCO_3$ (15 mL). The organic layer was separated, and the aqueous phase was saturated with NH_4Cl and extracted with CH_2Cl_2 (5 \times 30 mL). Combined organic solutions were dried with Na_2SO_4 and evaporated. Column chromatography (40 g SiO_2 , $CH_2Cl_2/MeOH$, 20:1, then $MeCN/H_2O$, 5:1) afforded 16 mg (49%) of **409-Me** and 11 mg (23%) of **409-H** as dark-violet solids.

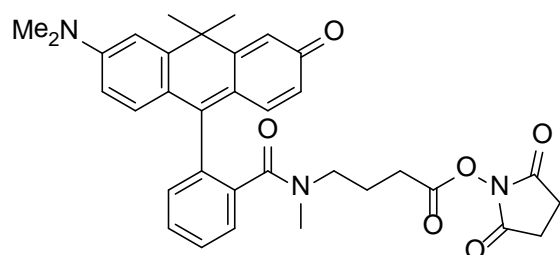
409-Me was an ~1:2.5 mixture of 2 diastereomers. 1H NMR (300 MHz, CD_3CN , only the signals of the major isomer are given): $\delta = 1.46$ (m, 2 H, CH_2), 1.55 (s, 3 H, Me), 1.68 (s, 3 H, Me), 1.86–1.94 (m, 2 H, CH_2), 2.78 (s, 3 H, NMe), 3.09 (s, 6 H, NMe_2), 3.10–3.32 (m, 2 H, NCH_2), 3.53 (s, 3 H, COOMe), 6.17 (dd, $J = 9.6$ and 2.0 Hz, 1 H, Ar), 6.55 (dd, $J = 9.1$ and 2.6 Hz, 1 H, Ar), 6.66 (m, $J = 2.0$ Hz, 1 H, Ar), 6.81 (m, $J = 9.1$ Hz, 1 H, Ar), 6.92 (m, $J = 9.6$ Hz, 1 H, Ar), 6.97 (m, $J = 2.6$ Hz, 1 H, Ar), 7.31 (m, 1 H, Ar), 7.45 (m, 1 H, Ar), 7.56 (m, 2 H, Ar) ppm. ^{13}C NMR (75.5 MHz, CD_3CN): $\delta = 22.6(-)$, 31.4(-), 31.8(+), 35.5(+), 37.6(+), 40.5(+), 40.9(-), 46.5(-), 51.8(+), 110.4(+), 111.3(+), 120.6(-),

120.9(-), 121.9(-), 123.5(+), 124.9(+), 127.6(+), 129.1(+), 129.5(+), 131.4(+), 134.8(+), 136.1(-), 137.7(-), 139.0(+), 152.1(-), 154.2(-), 157.2(-), 169.4(-), 174.1(-), 184.2(-) ppm. HRMS (ESI): found 499.2592; calc. for $C_{31}H_{35}N_2O_4$ [M^+] 499.2591. Lifetime of the excited state (τ): 2.2 ns (aq. PBS buffer).

409-H was an ~1:2.5 mixture of two diastereomers, 1H NMR (300 MHz, CD_3CN , only signals of the major isomer are given): δ = 1.38 (m, 1 H, CH_2), 1.43–1.57 (m, 1 H, CH_2), 1.53 (s, 3 H, Me), 1.66 (s, 3 H, Me), 1.83 (m, 1 H, CH_2COOMe), 1.93–2.00 (m, 1 H, CH_2COOMe), 3.09 (s, 3 H, NMe), 3.09–3.23 (m, 2 H, NCH_2), 3.27 (s, 6 H, NMe_2), 6.23 (dd, J = 9.6 and 2.1 Hz, 1 H, Ar), 6.55 (dd, J = 9.1 and 2.6 Hz, 1 H, Ar), 6.72 (m, 1 H, Ar), 6.81 (m, J = 9.1 Hz, 1 H, Ar), 6.95–6.99 (m, 2 H, Ar), 7.30 (m, 1 H, Ar), 7.45 (m, 1 H, Ar), 7.56 (m, 2 H, Ar). ^{13}C NMR (75.5 MHz, CD_3CN): δ = 23.0(-), 32.0(+), 32.7(-), 35.8(+), 37.9(+), 40.5(+), 47.1(-), 110.4(+), 111.5(+), 120.4(-), 121.5(-), 123.1(+), 124.5(+), 127.8(+), 129.5(+), 129.7(+), 131.4(+), 135.5(+), 135.6(-), 137.3(-), 140.0(+), 153.3(-), 154.6(-), 158.6(-), 170.1(-), 185.7(-) ppm. HRMS (ESI): found 485.2433; calc for $C_{30}H_{32}N_2O_4$ [$M + H$] $^+$ 485.2435.

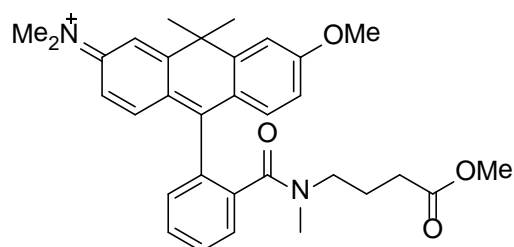
Preparation of 409-H from 409-Me

Compound **409-Me** (4 mg; 8 μ mol) was stirred for 1 h at r.t. in a 10:15:0.7 mixture of H_2O , THF, and 1 M aq. NaOH (2.5 mL). Then AcOH (1 mL) was added, and the reaction mixture was evaporated to dryness. Purification by flash chromatography (15 g SiO_2 , MeCN/ H_2O , 5:1) followed by evaporation, dissolution in CH_2Cl_2 , and filtration through a fine glass filter afforded 4 mg (quantitative yield) of the solid title compound. HPLC: B/A = 30/70 to 100/0 in 25 min, detection at 550 nm, t_R = 7.6 min (100%). Data in methanol: λ_{abs} (ϵ , $M^{-1}cm^{-1}$) = 573 nm (41000), λ_{em} = 613 nm, Φ_{fl} = 0.64, τ = 3.95 ns. Excitation spectrum in methanol: emission at 625 nm was monitored and found to be maximal at λ_{excit} = 588 nm. Data in PBS buffer at pH 7.4: λ_{abs} = 586 nm; ϵ = 58600 $M^{-1} cm^{-1}$, λ_{em} = 613 nm, Φ_{fl} = 0.32 (standard: perylene diimide, Φ_{fl} = 0.58 in H_2O), τ = 2.54 ns.



2,5-Dioxopyrrolidin-1-yl 4-(2-(6-*N,N*-dimethylamino)-10,10-dimethyl-3-oxo-3,10-dihydro-anthracen-9-yl)-*N'*-methyl benzamido)butanoate (409-NHS)

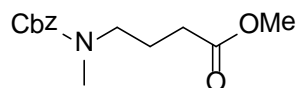
To a stirred solution of compound **409**-H (3 mg, 6.2 μmol) and *N*-hydroxysuccinimide (11 mg, 93 μmol) in MeCN/DMF mixture (2:1, 2 mL), HATU (10 mg, 25 μmol) was added followed by NEt_3 (16 μL , 112 μmol). The reaction mixture was stirred overnight and evaporated *in vacuo*. The residue was subjected to flash chromatography on SiO_2 (20 g, MeCN/ H_2O , 10:1). The main fraction was filtered through a fine glass filter and freeze-dried to give 3.1 mg (86%) of the title compound. HPLC: B/A = 30/70 to 100/0 in 25 min, detection at 550 nm, t_R = 9.7 min (100%). HRMS (ESI): found 582.2605; calc for $\text{C}_{34}\text{H}_{35}\text{N}_3\text{O}_6$ $[\text{M} + \text{H}]^+$ 582.2599. The conjugate with goat antirabbit antibodies (AB256): λ_{abs} = 585 nm, λ_{em} = 613 nm, DOL = 10.9, Φ_{fl} = 0.04 in PBS buffer at pH 7.4 (standard: rhodamine 101, Φ_{fl} = 1 in EtOH). The conjugate with goat antirabbit antibodies (AB257): λ_{abs} = 586 nm, λ_{em} = 614 nm, DOL = 12.4, Φ_{fl} = 0.04 in PBS buffer at pH 7.4 (standard: perylene diimide KP174, Φ_{fl} = 0.58 in H_2O , excitation at 550 nm).



***N*-(7-Methoxy-10-(2-(*N*'-(4-methoxy-4-oxobutyl)-*N*'-methylcarbamoyl)phenyl)-9,9-dimethylanthracen-2(9*H*)-ylidene)-*N*-methylmethanaminium (410)**

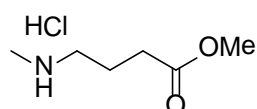
Into a Schlenk flask charged with a solution of compound **408**-Me (34 mg, 0.085 mmol) in dichloroethane (3 mL), POCl_3 (390 μL , 4.3 mmol) was injected. After stirring at 80 $^\circ\text{C}$ for 2 h, all volatile materials were evaporated *in vacuo* and the solid residue was dissolved in CH_3CN (5 mL). A solution of methyl 4-*N*-methylaminobutyrate hydrochloride (**413**) (71 mg, 0.425 mmol) in MeCN (3 mL) was added into the flask, followed by NEt_3 (360 μL , 2.5 mmol). After stirring at r.t. for 15 min, all volatile materials were removed *in vacuo*, and the residue was dissolved in CH_2Cl_2 (20 mL) and washed with a satd aq solution of NH_4Cl . The organic layer was separated, dried with Na_2SO_4 , and evaporated. The titled compound (36 mg, 76%) was isolated by column chromatography (40 g SiO_2 , MeCN/ H_2O , 15:1) as a red solid. ^1H NMR (300 MHz, CD_3CN): δ = 1.34 (m, 2 H, CH_2), 1.65 (s, 3 H, Me), 1.72–1.82 (m, 2 H, CH_2), 1.80 (s, 3 H, Me), 2.86 (s, 3 H, NMe), 3.11–3.23 (m, 2 H, NCH_2), 3.44 (s, 6 H, NMe_2), 3.53 (s, 3 H, COOMe), 3.94 (s, 3 H, OMe), 6.93 (m, 2 H, Ar), 7.17–7.24 (m, 2 H, Ar), 7.27 (m, 1 H, Ar), 7.39 (m, 1 H, Ar), 7.41 (m, 1 H, Ar), 7.56 (m, 1 H, Ar), 7.66 (m, 2 H, Ar) ppm. ^{13}C NMR (75.5 MHz, CD_3CN): δ =

22.5(-), 31.4 (-), 32.0(+), 35.0(+), 37.6(+), 42.6(+), 42.8(-), 46.7(-), 51.9(+), 57.0(+), 114.4(+), 114.5(+), 115.8(-), 116.5(+), 123.5(-), 124.2(-), 125.1(-), 128.0(+), 130.0(+), 130.2(+), 130.5(+), 131.1(+), 135.0(-), 137.0(+), 137.4(-), 141.3(+), 155.2(-), 160.0(-), 160.8(-), 166.8(-), 174.1(-) ppm. HRMS (ESI): found 513.2740; calc. for C₃₂H₃₇N₂O₄ [M⁺] 513.2748.



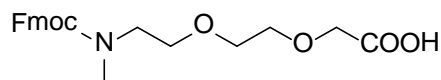
Methyl 4-(*N*-benzyloxycarbonyl-*N*-methylamino)butanoate (412)

Methylation of *N*-protected butyric acid **411** was performed according to the known procedure.^[176] To a solution of compound **411** (4.1 g, 17.4 mmol) in dry DMF (50 mL) MeI (13 mL, 209 mmol) and Ag₂O (24.2 g, 104 mmol) were added under cooling. The resulting mixture was stirred overnight at r.t. Afterwards, the reaction mixture was filtered through a pad of Celite eluting with CH₂Cl₂ (~300 mL). The filtrate was washed with 20% Na₂S₂O₃ (2×100 mL) and water (10 × 100 mL) dried with Na 100 mL) dried with Na₂SO₄ and evaporated *in vacuo*. The crude product (4.5 g, 98%) was used without further purification. ¹H NMR (300 MHz, CDCl₃): δ = 1.77–1.93 (m, 2 H, CH₂), 2.23–2.38 (m, 2 H, CH₂), 2.92 (s, 3 H, NMe), 3.33 (t, *J* = 7.0 Hz, 2 H, NCH₂), 3.64 (m, 3 H, COOMe), 5.11 (s, 2 H, CH₂), 7.22–7.42 (m, 5 H, Ar) ppm. MS (ESI): *m/z* = 288 (100) [M+Na]⁺.



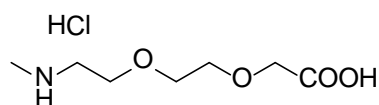
Methyl 4-*N*-methylaminobutanoate hydrochloride (413)

A dry 100 mL Schlenk flask was charged with Pd/C (200 mg, 0.19 mmol, 5 mol%) and EtOH (5 mL). The flask was purged with H₂, and a solution of compound **412** (1 g, 3.77 mmol) in EtOH (20 mL) mixed with 5 M HCl in *i*PrOH (1 mL) was added. The resulting suspension was stirred for 3 h at r.t. under slow flow of hydrogen. Afterwards, the reaction mixture was filtered through a plug of Celite eluting with CH₂Cl₂ (~100 mL). Evaporation of the filtrate gave an oil which was recrystallized from *n*-hexane/Et₂O to afford 450 mg (77%) of a white hygroscopic solid. ¹H NMR (300 MHz, CD₃OD): δ = 1.90–2.02 (m, 2 H, CH₂), 2.49 (t, *J* = 7.1 Hz, 2 H, CH₂), 2.70 (s, 3 H, NMe), 3.04 (m, 2 H, CH₂), 3.68 (s, 3 H, COOMe) ppm.



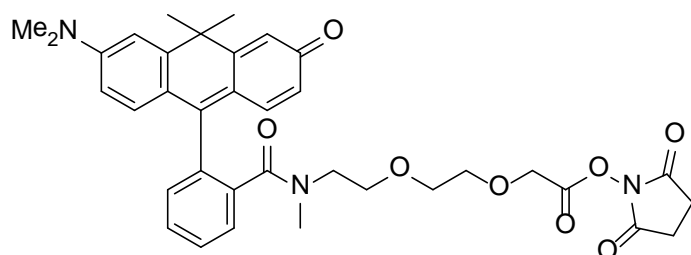
2-(2-(2-*N*-((9*H*-Fluoren-9-ylmethoxy)carbonyl)-*N*-methylaminoethoxy)ethoxy)acetic acid (415-Fmoc)

Methylation of *N*-protected amino acid **414** was carried out according to the known procedure.^[166] A mixture of compound **414** (100 mg, 0.26 mmol), TFA (1.6 mL), CHCl₃ (1.6 mL) and formaline (37%, 0.25 mL) was stirred for 30 min at r.t. Afterwards, triethylsilane (0.6 mL, 5.2 mmol) was added carefully with cooling. The resulting mixture was stirred for 30 min at r.t., and then all volatiles were evaporated *in vacuo*. The residue was subjected to column chromatography (50 g of SiO₂, CH₂Cl₂/MeOH, 5:1 → 3:1) to furnish 100 mg (96%) of the title compound. ¹H NMR (300 MHz, CD₃OD): δ = 2.81 (s, 3 H, NMe), 3.39–3.49 (m, 2 H, CH₂), 3.50–3.55 (m, 2 H, CH₂), 3.55–3.62 (m, 4 H, 2 × CH₂), 3.92 (s, 2 H, CH₂), 4.12 (s, 2 H, CH₂), 7.25–7.31 (m, 2H, Ar), 7.34–7.40 (m, 2H, Ar), 7.49 (d, *J* = 7.4 Hz, 2 H, Ar), 7.79 (d, *J* = 7.5 Hz, 2 H, Ar) ppm. MS (ESI): *m/z* = 422 (100) [M+Na]⁺.



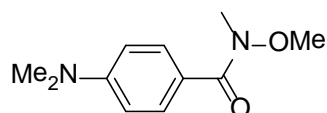
2-(2-(2-*N*-Methylaminoethoxy)ethoxy)acetic acid hydrochloride (415-H·HCl)

Compound **415-Fmoc** (50 mg; 0.125 mmol) was dissolved in a 30% solution of piperidine in DMF (2 ml). The resulting mixture was stirred for 30 min at r.t., and then, all volatiles were evaporated *in vacuo*. The residue was dissolved in diluted aq. HCl (20 ml), and this solution was extracted with Et₂O (3×20 mL). The aq. phase was evaporated, and the residue was subjected to column chromatography (25 g of SiO₂, CHCl₃/MeOH/H₂O/HCOOH, 75:25:5:1) to furnish 20 mg (74%) of the title compound. ¹H NMR (300 MHz, CD₃OD): δ = 2.38 (s, 3 H, NMe), 2.71–2.76 (m, 2 H, CH₂), 3.55–3.60 (m, 2 H, CH₂), 3.63 (s, 4 H, 2×CH₂), 3.87 (s, 2 H, CH₂), 8.52 (s, 1 H, NH) ppm. ¹³C NMR (75.5 MHz, CD₃OD): δ = 34.4(+), 50.1(-), 68.9(-), 69.3(-), 69.5(-), 70.2(-), 176.3(-) ppm. MS (ESI): *m/z* (positive mode, rel. int., %) = 178 (100) [M+H]⁺.



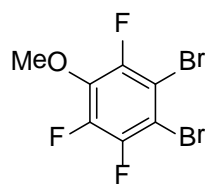
2,5-Dioxopyrrolidin-1-yl 2-(2-(2-(2-(6-*N,N*-Dimethylamino)-10,10-dimethyl-3-oxo-3,10-dihydroanthracen-9-yl)-*N'*-methylbenzamido)ethoxy)ethoxy)acetate (416-NHS)

To a stirred solution of compound **416-H** (3 mg, 5.5 μmol) and *N*-hydroxysuccinimide (0.8 mg, 6.6 μmol) in MeCN (1 mL), HATU (3.1 mg, 8.2 μmol) was added followed by NEt_3 (5 μL , 33 μmol). The reaction mixture was stirred overnight and then, evaporated *in vacuo*. The residue was subjected to flash chromatography on SiO_2 (5 g, MeCN/ H_2O , 10:1). The main fraction was filtered through a fine glass filter and freeze-dried to give 1.6 mg (45%) of the title compound. HPLC: B/A = 30/70 to 100/0 in 25 min, detection at 550 nm, t_R = 9.6 min (45%). MS (ESI): m/z (positive mode, rel. int., %) = 642 (100) $[\text{M}+\text{Na}]^+$.



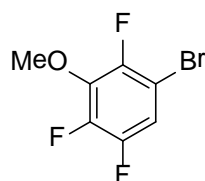
4-*N,N*-Dimethylamino-*N'*-methoxy-*N'*-methylbenzamide (418)

Compound **418** was prepared according to the known procedure:^[177] To a suspension of 4-*N,N*-dimethylaminobenzoic acid (1000 mg, 6 mmol) in CH_2Cl_2 (30 mL) triphosgene (891 mg, 3 mmol) and NEt_3 (4.3 mL, 30 mmol) were added at 0 °C under Ar. To the resulting blue solution, *N,O*-dimethylhydroxylamine hydrochloride (588 mg, 6 mmol) was added. The reaction mixture changed its color from blue to yellow, and a precipitate of $\text{NEt}_3\cdot\text{HCl}$ formed. The reaction mixture was allowed to warm up to r.t., and then was stirred for 3 h. The precipitate was filtered off, and the filtrate was shaken with water (20 mL). The organic layer was separated, and the aq. layer was extracted with CH_2Cl_2 (3 \times 20 mL). Combined organic solutions were dried with Na_2SO_4 and evaporated. The residue was subjected to column chromatography (30 g of SiO_2 , *n*-hexane/EtOAc, 2:3) to yield 1228 mg (98%) of the title compound. ^1H NMR (300 MHz, CDCl_3): δ = 3.02 (s, 6 H, NMe_2), 3.35 (s, 3 H, NMe), 3.59 (s, 3 H, OMe), 6.60–6.71 (m, 2 H, Ar), 7.66–7.77 (m, 2 H, Ar) ppm. MS (ESI): m/z (positive mode, rel. int., %) = 209 (41) $[\text{M}+\text{H}]^+$, 231 (100) $[\text{M}+\text{Na}]^+$.



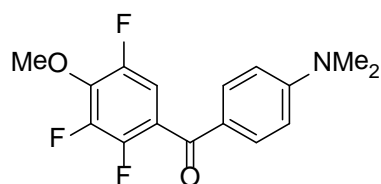
1,2-Dibromo-3,4,6-trifluoro-5-methoxybenzene (420)

Na (336 mg, 14.6 mmol) was dissolved in MeOH (30 mL) carefully, and to the resulting solution, 1,2-dibromo-3,4,5,6-tetrafluorobenzene (4000 mg, 13.3 mmol) was added. The reaction mixture was refluxed for 6 h, cooled down to r.t., and then, poured in water (100 mL). The resulting slurry was extracted with Et₂O (3×70 mL). Combined organic solutions were dried with Na₂SO₄ and evaporated *in vacuo* to give 4240 mg (99%) of the crude product which was used without further purification. ¹H NMR (300 MHz, CDCl₃): δ = 4.04 (m, 3 H, OMe) ppm. ¹⁹F NMR (282.2 MHz, CDCl₃): δ = -149.26 (dd, *J* = 21.9 and 5.4 Hz, 1 F), -126.52 (dd, *J* = 21.6 and 8.2 Hz, 1 F), -119.28 (m, 1 F) ppm.



1-Bromo-2,4,5-trifluoro-3-methoxybenzene (421)

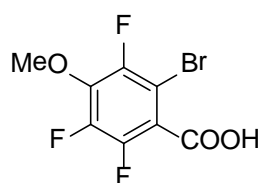
Compound **421** was prepared according to the known procedure:^[168b] In a 50 mL Schlenk flask to a solution of compound **420** (2000 mg, 6.25 mmol) in Et₂O (20 mL), 1.6 M solution of BuLi in hexanes (4.5 mL, 7.18 mmol) was injected carefully at -78 °C. After 4 h stirring at this temperature, the reaction mixture was quenched with 50% aq. EtOH (20 mL). The organic layer was separated, and the aq. layer was extracted with Et₂O (2×50 mL). Combined organic solutions were dried with Na₂SO₄ and evaporated. The residue was purified by column chromatography (70 g of SiO₂, *n*-hexane) to yield 855 mg (57%) of a colorless oil. ¹H NMR (300 MHz, CDCl₃): δ = 4.03 (m, 3 H, OMe), 7.04–7.13 (m, 1 H, Ar) ppm. ¹⁹F NMR (282.2 MHz, CDCl₃): δ = -151.31 (m, 1 F), -139.63 (m, 1 F), -125.67 (m, 1 F) ppm.



(4-*N,N*-dimethylaminophenyl)(2,3,5-trifluoro-4-methoxyphenyl)methanone (422)

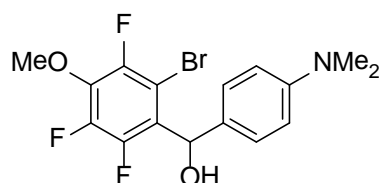
To a solution of compound **420** (1000 mg, 3.12 mmol) in THF (10 mL), 1.6 M solution of BuLi in hexanes (2.25 mL, 3.6 mmol) was injected at -78 °C. After 30 min stirring, a solution of compound **418** (844 mg, 4.07 mmol) in THF (5 mL) was added, the resulting solution was stirred for 30 min at -78 °C, for 10 min at 0 °C, and then, quenched with sat. aq. NH₄Cl (5 mL). The organic layer was separated, and the aq. layer was extracted with

EtOAc (3×20). Combined organic solutions were dried with Na₂SO₄ and evaporated. The crude product was purified by column chromatography (100 g of SiO₂, *n*-hexane/EtOAc, 4:1) to furnish 270 mg (28%) as a yellow oil. ¹H NMR (300 MHz, CDCl₃): δ = 3.07 (s, 6 H, NMe₂), 4.09 (m, 3 H, OMe), 6.61–6.67 (m, 2 H, Ar), 7.03 (ddd, *J* = 10.7, 5.6 and 2.4 Hz, 1 H, Ar) 7.69–7.73 (m, 2 H, Ar) ppm. ¹⁹F NMR (282.2 MHz, CDCl₃): δ = –150.62 (m, 1 F), –139.33 (m, 1 F), –132.96 (m, 1 F) ppm. ¹³C NMR (125.7 MHz, CDCl₃): δ = 40.0(+), 61.9(+, t, *J* = 4 Hz), 110.6(+), 111.2(+, dt, *J* = 22 and 4 Hz), 122.4(–, d, *J* = 15 Hz), 124.0(–), 132.3(+), 139.1(–, m), 143.9(–, ddd, *J* = 251, 16 and 6 Hz), 145.1(–, ddd, *J* = 249, 12 and 3 Hz), 150.6(–, dt, *J* = 246 and 3 Hz), 153.8(–), 187.8(–) ppm. HRMS (ESI): found 310.1044; calc. for C₁₆H₁₄NO₂F₃ [M+H]⁺ 310.1049.



2-Bromo-3,5,6-trifluoro-4-methoxybenzoic acid (423)

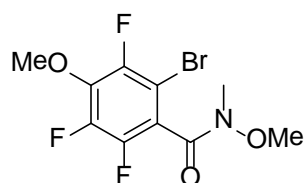
To a solution of compound **420** (100 mg, 0.31 mmol) in Et₂O (1 mL), 1.6 M solution of BuLi in hexanes (193 μL, 0.31 mmol) was injected over 7 min at –78 °C. After 30 min stirring at this temperature, an excess of solid CO₂ was added. The reaction mixture was allowed to reach r.t., and 1 M HCl was added (0.5 mL). The resulting slurry was extracted with CH₂Cl₂ (3×5 mL). Combined organic solutions were dried with Na₂SO₄ and evaporated *in vacuo*. The crude product was subjected to column chromatography (15 g of SiO₂, CH₂Cl₂/MeOH, 4:1) to afford 71 mg (81%) of the title product. ¹H NMR (300 MHz, CDCl₃): δ = 4.12 (m, 3 H, OMe) ppm. ¹⁹F NMR (282.2 MHz, CDCl₃): δ = –150.3 (m, 1 F), –137.7 (m, 1 F), –122.1 (m, 1 F) ppm. MS (ESI): *m/z* (negative mode, rel. int., %) = 239 (100) [M–COOH, ⁷⁹Br][–], 241 (96) [M–COOH, ⁸¹Br][–].



(2-Bromo-3,5,6-trifluoro-4-methoxyphenyl)(4-*N,N*-dimethylaminophenyl)methanol (424)

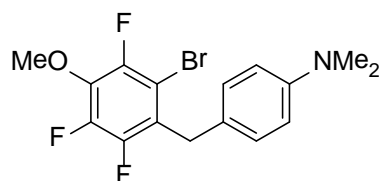
To a solution of compound **420** (320 mg, 1 mmol) in THF (3 mL), 1.6 M BuLi in hexanes was added dropwise at –78 °C. After 30 min stirring at this temperature, a solution of 4-

N,N-dimethylaminobenzaldehyde in Et₂O (5 mL) was injected. The resulted mixture was stirred for 30 min at -78 °C and then, allowed to warm to r.t. Afterwards, sat. aq. NH₄Cl (2 mL), water (5 mL) and CH₂Cl₂ (5 mL) were added. The organic layer was separated, and the aq. layer was extracted with CH₂Cl₂ (3×10 mL). Combined organic solutions were dried with Na₂SO₄ and evaporated. The crude product was purified by column chromatography (30 g of SiO₂, *n*-hexane/EtOAc, 2:1) to furnish 336 mg (86%) of a yellow oil. ¹H NMR (300 MHz, CDCl₃): δ = 2.73 (dd, *J* = 8.9 and 2.9 Hz, 1 H), 2.93 (s, 6 H, NMe₂), 4.03 (t, *J* = 1.2 Hz, 3 H, OMe), 6.24 (br. d, *J* = 8.6 Hz, 1 H, OH), 6.65–6.70 (m, 2 H, Ar), 7.20 (m, 2 H, Ar) ppm. ¹⁹F NMR (282.2 MHz, CDCl₃): δ = -151.15 (dd, *J* = 20.2 and 5.5 Hz, 1 F), -142.06 (dd, *J* = 20.1 and 9.3 Hz, 1 F), -122.97 (m, 1 F) ppm. MS (ESI): *m/z* (positive mode, rel. int., %) = 390 (100) [M+H, ⁷⁹Br]⁺, 392 (91) [M+H, ⁸¹Br]⁺.



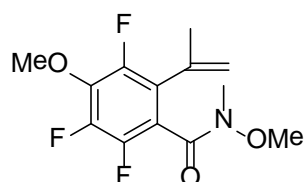
2-Bromo-3,5,6-trifluoro-*N*,4-dimethoxy-*N*-methylbenzamide (425)

To a suspension of compound **423** (1000 mg, 3.5 mmol) in CH₂Cl₂ (30 mL) triphosgene (727 mg, 2.45 mmol) and NEt₃ (2.5 mL, 17.5 mmol) were added at 0 °C under Ar. To the resulting solution, *N,O*-dimethylhydroxylamine hydrochloride (378 mg, 3.8 mmol) was added. The reaction mixture was allowed to warm up to r.t., and then was stirred for 1.5 h. The precipitate of NEt₃·HCl was filtered off, and the filtrate was shaken with water (20 mL). The organic layer was separated, and the aq. layer was extracted with CH₂Cl₂ (3×20 mL). Combined organic solutions were dried with Na₂SO₄ and evaporated. The residue was subjected to column chromatography (30 g of SiO₂, *n*-hexane/EtOAc, 3:1) to yield 741 mg (65%) of the title compound. ¹H NMR (300 MHz, CDCl₃): δ = 3.38 (s, 3 H, NMe), 3.55 (s, 3 H, OMe), 4.06 (t, *J* = 1.3 Hz, 3 H, OMe) ppm. ¹⁹F NMR (282.2 MHz, CDCl₃): δ = -150.61 (ddd, *J* = 21.6, 6.5 and 1.3 Hz, 1 F), -140.60 (dd, *J* = 21.6 and 10.2 Hz, 1 F), -124.10 (ddd, *J* = 10.0, 6.5 and 1.3 Hz, 1 F) ppm. HRMS (ESI): found 327.9792; calc. for C₁₀H₉NO₃F₃Br [M+H]⁺ 327.9791.



4-(2-Bromo-3,5,6-trifluoro-4-methoxybenzyl)-*N,N*-dimethylaniline (426)

Compound **424** (200 mg, 0.51 mmol) was dissolved in a CH₂Cl₂/TFA mixture (2:5, 7 ml), and to the resulting solution, Et₃SiH (1.5 mL, ~9.8 mmol) was added. The reaction mixture was stirred overnight at r.t. and 7 h at 40 °C. Afterwards, all volatiles were evaporated, the residue was dissolved in CH₂Cl₂ (~10 mL), the resulting solution was washed with sat. aq. NaHCO₃, dried with Na₂SO₄, and evaporated to dryness. The crude product was purified by column chromatography (30 g of SiO₂, *n*-hexane/Et₂O, 10:1) to furnish 187 mg (97%) of the title compound. ¹H NMR (300 MHz, CDCl₃): δ = 2.91 (s, 6 H, NMe₂), 4.01 (t, *J* = 1.1 Hz, 3 H, OMe), 4.07 (d, *J* = 2.8 Hz, 2 H, CH₂), 6.64–6.68 (m, 2 H, Ar), 7.12–7.17 (m, 2 H, Ar) ppm. ¹⁹F NMR (282.2 MHz, CDCl₃): δ = -151.98 (dd, *J* = 20.9 and 4.8 Hz, 1 F), -140.63 (ddt, *J* = 20.6, 10.2 and 2.7 Hz, 1 F), -123.29 (dd, *J* = 10.2 and 4.7 Hz, 1 F) ppm. MS (ESI): *m/z* (positive mode, rel. int., %) = 374 (100) [M+H, ⁷⁹Br]⁺, 376 (94) [M+H, ⁸¹Br]⁺.



2,3,5-Trifluoro-*N*,4-dimethoxy-*N*-methyl-6-(prop-1-en-2-yl)benzamide (427)

In a screw-cap tube compound **297** (200 mg, 0.6 mmol), isopropenylboronic acid (62 mg, 0.72 mmol), Pd(PPh₃)₄ (35 mg, 0.03 mmol, 5 mol%), 2 M Na₂CO₃ (1.2 mL, 2.4 mmol), EtOH (1.2 mL) and toluene (2 mL) were placed under argon. The mixture was heated to 110 °C and left overnight at this temperature with stirring. Afterwards, the reaction mixture was allowed to cool to r.t., diluted with CH₂Cl₂ (10 mL), passed through a plug of Celite (eluting with CH₂Cl₂), and the filtrate was evaporated *in vacuo*. Column chromatography (30 g of SiO₂, *n*-hexane/EtOAc, 4:1) furnished the title product as a yellow oil (110 mg, 64%). ¹H NMR (300 MHz, CDCl₃): δ = 2.03 (s, 3 H, Me), 3.27 (s, 3 H, NMe), 3.55 (s, 3 H, OMe), 4.04 (t, *J* = 1.3 Hz, 3 H, OMe), 4.98 (s, 1 H), 5.22 (m, 1H) ppm. ¹⁹F NMR (282.2 MHz, CDCl₃): δ = -152.83 (m, 1 F), -143.26 (dd, *J* = 21.7 and 12.3 Hz, 1 F), -134.81 (dd, *J* = 12.2 and 5.6 Hz, 1 F) ppm. HRMS (ESI): found 290.1002; calc. for C₁₃H₁₄F₃NO₃ [M+H]⁺ 290.0999.

Acknowledgments

Success of my doctoral project would have been impossible without inspiration, support and guidance from many people.

I would like to express my deepest gratitude to Prof. Stefan Hell who provided me an excellent opportunity to pursue my doctoral studies in a competitive and interdisciplinary environment of Department of NanoBiophotonics at MPI BPC. I am very thankful to Prof. Armin de Meijere for his careful reading of my yearly progress reports, giving me important feedback and his help in thesis preparation. A very special thanks goes to Dr. Vladimir N. Belov for suggesting the interesting topic of my doctoral studies, his great supervision and encouragement throughout the whole time of my stay at MPI BPC.

I would like to extend my thanks to all members of Organic Synthesis group in the NanoBiophotonics department for the wonderful working atmosphere, support and critical discussions. In particular, I am very thankful to Dr. Kirill Kolmakov and Dr. Shamil Nizamov for sharing their knowledge and rich experience in the synthesis of organic fluorophores. I am especially grateful to Dr. Heiko Schill for his readiness in teaching me how to work with absorption and fluorescence spectrometers and also for writing an Origin script that saved an enormous amount of time on data processing. A separate thanks goes to Dr. Matthias Bischoff who provided important synthetic intermediates.

I greatly appreciate assistance and commitment from the colleagues in Department of NanoBiophotonics without whose input the completion of this project would not have been possible. I would like to thank Dr. Christian Wurm, Dr. Katrin I. Willig and Elke Hebisch for recording numerous super-resolution images. I am also very thankful to Prof. Mariano L. Bossi, Nina Ohm, Marianne Pulst and Kurt Müller for their help in measuring important photophysical properties.

Finally, I would like to express the appreciation to Prof. Ulf Diederichsen, Prof. Claudia Höbartner, Prof. Konrad Koszinowski and Prof. Heinz Neumann for their readiness to serve as members of the examination board on my PhD defence. Thank you.

References

- [1] S. W. Hell, *Science* **2007**, *316*, 1153–1158.
- [2] B. Valeur, in *Molecular Fluorescence*, Wiley-VCH, **2001**, pp. 34–71.
- [3] S. A. Adam, *Genome Biol.* **2001**, *2*, Reviews0007.
- [4] S. W. Hell, J. Wichmann, *Opt. Lett.* **1994**, *19*, 780–782.
- [5] S. W. Hell, *Nat. Biotechnol.* **2003**, *21*, 1347–1355.
- [6] S. W. Hell, M. Kroug, *Appl. Phys. B: Lasers Opt.* **1995**, *60*, 495–497.
- [7] S. Bretschneider, C. Eggeling, S. W. Hell, *Phys. Rev. Lett.* **2007**, *98*, 218103.
- [8] M. Hofmann, C. Eggeling, S. Jakobs, S. W. Hell, *Proc. Natl. Acad. Sci. U.S.A.* **2005**, *102*, 17565–17569.
- [9] F. Lavoie-Cardinal, N. A. Jensen, V. Westphal, A. C. Stiel, A. Chmyrov, J. Bierwagen, I. Testa, S. Jakobs, S. W. Hell, *ChemPhysChem* **2014**, *15*, 655–663.
- [10] a) L. Song, E. A. Jares-Erijman, T. M. Jovin, *J. Photochem. Photobiol. A* **2002**, *150*, 177–185; b) L. Giordano, T. M. Jovin, M. Irie, E. A. Jares-Erijman, *J. Am. Chem. Soc.* **2002**, *124*, 7481–7489.
- [11] M. Bossi, J. Fölling, M. Dyba, V. Westphal, S. W. Hell, *New J. Phys.* **2006**, *8*, 275.
- [12] a) E. Betzig, G. H. Patterson, R. Sougrat, O. W. Lindwasser, S. Olenych, J. S. Bonifacino, M. W. Davidson, J. Lippincott-Schwartz, H. F. Hess, *Science* **2006**, *313*, 1642–1645; b) S. T. Hess, T. P. K. Girirajan, M. D. Mason, *Biophys. J.* **2006**, *91*, 4258–4272.
- [13] M. J. Rust, M. Bates, X. Zhuang, *Nat. Methods* **2006**, *3*, 793–796.
- [14] M. Heilemann, S. van de Linde, M. Schüttpelz, R. Kasper, B. Seefeldt, A. Mukherjee, P. Tinnefeld, M. Sauer, *Angew. Chem. Int. Ed.* **2008**, *47*, 6172–6176.
- [15] J. Fölling, M. Bossi, H. Bock, R. Medda, C. A. Wurm, B. Hein, S. Jakobs, C. Eggeling, S. W. Hell, *Nat. Methods* **2008**, *5*, 943–945.
- [16] V. Westphal, S. O. Rizzoli, M. A. Lauterbach, D. Kamin, R. Jahn, S. W. Hell, *Science* **2008**, *320*, 246–249.
- [17] A. Chmyrov, J. Keller, T. Grotjohann, M. Ratz, E. d'Este, S. Jakobs, C. Eggeling, S. W. Hell, *Nat. Methods* **2013**, *10*, 737–740.
- [18] G. Donnert, J. Keller, C. A. Wurm, S. O. Rizzoli, V. Westphal, A. Schönle, R. Jahn, S. Jakobs, C. Eggeling, S. W. Hell, *Biophys. J.* **2007**, *92*, L67–L69.

- [19] R. Schmidt, C. A. Wurm, S. Jakobs, J. Engelhardt, A. Egner, S. W. Hell, *Nat. Methods* **2008**, *5*, 539–544.
- [20] X. Liu, Z. Xu, J. M. Cole, *J. Phys. Chem. C* **2013**, *117*, 16584–16595.
- [21] a) G. A. Reynolds, K. H. Drexhage, *Opt. Commun.* **1975**, *13*, 222–225; b) K. H. Drexhage, G. R. Erikson, G. H. Hawks, G. A. Reynolds, *Opt. Commun.* **1975**, *15*, 399–403; c) A. N. Fletcher, D. E. Bliss, *Appl. Phys.* **1978**, *16*, 289–295; d) G. Jones II, W. R. Jackson, A. M. Halpern, *Chem. Phys. Lett.* **1980**, *72*, 391–395; e) G. Jones II, W. R. Jackson, S. Kanoktanaporn, A. M. Halpern, *Opt. Commun.* **1980**, *33*, 315–320; f) A. N. Fletcher, D. E. Bliss, J. M. Kauffman, *Opt. Commun.* **1983**, *47*, 57–61; g) G. Jones, W. R. Jackson, C. Y. Choi, W. R. Bergmark, *J. Phys. Chem.* **1985**, *89*, 294–300.
- [22] W.-C. Sun, K. R. Gee, R. P. Haugland, *Bioorg. Med. Chem. Lett.* **1998**, *8*, 3107–3110.
- [23] X. Jin, C. Uttamapinant, A. Y. Ting, *ChemBioChem* **2011**, *12*, 65–70.
- [24] D. P. Specht, P. A. Martic, S. Farid, *Tetrahedron* **1982**, *38*, 1203–1211.
- [25] a) E. Koller, O. S. Wolfbeis, *Monatsh. Chem.* **1985**, *116*, 65–75; b) O. S. Wolfbeis, E. Koller, P. Hoghmuth, *Bull. Chem. Soc. Jpn.* **1985**, *58*, 731–734.
- [26] G. Signore, R. Nifosi, L. Albertazzi, B. Storti, R. Bizzarri, *J. Am. Chem. Soc.* **2010**, *132*, 1276–1288.
- [27] T. Deligeorgiev, T. Tsvetkova, S. Stanimirov, *Color. Technol.* **2011**, *127*, 434–439.
- [28] D. H. McDaniel, H. C. Brown, *J. Org. Chem.* **1958**, *23*, 420–427.
- [29] O. S. Wolfbeis, H. Marhold, *Chem. Ber.* **1985**, *118*, 3664–3672.
- [30] P. Czerney, M. Wenzel, B. Schweder, F. Lehmann, EP 1318177 B1; US 7563907 B2.
- [31] J.-A. Richard, M. Massonneau, P.-Y. Renard, A. Romieu, *Org. Lett.* **2008**, *10*, 4175–4178.
- [32] a) P. Kele, X. Li, M. Link, K. Nagy, A. Herner, K. Lorincz, S. Beni, O. S. Wolfbeis, *Org. Biomol. Chem.* **2009**, *7*, 3486–3490; b) T. Ehrenschwender, B. R. Varga, P. Kele, H.-A. Wagenknecht, *Chem. Asian J.* **2010**, *5*, 1761–1764; c) K. Nagy, E. Orban, S. Bosze, P. Kele, *Chem. Asian J.* **2010**, *5*, 773–777; d) G. B. Cserep, K. N. Enyedi, A. Demeter, G. Mezo, P. Kele, *Chem. Asian J.* **2013**, *8*, 494–502.

- [33] I. I. Grandberg, L. K. Denisov, O. A. Popova, *Chem. Heterocycl. Compd.* **1987**, *23*, 117–142.
- [34] T. Hinohara, K. Amano, K. Matsui, *Nippon Kagaku Kaishi* **1976**, *1976*, 247–247.
- [35] K. Rechthaler, G. Köhler, *Chem. Phys.* **1994**, *189*, 99–116.
- [36] M. Weißenfels, A. Hantschmann, T. Steinführer, E. Birkner, *Z. Chem.* **1989**, *29*, 166–166.
- [37] L. A. Karandashova, M. A. Kirpichenok, D. S. Yufit, Y. T. Struchkov, I. I. Grandberg, *Chem. Heterocycl. Compd.* **1990**, *26*, 1338–1345.
- [38] N. A. Gordeeva, M. A. Kirpichenok, N. S. Patalakha, I. I. Grandberg, *Chem. Heterocycl. Compd.* **1990**, *26*, 1329–1337.
- [39] N. A. Gordeeva, M. A. Kirpichenok, N. S. Patalakha, V. M. Khutoretskii, I. I. Grandberg, *Chem. Heterocycl. Compd.* **1991**, *27*, 491–495.
- [40] M. A. Kirpichenok, V. M. Baukulev, L. A. Karandashova, I. I. Grandberg, *Chem. Heterocycl. Compd.* **1991**, *27*, 1193–1199.
- [41] M. A. Kirpichenok, N. S. Patalakha, L. Y. Fomina, I. I. Grandberg, *Chem. Heterocycl. Compd.* **1991**, *27*, 934–939.
- [42] N. S. Patalakha, D. S. Yufit, M. A. Kirpichenok, N. A. Gordeeva, Y. T. Struchkov, I. I. Grandberg, *Chem. Heterocycl. Compd.* **1991**, *27*, 32–37.
- [43] J. Gordo, J. Avó, A. J. Parola, J. C. Lima, A. Pereira, P. S. Branco, *Org. Lett.* **2011**, *13*, 5112–5115.
- [44] H. Takechi, Y. Oda, N. Nishizono, K. Oda, M. Machida, *Chem. Pharm. Bull.* **2000**, *48*, 1702–1710.
- [45] a) S. Nizamov, K. I. Willig, M. V. Sednev, V. N. Belov, S. W. Hell, *Chem. Eur. J.* **2012**, *18*, 16339–16348; b) H. Schill, S. Nizamov, F. Bottanelli, J. Bierwagen, V. N. Belov, S. W. Hell, *Chem. Eur. J.* **2013**, *19*, 16556–16565.
- [46] M.-S. Schiedel, C. A. Briehn, P. Bäuerle, *Angew. Chem. Int. Ed.* **2001**, *40*, 4677–4680.
- [47] K. Sivakumar, F. Xie, B. M. Cash, S. Long, H. N. Barnhill, Q. Wang, *Org. Lett.* **2004**, *6*, 4603–4606.
- [48] N. Kitamura, T. Fukagawa, S. Kohtani, S.-i. Kitoh, K.-K. Kunimoto, R. Nakagaki, *J. Photochem. Photobiol. A* **2007**, *188*, 378–386.
- [49] a) G. Chen, D. J. Yee, N. G. Gubernator, D. Sames, *J. Am. Chem. Soc.* **2005**, *127*, 4544–4545; b) G. Chen, N. Gubernator, D. Sames, D. J. Yee, **2006**.
- [50] T. Sheshashena Reddy, A. Ram Reddy, *Dyes Pigm.* **2013**, *96*, 525–534.

-
- [51] C. Murata, T. Masuda, Y. Kamochi, K. Todoroki, H. Yoshida, H. Nohta, M. Yamaguchi, A. Takadate, *Chem. Pharm. Bull.* **2005**, *53*, 750–758.
- [52] K. Komatsu, Y. Urano, H. Kojima, T. Nagano, *J. Am. Chem. Soc.* **2007**, *129*, 13447–13454.
- [53] B. N. Ahamed, P. Ghosh, *Dalton Trans.* **2011**, *40*, 6411–6419.
- [54] a) Y. Peng, Y.-M. Dong, M. Dong, Y.-W. Wang, *J. Org. Chem.* **2012**, *77*, 9072–9080; b) C. Wang, S. Yang, M. Yi, C. Liu, Y. Wang, J. Li, Y. Li, R. Yang, *ACS Appl. Mater. Interfaces* **2014**, *6*, 9768–9775.
- [55] T.-I. Kim, H. Kim, Y. Choi, Y. Kim, *Chem. Comm.* **2011**, *47*, 9825–9827.
- [56] P. Hou, S. Chen, H. Wang, J. Wang, K. Voitchovsky, X. Song, *Chem. Comm.* **2014**, *50*, 320–322.
- [57] a) M.-T. Le Bris, J. Mugnier, J. Bourson, B. Valeur, *Chem. Phys. Lett.* **1984**, *106*, 124–127; b) C. Trebaul, J. Roncali, F. Garnier, R. Guglielmetti, *Bull. Chem. Soc. Jpn.* **1987**, *60*, 2657–2662; c) S. Fery-Forgues, M. T. Le Bris, J. C. Mialocq, J. Pouget, W. Rettig, B. Valeur, *J. Phys. Chem.* **1992**, *96*, 701–710.
- [58] M. Monsigny, P. Midoux, M.-T. Le Bris, A.-C. Roche, B. Valeur, *Biol. Cell* **1989**, *67*, 193–200.
- [59] H. M. Kim, P. R. Yang, M. S. Seo, J.-S. Yi, J. H. Hong, S.-J. Jeon, Y.-G. Ko, K. J. Lee, B. R. Cho, *J. Org. Chem.* **2007**, *72*, 2088–2096.
- [60] I. Kim, D. Kim, S. Sambasivan, K. H. Ahn, *Asian J. Org. Chem.* **2012**, *1*, 60–64.
- [61] A. R. Sarkar, C. H. Heo, H. W. Lee, K. H. Park, Y. H. Suh, H. M. Kim, *Anal. Chem.* **2014**, *86*, 5638–5641.
- [62] L. G. Lee, G. M. Berry, C.-H. Chen, *Cytometry* **1989**, *10*, 151–164.
- [63] R. P. Haugland, J. Whitaker, US4945171 A.
- [64] J. E. Whitaker, R. P. Haugland, F. G. Prendergast, *Anal. Biochem.* **1991**, *194*, 330–344.
- [65] a) C. J. Chang, S. J. Lippard, E. Nolan, WO2005067580 A3; b) E. M. Nolan, S. J. Lippard, *J. Am. Chem. Soc.* **2007**, *129*, 5910–5918; c) A. Minta, P. R. Escamilla, WO2011047391 A1.
- [66] M. D. Pluth, M. R. Chan, L. E. McQuade, S. J. Lippard, *Inorg. Chem.* **2011**, *50*, 9385–9392.
- [67] R. M. Strongin, Y. Guo, L. Hakuna, M. A. Lowry, C. J. O. Escobedo, WO2013126816 A1.
- [68] D. Srikun, A. E. Albers, C. J. Chang, *Chem. Sci.* **2011**, *2*, 1156–1165.

- [69] S. H. Kim, J. R. Gunther, J. A. Katzenellenbogen, *Org. Lett.* **2008**, *10*, 4931–4934.
- [70] W. M. F. Fabian, S. Schuppler, O. S. Wolfbeis, *J. Chem. Soc., Perkin Trans. 2* **1996**, 853–856.
- [71] a) Y. Yang, M. Lowry, C. M. Schowalter, S. O. Fakayode, J. O. Escobedo, X. Xu, H. Zhang, T. J. Jensen, F. R. Fronczek, I. M. Warner, R. M. Strongin, *J. Am. Chem. Soc.* **2006**, *128*, 14081–14092; b) Y. Yang, M. Lowry, X. Xu, J. O. Escobedo, M. Sibrian-Vazquez, L. Wong, C. M. Schowalter, T. J. Jensen, F. R. Fronczek, I. M. Warner, R. M. Strongin, *Proc. Natl. Acad. Sci. U.S.A.* **2008**, *105*, 8829–8834.
- [72] a) K. Furukawa, H. Abe, J. Wang, M. Uda, H. Koshino, S. Tsuneda, Y. Ito, *Org. Biomol. Chem.* **2009**, *7*, 671–677; b) M. Sibrian-Vazquez, J. O. Escobedo, M. Lowry, R. M. Strongin, *Pure Appl. Chem.* **2012**, *84*, 2443–2456.
- [73] a) J. Chen, W. Liu, B. Zhou, G. Niu, H. Zhang, J. Wu, Y. Wang, W. Ju, P. Wang, *J. Org. Chem.* **2013**, *78*, 6121–6130; b) A. Chevalier, P.-Y. Renard, A. Romieu, *Chem.-Eur. J.* **2014**, *20*, 8330–8337.
- [74] Z. Tian, B. Tian, J. Zhang, *Dyes Pigm.* **2013**, *99*, 1132–1136.
- [75] L. Wu, K. Burgess, *Org. Lett.* **2008**, *10*, 1779–1782.
- [76] A. Zilles, K. H. Drexhage, N. U. Kemnitzer, J. Arden-Jacob, M. Hamers-Schneider, US20130224871 A1.
- [77] G. Ulrich, R. Ziessel, A. Harriman, *Angew. Chem. Int. Ed.* **2008**, *47*, 1184–1201.
- [78] Y. Chen, J. Zhao, H. Guo, L. Xie, *J. Org. Chem.* **2012**, *77*, 2192–2206.
- [79] a) A. Martin, C. Long, R. J. Forster, T. E. Keyes, *Chem. Commun.* **2012**, *48*, 5617–5619; b) A. Martin, R. D. Moriarty, C. Long, R. J. Forster, T. E. Keyes, *Asian J. Org. Chem.* **2013**, *2*, 763–778.
- [80] M. Verdoes, K. Oresic Bender, E. Segal, W. A. van der Linden, S. Syed, N. P. Withana, L. E. Sanman, M. Bogyo, *J. Am. Chem. Soc.* **2013**, *135*, 14726–14730.
- [81] A. Y. Bochkov, I. O. Akchurin, O. A. Dyachenko, V. F. Traven, *Chem. Commun.* **2013**, *49*, 11653–11655.
- [82] Y. Zhou, Y. Xiao, S. Chi, X. Qian, *Org. Lett.* **2008**, *10*, 633–636.
- [83] J. F. Araneda, W. E. Piers, B. Heyne, M. Parvez, R. McDonald, *Angew. Chem. Int. Ed.* **2011**, *50*, 12214–12217.
- [84] M. Mao, S. Xiao, T. Yi, K. Zou, *J. Fluorine Chem.* **2011**, *132*, 612–616.
- [85] Z. Li, X. Lv, Y. Chen, W.-F. Fu, *Dyes Pigm.* **2014**, *105*, 157–162.

- [86] a) X. Peng, F. Song, E. Lu, Y. Wang, W. Zhou, J. Fan, Y. Gao, *J. Am. Chem. Soc.* **2005**, *127*, 4170–4171; b) W. Pham, L. Cassell, A. Gillman, D. Koktysh, J. C. Gore, *Chem. Commun.* **2008**, 1895–1897.
- [87] F. Vollmer, W. Rettig, E. Birckner, *J Fluoresc* **1994**, *4*, 65–69.
- [88] B. Valeur, in *Molecular Fluorescence*, Wiley-VCH Verlag GmbH, **2001**, pp. 72–124.
- [89] B. Valeur, in *Molecular Fluorescence*, Wiley-VCH Verlag GmbH, **2001**, pp. 226–246.
- [90] J. Kasurinen, *Biochem. Biophys. Res. Commun.* **1992**, *187*, 1594–1601.
- [91] P. L. Paris, J. M. Langenhan, E. T. Kool, *Nucleic Acids Res.* **1998**, *26*, 3789–3793.
- [92] a) E. V. Bichenkova, A. Sardarian, H. E. Savage, C. Rogert, K. T. Douglas, *Assay Drug Dev. Technol.* **2005**, *3*, 39–46; b) E. V. Bichenkova, H. E. Savage, A. R. Sardarian, K. T. Douglas, *Biochem. Biophys. Res. Commun.* **2005**, *332*, 956–964; c) E. V. Bichenkova, A. Gbaj, L. Walsh, H. E. Savage, C. Rogert, A. R. Sardarian, L. L. Etchells, K. T. Douglas, *Org. Biomol. Chem.* **2007**, *5*, 1039–1051.
- [93] a) Y. N. Teo, E. T. Kool, *Chem. Rev.* **2012**, *112*, 4221–4245; b) H. Kashida, H. Asanuma, *Phys. Chem. Chem. Phys.* **2012**, *14*, 7196–7204.
- [94] a) J. Gao, C. Strässler, D. Tahmassebi, E. T. Kool, *J. Am. Chem. Soc.* **2002**, *124*, 11590–11591; b) J. Gao, S. Watanabe, E. T. Kool, *J. Am. Chem. Soc.* **2004**, *126*, 12748–12749; c) A. Cuppoletti, Y. Cho, J.-S. Park, C. Strässler, E. T. Kool, *Bioconjugate Chem.* **2005**, *16*, 528–534; d) J. N. Wilson, E. T. Kool, *Org. Biomol. Chem.* **2006**, *4*, 4265–4274; e) Y. N. Teo, J. N. Wilson, E. T. Kool, *Chem.-Eur. J.* **2009**, *15*, 11551–11558; f) Y. N. Teo, E. T. Kool, *Bioconjugate Chem.* **2009**, *20*, 2371–2380.
- [95] a) M. Nakamura, Y. Ohtoshi, K. Yamana, *Chem. Commun.* **2005**, 5163–5165; b) M. Nakamura, Y. Shimomura, Y. Ohtoshi, K. Sasa, H. Hayashi, H. Nakano, K. Yamana, *Org. Biomol. Chem.* **2007**, *5*, 1945–1951; c) M. Nakamura, Y. Murakami, K. Sasa, H. Hayashi, K. Yamana, *J. Am. Chem. Soc.* **2008**, *130*, 6904–6905.
- [96] C.-C. Hsieh, M.-L. Ho, P.-T. Chou, in *Advanced Fluorescence Reporters in Chemistry and Biology I, Vol. 8* (Ed.: A. P. Demchenko), Springer, **2010**, pp. 225–266.
- [97] J. Zhao, S. Ji, Y. Chen, H. Guo, P. Yang, *Phys. Chem. Chem. Phys.* **2012**, *14*, 8803–8817.

-
- [98] M. Van der Auweraer, Z. R. Grabowski, W. Rettig, *J. Phys. Chem.* **1991**, *95*, 2083–2092.
- [99] V. A. Galievsky, S. I. Druzhinin, A. Demeter, Y.-B. Jiang, S. A. Kovalenko, L. Pérez Lustres, K. Venugopal, N. P. Ernsting, X. Allonas, M. Noltemeyer, R. Machinek, K. A. Zachariasse, *ChemPhysChem* **2005**, *6*, 2307–2323.
- [100] K. Rotkiewicz, K. H. Grellmann, Z. R. Grabowski, *Chem. Phys. Lett.* **1973**, *19*, 315–318.
- [101] Z. R. Grabowski, K. Rotkiewicz, A. Siemiarczuk, *J. Lumin.* **1979**, *18–19*, 420–424.
- [102] T. Taniguchi, J. Wang, S. Irle, S. Yamaguchi, *Dalton Trans.* **2013**, *42*, 620–624.
- [103] J. Fan, M. Hu, P. Zhan, X. Peng, *Chem. Soc. Rev.* **2013**, *42*, 29–43.
- [104] B. Wieb van der Meer, in *FRET – Förster Resonance Energy Transfer* (Eds.: I. Medintz, N. Hildebrandt), Wiley-VCH, **2013**, pp. 23–62.
- [105] G.-S. Jiao, L. H. Thoresen, K. Burgess, *J. Am. Chem. Soc.* **2003**, *125*, 14668–14669.
- [106] L. Yuan, W. Lin, Z. Cao, J. Wang, B. Chen, *Chem.-Eur. J.* **2012**, *18*, 1247–1255.
- [107] S. Speiser, *Chem. Rev.* **1996**, *96*, 1953–1976.
- [108] W. Lin, L. Yuan, Z. Cao, Y. Feng, J. Song, *Angew. Chem. Int. Ed.* **2010**, *49*, 375–379.
- [109] D. Su, J. Oh, S.-C. Lee, J. M. Lim, S. Sahu, X. Yu, D. Kim, Y.-T. Chang, *Chem. Sci.* **2014**, *5*, 4812–4818.
- [110] B. R. Rankin, R. R. Kellner, S. W. Hell, *Opt. Lett.* **2008**, *33*, 2491–2493.
- [111] a) K. Kolmakov, V. N. Belov, J. Bierwagen, C. Ringemann, V. Müller, C. Eggeling, S. W. Hell, *Chem.-Eur. J.* **2010**, *16*, 158–166; b) C. Wurm, K. Kolmakov, F. Gottfert, H. Ta, M. Bossi, H. Schill, S. Berning, S. Jakobs, G. Donnert, V. Belov, S. Hell, *Opt. Nanoscopy* **2012**, *1*, 7; c) K. Kolmakov, C. A. Wurm, D. N. H. Meineke, F. Göttfert, V. P. Boyarskiy, V. N. Belov, S. W. Hell, *Chem.-Eur. J.* **2014**, *20*, 146–157.
- [112] Y. F. Hua, R. Sinha, C. S. Thiel, R. Schmidt, J. Huve, H. Martens, S. W. Hell, A. Egner, J. Klingauf, *Nat. Neurosci.* **2011**, *14*, 833–839.
- [113] K. Friedemann, A. Turshatov, K. Landfester, D. Crespy, *Langmuir* **2011**, *27*, 7132–7139.
- [114] P. A. Pellett, X. Sun, T. J. Gould, J. E. Rothman, M.-Q. Xu, I. R. Corrêa, J. Bewersdorf, *Biomed. Opt. Express* **2011**, *2*, 2364–2371.

- [115] C. Dean, H. Liu, T. Staudt, M. A. Stahlberg, S. Vingill, J. Bückers, D. Kamin, J. Engelhardt, M. B. Jackson, S. W. Hell, E. R. Chapman, *J. Neurosci.* **2012**, *32*, 5398–5413.
- [116] T. Karlsson, M. V. Turkina, O. Yakymenko, K.-E. Magnusson, E. Vikström, *PLoS Pathog.* **2012**, *8*, e1002953.
- [117] E. M. Mace, J. S. Orange, *Commun. Integr. Biol.* **2012**, *5*, 184–186.
- [118] C. Kempf, T. Staudt, P. Bingen, H. Horstmann, J. Engelhardt, S. W. Hell, T. Kuner, *PLoS ONE* **2013**, *8*, e62893.
- [119] G. Lavieu, M. H. Dunlop, A. Lerich, H. Zheng, F. Bottanelli, J. E. Rothman, *Mol. Biol. Cell* **2014**, *25*, 3028–3036.
- [120] B. Henkel, D. R. Drose, T. Ackels, S. Oberland, M. Spehr, E. M. Neuhaus, *Chem. Senses* **2014**, *40*, 73–87.
- [121] L. Westin, M. Reuss, M. Lindskog, A. Aperia, H. Brismar, *BMC Neurosci.* **2014**, *15*, 45.
- [122] F. Wilfling, A. R. Thiam, M.-J. Olarte, J. Wang, R. Beck, T. J. Gould, E. S. Allgeyer, F. Pincet, J. Bewersdorf, R. V. Farese, T. C. Walther, *eLife* **2014**, *3*, e01607.
- [123] A. Johnson, N. Bhattacharya, M. Hanna, J. G. Pennington, A. L. Schuh, L. Wang, M. S. Otegui, S. M. Stagg, A. Audhya, *The EMBO journal* **2015**, embj.201489032.
- [124] W. H. Perkin, *J. Chem. Soc.* **1868**, *21*, 53–63.
- [125] P. A. Vadola, D. Sames, *J. Org. Chem.* **2012**, *77*, 7804–7814.
- [126] W. D. Kumler, J. J. Eiler, *J. Am. Chem. Soc.* **1943**, *65*, 2355–2361.
- [127] L. D. Freedman, G. O. Doak, *Chem. Rev.* **1957**, *57*, 479–523.
- [128] C. Hansch, A. Leo, R. W. Taft, *Chem. Rev.* **1991**, *91*, 165–195.
- [129] M.-E. Theoclitou, L. A. Robinson, *Tetrahedron Lett.* **2002**, *43*, 3907–3910.
- [130] J. L. Luche, *J. Am. Chem. Soc.* **1978**, *100*, 2226–2227.
- [131] A. R. Katritzky, C. A. Ramsden, J. A. Joule, V. V. Zhdankin, in *Handbook of Heterocyclic Chemistry (Third Edition)* (Eds.: A. R. Katritzky, C. A. Ramsden, J. A. Joule, V. V. Zhdankin), Elsevier, **2010**, pp. 37–86.
- [132] A. R. Katritzky, C. A. Ramsden, J. A. Joule, V. V. Zhdankin, in *Handbook of Heterocyclic Chemistry (Third Edition)* (Eds.: A. R. Katritzky, C. A. Ramsden, J. A. Joule, V. V. Zhdankin), Elsevier, **2010**, pp. 242–382.
- [133] J. W. Perich, R. B. Johns, *Synthesis* **1988**, 1988, 142–144.

- [134] O. Valdes-Aguilera, D. C. Neckers, *Acc. Chem. Res.* **1989**, *22*, 171–177.
- [135] *The Molecular Probes Handbook: A Guide to Fluorescent Probes and Labeling Technologies*, 11th ed., Life Technologies, **2010**.
- [136] M. E. Kuipers, P. J. Swart, M. M. W. B. Hendriks, D. K. F. Meijer, *J. Med. Chem.* **1995**, *38*, 883–889.
- [137] G. Moneron, R. Medda, B. Hein, A. Giske, V. Westphal, S. W. Hell, *Opt. Express* **2010**, *18*, 1302–1309.
- [138] J. H. Blanch, *J. Chem. Soc. B* **1966**, 937–939.
- [139] R.-Z. Ma, Q.-C. Yao, X. Yang, M. Xia, *J. Fluorine Chem.* **2012**, *137*, 93–98.
- [140] R. Bentley, T. S. Stevens, M. Thompson, *J. Chem. Soc. C* **1970**, 791–795.
- [141] J. R. Lakowicz, in *Principles of Fluorescence Spectroscopy* (Ed.: J. R. Lakowicz), Springer, **2006**, pp. 331–351.
- [142] a) L. Kaczmarek, R. Balicki, J. Lipkowski, P. Borowicz, A. Grabowska, *J. Chem. Soc., Perkin Trans. 2* **1994**, 1603–1610; b) D. LeGourriérec, V. Kharlanov, R. G. Brown, W. Rettig, *J. Photochem. Photobiol., A* **1998**, *117*, 209–216; c) N. Basaric, P. Wan, *Photochem. Photobiol. Sci.* **2006**, *5*, 656–664.
- [143] C. Eggeling, J. Widengren, R. Rigler, C. A. M. Seidel, in *Applied Fluorescence in Chemistry, Biology and Medicine*, Springer, **1999**, pp. 193–240.
- [144] K. Muthuramu, V. R. Murthy, *J. Org. Chem.* **1982**, *47*, 3976–3979.
- [145] a) B. H. Winters, H. I. Mandelberg, W. B. Mohr, *Appl. Phys. Lett.* **1974**, *25*, 723–725; b) R. J. von Trebra, T. H. Koch, *J. Photochem.* **1986**, *35*, 33–46.
- [146] O. V. Zinkovskaya, N. A. Kuznetsova, O. L. Kaliya, *J. Appl. Spectrosc.* **1984**, *41*, 1171–1174.
- [147] M. Krzeszewski, O. Vakuliuk, D. T. Gryko, *Eur. J. Org. Chem.* **2013**, *2013*, 5631–5644.
- [148] a) T. R. Kelly, M. H. Kim, *J. Org. Chem.* **1992**, *57*, 1593–1597; b) G.-H. Kuo, A. Wang, S. Emanuel, A. DeAngelis, R. Zhang, P. J. Connolly, W. V. Murray, R. H. Gruninger, J. Sechler, A. Fuentes-Pesquera, D. Johnson, S. A. Middleton, L. Jolliffe, X. Chen, *J. Med. Chem.* **2004**, *48*, 1886–1900.
- [149] T. Bakos, I. Vincze, *Synth. Commun.* **1989**, *19*, 523–528.
- [150] A. N. Shaw, K. J. Duffy, R. Tedesco, K. Wiggall, WO2007136990 A2.
- [151] J.-H. Lee, W.-S. Kim, Y. Y. Lee, C.-G. Cho, *Tetrahedron Lett.* **2002**, *43*, 5779–5782.
- [152] X. Han, B. M. Stoltz, E. J. Corey, *J. Am. Chem. Soc.* **1999**, *121*, 7600–7605.

- [153] R. L. Atkins, D. E. Bliss, *J. Org. Chem.* **1978**, *43*, 1975–1980.
- [154] H. Takechi, S. Kamada, M. Machida, *Chem. Pharm. Bull.* **1996**, *44*, 793–799.
- [155] J. E. Whitaker, R. P. Haugland, D. Ryan, P. C. Hewitt, R. P. Haugland, F. G. Prendergast, *Anal. Biochem.* **1992**, *207*, 267–279.
- [156] a) J. Arden-Jacob, J. Frantzeskos, N. U. Kemnitzer, A. Zilles, K. H. Drexhage, *Spectrochim. Acta, Part A* **2001**, *57*, 2271–2283; b) P. V. Fisher, R. O'Neill, WO2004003510 A3; c) J. Arden-Jacob, K. H. Drexhage, J. Frantzeskos, A. Zilles, EP1173519 B1; d) K. Kolmakov, V. N. Belov, C. A. Wurm, B. Harke, M. Leutenegger, C. Eggeling, S. W. Hell, *Eur. J. Org. Chem.* **2010**, *2010*, 3593–3610.
- [157] K. Kolmakov, C. Wurm, M. V. Sednev, M. L. Bossi, V. N. Belov, S. W. Hell, *Photochem. Photobiol. Sci.* **2012**, *11*, 522–532.
- [158] J. B. Grimm, A. J. Sung, W. R. Legant, P. Hulamm, S. M. Matlosz, E. Betzig, L. D. Lavis, *ACS Chem. Biol.* **2013**, *8*, 1303–1310.
- [159] G. W. Gribble, C. F. Nutaitis, *Synthesis* **1987**, *1987*, 709–711.
- [160] H. Mansilla, D. Regás, *Synth. Commun.* **2006**, *36*, 2195–2201.
- [161] A. Thurkauf, A. E. Jacobson, K. C. Riee, *Synthesis* **1988**, *1988*, 233–234.
- [162] L. Alig, J. Alsenz, M. Andjelkovic, S. Bendels, A. Bénardeau, K. Bleicher, A. Bourson, P. David-Pierson, W. Guba, S. Hildbrand, D. Kube, T. Lübbers, A. V. Mayweg, R. Narquizian, W. Neidhart, M. Nettekoven, J.-M. Plancher, C. Rocha, M. Rogers-Evans, S. Röver, G. Schneider, S. Taylor, P. Waldmeier, *J. Med. Chem.* **2008**, *51*, 2115–2127.
- [163] W. P. Neumann, W. Uzick, A. K. Zarkadis, *J. Am. Chem. Soc.* **1986**, *108*, 3762–3770.
- [164] A. Ono, N. Suzuki, J. Kamimura, *Synthesis* **1987**, *1987*, 736–738.
- [165] L. Gu, B. Yang, F. Liu, Y. Bai, *Chin. J. Chem.* **2009**, *27*, 1199–1201.
- [166] R. W. A. Luke, P. G. T. Boyce, E. Kate Dorling, *Tetrahedron Lett.* **1996**, *37*, 263–266.
- [167] W.-C. Sun, K. R. Gee, D. H. Klaubert, R. P. Haugland, *J. Org. Chem.* **1997**, *62*, 6469–6475.
- [168] a) J. Burdon, B. L. Kane, J. C. Tatlow, *J. Fluorine Chem.* **1971**, *1*, 185–192; b) A. M. Kenwright, G. Sandford, A. J. Tadeusiak, D. S. Yufit, J. A. K. Howard, P. Kilickiran, G. Nelles, *Tetrahedron* **2010**, *66*, 9819–9827.
- [169] S. Nahm, S. M. Weinreb, *Tetrahedron Lett.* **1981**, *22*, 3815–3818.

-
- [170] D. N. Kursanov, Z. N. Parnes, N. M. Loim, *Synthesis* **1974**, 1974, 633–651.
- [171] K. Kolmakov, C. A. Wurm, R. Hennig, E. Rapp, S. Jakobs, V. N. Belov, S. W. Hell, *Chem.-Eur. J.* **2012**, 18, 12986–12998.
- [172] a) M. M. Martin, L. Lindqvist, *J. Lumin.* **1975**, 10, 381–390; b) E. Martin, A. Pardo, M. S. Guijarro, J. I. Fernandez-Alonso, *J. Mol. Struct.* **1986**, 142, 197–200; c) R. Sjöback, J. Nygren, M. Kubista, *Spectrochim. Acta, Part A* **1995**, 51, L7–L21; d) N. Klonis, W. Sawyer, *J. Fluoresc.* **1996**, 6, 147–157.
- [173] T. Peng, D. Yang, *Org. Lett.* **2010**, 12, 496–499.
- [174] J. Bückers, D. Wildanger, G. Vicidomini, L. Kastrop, S. W. Hell, *Opt. Express* **2011**, 19, 3130–3143.
- [175] N. Senda, A. Momotake, Y. Nishimura, T. Arai, *Bull. Chem. Soc. Jpn.* **2006**, 79, 1753–1757.
- [176] R. K. Olsen, *J. Org. Chem.* **1970**, 35, 1912–1915.
- [177] K.-J. Han, M. Kim, *Lett. Org. Chem.* **2004**, 4, 20–22.

Curriculum vitae

Name: Maksim Sednev
Date of birth: 21.10.1988
Place of birth: Nizhny Tagil
Nationality: Russian

EDUCATION

2011 – present **University of Göttingen and Max Planck Institute for Biophysical Chemistry, Germany**
PhD in Organic Chemistry

Thesis: Fluorescent dyes with large Stokes shifts of 80–200 nm and their use in super-resolution microscopy

Supervisors: Prof. Dr. Stefan W. Hell, Prof. Dr. Armin de Meijere

2011 **Max Planck Institute for Biophysical Chemistry, Germany**

Visiting student

Project: Masked red-emitting carbopyronines with photosensitive 2-diazo-1-indanone caging group

Supervisor: Prof. Dr. Stefan W. Hell

2005 – 2010 **Saint Petersburg State University, Russia**

MSc with Distinction in Chemistry

Thesis: 1,3-Dipolar cycloaddition of (*Z*)-1-arylmethylidene-3-oxopyrazolidine-1-ium-2-ide to *N*-arylmaleimides

Supervisor: Assoc. Prof. Yuri B. Koptelov

AWARDS AND FELLOWSHIPS

2013 Microsoft Fellowship for the participation in the 63rd Lindau Nobel Laureate Meeting, Lindau, Germany

2013 Best poster presentation, 15th JCF-Frühjahrsymposium, Berlin, Germany

2011 – 2014 Max Planck Society Graduate Fellowship

PUBLICATIONS

6. *submitted*: **Sednev, M.V.**; Belov, V.N.; Hell, S.W: Fluorescent dyes with large Stokes shifts for super-resolution optical microscopy of biological objects. *Methods Appl. Fluoresc.*, 2015
5. **Sednev, M.V.**; Wurm, C.A.; Belov, V.N.; Hell, S.W: Carborhodol: A New Hybrid Fluorophore Obtained by Combination of Fluorescein and Carbopyronine Dye Cores. *Bioconjugate Chem.* 24 (4), 690–700, 2013
4. Nizamov, S; Willig, K.I; **Sednev, M.V.**; Belov, V.N.; Hell, S.W.: Phosphorylated 3-Heteroarylcoumarins and Their Use in Fluorescence Microscopy and Nanoscopy. *Chem. Eur. J.* 18 (51), 16339–16348, 2012
3. Kolmakov, K.; Wurm, C.; **Sednev, M. V.**; Bossi, M. L.; Belov, V.N.; Hell, S. W.: Masked Red-emitting Carbopyronine Dyes with Photosensitive 2-Diazo-1-indanone Caging Group. *Photochem. Photobiol. Sci.* 11 (3), 522–532, 2012
2. Koptelov, Yu. B.; **Sednev, M.V.**; Kostikov, R.R.: (Z)-1-Alkylidene- and 1-Arylmethylidene-5,5-dimethyl-3-oxopyrazolidin-1-ium-2-ides and Their Cycloaddition to *N*-Arylmaleimides. *Russ. J. Org. Chem.* 48 (6), 804–814, 2012
1. Koptelov, Yu. B.; **Sednev, M.V.**: Stable Azomethine Imines Derived from Pyrazolidin-3-one and Their Cycloaddition to *N*-Arylmaleimides. *Russ. J. Org. Chem.* 47 (3), 547–555, 2011

CONFERENCES AND MEETINGS

- 2014** **Labeling and Nanoscopy**, Heidelberg, Germany
“Design of Red-Emitting Dyes for Microscopy and Nanoscopy” (*poster*)
- 2013** **63rd Lindau Nobel Laureate Meeting**, Lindau, Germany
- 2013** **15th JCF-Frühjahrsymposium** (A meeting of young chemists organized by German Chemical Society), Berlin, Germany
“(Iso)quinolinocoumarins: a novel class of bright fluorescent dyes with large Stokes shift” (*talk and poster*)
- 2012** **13th Belgian Organic Synthesis Symposium**, Leuven, Belgium
“Novel coumarin dyes for microscopy applications” (*poster*)
- 2011** **V International Symposium “Aliphatic Diazo Compounds**, St. Petersburg, Russia
“Cycloaddition of *N*-arylmaleimides to *C*-alkyl- and *C*-arylsubstituted azomethine imines generated from 5,5-dimethylpyrazolidin-3-one” (*poster*)

TEACHING EXPERIENCE

- 2013** Teaching assistant, Introductory Organic Synthesis Lab, University of Göttingen
- 2012** Teaching assistant, Introductory Organic Synthesis Lab, University of Göttingen
- 2011 – 2012** Teaching assistant, Advanced Organic Synthesis Lab, University of Göttingen

Date:

Signature: